School of Chemical and Petroleum Engineering

Synthesis and Evaluation of Nanostructured Membrane Catalytic Systems for Water Treatment

Ping Liang

This thesis is presented for the Degree of
Doctor of Philosophy
of
Curtin University

June 2017

Declaration

To the best of my knowledge and belief this thesis contains no material previously published by any other person except where due acknowledgement has been made.

This thesis contains no material which has been accepted for the award of any other degree or diploma in any university.

Signature:.....Ping Liang.....

Date:...05/06/2017.....

Acknowledgement

Firstly, I would like to express my sincere gratitude to my supervisor, Prof. Shaobin Wang, for the opportunity to join the research group and instructive guidance. He is nice, patient and erudite. I am proud and lucky to be one of his students. During the past three years, my academic life was happy and fruitful with the great help of Prof. Wang. Without him, my research and thesis cannot be completed smoothly.

Equally, I am deeply grateful to my co-supervisor, Dr. Hongqi Sun. I have learnt a lot from him about academic writing and he gave me great suggestions about academic research. Thanks to his painstaking effort in polishing my manuscripts, the research results can be published successfully. I would also like to thank Prof. Shaomin Liu for the great assistance in my studies and life.

I would like to thank the staff members from the Department of Chemical Engineering: Guanliang Zhou, Anja Werner, Roshanak Doroushi, Jason Wright, Araya Abera, Yu Long, Xiao Hua and Andrew Chan. I am also grateful to staff from Department of Applied Physics, for their assistance in XRD and SEM training.

I also express my gratitude to my friends, Stacey, Fern, Yuxian Wang, Spark, Hao Tian, Xiaochen Guo, Mingming Zhang, Xin Pang, Wenran Gao, Huayang Zhang, Wenjie Tian, Xiaoguang Duan, Chen Wang, Yu Liu, Wei Wang, Jian Kang, Yilin Liu, Jijiang He, Yazi Liu, Qi Yang, Li Zhou, Qiaoran Liu, Jun Ke, Jie Liu, Leon, Sharon, Min Ao, Bing Song, Chao Feng, Sui Boon, Chow, Lee, Pae and many others. Thank you all for the great help during my Ph.D life. I will treasure our friendship forever.

Last but not least, I would like to express my deepest gratitude to my family — my parents, my husband, and my siblings, for their supports and love to me. Especially, I

owe my deep gratitude to my husband, Chi Zhang. With his love, tolerance and help, I overcame the troubles and pressures successfully.

Abstract

Wastewater treatment technologies, such as adsorption, photocatalytic reaction, advanced oxidation process and so on, are widely reported during the past years. Nanocarbons, metals/metal-oxides, and their hybrids have been explored as the adsorbents and catalysts for environmental remediation. Metal-organic frameworks (MOFs), consisting of metal ions and organic linkers, have been considered as promising precursors for the materials mentioned above, due to the tunable porous structures and good configuration of elements. Therefore, the purpose of this research is to explore MOFs-derived catalysts for wastewater treatment. In this study, carbon and nitrogen co-doped zinc oxide and nitrogen-doped graphene have been synthesized by the controlled pyrolysis of MOFs like ZIF-8 (Zn) and MIL-100 (Fe). Additional nitrogen sources and post-acid treatment have also been employed. The as-synthesized materials were characterized and evaluated by catalytic degradation of organic pollutants in water. It was found that the pyrolysis routes, temperatures and time imposed great influences on the photocatalysis for dye degradation and water oxidation. The proper carbon and nitrogen doping in zinc oxide could improve the photocatalytic efficiency. In addition, the catalytic degradation of organic pollutants in the presence of peroxymonosulfate was influenced by the nitrogen doping, conductive graphene and high specific surface area of the catalysts. The transformation from MOFs to graphitic carbon has also been uncovered. The mechanism of peroxymonosulfate activation by N-doped graphene have been studied by electron paramagnetic resonance and quenching tests, showing that singlet oxygen was generated and contributed mainly to the decomposition of organic pollutants besides hydroxyl and sulfate radicals.

Publications by the author

1. **P. Liang**, C. Zhang, H. Sun, S. Liu, M. Tade, S. Wang*, Solar photocatalytic water oxidation and purification on ZIF-8 derived C-N-ZnO composites, Energy & Fuels, 2017, 31, 2138-2143.
2. **P. Liang**, C. Zhang, H. Sun, S. Liu, M. Tade, S. Wang*, Photocatalysis of C, N-doped ZnO derived from ZIF-8 for dye degradation and water oxidation, RSC Advances, 2016, 6, 95903-95909.
3. **P. Liang**, C. Zhang, X. Duan, H. Sun, S. Liu, M. Tade, S. Wang*, An insight to metal organic framework derived N-doped graphene towards oxidative degradation of persistent contaminants: Generation of singlet oxygen from peroxymonosulfate, Environmental Science: Nano, 2017, 4, 315-324.
4. **P. Liang**, C. Zhang, X. Duan, H. Sun, S. Liu, M. Tade, S. Wang*, N-doped graphene from metal organic frameworks for catalytic oxidation of p-hydroxylbenzoic acid: N functionality and mechanism, ACS Sustainable Chemistry & Engineering, 2017, 5(3), 2693-2701.
5. Z. Shen, **P. Liang**, S. Wang, L. Liu, S. Liu*, Green synthesis of carbon- and silver-modified hierarchical ZnO with excellent solar light driven photocatalytic performance, ACS Sustainable Chemistry & Engineering, 2015, 3, 1010-1016.
6. C. Wang, J. Kang, **P. Liang**, H. Zhang, H. Sun, M. Tade, S. Wang*, Ferric carbide nanocrystals encapsulated in nitrogen-doped carbon nanotubes as an outstanding environmental catalyst, Environmental Science: Nano, 2017, 4, 170-179.
7. J. Ke, J. Liu, H. Sun, H. Zhang, X. Duan, **P. Liang,** X. Li, M. Tade, S. Liu, S. Wang*, Facile assembly of $Bi_2O_3/Bi_2S_3/MoS_2$ *n-p* heterojunction with layered *n*-Bi_2O_3 and *p*-MoS_2

for enhanced photocatalytic water oxidation and pollutant degradation, Applied Catalysis B: Environmental, 2017, 200, 47-55.

8. J. Liu, J. Ke, D. Li, H. Sun, **P. Liang,** X. Duan, W. Tian, M. Tade, S. Liu, S. Wang*, Oxygen vacancies in shape controlled Cu_2O/reduced graphene oxide/In_2O_3 hybrid for promoted photocatalytic water oxidation and degradation of environmental pollutants, ACS Applied Materials & Interfaces, 2017, 9, 11678−11688.

Table of Contents

Chapter 1: Introduction

1.1. Background

Severe water pollution is bringing about detrimental effects on the human health with the fast development in industrialisation and population expansion. As a result, various strategies for water purification are reported, such as adsorption, photocatalysis, advanced oxidation and so on. The adsorbents like porous carbons with high surface area and rich porosity, as well as the carbon and metal oxide hybrids are explored[1-3]. Meanwhile, zinc oxide, titanium oxide and carbon nitride, as well as their derivatives through modification by carbon or nitrogen, are commonly employed as photocatalysts[4, 5]. Much endeavour is made on narrowing the bandgap between the valence band and conductive band of a photocatalyst, and hindering the recombination of photo-excited electrons and holes, aiming to improve the photocatalytic efficiency. In addition, advanced oxidation process is attracting considerable attention due to the high efficiency, non-selective and complete removal of organic pollutants, releasing in the form of gases like CO_x, NO_x or SO_x. The superoxides like hydrogen peroxide, peroxymonosulfate, persulfate and ozone are supposed to be activated by the catalysts, generating free radicals like hydroxyl and sulfate radicals, which would decompose the pollutants effectively[6, 7]. Moreover, a nonradical process is also proposed to initiate the reaction. As reported by Zhang *et al.*, peroxydisulfate is firstly activated by CuO through outer-sphere interaction instead of chemical bond, and then decomposes the pollutants directly without the formation of free radicals[8]. The metallic catalysts, like metal oxides, metal sulfides and zero-valent metals, have been reported[9, 10]. In order to solve the problems of metal leaching and second contamination, metal-free catalysts, such as graphene, carbon nanotubes and so on, are also investigated[11]. Heteroatom doping into the carbons, like nitrogen, boron, sulfur and phosphide, could decrease the rigidity of the carbons and improve the catalytic effect[12, 13].

The conventional methods to synthesize the catalysts mentioned above, like chemical vapor deposition, arc-discharge and post-synthesis treatment, commonly require critical synthesis conditions. As an alternative, using metal-organic frameworks (MOFs) as the precursors or templates to synthesize the catalysts is supposed to be promising due to their unique structures. MOFs, consisting of metal ions and organic linkers, own tuneable pores and open channels, which allow alien molecules to access and facilitate the formation of porous derivatives *via* facile routes like thermolysis and ultrasonic treatment. MOFs sacrifice themselves into the formation of derivatives, including metal or metal oxide, carbon, and their composites[14-16]. In addition, uniform element distribution is expected while MOFs are being employed as the precursors.

To our best knowledge, few reports have focused on the MOFs-derived catalysts for water treatment. In addition, the mechanisms of catalysis during photocatalytic and advanced oxidation processes are still demanded to be further studied.

1.2. Objectives

This research aims to develop the catalysts by using MOFs as the precursors, in order to remove the pollutants in water, like dyes, phenol, and *p*-hydroxylbenzoic acid. In addition, the mechanisms of photocatalysis and peroxymonosulfate activation by the derivatives are deeply investigated. To this end, the following sections have been included and accomplished in this thesis.

1) Summarizing the recent progress of MOFs-derived materials for energy storage and environmental catalysis;
2) Developing carbon and nitrogen co-doped ZnO as the photocatalysts for dye degradation and water oxidation by the controllable pyrolysis of zeolitic imidazolate framework-8 (ZIF-8).

3) Investigating the influences of MOFs carbonization temperature and calcination time in air on the photocatalytic effect of as-derived C, N-doped ZnO, as well as the mechanism of photocatalysis on the dye degradation.
4) Employing MIL-100 (Fe) and dicyandiamide (DCDA) as the precursors to synthesize nitrogen-doped graphene for peroxymonosulfate activation in the presence of phenol solution and identifying the mechanism of peroxymonosulfate activation by N-graphene.
5) Exploring the catalytic effect of MIL-100 (Fe)-templated N-graphene on degradation of *p*-hydroxylbenzoic acid in the presence of peroxymonosulfate by using DCDA, melamine and urea as the nitrogen precursors, and the mechanism of peroxymonosulfate activation as well as the degradation pathway of *p*-hydroxylbenzoic acid.

1.3. Thesis outline

This thesis consists of seven chapters, of which this chapter is the introduction section. Chapter 2 summarizes the recent progress of MOFs-derived materials related to this thesis. Chapters 3-6 are results and discussions of the experimental studies, which have been published. The conclusions and future perspectives of this thesis is presented in Chapter 7.

Chapter 1: Introduction

This chapter mainly introduces the significance of MOFs-derived materials for water treatment, including the strategies for water treatment related to the thesis, and the advantages of materials synthesis by using MOFs as the precursors. The research objectives and thesis outline are also presented in this chapter.

Chapter 2: Literature Review

This chapter provides a comprehensive review of recent progress in MOFs-derived materials,

including the synthesis strategies of materials and applications in energy storage and environmental catalysis.

Chapter 3: Solar Photocatalytic Water Oxidation and Purification on ZIF-8 Derived C-N-ZnO Composites

In this chapter, carbon and nitrogen modified ZnO photocatalysts were prepared by the controlled thermal decomposition of Zeolitic Imidazolate Framework (ZIF)-8: single-step air combustion, N_2 annealing, and two-step N_2 annealing followed by air calcination. The photocatalytic performances were evaluated in both oxygen evolution and degradation of dye under solar light. It was found that the two-step synthesis delivered better photocatalyst materials than that from one-step process. The co-existence of nitrogen and carbon in ZnO was suggested to be favorable to the enhanced photocatalysis.

Chapter 4: Photocatalysis of C, N-doped ZnO derived from ZIF-8 for dye degradation and water oxidation

In this chapter, carbon and nitrogen co-doped ZnO was synthesized by a simple, two-step pyrolysis of ZIF-8: carbonized in the nitrogen atmosphere, followed by the pyrolysis in air. The carbonization temperature under N_2 and annealing time in air appeared to influence the photocatalytic performances of the hybrids, including photocatalytic dye degradation and oxygen evolution reaction. The mechanistic study showed that hydroxyl radicals and photo-excited electrons contributed to the dye degradation. The carbon-zinc oxide hybrid also demonstrated a great potential for water oxidation because of the more active sites induced by the dopants.

Chapter 5: An insight to metal organic framework derived N-doped graphene towards oxidative degradation of persistent contaminants: Formation mechanism and generation of singlet oxygen from peroxymonosulfate

In this Chapter, nitrogen doped graphene was synthesized by simple pyrolysis of MIL-100 (Fe) and DCDA, showing excellent performances in peroxymonosulfate (PMS) activation in the presence of phenol solution. The formation process of N-graphene derived from MIL-100 (Fe) and DCDA was firstly revealed. In addition, the mechanism of PMS activation by N-doped graphene was also investigated by the electron paramagnetic resonance (EPR) and radical quenching, showing that singlet oxygen ($^1O_2$) was mainly produced and contributed to the catalytic oxidation instead of sulfate and/or hydroxyl radicals. These findings provided new insights into PMS activation by metal-free carboncatalysis.

Chapter 6: N-doped graphene from metal organic frameworks for catalytic oxidation of p-hydroxylbenzoic acid: N functionality and mechanism

In this chapter, MIL-100 (Fe)-templated N-doped graphene samples were synthesized using DCDA, melamine and urea as the nitrogen precursors, showing excellent catalytic oxidation of *p*-hydroxylbenzoic acid *via* peroxymonosulfate activation, attributed to the high surface area and N doping. The mechanistic investigation confirmed that singlet oxygen was generated and dominated the PHBA degradation on N-doped graphene other than hydroxyl/sulfate radicals, due to the N doping. In addition, the degradation pathway of *p*-hydroxylbenzoic acid was also revealed. This study illustrates the formation mechanism of nitrogen functionalities for reactive radicals *via* PMS activation for removal of organic contaminants in water.

Chapter 7: Conclusions and future perspectives

This chapter summarizes the results in this thesis and proposes the future perspectives in this area.

1.4. References

1. W. Guan, R. Wei, T. Hui Ru and L. Ye, *Nanotechnology*, 2017, **28**, 085703.
2. S. Wang, H. Sun, H. M. Ang and M. O. Tadé, *Chem. Eng. J.*, 2013, **226**, 336-347.
3. A. Banerjee, R. Gokhale, S. Bhatnagar, J. Jog, M. Bhardwaj, B. Lefez, B. Hannoyer and S. Ogale, *J. Mater. Chem.*, 2012, **22**, 19694.
4. S. Liu, H. Sun, S. Liu and S. Wang, *Chem. Eng. J.*, 2013, **214**, 298-303.
5. F. X. Qin, S. Y. Jia, Y. Liu, X. Han, H. T. Ren, W. W. Zhang, J. W. Hou and S. H. Wu, *Mater. Lett.*, 2013, **101**, 93-95.
6. G. P. Anipsitakis and D. D. Dionysiou, *Environ. Sci. Technol.*, 2003, **37**, 4790-4797.
7. S. Wang, *Dyes Pigm.*, 2008, **76**, 714-720.
8. T. Zhang, Y. Chen, Y. Wang, J. Le Roux, Y. Yang and J. P. Croue, *Environ. Sci. Technol.*, 2014, **48**, 5868-5875.
9. Y. Wang, H. Sun, X. Duan, H. M. Ang, M. O. Tadé and S. Wang, *Appl. Catal., B-Environ*, 2015, **172-173**, 73-81.
10. E. Saputra, S. Muhammad, H. Sun, A. Patel, P. Shukla, Z. H. Zhu and S. Wang, *Catal. Commun.*, 2012, **26**, 144-148.
11. H. Sun, S. Liu, G. Zhou, H. M. Ang, M. O. Tade and S. Wang, *ACS Appl. Mater. Interfaces*, 2012, **4**, 5466-5471.
12. X. Duan, K. O'Donnell, H. Sun, Y. Wang and S. Wang, *Small*, 2015, DOI: 10.1002/smll.201403715.
13. S. Indrawirawan, H. Q. Sun, X. G. Duan and S. B. Wang, *J. Mater. Chem. A*, 2015, **3**, 3432-3440.
14. X. Yan, X. Li, Z. Yan and S. Komarneni, *Appl. Surf. Sci.*, 2014, **308**, 306-310.
15. L. Zhang, H. B. Wu, S. Madhavi, H. H. Hng and X. W. Lou, *J. Am. Chem. Soc*, 2012, **134**, 17388-17391.

16. A. Aijaz, J. Masa, C. Rosler, W. Xia, P. Weide, A. J. Botz, R. A. Fischer, W. Schuhmann and M. Muhler, *Angew. Chem., Int. Ed. Engl.*, 2016, **55**, 4087-4091.

Chapter 2: Literature Review

2.1. Introduction

Metal-organic frameworks (MOFs), as a class of promising crystalline microporous materials, have attracted extensive research interests [1-5]. They are constituted of inorganic metal ion nodes and organic linkers, and the structures can be tailored according to rational design [6-8]. MOFs own incredible high porosities (up to 90% free volume) and the Langmuir surface areas (beyond 10,000 $m^2 g^{-1}$) [9-11], enabling them to be widely used in storage and separation [12-15], sensing [16-18], drug delivery [19-21], catalysis [22-24] and adsorption [25, 26]. Meanwhile, the versatile structures and properties make MOFs beneficial for potential applications in membrane technology and thin-film devices [27-30]. However, MOFs suffer from some defects such as poor chemical or hydrothermal stability which would impede their potentialities. Incorporation of selected functional materials such as oxides, polyoxometalates, graphene, carbon nanotubes (CNTs) or other nanocarbons into MOFs would be able to overcome the shortages, resulting in enhanced performances for more versatile applications [31-35]. The synthesis strategy, including room temperature synthesis [36], conventional electric heating [37], microwave heating [38], electrochemistry [38], mechanochemistry [39] and ultrasonic methods [40], plays a crucial role in designing various MOFs with specific functions.

The unique structures and expanding kinds of metals and organic components in MOFs, in addition, can prepare themselves readily as starting blocks for a high level materials design. For example, MOFs have been considered to be promising precursors/templates for synthesis of nanoporous carbon and other functional materials, *e.g.* metal/metal oxide (M/MO) and carbon-metal/metal oxide (C-M/MO) hybrids [41-43]. Compared to conventional methods such as soft/hard templating [44, 45], self-assembly [46, 47], arc discharge [48], and chemical vapor deposition (CVD) [49], synthesis using MOFs as the starting materials exhibits the following advantages. At first, porous MOFs own permanent nanoscale pores and open channels for small alien

molecules to access, allowing the elements involved to disperse uniformly. Secondly, MOFs sacrifice themselves to the formation of new materials as the carbon and metal sources, avoiding additional costs from precursors and elimination of templates. At last, conversion of MOFs mainly by pyrolysis is simple and scalable without complex equipment and procedures, holding the potential for industrial-scale production.

In the past, reviews on MOFs, such as introduction, chemistry, water adsorption properties, development, synthesis and applications, have been published[2, 4, 14-16, 50, 51]. Moreover, Zhu *et al.* reviewed the MOF composites synthesized by controllable integration of MOFs and functional materials[35]. Xia *et al.* reviewed the MOFs and their derived nanostructures for electrochemical energy storage and conversion[52]. However, their attention was still mainly paid on MOFs with brief introduction on the derived materials. There is a lack of systematic review on MOFs-derived materials. Furthermore, the development of MOFs-derived materials is fast and a multitude of new research results are reported during the past five years. Herein, we critically reviewed recent advances in the fabrication of nanostructures based on conversion of MOFs, aiming at providing insights into the structure control strategies for MOFs-derived materials. With the unique structure-dependent performances, the prospect and challenges of MOFs-derived materials are presaged. The overlapping with other available reviews is avoided as much as possible.

2.2. MOFs-derived materials

MOFs are considered to be an emerging kind of templates and precursors because of the intriguing topologies and tuneable pore size. The metal species in MOFs are expected to convert into metals oxides by pyrolysis in air and zero-valence metals in inert atmosphere while the organic ligands in MOFs are combusted into gas and released in air. Moreover, carbonization of MOFs under inert atmosphere followed by removal of metal species would produce designed carbon materials. Furthermore, the hybrids of carbon and metals (metal

carbide or nitride) could also be derived from MOFs by a rational design. In this part, we specifically reviewed the novel synthesis of MOFs-derived materials with effective morphology and structural control.

2.2.1. MOFs-derived metals and metal oxides

Nanoporous metals or metal oxides are attracting significant attention because of the wide applications such as energy storage and environmental remediation. The controllable morphology on M/MO like core-shell and hollow shapes is considered to exert great influences on the catalytic effect. MOFs, owning versatile morphologies and tuneable pore sizes, can be used as intriguing templates for a rational design of MOFs-derived M/MO. Synthetic protocols utilizing MOFs as the precursors to fabricate M/MO are explored and reviewed here.

2.2.1.1. M/MO derived from single-metal MOFs

Iron (III) oxides, including α-, β- and γ-Fe_2O_3, are considered to be important transitional-metal materials for catalysis and separation due to its unique catalytic and magnetic properties. As a result, iron-based MOFs have been evolving to produce iron oxides recently. Cubic mesoporous mixed β- and γ-Fe_2O_3 templated from Prussian blue (PB, $Fe_4[Fe(CN)_6]_3$) and spindle-like mesoporous α-Fe_2O_3 from MIL-88-Fe were reported by Hu *et al.* and Xu *et al.,* respectively[53, 54]. Zhang *et al.* reported the formation of Fe_2O_3 microboxes with hierarchically structured shells by conversion of PB[55](Figure 2.1). PB was oxidized into Fe_2O_3 microbox with dense shell at 350 ˚C and further converted into porous Fe_2O_3 shell with the growth of grain at 550 ˚C. When the calcination temperature increased to 650 ˚C, hierarchical microboxes consisting of Fe_2O_3 nanoplatelets formed. Subsequently, their group reported the synthesis of hollow microboxes with multi-shell structure and multi-compositional microboxes by adjusting the reactions between PB template and alkaline substances[56]. Three-dimensional (3D) porous materials are in the spotlight of research due to the high specific surface area (SSA) and accessible pore channels. Kong *et al.* fabricated 3D mesoporous iron oxide (3DMI) by the

interface-mediated growth of PB nanocubes on polyurethane sponge followed by thermal conversion of PB[57]. The 3DMI architectures exhibited a large surface area (117 $m^2 g^{-1}$) and the surface wettability of 3DMI could be tuned by the surface functionalization. Furthermore, 3DMI could be conveniently tailored into various shapes like films and cylinders due to the low density (6 mg cm^{-3}) and non-rigid connection of the nanocube building blocks.

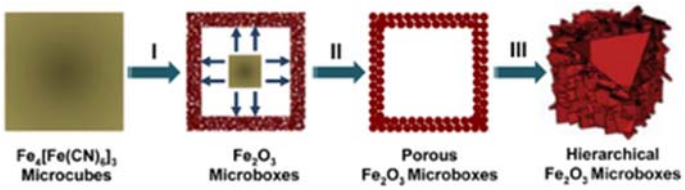

Figure 2.1. Schematic illustration of the formation of hollow Fe_2O_3 microboxes and the evolution of the shell structure with the increasing calcination temperature[55]. Reproduced with permission of the American Chemical Society.

Cobalt oxide (Co_3O_4), as another transition metal oxide, is also essential in various applications and has been extensively studied by many researchers. Zeolitic imidazolate frameworks (ZIFs) are popular porous MOFs, among which ZIF-67 is a typical cobalt-based MOF and was utilized as the precursor of morphology-inherited Co_3O_4 by many researchers. Shao and co-workers synthesized ball-in-dodecahedron and concave-dodecahedron Co_3O_4 *via* one-step calcination in air and two-step calcination in N_2 followed by in air of ZIF-67, respectively[58]. In addition, porous Co_3O_4 hollow dodecahedra derived from ZIF-67 was studied by Wu *et al.via* synthesis by a two-step route as above[59]. Other cobalt-based MOFs were also utilized to synthesize Co_3O_4 with unique morphologies. Su *et al.* firstly reported the synthesis of Co_3O_4 with hexagonal nanorings, nanoplates and nanoparticles derived from Co-MOF *via* chemical method. Co-MOF was synthesized by a hydrothermal method and then treated with tetrapropylammonium or tetramethylammonium hydroxide solutions to form $Co(OH)_2$, followed by calcination in air[60].

Copper oxide is well known due to the earth abundant, eco-friendly and low-cost properties, and thus widely used as catalysts. MOFs-derived CuO or Cu_2O nanostructures with various morphologies are reported recently for catalytic applications. The pyramidal-like pure CuO nanostructure templated by Cu-MOF (MOF-199) was synthesized by Banerjee *et al.* through simple pyrolysis at 550°C for 2 h in air[61]. Later, Wu *et al.* reported the synthesis of hollow CuO with a well-defined octahedral structure by two-step pyrolysis of Cu-BTC MOF[62]. CuO/Cu_2O hollow polyhedrons with porous and rough shells were also synthesized by one-step pyrolysis of Cu-BTC MOF at 350 °C in air[63]. Besides the morphology-inherited copper oxide mentioned above, Zhan *et al.* successfully synthesized two-dimensional (2D) Cu-based MOFs (nanofibers, nanorods and nanosheets) by utilization of a solid-state metal ion source and the growth-blocking agents. As a result, CuO and CuO/Cu_2O nanocomposites derived from 2D Cu-MOF with the platelet morphology could be synthesized by controlling pyrolysis conditions under static air [64].

Metal oxide particles are inclined to aggregate together during the calcination, inducing the deterioration of catalytic effect and limitation in other applications. In order to solve this problem, controllable synthetic protocols have been proposed. Kim *et al.* reported nanoporous magnesia (MgO) and ceria (CeO_2) derived from an aliphatic ligand-based MOF which is thermally labile[42]. The aliphatic ligands would be decomposed into organic moieties upon thermolysis and confined as vesicles which would evaporate, generating highly porous nanostructures and preventing the aggregation of metal oxide particles. Cao *et al.* firstly reported mini-hollow polyhedron Mn_2O_3 by annealing Mn-MOF at 750 °C for 4 h with a temperature ramp of 5 °C/min [65]. The cycling performance of the mini-hollow structure as the anode of lithium ion batteries outperformed that of bulk and large-hollow structures due to the nanosize effect (Figure 2.2). The small interior cavity provided a proper room for the inward volume expansion during electrochemical reactions, inducing a homogeneous dispersion of the

rearranged nanoparticles. The bulk sample lacked the room to alleviate the tension resulting from the inward volume expansion, and the non-equilibrium status would induce the nonuniform dispersion of particles. Hollow reconstructed hierarchical nanostructure formed after the first cycle, and then collapsed finally with the expansion of nanoparticles near the inner cavity due to the weak interaction with each other.

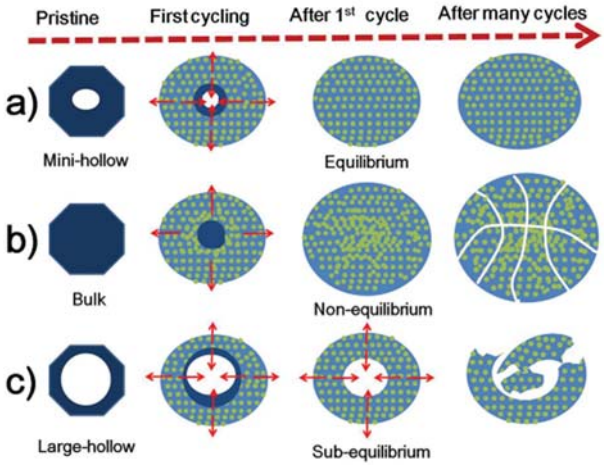

Figure 2.2. Schematic illustration of the structure evolutions of (a) mini-hollow, (b) bulk, and (c) large-hollow polyhedron Mn_2O_3 electrodes with cycling[65]. Acknowledgement to Royal Society of Chemistry.

2.2.1.2. M/MO derived from multi-metallic MOFs

Inspired by the synergistic effect and homogeneous dispersion of multi-metal oxide composites, scientists have explored multi-metallic MOFs as the precursors to synthesize metal oxide composites. To preserve the homogeneity of metal ions and shapes of MOFs, they made efforts to find out the well-defined MOFs with low residual stresses.

In 2014, Wu *et al.* firstly reported the synthesis of heterobimetallic ZIFs (Zn-Co-ZIFs) with different Zn/Co molar ratios by co-precipitation of Zn and Co ions in the presence of 2-methylimidazolate[66]. Meanwhile, highly symmetric porous anisotropic $Zn_xCo_{3-x}O_4$ hollow polyhedra were produced by two-step thermolysis of the ZIFs (Figure 2.3a). X-ray diffraction

(XRD) and selected area electron diffraction (SAED) results confirmed that the zinc atoms were perfectly incorporated into the Co_3O_4 lattice, forming polycrystalline texture of $Zn_xCo_{3-x}O_4$. The as-synthesized $Zn_xCo_{3-x}O_4$ inherited the size and rhombic dodecahedral shape of the Zn-Co-ZIFs, and the elemental mapping ensured the uniform distribution of the elements Zn, Co and O. Core-shell porous ZnO@Co_3O_4 was firstly synthesized by a two-step thermal conversion of core-shell ZIF-8@ZIF-67[67]. The porous structure of the composite and co-catalytic effect of Co_3O_4 resulted in the superior photocatalytic reaction for CO_2 photoreduction. Meanwhile, Co_3O_4 would protect ZnO from photocorrosion, inducing an excellent stability. Hierarchical nanosheet structure exposes more active sites compared to bulk architectures. Xu *et al.* synthesized Zn-Co-MOF by co-precipitation of zinc and cobalt ions in the presence of terephthalic acid and subsequently fabricated 3D hierarchical porous ZnO/$ZnCo_2O_4$ (ZZCO) nanosheets by one-step thermolysis of as-synthesized Zn-Co-MOF[68]. The nanosheets were composed of interconnected nanoparticles and pores between them, which was positive to the electrochemical performance as the anode material in lithium ion batteries.

The Prussian Blue Analogues (PBA) $M_3^{II}[M^{III}(CN)_6]_2 \bullet nH_2O$ are composed of octahedral $M^{III}(CN)_6^{3-}$ complexes which are bridged into a cubic lattice by M^{2+} ions. PBA have been selected as the precursors for hetero-metal oxides *via* thermal oxidation. Porous $Mn_xCo_{3-x}O_4$, ZnO/Co_3O_4, $ZnFe_{2-x}O_4$-ZnO and Fe_2O_3@$NiCo_2O_4$ nanocomposites were synthesized by directly calcination of $Mn_3[Co(CN)_6]_2$ nanocubes, $Zn_3[Co(CN)_6]_2$ nanospheres, $K_2Zn_3[Fe(CN)_6]_2$ microplates and core-shell $Co_3[Fe(CN)_6]_2$@ $Ni_3[Co(CN)_6]_2$ nanocubes, respectively[69-72]. PBA materials with high surface-area-to-volume ratios as the precursors are expected to overtake conventional MOFs. Han *et al.* firstly prepared Ni-Co PBA nanocages with pyramid-like walls by etching Ni-Co PBA cubes with ammonia[73] (Figure 2.3b). As the corners of PBA cubes have a higher surface energy than flat planes and the interior cores are defect-rich compared with the exterior shells, etching occurs preferentially on the corners and

then along the body diagonal direction of the cubes, forming interior voids with six pyramid-like walls. After annealing in air, the Ni-Co mixed oxides retain the nanocage structure with rougher surfaces, showing better electrocatalytic performance on OER with an over potential of 0.38V compared with hollow urchin-like and nanoneedle $NiCo_2O_4$[74, 75].

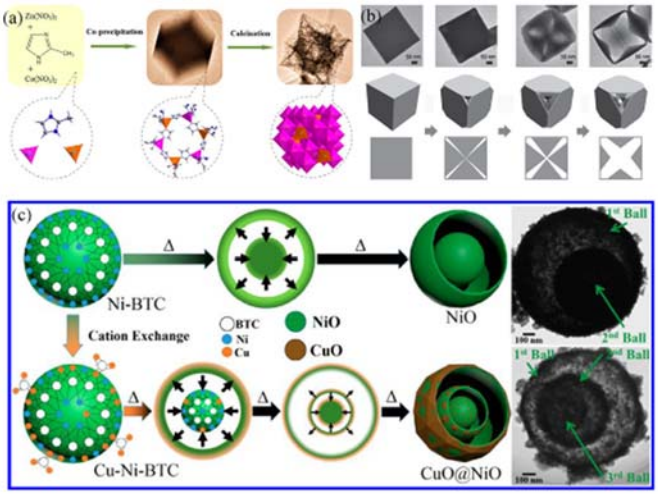

Figure 2.3. Schematic illustrations for (a) the preparation of bimetallic ZIFs and their conversion to spinel $Zn_xCo_{3-x}O_4$ hollow polyhedra[66], reproduced with permission of the American Chemical Society; (b) the formation process of the Ni-Co PBA cages[73], reproduced with permission from Wiley-VCH Verlag GmbH & Co. KGaA; and (c) the cationic exchange process of MOF and its conversion to multi-layer hollow structure[76]. Reproduced with permission of the American Chemical Society.

Guo *et al.* synthesized multi-shell ball-in-ball CuO@NiO microsphere by post-annealing of Cu-Ni-BTC MOF [76]. A multi-layer yolk-shell structure was formed due to the temperature gradient from the shell to the core of MOF during pyrolysis in air (Figure 2.3c): the exterior surface would be decomposed prior to the core of MOF, as a result, the adhesion force between the surface shell and inner core with the contraction force by decomposition of the core was generated and separated the core and shell layers. The interior Cu-Ni-BTC ball would undergo the similar process, inducing the secondary shell and core layer. Three-layer hollow CuO@NiO

microsphere formed eventually and more CuO on the shell while more NiO in the core due to controlled cationic exchange reactions.

2.2.1.3. M/MO derived from MOFs and additives

Co-precipitating heterometallic ions in the presence of organic linkers incline to induce the collapse of as-synthesized multimetallic MOFs due to the residual stress. In order to obtain more abundant M/MO composites, and optimize the structures and compositions of the derivatives, many researchers chose to introduce other precursors into the MOFs, generating various metal-based composites.

Hu *et al.* synthesized starfish-shaped porous nanocomposite for the first time using Co_3O_4 nanocages and Fe^{III}-MOF-5 as precursors, consisting of "starfish head" Co_3O_4 and "starfish arm" $ZnFe_2O_4$ nanotubes[77]. The formation mechanism of starfish-shape structure and transmission electron microscope (TEM) images were shown in Figure 2.4a-b: Co_3O_4 cages derived from Co-PBA were utilized as the seed for the nucleation of Fe^{III}-MOF-5 in one direction outward. In order to reduce the surface energy, Fe^{III}-MOF-5 grew into the nanotube shapes. As a result, $Co_3O_4/ZnFe_2O_4$ composites obtained by pyrolysis of Co_3O_4 nanocages/ Fe^{III}-MOF-5 appeared to be in a starfish hollow shape.

Hu *et al.* reported a novel method for synthesis of $Co_3O_4/NiCo_2O_4$ double-shelled nanocages (DSNCs), as shown in Figure 2.4c-d. ZIF-67 was soaked in the ethanol solution of $Ni(NO_3)_2$ for 30 min at room temperature. Then the proton was generated due to the hydrolysis of Ni^{2+} ions attacked ZIF-67 and part of Co^{2+} (some were oxidized into Co^{3+}) was released, which would co-precipitate with Ni^{2+} to form Ni-Co layered double hydroxides (LDH) shells. $Co_3O_4/NiCo_2O_4$ DSNCs formed after the thermal oxidation of yolk-shell ZIF-67@Ni-Co LDH[78]. The gap in the yolk-shell structure would alleviate the strain between cores and shells generated during pyrolysis, making it possible to form multi-shelled hollow structure with

different shell compositions. The longer soaking time and higher temperature would induce the total dissolution of ZIF-67, generating hollow NiCo-LDH and porous $NiCo_2O_4$/NiO hollow dodecahedra after thermal treatment, as reported by Sun *et al.*[79]. The synthesis of hollow ZnO/$ZnCo_2O_4$ core-shell nanocages was also reported using the similar procedures, except that the precursor was ZIF-8/Co-Zn core-shell hydroxide which was fabricated by soaking ZIF-8 in ethanol solution containing $Co(NO_3)_2$ at room temperature[80].

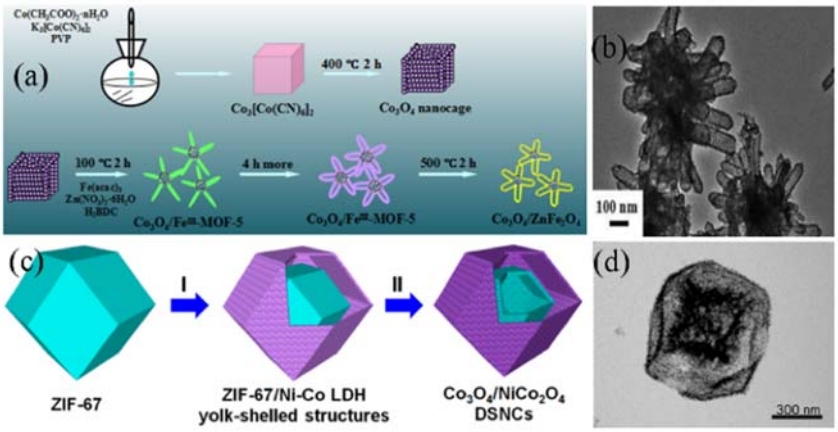

Figure 2.4. (a) Synthesis procedure of the starfish-shaped porous $Co_3O_4/ZnFe_2O_4$ nanocomposite[77]; (b) TEM image of $Co_3O_4/ZnFe_2O_4$ nanocomposite[77], reproduced with permission of the American Chemical Society; (c) Schematic illustration of the formation process of $Co_3O_4/NiCo_2O_4$ DSNCs[78]; and (d) TEM image of $Co_3O_4/NiCo_2O_4$ DSNCs[78]. Reproduced with permission of the American Chemical Society.

The multi-compositionally yolk-shell structures were also investigated. Wu *et al.* synthesized multi-faceted hollow nanocomposites, *e.g.* Co_3O_4/SiO_2, Co_3O_4/TiO_2, ZnO/SiO_2 and ZnO/TiO_2, by thermolysis-induced transformation of ZIF-67 or ZIF-8 in air which were coated with a SiO_2 or TiO_2 shell by a sol-gel method initially[81]. The hollow oxide composites could combine the merits of their constituents, and thus exhibit inspiring physiochemical properties.

Heteroatom doping like N, P and S in the metal lattices is a promising method to tune the

inherent electronic and surface structures of the host materials in order to improve the activities. Yu *et al.* successfully synthesized CoS_2 nanobubble hollow prisms derived from ZIF-67 hollow prisms by a sulfidation reaction with thioacetamide[82]. Homobimetallic sulphides, like hollow $M_xCo_{3-x}S_4$ (M= Zn, Ni, Cu) polyhedra, were synthesized by solvothermal sulfidation of bimetallic MOFs, followed by annealing under N_2 at 350 °C to remove oxygen groups[83]. The formation of bimetallic cobalt sulfides hollow structure was attributed to the larger ionic radius of S^{2-} ions (184 pm) than that of metal ions (72-74 pm), leading to the slower inward diffusion of S^{2-} ions compared with the outward diffusion of metal ions. Therefore, the inner organic clusters dissolved and the metal ions moved outward to react with S^{2-} ions on the outer surface, leading to the hollow voids inside the shell. In 2016, Bendi *et al.* fabricated Ni-MOF-derived hollow, porous nickel phosphate ($Ni_xP_yO_z$) *via* substitution of benzene-1,3,5-tricarboxylic acid (BTC) ligands in the MOF with the phosphoric ions[84].

In order to immobilize the guest species totally and homogeneously into the pores of MOFs, Wang *et al.* immobilized ammonium meta-tungstate into UiO-66 by a double-solvent technology (utilization of water and hexane), followed by thermal oxidation to obtain grape clusters-like tungstated zirconia (WZ) particles[85]. The water (hydrophilic) would carry ammonium meta-tungstate into the hydrophilic pores of UiO-66 with impulsion of capillary force and hydrophilic interaction, while hexane (hydrophobic) facilitated the suspension of UiO-66.

As the organic linker of 2-methylimidazole could coordinate with Ce ions on the surface, Wang *et al.* successfully synthesized CeO_2 nanowires self-inserted into ZIF-67 nanostructures[86]. After annealing at 400 °C for 1 h, the one-dimensional CeO_2 inserted into porous Co_3O_4 frameworks were produced. The self-inserted structure and surface nucleation of ZIF-67 on CeO_2 nanowires induced the strong combination of CeO_2 and Co_3O_4. The synthetic strategy can also be applied in preparation of CeO_2 nanowires inserted into $ZnCo_2O_4$

and $NiCo_2O_4$ hybrids.

2.2.2. MOFs-derived carbon

Carbon materials, including amorphous carbon, graphene, carbon nanotubes and so on, were attracting tremendous interests in the fields of adsorption, catalysis and electrochemistry. Porous MOFs possess enriched nanoscale pores and open channels, which are considered to be ideal precursors or templates for the synthesis of carbon materials.

2.2.2.1. Amorphous carbon

The porous amorphous carbons with large specific surface areas and large pore volumes have been synthesized using zinc or aluminium-based MOFs as the precursors during the past few years.

MOF-5, as one of the most representatives of MOFs, could be prepared rapidly at room temperature. It has then been decomposed to prepare porous carbon by many researchers. No corrupting and washing process is needed while the carbonization temperature is above 900 °C because the zinc cation in the MOF-5 could be reduced into zero-valent zinc and vaporized away. In addition, other carbon sources could also be impregnated in or covered outside the pores of MOF-5. Hu *et al.* prepared porous carbon by using MOF-5 as both a template and carbon source while carbon tetrachloride and ethylenediamine were employed as the additional carbon sources[87]. After carbonization at 900 °C under N_2 followed by activation with KOH, the surface area of as-synthesized carbon reached 2222 $m^2 g^{-1}$ and the pore volume was 1.14 $cm^3 g^{-1}$. Liu *et al.* introduced furfuryl alcohol (FA) into MOF-5 as the additional carbon source, treated by carbonization under argon and acid washing without activation of KOH[41]. The surface area of the obtained carbon reached between 1140 and 3040 $m^2 g^{-1}$ at carbonization temperatures from 530 to 1000˚C.

Zeolitic imidazolate framework-8 (ZIF-8), which could be prepared in a facile way at room

temperature, was selected as another Zn-based MOF for the synthesis of porous carbon. In 2012, commercial ZIF-8 was directly carbonized under N_2 at various temperatures (600~1000 ˚C) followed by HF acid washing and a surface area of 1110 $m^2 g^{-1}$ was obtained at 1000 ˚C, as reported by Chaikittisilp *et al.*[88]. Zhong *et al.* introduced additional carbon and nitrogen sources including melamine, urea, xylitol and sucrose into ZIF-8 to produce nitrogen-doped porous carbons[89]. The results indicated that sucrose could reduce the nitrogen loss during carbonization while the addition of urea induced the great specific surface area of 2159 $m^2 g^{-1}$.

Besides improving the surface area and pore volume of the porous carbon, hierarchical porosity construction is also an important issue in consideration of improving the performances effectively. Ding *et al.* proposed the synthesis of ZIF-8@ZnO core-shell nanostructure using ZnO sheets as the template and Zn^{2+} source[90]. The 2D carbon nanosheets derived from ZIF-8@ZnO exhibited a high surface area of 1228 $m^2 g^{-1}$ and hierarchical porosity with high ratio of meso-/macropore volume to micropore volume (2.46). Zhao *et al.* introduced a solvent-assistant-linker-exchange method to synthesize a new type of ZIF-8 (immersing the typical ZIF-8 in the 1H-1,2,3-triazole methanol solution) and obtained a hierarchically porous carbon with larger surface area and pore volume (1257 $m^2 g^{-1}$ and 4.4 $cm^3 g^{-1}$, respectively) in comparison with typical ZIF-8-derived carbon (811 $m^2 g^{-1}$ and 0.4 $cm^3 g^{-1}$, respectively)[91]. Lai *et al.* further systematically studied the control strategy and mechanism on porosity of ZIF-8-derived nitrogen-enriched meso-microporous hierarchical carbon (NEMC) by adding polyvinyl pyrrolidone (PVP) [92]. As shown in Figure 2.5, under low pyrolysis temperature, ZIF-8 was encapsulated by PVP from the coordination effect between Zn^{2+} in ZIF-8 and C=O in PVP. At 500 °C, PVP was decomposed into mesopore-dominated carbon and still confined the ZIF-8 crystal polyhedrons by strong cohesive interface interaction. With the increase of pyrolysis temperature, ZIF-8 shrank from center to outside due to ZIF-8-derived carbon and kept adhering to the PVP-derived carbon shell. As a result, mesoporous structure was formed

with some ZIF-8-derived micropores surviving in the shell. Similarly, Lee *et al.* reported the growth of ZIF-8 on carboxylic acid-terminated polystyrene surface to form the core-shell structure[93]. After pyrolysis under N_2, polystyrene vanished and hollow porous carbon with a surface area of 1724 $m^2 g^{-1}$ could be derived from the core-shell polystyrene@ZIF-8.

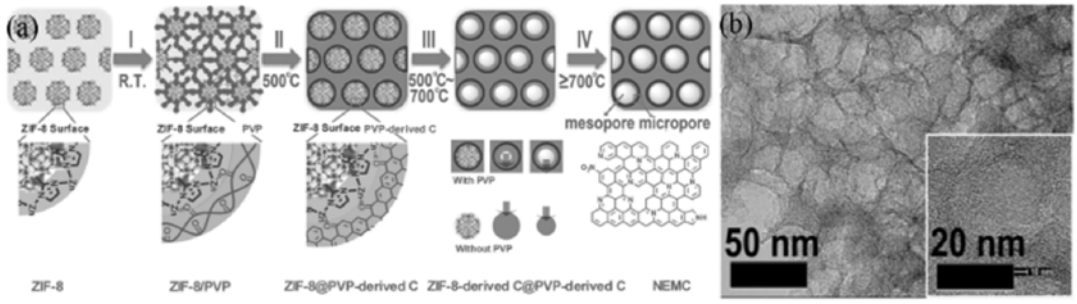

Figure 2.5. (a) The formation mechanism of nitrogen-doped carbon from ZIF-8 with a meso-microporous hierarchical structure; and (b) TEM image of NEMC[92]. Reproduced with permission from Wiley-VCH Verlag GmbH & Co. KGaA.

MIL-100 (Al), an aluminium-based zeolite-type MOF, was chosen as the precursor and template for synthesis of shape-controlled porous carbon because of the 3D mesoporous structure, high stability, large surface area and micro-sized crystal. Aijaz *et al.* reported the thermal transformation of MIL-100 (Al) followed by HF washing towards hierarchical hollow octahedral carbon cages, exhibiting a surface area of 1711 $m^2 g^{-1}$[94]. Sun and co-workers firstly synthesized porous carbon materials by a double-template method: Al-MIL-101-NH_2 as one template and copper ions (Cu^{2+}) as the second template[95]. The hydrophilic inner pores of Al-MIL-101-NH_2 facilitated the incorporation of Cu^{2+} into the MOF. The *in situ* generated Cu nanoparticles from Cu^{2+} during carbonization were acting as the pore-forming agent and Cu^{2+} could also tune the crystal size of Al_2O_3, generating the hierarchical porous carbon with a surface area of 2116 $m^2 g^{-1}$.

2.2.2.2. Graphitic carbon and carbon nanotubes

Graphene is widely used in electrochemical and catalytic applications due to its large surface

area, good electrical conductivity, excellent flexibility and chemical stability. Nowadays, graphene-based materials derived from graphite achieve mass production at low cost. However, the graphene sheets synthesized *via* such a route apt to agglomerate together, inducing small surface areas. Therefore, exploring graphitic carbon with a large surface area and superb performances is highly needed. MOFs have attracted more and more attention to prepare graphitic carbons as the excellent precursors.

As cobalt could catalyze the graphitization of carbon, ZIF-67 is an ideal candidate to be a precursor for graphene synthesis. Yamauchi *et al.* prepared highly graphitized nanoporous carbon by thermal conversion of ZIF-67 followed by acid etching, showing a surface area of 943 m^2 g^{-1} and average pore volume of 0.84 cm^3 g^{-1} [96]. Later, their group synthesized nanoporous hybrid carbon consisting of nitrogen-doped amorphous carbon (NC, core) and graphitic carbon (GC, shell) (NC@GC) *via* thermal conversion of core-shell ZIF-8@ZIF-67[97].

As shown in Figure 2.6, the core-shell NC@GC could combine the merits of NC and GC, inducing a large surface area, a high nitrogen content, high crystallinity, good conductivity and stability. The surface area of 1276 m^2 g^{-1} and N content of 10.6 at.% could be obtained on NC@GC by adjusting the molar ratio of zinc and cobalt ions.

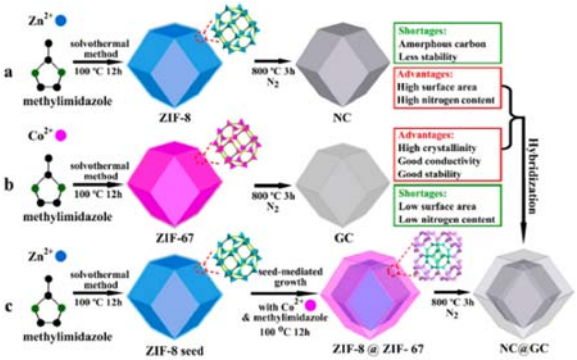

Figure 2.6. Synthetic scheme for the preparation of (a) ZIF-8 and NC, (b) ZIF-67 and GC, and (c) core-shell ZIF-8@ZIF-67 and NC@GC[97]. Reproduced with permission of the American Chemical Society.

Carbon nanotubes derived from MOFs have also been investigated. Su *et al.* successfully synthesized nitrogen-doped carbon nanotubes using Zn-Fe-ZIF and dicyandiamide (DCDA) as the precursors at a low temperature, demonstrating that DCDA facilitated the formation of carbon nanotubes[98]. Li *et al.* introduced DCDA and iron acetate into cage-containing Co-MOF with a great void volume and produced onion-like carbon, N-doped carbon tube and N-doped graphene/graphene-tube nanocomposites at different carbonization temperatures[99]. Xia *et al.* synthesized N-doped carbon nanotube frameworks (NCNTFs) by pyrolysis of ZIF-67 under argon/H_2 mixed atmosphere[100]. The as-synthesized NCNTFs inherited well the morphology of the initial ZIF-67 particles, and the presence of H_2 was responsible for the formation of carbon nanotubes instead of inert gas.

As most of the MOFs do not contain the catalytic metal ions or clusters (such as Fe, Mn, Ni and Co) for graphitization of carbon, post-addition of catalytic metals is demanding. Zhang *et al.* synthesized the hybrids of nitrogen-doped graphitic porous carbon and carbon nanotube (NGPC/NCNT) derived from MOF-5 by post-addition of Ni^{2+} and urea[101]. The specific surface area of NGPC/NCNT could reach 1053 $m^2\ g^{-1}$, comparable to that of nitrogen-doped amorphous carbon derived directly from MOF-5 (1157 $m^2\ g^{-1}$). In addition, incorporation of graphene oxide (GO) is also an alternative because GO would be reduced into graphene after carbonization. The coating of ZIF-8 on graphene oxide (GO) would be uniform with the addition of poly(vinylpyrrolidone) (PVP) as reported by Zhong *et al.*[102]. The surface area of as-synthesized nanoporous carbon by carbonization of ZIF-8/GO could reach 911 $m^2\ g^{-1}$. Thomas *et al.* fabricated the nanoporous carbon containing 6.12 at.% nitrogen with a surface area of 502 $m^2\ g^{-1}$, using ZIF-8 wrapped by GO as the precursor[103]. It demonstrated that the core-shell structure of ZIF-8@GO could reduce the nitrogen loss during pyrolysis under inert atmosphere.

2.2.2.3. Other carbon materials

During the carbonization process, MOFs are inclined to convert into bulk carbon materials after the high temperature pyrolysis, reducing the active surface areas. Therefore, rational design of the shape and size of the MOFs derived materials is essential, in order to improve the performances. Tuning the shapes of MOFs using templates or modulators have been explored, and thus the architectures of as-derived carbon materials are also altered.

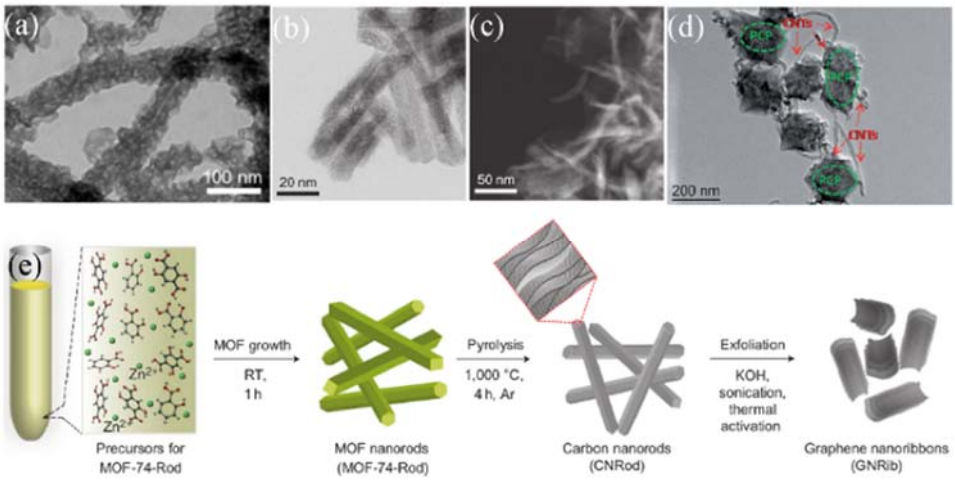

Figure 2.7. TEM images of (a) carbon nanowires[104], reproduced with permission of the American Chemical Society; (b) carbon nanorods[105]; (c) graphene nanoribbons[105]; (d) CNT/PCP[106], acknowledgement to Royal Society of Chemistry; and (e) Scheme of synthesis of MOF-74-Rod, carbon nanorods and graphene nanoribbons[105]. Reproduced with permission of the nature publishing group.

Zhang *et al.* synthesized ZIF-8 nanowires by introducing ultrathin tellurium nanowires as templates and obtained porous carbon nanowires by pyrolysis under N_2 (Figure 2.7a). The as-obtained carbon nanowires showed a larger surface area (2270 $m^2 g^{-1}$) than carbon derived directly from ZIF-8 (1481 $m^2 g^{-1}$)[104]. Pachfule *et al.* synthesized successfully rod-shaped MOF-74 by the addition of salicylic acid as a shape modulator[105]. As shown in Figure 2.7e, the one-dimensional carbon nanorods (Figure 2.7b) were produced by a morphology-preserved thermal

transformation process, exhibiting a surface area of 1559 $m^2 g^{-1}$. After KOH treatment under ultrasound followed by thermal activation at 800 °C, two-dimensional graphene nanoribbons (Figure 2.7c) were generated with a surface area of 1492 $m^2 g^{-1}$. Xu *et al.* fabricated porous carbon nanotube/porous carbon polyhedral (CNT/PCP) hybrid by pyrolysis of CNT inserting ZIF-8 (Figure 2.7d). Due to the insertion of CNT into PCP, the surface area of the hybrid (898 $m^2 g^{-1}$) was higher than that of PCP derived directly from ZIF-8 (825 $m^2 g^{-1}$).

2.2.3. MOFs-derived carbon-metal/metal oxide hybrids

Carbon-metal or metal oxide (C-M/MO) hybrids are of great importance in the fields of electrochemistry and environmental application. Conventionally, the hybrids can be synthesized by direct nucleation, growth, and anchoring of metal oxides on the carbon atoms. MOFs are becoming popular as the precursors or templates for preparation of the composites recently.

As metal-based nanoparticles are inclined to aggregate together during the conversion of MOFs, preparation of C-M/MO hybrids with highly dispersed nanoparticles is needed to be improved. Yang and co-workers developed a facile one-step thermal-pyrolysis route to fabricate porous carbon-coated ZnO quantum dots (~3.5 nm) without aggregation and intrinsic defects, using IRMOF-1 as the template and single precursor[107]. IRMOF-3 could coordinate with metal precursors (i.e., Ru, W, V and Ti) due to the amine group, resulting homogeneous distribution of metal with small particle sizes in the nanoporous carbon (M/NC) after carbonization and carbothermal reduction[108]. The M/NC exhibited a large surface area (900-2000 $m^2 g^{-1}$) and the carbide phase metals formed at a lower temperature (1000 °C). Chen *et al.* found that introduction of water steam during carbonization of ZIF-8 facilitated the homogeneous distribution of ZnO nanoparticles and a larger surface area in comparison to pyrolysis under dry argon atmosphere[109]. Santos *et al.* impregnated Basolite F300 (Fe-based MOF) with furfuryl alcohol (FA) by incipient wetness impregnation, and obtained the catalysts

(Fe@C) after a series of polymerization and carbonization under N_2 atmosphere [110]. Fe@C presented a high content of Fe_3C and capsulation of the highly dispersed metal phase by carbon. You *et al.* synthesized nanoporous Co-NC hybrid by using bimetal-organic framework (Zn-Co-ZIF) as the precursor *via* carbonization at 900°C[111]. The existence of Zn would suppress the sintering of Co during pyrolysis by spatial isolation and the porosity was tuned by the evaporation of Zn. It was reported that coating catalysts with an oxide shell, such as silica, could prevent aggregation during high-temperature pyrolysis[112]. Shang *et al.* coated mesoporous-silica ($mSiO_2$) on ZnCo-ZIFs and fabricated hierarchically porous Co, N-doped carbon nanoframework (Co, N-CNF) after the subsequent pyrolysis and acid washing (Figure 2.8a-d)[113]. The specific surface area and pore volume of Co, N-CNF (1170 $m^2 g^{-1}$and 1.52 $m^3 g^{-1}$) were much higher than those of the catalyst derived from ZnCo-ZIFs without a silica shell (540 $m^2 g^{-1}$and 0.46 $m^3 g^{-1}$), and exhibited rich porosity, indicating that the SiO_2 shell successfully prevented the agglomeration of nanoparticles during thermal treatment. Meanwhile, their group successfully synthesized monodisperse carbon nanospheres containing porphyrin-like zinc centers by pyrolysis of ZIF-8 coated with SiO_2 followed by removal of SiO_2 with NaOH etching[114]. Yang *et al.* tackled the problems of bimetallic phase separation and aggregation during high-temperature treatment[115]. Platinum nanoparticles were loaded on ZIF-8 followed by coating with tannic acid. The second metallic particles like cobalt were then incorporated into the acid layer *via* cation exchange. During pyrolysis, Pt nanoparticles would firmly locate the metallic particles in the walls of final capsules and thus, prevent the aggregation of nanoparticles (Figure 2.8e-i). Wang *et al.* utilized Fe^{2+} as the iron source during synthesis of Fe-doped ZIF-8[116]. As Fe^{2+} and Zn^{2+} have similar ion radius, the participation of Fe^{2+} would not cause structure distortion, inducing the homogeneous distribution of Fe in Fe-doped ZIF-8 which further facilitated the well-distribution of Fe in the Fe-NC after conversion of the MOF under O_2-free environment.

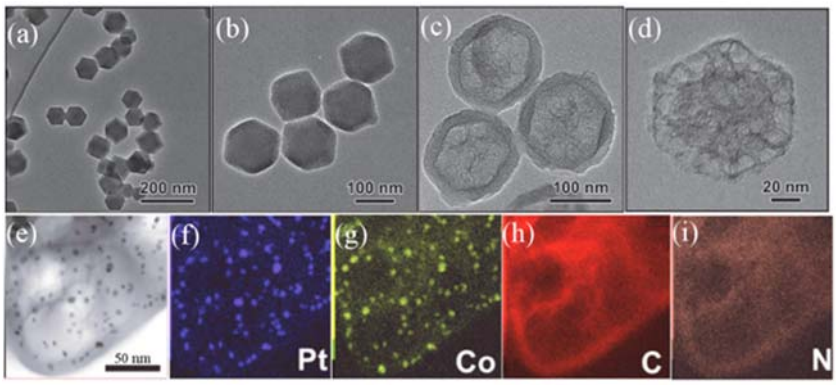

Figure 2.8. TEM images of (a) ZnCo-ZIFs[113]; (b) ZnCo-ZIFs@mSiO$_2$[113]; (c) Co, N-CNF@mSiO$_2$[113]; (d) Co, N-CNF[113]; reproduced with permission from Wiley-VCH Verlag GmbH & Co. KGaA; (e) Scanning TEM (STEM) image of PtCo@NC[115]; and (f-i) Elemental mapping of PtCo@NC[115]. Reproduced with permission of the American Chemical Society.

Unlike the oxygen-containing MOFs which could be converted into corresponding carbon-metal oxide (C-MO) hybrids through one-step calcination under inert atmosphere, the conversion of oxygen-free MOFs into C-MO hybrids typically requires two steps. Nanoporous carbon-cobalt-oxide hybrids derived from ZIF-9 were synthesized *via* a two-step method (pyrolysis under N_2 and subsequently in air), as reported by Chaikittisilp *et al.* [117]. Metallic cobalt embedded in carbon would be formed if pyrolysis was conducted under N_2 without any air. Metallic cobalt would convert into cobalt oxide such as Co_3O_4 and CoO after calcination in air. In order to avoid the loss of carbon and heteroatoms during the calcination in air, Wang *et al* developed a one-step calcination method to synthesize pure phase of CoO in carbon matrix[118]. They employed ZIF-67 as the precursor and subjected it to calcination under a flow of mixed atmosphere consisting of argon and dry air. It was investigated that the calcination temperature, holding time and air fraction would influence the valence of cobalt. CoO and carbon hybrid was synthesized by pyrolysis at 530 ˚C for 20 min in the atmosphere of 1.5 mL of air and 48.5 mL of argon.

In order to improve the graphitic degree of the derived carbon, metal or metal oxide

embedded in carbon nanotubes using MOFs as the precursors was also studied. Aijaz *et al.* fabricated core-shell Co@Co_3O_4 embedded in N-doped carbon nanotube-grafted carbon polyhedra (Co@Co_3O_4/CNT-NC) derived from ZIF-67 by carbonization under H_2 and a subsequent mild calcination in O_2 (Figure 2.9) [119]. It was found that H_2 atmosphere facilitated the formation of carbon nanotube to improve the graphitic degree. In addition, Li *et al* synthesized Co/Co_3ZnC dodecahedron with N-doped carbon overlayer and rooted CNTs derived from CoZn-ZIFs *via* pyrolysis under acetylene (5%) and N_2 (95%) gas mixture[120]. Compared to pure N_2, acetylene gas could be used as the carbon source in the formation of CNTs by the catalysis of Co metal. As H_2 and acetylene are risky due to combustion, Ahn *et al.* introduced a facile method to synthesize cobalt and N-doped carbon (Co-NC) microtubular structure by using cobalt oxalate microtubes as the cobalt precursor of ZIF-67 and template for the 1D tubular structure[121]. The as-obtained carbon microtubes were composed of hollow spheres and carbon nanotubes.

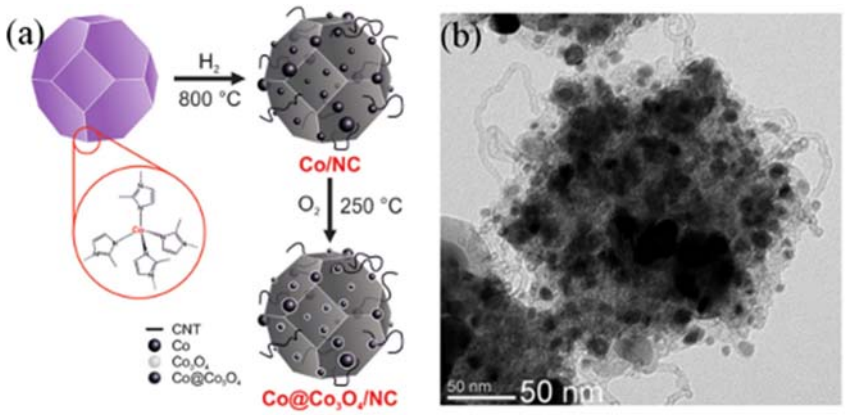

Figure 2.9. (a) The formation of Co@Co_3O_4/CNT-NC *via* reductive carbonization of ZIF-67; and (b) TEM image of Co@Co_3O_4/CNT-NC[119]. Reproduced with permission from Wiley-VCH Verlag GmbH & Co. KGaA.

The incorporation of reduced graphene oxide (RGO) in the C-M/MO hybrids is expected to improve the catalytic and electrochemical efficiencies of the systems due to the improved

conductivity. Two routes have been explored for the addition of RGO. One is growth of the MOFs directly on the GO followed by post treatment. Cao *et al.* proposed the direct growth of ZIF-8 and MIL-88-Fe on three-dimensional graphene networks (3DGN)[122]. After a two-step pyrolysis, ZnO/3DGN and Fe_2O_3/3DGN composites with good mechanical properties would be derived from the as-synthesized MOFs/3DGN (Figure 2.10a-e). Similarly, graphene-supported Co_3O_4, Fe_3O_4 and Mn_2O_3 nanocrystallites derived from the growth of MOFs on GO nanosheets were also obtained [123-125]. Hou *et al.* fabricated the porous N-doped Fe/Fe_3C@C/RGO derived from PB/GO composites through one-step carbonization treatment[126]. In this study, PB was firstly synthesized and then mixed with GO at 80˚C, followed by a thermal treatment. The Fe/Fe_3C was coated with carbon shells and then further covered by RGO sheets. In addition, RGO was considered as a bridge to connect the Fe/Fe_3C@C nanoboxes. The other route towards the addition of RGO is calcination of MOFs at first and then wrapping RGO on the derived C-M/MO hybrids. Li *et al.* proposed a new method to synthesize RGO wrapped MOF-derived cobalt-doped carbon polyhedrons (Figure 2.10f-g)[127]: firstly, ZIF-67 was annealed under H_2/Ar (10%/90%) flow to obtain C-Co, and the H_2 atmosphere facilitated the formation of Co; subsequently, acid washing would eliminate part of Co particles, generating more pores; then, the C-Co polyhedrons were treated by poly(diallyldimethylammoniumchloride) (PDDA) to gain positive charge surface. As a result, the negative charged graphene oxide would wrap the positive charge C-Co polyhedrons, producing GO-C-Co as a sulfur immobilizer. After heating under vacuum, the sulfur was impregnated into pores of GO-C-Co and GO was reduced into RGO, generating RGO/C-Co-S nanohybrids. Zhu *et al.* fabricated MnO_2 nanowires self-inserted with Co_3O_4 nanocages (MnO_2/Co_3O_4) derived from MnO_2/ZIF-67 by calcinating in air. The as-obtained MnO_2/Co_3O_4 was then wrapped by reduced graphene oxide *via* hydrothermal treatment at 160˚C for 12 h.

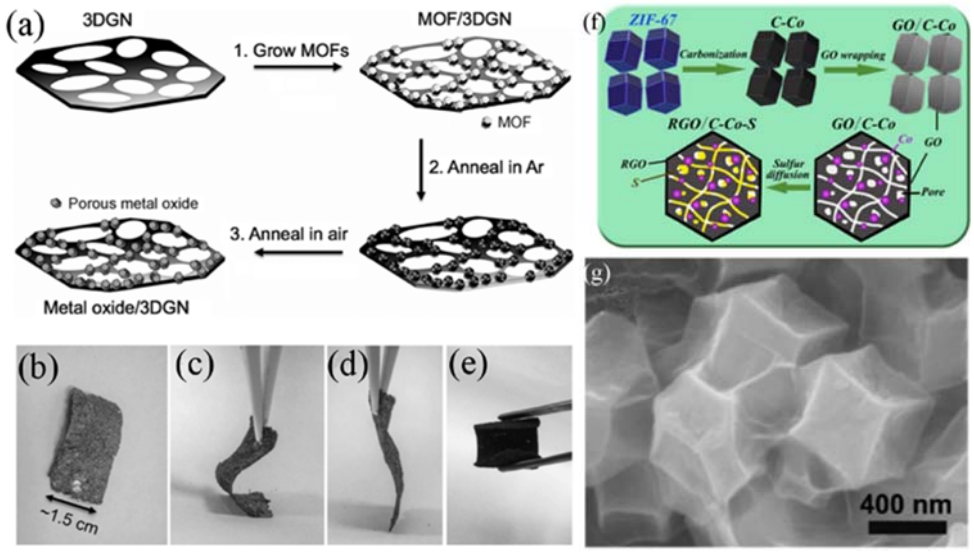

Figure 2.10. (a) Schematic illustration of the process for synthesis of metal oxide/3DGN composites[122]; (b-d) Photographs of the ZnO/3DGN composite[122]; (e) Photographs of the Fe_2O_3/3DGN composite[122]; Reproduced with permission from Wiley-VCH Verlag GmbH & Co. KGaA. (f) Schematic illustration of the formation of RGO/C-Co-S nanohybrids[127]; (g) Scanning electron microscopy (SEM) image of RGO/C-Co-S nanohybrids[127]. Reproduced with permission from Elsevier.

Direct growth of MOFs on the self-standing backbones like copper foil or carbon cloth is observed to be an excellent method for synthesis of C-M/MO composites. Ma *et al.* synthesized hybrid Co_3O_4-carbon porous nanowire arrays (Co_3O_4C-NA, Figure 2.11a) by carbonization of Co-naphthalenedicarboxylate MOF which was grown on Cu foil[128]. Co_3O_4C-NA showed a surface area of 251 $m^2\ g^{-1}$ and slit-like mesopores. Similarly, ZnO@ZnO quantum dots/C nanorod arrays (ZnO@ZnO QDs/C NRA, Figure 2.11b) on flexible carbon cloth (CC) were fabricated by an in-situ ion exchange process[129]. In addition, Zn-doped $CoSe_2$ grown on a free-standing carbon fabric collector (CFC) was reported by Dong and co-workers, derived from ZnCo-ZIF on CFC followed by a selenylation process[130]. 2D layered double hydroxides (LDHs) could also be used as a matrix for growth of MOFs. Li *et al.* reported the impregnation of ZIF-67 on CoAl-LDH nanoplatelets and formation of a honeycomb-like carbon network embedded

with Co nanoparticles (LDH/ZIF-67-800, Figure 2.11c) by carbonization of ZIF-67/CoAl-LDH at 800 ˚C [131]. The investigation showed that the CoAl-LDH facilitated the formation of a well-organized carbon architecture *via* proper pyrolysis temperature. Meanwhile, they proposed the growth of ZnCo-ZIFs on CoAl-LDH nanoplatelets and found that the molar ratio of Co^{2+} /Zn^{2+} in the ZnCo-ZIFs exerted great influence on the formation of honeycomb-like carbon network[85].

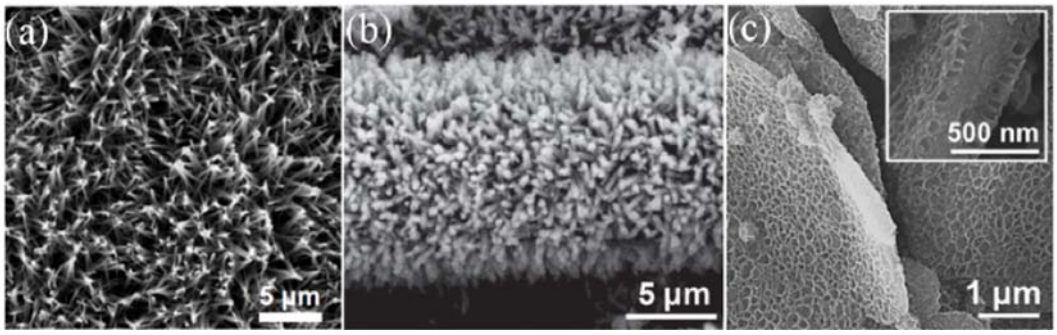

Figure 2.11. SEM images of (a) Co_3O_4C-NA[128], reproduced with permission of the American Chemical Society; (b) ZnO@ZnO QDs/C NRA[129], reproduced with permission from Wiley-VCH Verlag GmbH & Co. KGaA; (c) LDH/ZIF-67-800[131], reproduced with permission from Wiley-VCH Verlag GmbH & Co. KGaA.

2.3. Electrochemical energy storage and environmental remediation

2.3.1. Electrochemical energy storage

The growing demand for clean and sustainable energy has boosted the research on electrochemical energy storage (EES), including fuel cells, batteries and supercapacitors. Many efforts have been made on the advancement of EES. However, it is still dragged by several troubles, such as the low electrochemical activity and unsatisfactory stability. MOFs-derived materials, as a new hope in the field of EES, are emerging during the past few years. In this section, the electrochemical performances of the MOF-derived materials on EES are reviewed and the crucial factors influencing the activities are also summarized.

2.3.1.1. Fuel cells

Electrochemical conversion between oxygen and water is attracting great interest due to its potential to make contributions to the next generation energy devices like regenerative fuel cells. A regenerative fuel cell would provide electricity in the galvanic mode and produce hydrogen and oxygen in the electrolytic mode. The electrocatalytic reactions, for example, oxygen reduction reaction (ORR), oxygen evolution reaction (OER) and hydrogen evolution reaction (HER) are involved in the fuel cells. The major problems to be addressed are the high overpotential and poor stability in the reactions above. Various electrocatalysts have been explored and reported in the past decades and noble metals such as Pt or Ru were considered to be the best choices due to the low overpotential. However, the exploration of better alternatives is continuing due to the high cost and weak stability of the noble metals hindering the mass production. Based on the advantages of MOFs as the precursors, the MOFs-derived electrocatalysts are booming and the performances on ORR, OER and HER are summarized in Table 2.1([73, 78, 83, 85, 92, 98-104, 111, 113, 116, 119, 121, 126-128, 130-159]). Hereafter, all of the electrode potentials are reported relative to the reversible hydrogen electrode (RHE) potential, if not specified.

2.3.1.1.1. Oxygen reduction reaction

Catalytic materials with high activity for ORR are highly demanding as the alternatives of Pt-based materials. Therein, metal-free or non-precious transitional metal-based (Fe, Co, *etc*.) materials have attracted considerable attention due to low cost, high abundance as well as inspiring catalytic activity.

Zhao *et al.* reported the non-platinum electrocatalysts (Fe-NC) derived from FeIM/ZIF-8 as cathode materials for ORR, exhibiting an onset potential (E_{onset}) of 0.915 V[132]. They proved that the excellent ORR catalytic activity was attributed to high N content and large specific surface area. Zhang *et al.* found that doping Fe in ZIF-8 was favorable for the uniform

distribution of the ORR active sites of FeN_x in the as-derived Fe-NC hybrid[133]. In addition, they reported that the incorporation of FA and insertion of multi-wall carbon nanotubes in the Fe-doped ZIF-8 would improve the intrinsic activity and enhance the conductivity of the catalysts, respectively. Armel *et al.* investigated the influence of property of the pristine MOF on the ORR activity of the derived materials, taking Fe-NC derived from Fe-doped ZIFs as examples[160]. The result showed that the large cavity size and specific pore volume of the pristine ZIFs were the keys to the formation of the active sites of $Fe\text{-}N_4$ moieties. In contrast, the chemical composition of the pristine ZIFs was not the primary factor for the ORR activity.

Wang *et al.* synthesized Co-NC derived from ZIF-67 and pointed out that the density of exposed active site of CoN_x played a crucial role in determining the ORR performance in alkaline electrolyte which was not dependent directly on the content of Co and N[134]. In 2016, You *et al.* further reported the ORR performance of Co-NC derived from ZIF-67 in pH-neutral media, which was superior to that of commercial Pt-C catalyst[161]. Chen *et al.* synthesized CNCo-*n* (n indicated the molar ratio of Zn/Co in the precursors) and P-CNCo-*n* for ORR using Zn-Co-ZIFs (BMZIFs) as precursors, realizing simultaneously the conditions beneficial to ORR activity: hierarchical porosity and high surface area, graphitic carbon, formation of active site of CoN_x, uniform distribution of N or P doping (Figure 2.12a)[135]. The linear sweep voltammetry (LSV) data in Figure 2.12b-d showed that P-CNCo-20 exhibited more positive onset potential (0.93 V) and half-wave potential (0.85 V), superb stability and methanol tolerance compared with Pt/C. Zhang *et al.* synthesized Co_3O_4@N-doped carbon hybrids by using Co-I-MOF as a single precursor, showing excellent ORR properties which were attributed to Co^{3+} ions, core-shell structure and pyridinic/pyrrolic nitrogen doped in the carbon shell[136]. Li *et al.* synthesized well-organized honeycomb-like cobalt-carbon framework derived from ZIF-67 grown on CoAl-LDHs, showing excellent ORR performance (half wave potential at 0.83 V) which is superior to commercial Pt/C (catalyst half wave potential at 0.805 V)[131].

They found that the Co nanoparticles would alter the electron structure of the surrounding carbon shell and facilitated the ORR activity. In addition, pyridinic N and graphitic N were observed to be responsible for the ORR performances. Shang *et al.* synthesized Co, N-doped carbon nanoframes derived from ZnCo-ZIFs which were coated with SiO_2 as the protector[113]. A near ideal compromise between surface area, N and Co contents and graphitic degree could be obtained on the carbon nanoframes, showing the excellent ORR catalytic performance which is superior to commercial Pt/C in alkaline electrolyte and comparable to Pt/C in acid media.

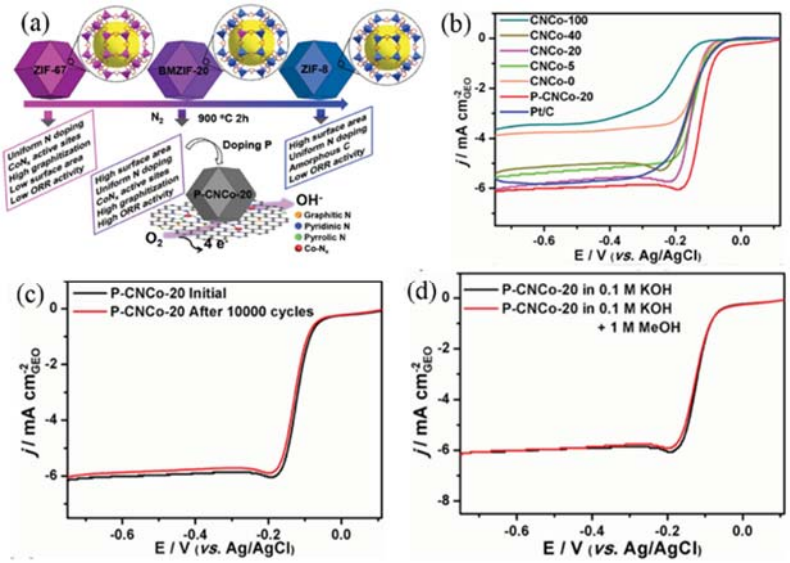

Figure 2.12. (a) Schematic illustration for the preparation of catalysts from BMZIFs for ORR; LSV curves of (b) different samples in O_2-saturated 0.1 M KOH at a rotation rate of 1600 rpm; (c) P-CNCo-20 before and after 10000 potential cycles in O_2-saturated 0.1 M KOH; (d) P-CNCo-20 samples in O_2-saturated 0.1 M KOH without and with 1 M methanol[135]. Reproduced with permission from Wiley-VCH Verlag GmbH & Co. KGaA.

Besides Fe and Co, cheap and abundant Cu is also expected to be an alternative electrocatalyst for ORR. Yu *et al.* fabricated Cu, N-codoped porous carbon (Cu-NC) derived from Cu-doped ZIF-8, showing excellent ORR performance which was comparable to

commercial Pt/C[138]. Their studies revealed that a large porosity, a high level of pyridinic N and metal-N co-doping were beneficial to the electrochemical reactions.

Nitrogen-doped RGO (NRGO) with unique two-dimensional structure and excellent conductivity is considered to be a promising candidate as the catalytic material for ORR. Combining NRGO with transition metal-based catalysts is expected to integrate their merits, inducing superior catalytic activity towards ORR. Inspired by the prediction above, Hou *et al.* synthesized core-shell porous N-doped Fe/Fe_3C@C/RGO derived from RGO/PB[126]. Nitrogen was not only doped on the carbon shell of Fe/Fe_3C, but also on the RGO sheets. The N-doped Fe/Fe_3C@C/RGO displayed a more positive ORR onset potential (1 V) and half-wave potential (0.93) than N-doped Fe/Fe_3C@C (onset potential = 0.91 V, half-wave potential = 0.83 V), indicating that NRGO sheets were also the active sites for ORR as well as the N-doped Fe/Fe_3C@C (Figure 2.13a). In addition, the synergistic effect between the NRGO sheets and N-doped Fe/Fe_3C improved methanol tolerance and stability of the material (Figure 2.13b).

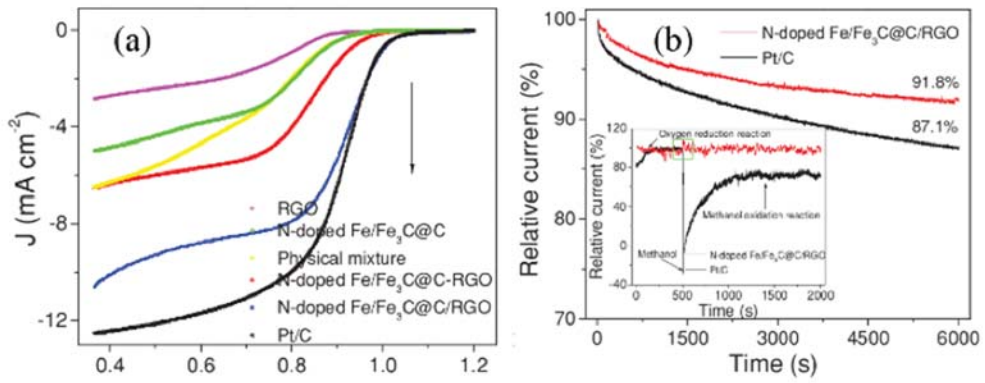

Figure 2.13. (a) LSV curves of samples at a rotation rate of 1600 rpm in O_2-saturated 0.1 M KOH at a rotation rate of 1600 rpm; (b) Current-time chronoamperometric response of N-doped Fe/Fe_3C@C/RGO and Pt/C at 0.8 V in O_2-saturated 0.1 M KOH (1600 rpm); inset are chronoamperometric response of N-doped Fe/Fe_3C@C/RGO and Pt/C at 0.8 V in O_2-saturated 0.1 M KOH (1600 rpm) followed by 3 M methanol[126]. Reproduced with permission from Wiley-VCH Verlag GmbH & Co. KGaA.

As metal leaching may happen on metal-containing ORR catalysts in the strong basic media, carbon-based catalysts were proposed. Graphene/graphene tubes were synthesized by using cage-containing MOF with the addition of DCDA and iron precursor, showing excellent ORR performance as the cathode for Li-O_2 batteries[99]. The half-wave potentials of the material in 0.5 M H_2SO_4, 1 M KOH and 0.1 M $LiPF_6$ tetraethylene glycol dimethyl ether were 0.79, 0.88 and 2.67 V, respectively. It was observed that the graphene/graphene tubes with abundant defects and edge sites are mainly responsible for the outstanding activity.

2.3.1.1.2. Oxygen evolution reaction

Oxygen evolution reaction is generally sluggish due to the high energy barrier to break O-H bond and form O-O bond. IrO_2 and RuO_2 have widely acted as the efficient catalytic materials for OER because of the competitive advantages in high efficiency, fast response and low overpotentials. However, the defects in scarcity and high cost hinder the industrial applications. Consequently, candidates with low cost, high efficiency and abundance are highly needed. During the past few years, MOFs-derived transition oxide, carbon and metal hybrids, metal hydroxides, metal sulfides and metal phosphides for OER have been reported and reviewed in this section.

A transition metal oxide hybrid, $Co_3O_4/NiCo_2O_4$ double-shelled nanocages derived from ZIF-67/Ni-Co LDH, showed an onset potential of 1.53 - 1.57 V at a current density of 10 mA cm^{-2} while the onset potential for Co_3O_4 nanocages appeared at 1.57 - 1.64 V at 10 mA cm^{-2} [78]. The superior OER performance of $Co_3O_4/NiCo_2O_4$ was attributed to the incorporation of Ni^{2+} cations and complex structure, which improved the conductivity, and created or revealed more active sites.

The weak stability and limited conductivity of metal oxides in the alkaline media limited the wide applications. Hybridization of conductive carbon with metals or metal oxides is expected

to solve the problem. Li *et al.* synthesized Co^{3+}-rich cobalt selenide coated with carbon shell deriving from ZIF-67, showing an onset potential of 1.52 V as an OER electrocatalyst[141]. They reported that the surface area was not the primary contributor to the excellent OER performance. Instead, the N-doped carbon shell and abundant Co^{3+} are attributed to the outstanding catalytic effect. FeNi alloy and $NiFe_2O_4$ encapsulated in N-doped carbon (FeNi/$NiFe_2O_4$@NC) nanoboxes were prepared by calcination of FeNi-BTC nanocubes in N_2, showing superior OER performance (overpotential of ~316 mV at 10 mA cm^{-2}) compared with commercial IrO_2[142]. In addition, the polarization curve after continuous 5000 cycles kept coincidence with the initial one, indicating the robust durability. The carbon nitride shells would protect FeNi/$NiFe_2O_4$ from agglomerating, pulverizing, and leaching.

Two-dimensional metal hydroxides are considered to facilitate the electrochemical reactions due to the high surface area and exposure of more active sites, inducing fast interfacial charge transfer. He *et al.* explored the synthesis of CoNi-hydroxide nanosheets derived from CoNi-MOF by ultrasonication, showing overpotentials of 324 and 372 mV at current densities of 10 and 100 mA cm^{-2} which were superior to those of IrO_2 commercial electrocatalyst[139]. Besides the synergistic effect of Co and Ni, the excellent OER performance of the as-synthesized materials was attributed to the numerous active sites exposed in the alkaline electrolyte. In addition, CoNi-hydroxide nanosheets tended to break into smaller fragments, generating more sheet edges containing unsaturated coordination sites, which could act as the active sites for OER.

Metal sulfide or phosphides have also been attempted to act as the catalytic materials for OER. Yu *et al.* synthesized $Ni(OH)_2$, NiO, and Ni-P derived from the same precursor Ni-Ni PBA, exhibiting similar porous plate-like structures (Figure 2.14a)[145]. The OER activity of Ni-P outperformed that of $Ni(OH)_2$ and NiO, showing an onset potential of 1.48 and 1.53 V at 10 mA cm^{-2}, respectively (Figure 2.14b). The oxidation peaks at around 1.37 V in the LSV curves

of Ni-P represented the oxidation of Ni(II)/Ni(III), suggesting the nickel phosphides were partially oxidized into nickel oxides/hydroxides on the surface during the OER reaction which served as the primary active sites for OER. Inspired by the synergistic effect of multicomponents, Zhang *et al.* synthesized CoFe-P derived from CoFe-MOF, exhibiting a low overpotential of 244 mV at a current density of 10 mA cm^{-2} in 1 M KOH solution[143]. The hybrid of NiS nanoparticles embedded in nitrogen and sulfur co-doped carbon (NiS@N/S-C) was fabricated using Ni-MOF as the precursor, revealing an onset potential of 1.54 V and overpotential of 417 mV at 10 mA cm^{-2}[146]. The doped nitrogen and thiophene S were reported to contribute greatly to the excellent OER activity.

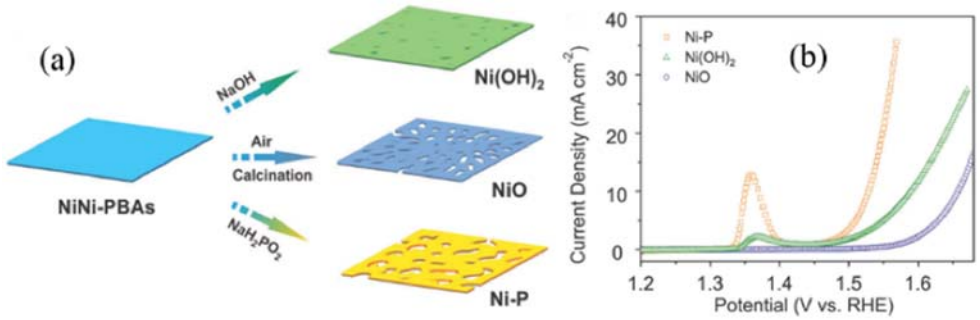

Figure 2.14. (a) Scheme for the preparation of $Ni(OH)_2$, NiO, and Ni-P porous nanoplates; (b) LSV curves of $Ni(OH)_2$, NiO, and Ni-P porous nanoplates in 1.0 M KOH[145]. Acknowledgement to Royal Society of Chemistry.

2.3.1.1.3. Hydrogen evolution reaction

Hydrogen, as a clean energy source, could be produced by the friendly electrocatalytic HER. Due to the defects of Pt and Pt-based electrocatalysts mentioned above, non-precious transition metal-based materials are investigated and act as the promising catalysts for HER.

The economic-friendly transition metal phosphides (TMP) are attracting great interest due to the desired stability in both acidic and alkaline media. Metal atoms appear to be cationic state and P atoms to be anionic state, due to the electron density transfer from transition metal

to phosphorus. The P atoms with anionic state, as an active site, boost the proton discharge in HER. In order to generate more anionic state, binary metal phosphides were proposed. Hao *et al.* synthesized $Co_xFe_{1-x}P$ by pyrolysis of CoFe-PBA and NaH_2PO_2 under N_2 flow, showing excellent HER activity in 0.5 M H_2SO_4 (onset potential: 31 mV) and 1.0 M KOH electrolyte (onset potential: 39 mV)[147]. The study proved that the binary transition metal system is favorable to the HER process due to redistribution of valence. Feng *et al.* reported the synthesis of quasi-hollow nickel cobalt phosphide (Ni-Co-P) microcubes derived from Ni-Co-PBA, requiring an overpotential of 150 mV at a current density of 10 mA cm^{-2}[148]. The quasi-hollow porous structure, as well as the synergistic effect between Ni_2P and CoP, may be beneficial to the superior HER activity.

Second metal-doping is also applied on the metal sulfides. Huang *et al.* reported the synthesis of hollow $M_xCo_{3-x}S_4$ (M: Ni, Zn, Cu) by sulfidation and thermal annealing of homogeneous bimetallic MOFs (MCo-MOF), showing superior HER performance in a wide pH range compared with pristine Co_3S_4 (Figure 2.15a-c)[83]. The calculated density of states in Figure 2.15d showed that second-metal doping (Zn^{2+}, Ni^{2+} and Cu^{2+}) would narrow the bandgap from 0.82 eV for pristine Co_3S_4 to 0.68, 0.43 and 0.45 eV, respectively, suggesting the enhanced electrical conductivity. The reduced bandgap was induced by improved hybridization between Co d orbital and S p orbital (Figure 2.15e). In addition, the density functional theory (DFT) calculations (Figure 2.15f) proved that second-metal doping like Zn^{2+} and Ni^{2+} would decrease the free energy for H adsorption (ΔG_{H*}) of Co_3S_4, thus dramatically improving the HER activity by collaborating with the enhanced conductivity.

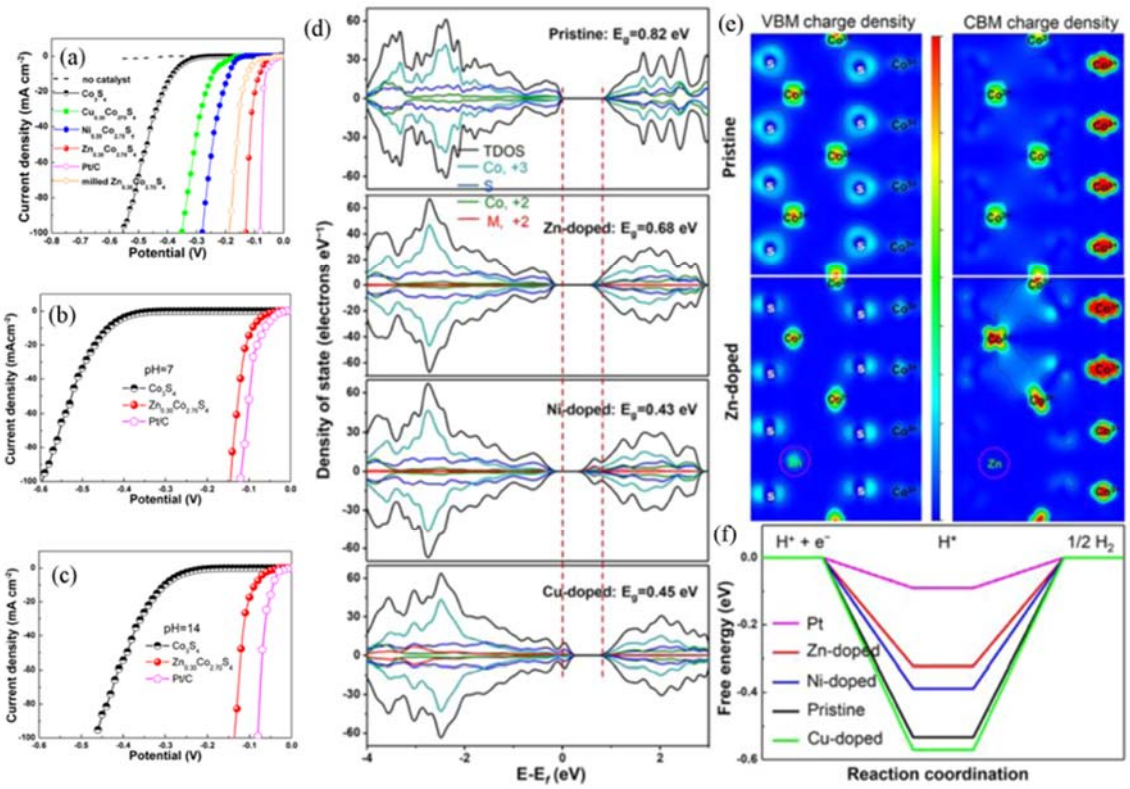

Figure 2.15. The polarization data of materials in (a) 0.5 M H_2SO_4; (b) 0.1 M phosphate buffer; (c) 1 M KOH; (d) Projected density of states of materials; (e) Difference charge density of valence band and conduction band in Co_3S_4 and Zn-doped Co_3S_4 (red and blue colors represent electron accumulation and depletion); and (f) Calculated free-energy diagram of HER at equilibrium potential on the materials[83]. Reproduced with permission of the American Chemical Society.

Besides the second metal-doping in the electrocatalysts, tuning the proportion of metal components is also a strategy to improve the HER activity. Yang *et al.* synthesized ternary alloys embedded on carbon (metal@carbon) by pyrolysis of $Fe_3[Co(CN)_6]_2$ encapsulated by $Ni_3[Co(CN)_6]_2$ and unveiled the relationship between activity and proportion of alloys by DFT calculations[162]. The results showed that the change of proportion would influence the number of transferred electrons between metal and carbon, thus changing the electronic structure of the metal@carbon and further impacting the activity.

Heteroatom doping into carbon, such as nitrogen (N), boron (B), sulfur (S), and phosphorus (P), would modify the electronic structure of the carbon, and thus enhance the catalytic efficiency. Inspired by this conclusion, Yang *et al.* reported the HER performance of FeCo@N-graphene (FeCo@NG) derived from $Fe_3[Co(CN)_6]_2$, showing a low onset overpotential (88 mV) and overpotential (262 mV) at 10 mA cm^{-2} [149]. They also pointed out by DFT calculations that the appropriate nitrogen doping and metal-graphene structure would decrease ΔG_{H*}, thus improve the HER activity. Zhang *et al.* synthesized cobalt encapsulated in N, B-codoped carbon (Co@N,B-C) by pyrolysis of ZIF-67 and H_3BO_3, exhibiting an onset potential of ~0 V and overpotential of 96 mV at 10 mA cm^{-2} in acidic media while an overpotential of 183 mV at 10 mA cm^{-2} in 1 M KOH[127]. No significant decrease of HER activity was found after adding SCN^- ions in the electrolyte, suggesting that N, B-codoped carbon shells contributed primarily to the HER performance instead of cobalt species. The DFT calculation results proved that the encapsulated cobalt species and heteroatom doping in the carbon shells facilitated in the tunning of ΔG_{H*} near to zero, inducing the superb HER performance.

2.3.1.1.4. ORR and OER

The noble Pt-based materials are famous for the ORR activity but exhibit poor OER performance while RuO_2 and IrO_2 are widely used as the OER catalysts but not ideal for ORR. Consequently, exploring bifunctional materials with high efficiency and reliable stability for both ORR and OER is urgent. MOFs-derived metal oxide-carbon hybrids and nanocarbons are attracting more attention and studied for the bifunctional capability.

The carbon incorporated into the metal oxides is expected to facilitate the electrochemical activities for OER and ORR. Ma *et al.* reported the synthesis of Co_3O_4 and carbon nanowire array (Co_3O_4C NA) by using Co-MOF grown on the current collector Cu foil[128]. The as-obtained Co_3O_4C NA on Cu foil could be directly used as the electrode without extra substrates or binders, exhibiting an onset potential at 1.47 V for OER and a half-wave potential of 0.78

V for ORR. The incorporation of carbon, the mesoporous nanowire array structure and the Cu foil facilitated the excellent electrochemical performances. Aijaz *et al.* reported the synthesis of core-shell Co@Co_3O_4 embedded in carbon nanotube-grafted N-doped carbon (Co@Co_3O_4/CNT-NC) by pyrolysis of ZIF-67 *via* a two-step route[119]. As a bifunctional material for ORR and OER, the low overvoltage (0.85 V *vs* RHE) was attributed to highly graphitic CNT-grafted polyhedral, synergistic effect between Co cores and Co_3O_4 shells as well as the nitrogen-containing groups and N-doped carbon shells. Gadipelli *et al.* synthesized Co/NC derived from ZnCo-ZIFs as a bifunctional material for ORR and OER[163]. They systematically studied the control of graphitic degree and nitrogen/cobalt concentrations by changing carbonization temperature and time, and molar ratio of Zn^{2+} and Co^{2+} of ZnCo-ZIF, realizing highly effective performances for both ORR and OER.

The bifunctional capability of carbon catalysts for ORR and OER is reported to be impacted by the graphitization degree and heteroatom doping. Qian *et al.* firstly reported the synthesis of N, B-co-doped nanoporous carbon (N, B-C) as the bifunctional catalyst by pyrolysis of Zn-MOF (MC-BIF-1S) under H_2/Ar atmosphere[156]. The results showed that pyrolysis at 1100 °C under H_2 was favorable to the ORR and OER activities due to the high porosity and B, N co-doping. Liu *et al.* synthesized sandwich-like N-doped porous carbon@graphene (NC@graphene) derived from ZIF-8 grown on graphene oxide, exhibiting excellent ORR ($E_{1/2}$ = 0.8 V, $E_{1/2}$ represents half-wave potential) and OER ($E_{j=10}$ = 1.63 V, $E_{j=10}$ is potential at a current density of 10 mA cm^{-2}) performances[154]. The large surface area (1094.3 m^2 g^{-1}), high graphitic degree of graphene, and the synergistic effect between N-doped porous carbon and graphene were the positive factors influencing the electrocatalytic activity by creating more active sites and boosting the mass transport as well as electron transfer. *Xia et al.* synthesized hollow N-doped carbon nanotube frameworks (NCNTFs) derived from ZIF-67 consisting of interconnected carbon nanotubes (Figure 2.16a) [100]. The graphitic layers in the CNT walls were

not completely parallel to the axis direction of the CNTs, inducing exposure of more edges which contained more defect sites than basal planes (Figure 2.16b). The NCNTF exhibited excellent catalytic performances for ORR ($E_{1/2}$ = 0.87 V, Figure 2.16c) and OER ($E_{j=10}$ = 1.6 V, Figure 2.16d) activities, which were attributed to the robust framework constructed by interconnected carbon tubes, and defects induced by the unique structure and N doping.

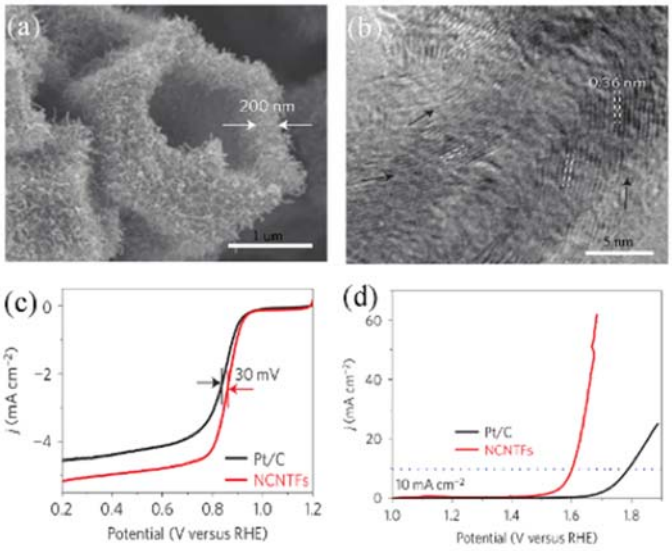

Figure 2.16. (a) SEM image of NCNTFs; (b) High-resolution TEM (HRTEM) of NCNTFs; LSV curves of Pt/C and NCNTFs for (c) ORR and (d) OER[100]. Reproduced with permission of the nature publishing group.

2.3.1.1.5. HER and OER

Electrochemical water splitting including HER and OER has been considered as an efficient method to produce clean hydrogen fuel. The development of highly active catalysts for overall water splitting is required. Transition metal phosphides and sulfides are promising due to the abundance, low cost, and high tolerance in harsh environment. MOFs have been highly appreciated as the precursors of the bifunctional catalysts for HER and OER in the past few decades.

You *et al.* firstly reported Co-P/NC (CoP and Co_2P encapsulated in the carbon matrix) for

water splitting by pyrolysis of ZIF-67 and subsequent phosphidation, showing robust HER and OER (overpotential of -191 and 354 mV at 10 mA cm^{-2}, respectively) performances in 1.0 M KOH, as well as inspiring stability[157]. The cobalt phosphides were responsible for the high HER and OER activity, and N-doped carbon matrices guaranteed the stability and conductivity. The mesoporous structure and high surface area (183 m^2 g^{-1}) facilitated the diffusion of gas (H_2 and O_2) and exposure of active sites. Meanwhile, Jiao *et al.* rationally combined GO into ZIF-67 as precursors for CoP/RGO, which showed superb OER ($E_{j=10}$ = 1.57 V) and HER ($E_{j=10}$ = -150 mV) performances under alkaline condition[158]. The participation of RGO in the catalyst improved the conductivity which is beneficial to the electron transfer.

Zhang *et al.* fabricated cobalt sulphide anchored onto N, S co-doped graphene (Co/Co_9S_8@SNGS) derived from thiophene-2,5-dicarboxylate (Tdc) and 4,4'-bipyridine (Bpy) ligands assembled Co-MOF grown on GO sheets[116]. An overpotential of 290 mV for OER at 10 mA cm^{-2} and 350 mV for HER at 20 mA cm^{-2} were obtained in 0.1 M KOH electrolyte, due to suitable N and S doping, Co/Co_9S_8 core-shell structure, Co-N_x active sites, high porosity, and good conductivity.

2.3.1.2. Batteries

Rechargeable batteries are fast-developing due to the wide applications of electric devices. High specific capacity, rate performance and robust stability are the essential criteria of battery performance. Scientific research toward high-performance electrode materials including anode and cathode materials have been encouraged. In this section, we summarized and reviewed the MOFs-derived anode and cathode materials for batteries, such as lithium ion batteries (LIBs), sodium ion batteries (SIBs) and lithium sulfur batteries (LSBs).

2.3.1.2.1. Anode materials

MOFs-derived anode materials, including carbon, metal or metal oxide, and metal-carbon

hybrids, are generally employed on LIBs and SIBs. Rational components and structures are expected to facilitate the battery performances. The performances of MOFs-derived anode materials on LIBs and SIBs are summarized in Table 2.2 ([43, 54-56, 58-63, 65, 66, 68, 72, 76, 79, 82, 107, 118, 120, 122, 123, 125, 129, 148, 164-187]).

2.3.1.2.1.1. Lithium ion batteries

LIBs, as a promising power source, have attracted considerable attention during the past few decades. The principle for LIBs is that Li in the anode materials is oxidized into Li^+ which is subsequently transferred to the cathode. A volume change during cycling would induce the sharp decline in capacity. The commercial anode material, graphite, is facing the challenge due to the low theoretical specific capacity (372 mA h g^{-1}). In consideration of the problems above, various materials have been exploited, aiming to improve the cycling performance while boost the capacity. MOFs-derived materials have gained popularity as the anode materials for LIBs, exhibiting high capacity and minimal volume change.

MOFs-derived metal oxide is considered as a fascinating candidate for the anode material of LIBs due to the tuneable structures and components. Anatase TiO_2 derived from MIL-125 (Ti) was firstly reported by Wang *et al.*, exhibiting a reversible capacity of 166 mA h g^{-1} at a current density of 1 C after 500 cycles[175]. Speedle mesoporous α-Fe_2O_3 derived from MIL-88-Fe *via* a two-step pyrolysis route was also fabricated and showed a reversible capacity of 911 mA h g^{-1} at 200 mA g^{-1} after 50 cycles[54]. Banerjee *et al.* studied the performance of CuO derived from Cu-MOF (MOF-199) on LIBs, exhibiting a high reversible capacity of ~484 mA h g^{-1} at 100 mA g^{-1} after 40 cycles[61]. Core-shell $Co_3[Fe(CN)_6]_2$@$Ni_3[Co(CN)_6]_2$ nanocubes-derived Fe_2O_3@$NiCo_2O_4$ porous nanocages showed a reversible capacity of 1079.6 mA h g^{-1} at 100 mA g^{-1} after 100 cycles, reported by Huang *et al.*[72]. The synergistic effect between Fe_2O_3 and $NiCo_2O_4$ as well as the unique structure contributed to the enhanced specific capacity and stability.

Carbon-based anode materials, such as carbon nanotubes, graphene and partially graphitic carbon, have been studied for applications in LIBs. Heteroatom (like N, S, B and P) doping would modify the electronic properties of carbon and generate better electrochemical performances compared with the non-doped carbon. Zheng *et al.* synthesized N-doped nanoporous carbon containing a multitude of small graphene analogous particles by using ZIF-8 as the precursor, obtaining a high N content of 17.72 wt.%. A reversible capacity of 1147 mA h g^{-1} at 500 mA g^{-1} after 200 cycles was delivered[174]. The DFT calculations confirmed that high N content, especially pyridinic N and pyrrolic N, was responsible for the excellent LIBs performances.

Incorporating carbon into the metal oxides would facilitate to alleviate the volume shift during cycling. Yang *et al.* firstly synthesized carbon and ZnO quantum dots (ZnO QDs/C) hybrid (IRMOF-1 as the precursor) for using as the anode materials for LIBs, exhibiting a specific charge capacities of 1200 mA h g^{-1} at 75 mA g^{-1} [107]. The excellent performance was attributed to the long-range-ordered structure and the hindering of volume expansion by carbon layers. Han *et al.* found that ZnO/C composites originating from ZIF-8 coated with organic compounds like chitosan showed higher specific capacity and lower internal impedance compared with the composites derived from single ZIF-8[164]. A porous ZnO/$ZnFe_2O_4$/C hybrid (Figure 2.17a) derived from Fe^{III}-modified MOF-5 was reported by Zou *et al.*[43], exhibiting high rate performance (Figure 2.17b) and excellent stability (Figure 2.17c): high reversible capacities of 1060, 934, 887 and 842 mA h g^{-1} were achieved at 0.5, 1, 2 and 5 A g^{-1}, respectively. In addition, a capacity of over 1200 mA h g^{-1} was recovered when the current density went back to 0.5 A g^{-1}; and moreover, a capacity of 1390 mA h g^{-1} was obtained at a current density of 0.5 A g^{-1} after 100 cycles. The better electrochemical performance of ZnO/$ZnFe_2O_4$/C than that of ZnO/$ZnFe_2O_4$ (Figure 2.17d) demonstrated that the 3D inter-connected carbon shell with hollow interior could buffer the volume effect and effectively

counteract pulverization.

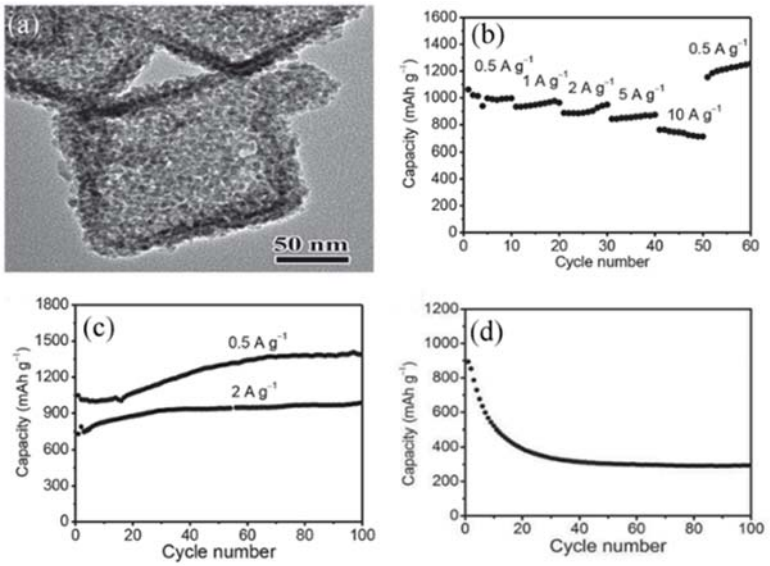

Figure 2.17. (a) TEM image of $ZnO/ZnFe_2O_4/C$ hybrid; (b) Rate capability of $ZnO/ZnFe_2O_4/C$ at current densities of 0.5, 1, 2, 5, 10 A g^{-1}; (c) Cycling performance of $ZnO/ZnFe_2O_4/C$ at current densities of 0.5 and 2 A g^{-1}; (d) Cycling performance of $ZnO/ZnFe_2O_4$ at current densities of 2 A g^{-1} [43]. Reproduced with permission from Wiley-VCH Verlag GmbH & Co. KGaA.

Hybridization of graphene into metal oxides could not only alleviate the volume change but also improve the conductivity of the system. Graphene/Co_3O_4 was synthesized by Qu and co-workers using ZIF-67 grown on graphene oxide as precursors and showed a capacity of 877 mA h g^{-1} at a current density of 5000 mA g^{-1}, which was much higher than pure Co_3O_4[123]. On one hand, the graphene-supported Co_3O_4 structure facilitated the access of electrolyte and shorten the diffusion length of Li^+ ion. On the other hand, the conductive graphene substrate in the hybrid could also enhance the electrode reaction kinetics.

Unique shapes and structures of the electrode materials are regarded as key factors for the excellent electrochemical performances on LIBs. Yolk-shell NiO@C derived from a Ni-MOF was synthesized by Liu *et al.*, showing a specific capacity of 962 mA h g^{-1} at a current density

of 1 C after 200 cycles[165]. It was validated that the yolk-shell nanostructure had a high specific surface area (182 $m^2 g^{-1}$). In addition, it could effectively shorten the diffusion pathway of Li^+ ions. Moreover, the void space would buffer the volume change during cycling. Yu *et al.* synthesized NiSb nanoparticles embedded in the hollow carbon spheres by using hollow Ni-MOF and $SbCl_3$ as the precursors, showing high capacity, great rate capability and excellent stability[166]. As reported, the hollow and porous structure of the electrode material would shorten the Li^+ ion diffusion length, boost the mass transfer and alleviate the volume change during the reaction. Wu and co-workers synthesized the porous ternary $Zn_xCo_{3-x}O_4$ by using heterobimetallic ZIFs (Zn-Co-ZIFs) as precursors, showing a high reversible capacity of 990 mA h g^{-1} at 100 mA g^{-1} and excellent stability due to the nano-sized subunits and hollow porous structure[66]. Yu *et al.* synthesized hierarchical CoS_2 nanobubble-like prisms with multilevel hollow interiors (Figure 2.18a) by using ZIF-67 hollow prisms as the precursor followed by sulfidation reaction. High rate performance was delivered (Figure 2.18b), for example, reversible specific capacities of 910, 778, 681, and 470 mA h g^{-1} at the current densities of 200, 500, 1000, and 5000 mA g^{-1}, respectively. The capacity recovered to 864 mA h g^{-1} when the current density returned to 200 mA g^{-1}. In addition, a reversible capacity of 737 mA h g^{-1} could be maintained after 200 cycles at 1000 mA g^{-1} (Figure 2.18c). The excellent electrochemical performance of CoS_2 was attributed to the unique structures. First, the nanobubbles would shorten the diffusion pathway of Li^+ to boost the kinetics. Moreover, the multilevel hollow interior could buffer the structural stress and volume shift, improving the cycling performance. Fang *et al.* fabricated ZIF-67 on a 3D electro-conductive substrate (3D nickel foam, 3DNF) and obtained a Co_3O_4 nanosheet/3DNF hybrid by subsequent calcination[177]. The reversible capacities of 1226, 1130, 923, 751 and 543 mA h g^{-1} could be maintained at the current densities of 1, 2, 3, 10, and 20 A g^{-1}, respectively. About 600 mA h g^{-1} could still be found after 2000 cycles at 5 A g^{-1}, suggesting excellent cycling performance. The leaf-like porous Co_3O_4

nanosheets facilitated the exposure of active sites, shortened Li ion diffusion length and buffered the volume expansion. In addition, the conductive 3DNF was beneficial to the electron transportation. The synergistic effect of Co_3O_4 nanosheets and 3DNF made the Co_3O_4 nanosheet/3DNF hybrid to be a promising anode material.

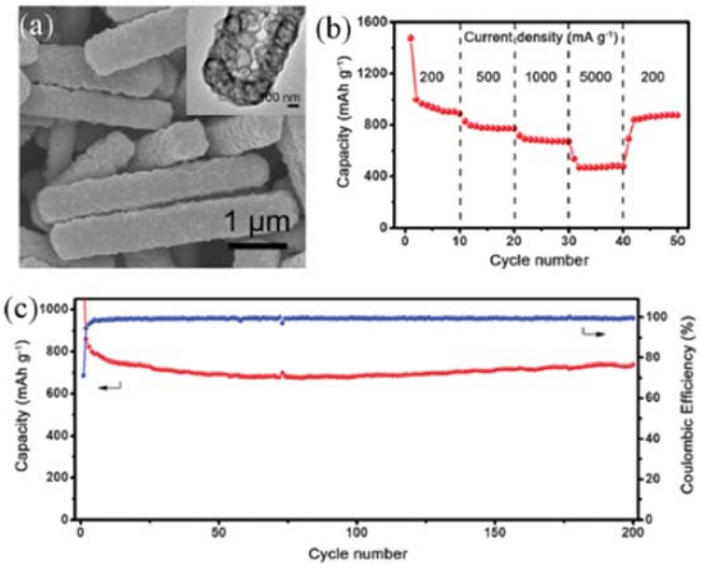

Figure 2.18. (a) SEM and TEM (inset) images of CoS_2 nanobubble-like prisms; (b) Rate capabilities of CoS_2 nanobubble-like prisms at various current densities; and (c) Cycling performance of CoS_2 nanobubble-like prisms at 1000 mA g^{-1} [82]. Reproduced with permission from Wiley-VCH Verlag GmbH & Co. KGaA.

2.3.1.2.1.2. Sodium-ion batteries

In consideration of the availability and cost of lithium in the future, as well as the safety problem of formation of metal dendrites on the negative electrode of LIBs, alternatives to LIBs are demanding. Sodium ion batteries have thus attracted the scientific research due to the low cost and abundance of sodium. However, the development of electrode materials for SIBs is hindered, because Na^+ has a large ionic radius (1.02 Å) than Li^+ (0.76 Å), inducing the frustrating movement of Na^+ in the electrode materials. The graphite, which is a common anode material for LIBs, exhibited poor electrochemical performances on the SIBs. During the past

few years, carbon materials, metal oxides, and carbon/metal hybrids have been attempted to act as the anode materials for SIBs. Here, we review the MOFs-derived anode materials for SIBs.

The carbon anode materials for SIBs are expected to own micro/mesoporous structure and high specific surface area, aiming to increase the contact area between the anode materials and electrolyte. Cube-like porous carbon (CPC) possessing a high surface area of 2316 m^2 g^{-1} was synthesized using MOF-5 as the precursor, showing a specific capacity of 240 mA g^{-1} at 100 mA g^{-1} after 100 cycles and 100 mA g^{-1} at 3200 mA g^{-1} after 5000 cycles[186]. The high surface area and hierarchical porosity (pore size mainly at 1.06 and 3.65 nm) would effectively improve the contact area and boost the mass transfer while the carbon skeleton buffers the volume change.

The large volume change is the main problem for metal oxides as the anode materials for SIBs, which will induce the sharp decline of capacity and poor rate performance. In order to accommodate the volume shift and improve the contact area between anode materials and electrolyte, Zhang *et al.* synthesized a porous CuO/Cu_2O composite in hollow octahedrons as the anode material for SIBs by calcination of Cu-based MOF, showing a reversible capacity of 415 mA h g^{-1} at 50 mA g^{-1} after 50 cycles[181]. The hollow structure afforded void to alleviate stresses generated by the volume change and the porous structure facilitated the contact between the active material and electrolyte.

Coating carbon or incorporation of graphene or CNTs on the metal oxide is an effective strategy to improve the performance of metal oxide as the anode materials for SIBs. Zhang *et al.* synthesized graphene@nitrogen-doped carbon@ultrafine TiO_2 nanoparticles (G-NC@TiO_2) using GO wrapped NH_2-MIL-125(Ti) as the precursor, delivering an outstanding cycling performance (a capacity retention of 93% after 5000 cycles at 1 A g^{-1})[183]. The wrapping

graphene and nitrogen-doped carbon coating would enhance the conductivity, and the porous structure and ultrafine TiO_2 nanoparticles ensured the stability and rate performance. An amorphous carbon nitride and zinc oxide hybrid (ACN/ZnO) was synthesized by pyrolysis of ZIF-8, delivering a reversible capacity of 430 and 140 mA h g^{-1} at 83 and 8330 mA g^{-1}, respectively[180]. In addition, only 0.016% capacity degradation per cycle was found in 2000 cycles at 1.67 A g^{-1}, indicating the excellent long-term cycling performance. The stable amorphous carbon nitride facilitated the high reversible capacities while ZnO particles are responsible for the superb cycling stability due to the rigid structure. Chen *et al.* synthesized Co_3ZnC/carbon nanotube-inserted N-doped carbon concave-polyhedrons (Co_3ZnC/CNT-NCCPs) by using Zn-Co-ZIFs as the precursor[185]. A discharge capacity of 500 mA h g^{-1} at 200 mA g^{-1} after 200 cycles was delivered. Meanwhile, a discharge capacity of 754 mA h g^{-1} at 500 mA g^{-1} after 200 cycles was also obtained while it was used as the anode material for Li-ion batteries. The 3D porous carbon matrix could facilitate the electron transfer and weaken the volume change. The carbon nanotubes enhanced the conductivity thus improving the rate performance. It is noteworthy that the N doping introduced more active sites to adsorb extra Li^+ and Na^+, resulting in high storage performances.

2.3.1.2.2. Cathode materials

MOFs-derived cathode materials, especially for lithium sulfur batteries, have been a spot of scientific research. Lithium sulfur batteries, using sulfur as the cathode material, have been considered as a promising battery system due to the high theoretical specific capacity of 1672 mA h g^{-1} and an energy density of 2500 Wh kg^{-1}. However, the sulfur cathode owned drawbacks: (i) the low conductivity (5×10^{-30} S cm^{-1}) of sulfur hinders the ultilization of sulfur, and (ii) polysulfides forming during the electrochemical reaction apt to dissolve in organic electrolytes and deposit on the surface of electrodes, inducing fast capacity fading. Exploring hosts for sulfur as the cathode materials is an efficient approach to address the problems above by

immobilizing the sulfur and polysulfides, meanwhile, improving the conductivity of the cathode. The MOFs-derived cathode materials for LSBs are summarized in Table 2.3 ([127, 188-197]).

Nanoporous carbons can provide an exceptionally high specific surface area and hierarchical pores to host sulfur and suppress the shuttle effect of polysulfides *via* absorbability. A nitrogen-doped carbon derived from ZIF-8 as the host of sulfur as a cathode for Li-S batteries was reported by Wu *et al.* and Li *et al.*, showing excellent cycling and rate performances[188, 189]. The small S_{2-4} molecules confined in the micropores of the carbon matrix would suppress the loss of soluble Li polysulfides, avoiding the shuttle effect. The doped nitrogen enhanced the conductivity of the carbon network, improving the charge transfer between the electrode and electrolyte. Xi *et al.* studied the influence of pore volume and pore size distribution of MOF-derived carbon on the LSBs performance[190]. ZIF-8, room temperature synthesized MOF-5 (RT-MOF-5), solvothermally synthesized MOF-5 (solvo-MOF-5) and $[Zn_3(fumarate)_3(dmf)_2]$ (ZnFumarate) were used as the precursors, generating hierarchically porous carbon with different textural characteristics. Combined the porosity and electrochemical activity on LSBs, they proposed that micropores (< 2 nm) are responsible for the cycle performance due to firmly confinement of polysulfide anion diffusion in the electrolyte. Mesopores (2 - 50 nm) enhanced the transport of electrolyte and lithium ions, inducing the high initial capacities. Macropores (> 50 nm) could explained the loss of capacity during cycling.

Polar metallic oxides with a high surface area could afford “sulfiphilic” surfaces and electron transport to locate polysulfides deposition and boost the redox reactions. Carbon and metal oxide hybrids as the host of sulfur are expected to combine the merits of metal oxides and carbon. Cobalt and N-doped graphitic carbon (Co-N-GC) derived from ZIF-67 as a sulfur host was synthesized and used as the cathode material for Li-S batteries, delivering a reversible capacity of 850 mA h g^{-1} at 0.2 C after 200 cycles[194]. The 3D porous structure and high surface

area (308 m^2 g^{-1}) enabled a high sulfur loading of 70 wt.% in the total electrode weight. The nitrogen doping in GC, especially pyridinic-N, provided one pair of long electrons to trap polysulfides through the strong chemical bonding between Li in Li_2S_n with N atoms, inducing the high utilization of S as well as excellent rate and cycling performances. Most importantly, the Co-N-GC hybrid acted as a dual-catalyst on S reduction and oxidation (Figure 2.19). For instance, Co nanoparticles could effectively transform long-chain polysulfides into short-chain ones (like Li_2S_2 and Li_2S), inducing a high specific capacity and reaction kinetics. The doped N facilitated the oxidation of $Li_2S_6 \rightarrow Li_2S_8 \rightarrow S_8$, improving the cycling performance.

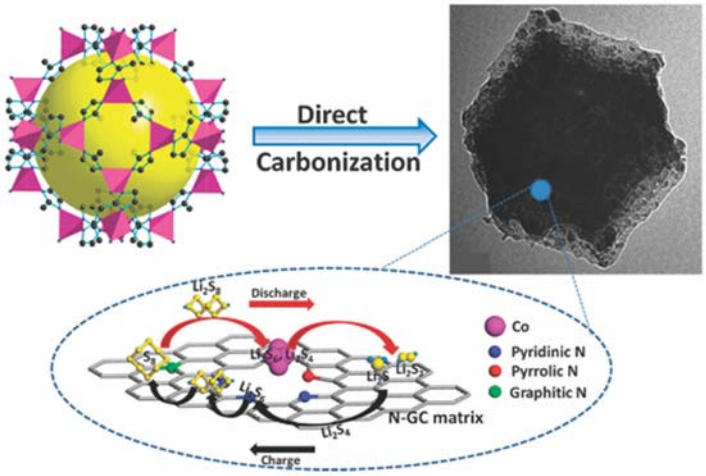

Figure 2.19. Schematic illustration of Co-N-GC composite preparation and its interaction with polysulfides during the charge/discharge processes of a Li-S battery[194]. Acknowledgement to Royal Society of Chemistry.

Similarly, He *et al.* employed graphitic carbon co-doped with cobalt and nitrogen (C-Co-N) derived from ZIF-67 as the host for lithium sulphide (Li_2S) which is another promising cathode material for Li-S batteries[196]. The doped N in the carbon matrix, especially pyridinic-N, could confine the polysulfides by the interaction between Li in Li_2S_n and N atoms while the Co nanoparticles enhanced the electrochemical performance of Li_2S by favoring the conversion of long-chain polysulfides to short-chain ones. The DFT calculation results confirmed that the

C-Co-N could effectively stabilize the soluble lithium polysulfides by the physical spatial restriction. As a result, the Li_2S@C-Co-N composite exhibited a reversible capacity of 929.6 mA h g^{-1} at 0.2 C after 300 cycles.

Li *et al.* wrapped GO on the cobalt doped carbon (C-Co) derived from ZIF-67, forming GO@C-Co as the host of sulfur. The obtained RGO@C-Co-S as the cathode material of Li-S batteries showed a capacity of 949 mA h g^{-1} at 300 mA g^{-1} after 300 cycles[127]. The homogeneously dispersed cobalt nanoparticles, as well as the meso- and micro-porous structures, facilitated the loading of sulfur by chemical and physical interactions. In addition, the wrapped RGO nanosheets as barrier layers would hinder the diffusion of polysulfide, thus suppressing the shuttle effect. The excellent electrochemical performance in this study could be attributed to the synergistic effect of carbon matrix originated from ZIF-67, cobalt nanoparticles and RGO nanosheets.

2D metal carbides with high conductivity are favorable as the cathode materials for LSBs due to the active hydrophilic surfaces, which can immobilize the polysulfides *via* strong chemical bonding. Bao *et al.* synthesized 3D metal carbide@mesoporous carbon hybrid ($Ti_3C_2T_x$@Meso-C, $T_x \approx F_xO_y$, Figure 2.20a) by using $Ti_3C_2X_x$@Meso-MOF-5 ($X_x \approx F_xOH_yO_z$) as the precursor[197]. The mesoporous carbon could inhibit the restacking of $Ti_3C_2T_x$ nanosheets due to the hydrophilic surface of $Ti_3C_2T_x$. In addition, the highly porous structure facilitated the loading of sulfur, forming $Ti_3C_2T_x$@Meso-C/S (Figure 2.20b). The $Ti_3C_2T_x$@Meso-C/S as the cathode materials for Li-S batteries showed a discharge capacity of 704.6 mA h g^{-1} at 0.5 C after 300 cycles (Figure 2.20c). The DFT calculations revealed that the strong ionic attraction existed between $Ti_3C_2T_x$ and S cations, which induced the trapping of polysulfides, avoiding the shuttle effect.

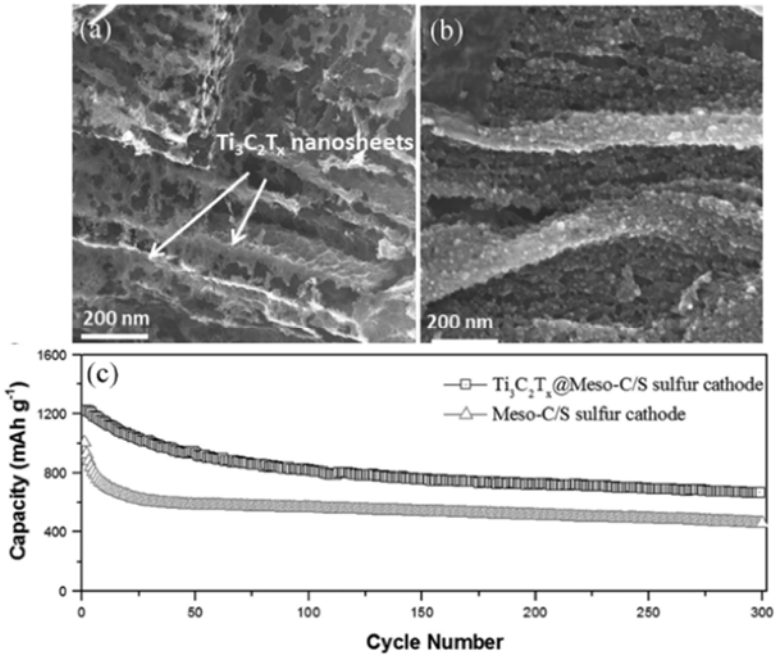

Figure 2.20. SEM images of (a) $Ti_3C_2T_x$@Meso-C; (b) $Ti_3C_2T_x$@Meso-C/S; and (c) Cycling performance of $Ti_3C_2T_x$@Meso-C/S and Meso-C/S at 0.5 C[197]. Reproduced with permission from Wiley-VCH Verlag GmbH & Co. KGaA.

2.3.1.3. Supercapacitor

Supercapacitors have attracted extensive attention as a power source for the electrical vehicles, electronic devices, *etc*. Unlike a common capacitor, supercapacitors can satisfy the criteria of high energy density and fast charge-discharge rate simultaneously. There exist two types of supercapacitors, *e.g.*, electric double layer capacitors (EDLCs) and Faradaic capacitors. Energy is stored on EDLCs by accumulation of electrostatic charge in the electric double layers at the electrolyte-electrode interface without electrochemical reactions. Carbonaceous materials are customarily utilized as the electrode materials for EDLCs. Faradaic capacitors store energy through pseudo-capacitive redox reaction at the electrode materials like metal oxides and heteroatom-doping carbon. MOFs-derived electrode materials for supercapacitors are summarized in Table 2.4 ([77, 78, 84, 88, 89, 95-97, 105, 124, 198-206]).

Porous carbons as the electrode can provide high surface area and rich porosity for ion

diffusion. Solvation shells form in the pores due to the ion diffusion, and are distorted when the pore size is below 2 nm, leading to closer distance between the ion center and electrode surface, thus improving the capacitance of a supercapacitor (Equation (2.1)).

$$C = \frac{\varepsilon A}{d} \qquad (2.1)$$

C: the capacitance of a supercapacitor; ε: electrolyte dielectric constant; *A*: electrode surface area accessible to electrolyte ions; *d*: small separation between electrolyte ions and porous carbon electrodes.

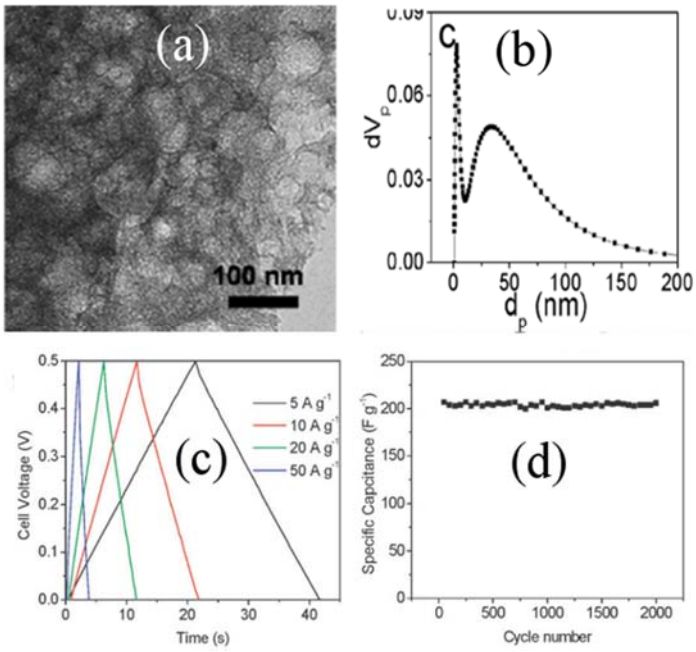

Figure 2.21. (a) TEM image of HPC; (b) Pore size distribution of HPC; (c) Galvanostatic charge-discharge curves of HPC at high current densities; (d) Cycling stability of HPC at 5 A g-1 for an electrochemical capacitor[198]. Acknowledgement to Royal Society of Chemistry.

Based on the conclusion above, nanoporous carbon (NPC) with a high specific surface area (1523 m^2 g^{-1}) and an average pore diameter of ~1 nm was fabricated by Salunkhe *et al.*, using ZIF-8 as the precursor[199]. High capacitances of 98 and 62 F g^{-1} were delivered at 0.5 and 5 A g^{-1}, respectively. A negligible loss of 8% after 2000 cycles was found, indicating an excellent

stability. Apart from micropores, large pores in carbons allow for the accommodation of solvation and diffusion layers, and shorten the ion diffusion length, which are also favorable for supercapacitors. Therefore, hierarchical porous carbon (HPC) with well- interconnected micro-, meso- and macropores was synthesized by pyrolysis ZIF-8 followed by KOH activation (Figure 2.21a-b). The specific capacitance reached 204 F g^{-1} at the current densities of 50 A g^{-1}, (Figure 2.21c)[198]. Moreover, excellent cycling stability can be found in Figure 2.21d. The synergistic effect of interconnected pores facilitated the ion mobility and charge storage, resulting in the fast kinetic, a high capacitance and a reliable stability.

Wang *et al.* added GO in MOF-5 as the precursors for porous carbon with "brick-and-mortar" architecture (C-GMOF), in which the mesoporous carbon derived from MOF-5 was confined in the conductive graphene sheets (Figure 2.22a)[201]. A specific capacity of 345 F g^{-1} at 2 mV s^{-1} and 99 % retention over 100000 cycles were realized, which were much higher than the traditional carbons derived from MOF-5 (C-MOF) and RGO. They pointed out that the "brick-and-mortar" structure was beneficial for fast ion diffusion, overcoming the problems of mass transport limitation of RGO and long ion diffusion pathway of C-MOF (Figure 2.22b). In order to investigate the effect of graphitic degree and heteroatom doping in the carbon, Tang *et al.* designed core-shell NC@GC derived from ZIF-8@ZIF-67 as discussed in Figure 2.6, showed a specific capacity of 270 F g^{-1} at 2 A g^{-1} and almost 100% of the capacitance was retained in 10000 cycles[97]. Besides EDLC, pseudocapacitance was also generated due to the nitrogen doping. The high graphitic degree in the GC shells improved the electrical conductivity of the system, and thus reduced the internal resistance, resulting in a high capacitance. Conclusively, the excellent supercapacitor performances of NC@GC are attributed to the proper balance between surface area, porosity, graphitic degree and N doping, which could be tuned by the thickness of GC shells.

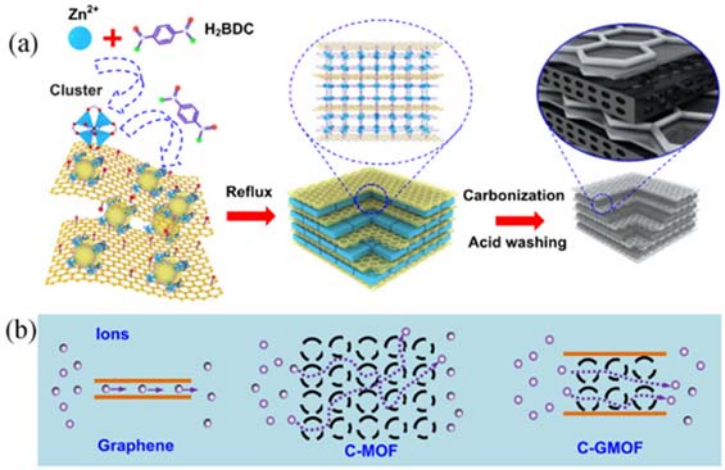

Figure 2.22. Schematic illustrations of (a) the fabrication process for C-GMOF; (b) ion diffusion into different pore-structure[201]. Reproduced with permission of Elsevier.

The specific pseudocapacitance is determined by the structure and constitution of the electrode materials. Hu *et al.* found that $Co_3O_4/NiCo_2O_4$ double-shelled nanocages exhibited a better pseudocapacitive performance compared with Co_3O_4 nanocages, due to more active sites and increased conductivity generated by the incorporation of Ni^{2+}, as well as the higher specific surface area[78]. The hollow porous nickel phosphate ($Ni_xP_yO_z$) derived Ni-MOF exhibited a specific capacitance of 1627 F g^{-1} at the current density of 1 A g^{-1}, as reported by Bendi *et al.*[84]. Apart from porous structure and high specific surface area (142 m^2 g^{-1}), the phosphate ions could improve the conductivity and enhance the faradaic reactions across the interface.

The energy density of the pseudocapacitor positively relates to the specific capacitance and potential window, as shown in Equation (2.2). Thereby, besides the specific capacitance, a wide potential window is essential to achieve high energy density. The charge storage efficiency sharply declines when the potential window expands. The metal oxides (like Co_3O_4, NiO, MnO_2, *etc.*) for the pseudocapacitor owned limited potential windows in certain electrolytes. Designing metal oxide composites for complementation of the potential windows is an effective approach to realize high energy density.

$$E = \frac{1}{2}CV^2 \qquad (2.2)$$

E: the energy density; C: the specific capacitance; V: the potential window.

Hu *et al.* synthesized starfish-shaped $Co_3O_4/ZnFe_2O_4$ hollow nanocomposite by pyrolysis of Co_3O_4/Fe^{III}-MOF-5 as discussed in Figure 2.4, exhibiting a higher specific capacity (326.7 F g^{-1} at the current density of 1 A g^{-1}) compared with the individual components (Co_3O_4: 142 F g^{-1}; $ZnFe_2O_4$: 112 F g^{-1}) due to the unique starfish structure, which provided more active sites and facilitated the electron transfer[77]. The potential window expanded to 1.35 V, and the enlarged potential window favoured the energy density of $Co_3O_4/ZnFe_2O_4$ to reach 82.5 Wh kg^{-1} at a power density of 675 W kg^{-1}, which outperformed that of pure Co_3O_4 (17.8 Wh kg^{-1} at a power density of 250 W kg^{-1}) and $ZnFe_2O_4$ (44.3 Wh kg^{-1} at a power density of 722.5 W kg^{-1}).

Incorporating carbon into metal oxides can improve the conductivity of the electrode and suppress the volume change during the charge-discharge process. Three-dimensional graphene network (3DGN) is expected to be a superb current collector for energy storage and conversion due to the large surface area as well as good mechanical and conductive properties. Ji *et al.* reported the production of 3DGN/Mn_2O_3 hybrids using Mn-MOF grown on 3DGN as the precursor, exhibiting a specific capacitance of 471.1 F g^{-1} at the current density of 0.2 A g^{-1}[1124]. The working electrodes could be used directly without any conductive material or binders due to the free-standing 3DGN in this study as the backbone. In addition, 3DGN facilitated the diffusion of electrolyte ions and buffered the volume expansion, resulting in the high specific capacitance and excellent stability. Harsh temperatures tolerance of the carbon and metal oxide composite was investigated by Meng *et al.* and the specific capacitance of Fe_3O_4/carbon composite derived from Fe-MIL-88B-NH_2 was tested at various temperatures[205]. The composite obtained a specific capacitance of 139 F g^{-1} at the current density of 0.5 A g^{-1} at 20

°C. Higher capacitance at elevated temperature was observed due to the reduced effective internal resistance from 0 to 60 °C. Excellent long-term stability was observed under a series of temperatures, with 83.3% retention of specific capacitance after 4000 cycles.

2.3.2. Environmental remediation

Environment issues have attracted considerable attention during the past few decades, and therein the remediation technology is a hotspot of scientific and industrial research. The pollutants in water including organic compounds, antibiotics and heavy metals have been causing adverse effects on human health. The widely used strategies on pollutant removal include adsorption, photodegradation and advanced oxidation. Therefore, the super adsorbents as well as the catalysts for photodegradation and advanced oxidation are demanded. In this section, the MOFs-derived materials for water treatment are reviewed.

2.3.2.1. Adsorption

Adsorption is popular for water purification due to the low cost, convenience and recycling. Various adsorbent materials, like carbon and carbon-metal oxide hybrids, have been explored. The pollutant removal can be realized by the interactions (*e.g.*, van der Waals force and π–π interactions) between adsorbents and pollutants. The sorption can be affected by the ambient temperature, solution pH value and ionic strength. The adsorption ability is generally evaluated by the adsorption capacity according to Equation (2.3).

$$q = \frac{(C_0 - C_t) \times V}{m} \qquad (2.3)$$

q: the adsorption capacity (mg/g); C_0: the initial concentration of pollutants in solution (mg/L); C_t: the concentration of pollutants in solution at time t (mg/L); m: the mass of the adsorbent (g); and V: the volume of the solution (L)

Carbon-based materials are expected to be promising adsorbents for removing pollutants in

water due to the high surface area, rich porosity and functional groups on the carbon. Li *et al.* tested the adsorption of ciprofloxacin (CIP) on ZIF-8-derived nanoporous carbon, showing a specific surface area of 750 $m^2 g^{-1}$ and total pore volume of 0.65 $cm^3 g^{-1}$ [207]. The adsorption capacity could reach 416.7 mg/g at an initial CIP concentration of 100 mg/L at pH 6.0. The hydrophobic and electrostatic interactions between CIP and carbon contributed to the adsorption. In addition, nitrogen atoms doped in the carbon increased the defects and induced higher adsorption energy.

Magnetic carbon composites are of great importance in the adsorption field due to their facile separation, besides the high surface area or conductivity originating from carbon. Banerjee *et al.* synthesized MOF-derived Fe_3O_4/C nanocomposite and the saturation magnetization of the composite reached 49 emu g^{-1}, which was strong enough to separate the adsorbent from solution. The hydrophobicity and polarity of the composite surface exerted great influence on the adsorption. Fe_3O_4/C exhibited to be a super-adsorbent for both superhydrophobic (oil and hydrocarbon) and less hydrophobic (dyes and phenol) pollutants *via* strong van der Waals force and π–π interactions, respectively[208]. The uniform disperse of metal species in the composites is favorable to the adsorption. Inspired by the fact, uniformly dispersed cobalt nanoparticles embedded in nanoporous carbon (Co/NPC) derived from ZIF-67 were synthesized and the saturation magnetization was 58.9 emu g^{-1}, facilitating the easy magnetic separation and recycling[209]. An adsorption capacity of 500 mg g^{-1} for methylene blue (MB) on Co/NPC was 10 times larger than that on activated carbon. During adsorption, MB interacted with carbon surface by the π–π interactions and was captured by Co nanoparticles through forming bi-dentate complexes due to an organic-ligand interaction corresponding to the Equations (2.4-2.7).

$$MB_{solution} \rightarrow MB^{+}_{(aq)} + Cl^{-}_{(aq)} \quad (2.4)$$

$$Co_{(solid)} + 2CoO_{(solid)} + 6Cl^{-}_{(aq)} + 24H_2O_{(l)} \rightarrow 3CoCl_2{\bullet}6H_2O_{(aq)} + [Co(H_2O)_6]^{+}_{(aq)} \quad (2.5)$$

$$[Co(H_2O)_6]^{+}_{(aq)} + 4Cl^{-}_{(aq)} \rightleftharpoons [CoCl_4]^{2-}_{(aq)} + 6H_2O_{(l)} \quad (2.6)$$

$$[CoCl_4]^{2-}_{(aq)} + 2MB^{+}_{(aq)} \rightarrow MB_2[CoCl_4]_{(aq)} \quad (2.7)$$

The bonding site on the adsorbents is as important as the specific surface area and porosity. Abney *et al.* synthesized MOF-derived $H_xNa_{1-x}InS_2$ *via* a wet-treatment process without carbonization or activation, showing a rapid sorption rate and a high adsorption capacity towards heavy metals in water like Hg^{2+}[210]. The Hg^{2+} removal was realized by the formation of bonding sites consisting of one Hg^{2+} and three equidistant S atoms. In addition, the porous structure favored the diffusion of Hg^{2+} through the adsorbent.

2.3.2.2. Photocatalytic degradation

Photocatalytic degradation of pollutants in wastewater is widely reported during the past few years. The mechanism of photodegradation is as below. (i) Under light irradiation, the electrons transit from the valence band (VB) to conduction band (CB), generating light-excited electrons (e^-) and holes (h^+). (ii) The electrons are trapped by the dissolved oxygen, forming superoxide anion. Meanwhile, the hydroxide ions and water are oxidized into hydroxyl radicals by holes. (iii) Finally, the pollutants, especially organic compounds, are decomposed into CO_2 and H_2O by superoxide and hydroxyl radicals. The bandgap of the photocatalysts, as well as the recombination rate of electrons and holes, determine the photocatalytic efficiency. In this section, the effort on MOFs-derived photocatalysts for water treatment is summarized.

The applications of photocatalysts like ZnO are restrained because of the wide bandgap (3.37 eV) and rapid recombination of light-excited electrons and holes. To address the problems, various strategies have been attempted, such as morphology modification and heteroatom

doping. In our previous work, we synthesized carbon and nitrogen co-doped ZnO by using ZIF-8 as the precursor, showing better photocatalytic effect on methylene blue (MB) degradation under sunlight-simulated irradiation compared with ZIF-8-derived ZnO[211, 212]. The light absorption threshold was extended inducing more light absorption. Meanwhile, the bandgap was narrowed, and thus more electrons and holes were excited, generating more free radicals to degrade the pollutant. Yang *et al.* synthesized ZnO/C derived MOF-5 *via* pyrolysis, exhibiting superb photocatalytic activity towards Rhodamine-B (RhB) degradation under UV irradiation comparable to commercial P25, due to the low recombination ability of photogenerated electrons and holes[213]. Chen *et al.* fabricated ZnO/C by water stream carbonization of ZIF-8, showing excellent photocatalytic degradation of under visible light irradiation, attributed to high porosity, high crystallinity degree of metal oxide and rich oxygen-containing functional groups in the N-doped carbon[109]. In addition, Zhu *et al.* revealed that the ZIF-8-derived ZnO incorporated by GO showed enhanced photocatalytic effect on MB degradation under visible light irradiation, compared to pure ZnO[214]. The participation of GO facilitated the photocatalytic reaction by improving light absorption, separating the electrons and holes as well as hindering the recombination of charge carriers.

Incorporating metal species into the photocatalysts is also an effective route to improve the photocatalytic performance. Zhang *et al.* fabricated magnetic Fe_3O_4@C/Cu nanocomposites by thermal conversion of Fe_3O_4@HKUST-1 microspheres, showing a much better photocatalytic effect on MB degradation under visible light in the presentation of H_2O_2 in comparison with Fe_3O_4@CuO, g-C_3N_4 and TiO_2[215]. The carbon acted as the photosensitizer as well as adsorbent of MB. H_2O_2 was the provider of hydroxyl radicals ($OH^{\bullet}$) by reduction. The copper nanoparticles (Cu NPs) would induce the equilibrium of Fermi level which was close to the conduction band of Fe_3O_4 and accept the photo-excited electrons from Fe_3O_4, resulting in rapid electron transfer and hindering the recombination of holes and electrons (Figure 2.23a).

The photocatalytic activity of Ag/ZnO/$ZnFe_2O_4$ hollow nanocubes derived from Ag-ZnPBA was reported by Wu *et al.* and the reaction constant of MB degradation on Ag/ZnO/$ZnFe_2O_4$ was much higher than that of ZnO/$ZnFe_2O_4$ under simulated sunlight irradiation[216]. The optimal Ag and ZnO contents loading on $ZnFe_2O_4$ facilitated the photocatalytic activity as shown in Figure 2.23b. On one hand, a type-II band alignment formed during the coupling of ZnO and $ZnFe_2O_4$. The electrons transited to CB of ZnO, leaving the holes in the VB of $ZnFe_2O_4$. As a result, the light-induced electron-hole pairs were separated. On the other hand, some of the light-excited electrons transferred to the surface of silver and trapped due to Schottky barrier forming between ZnO and Ag. Therefore, the recombination of electrons and holes could be effectively suppressed.

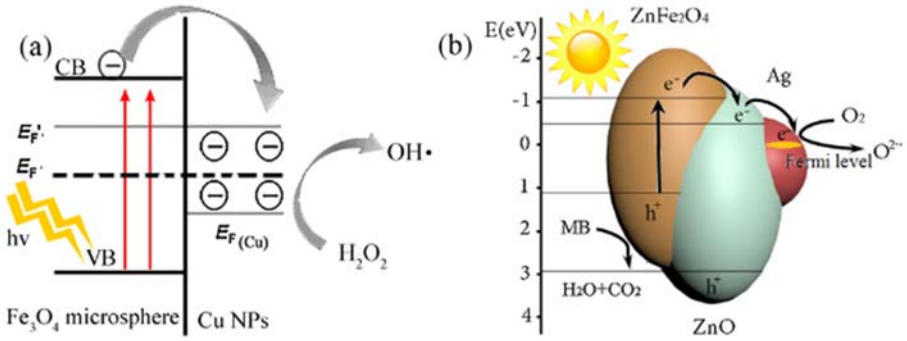

Figure 2.23. The proposed degradation mechanism of organic pollutants over (a) Fe_3O_4@C/Cu (EF and EF' refer to Fermi levels of Fe_3O_4 before and after equilibrium)[215], reproduced with permission of Elsevier; and (b) Ag/ZnO/$ZnFe_2O_4$[216]. Reproduced with permission of Elsevier.

2.3.2.3. Catalytic oxidation

Advanced oxidation processes (AOPs) have been highly valued, as the pollutants can be decomposed completely through AOPs. The superoxides, such as hydrogen peroxide (H_2O_2), ozone (O_3), peroxymonosulfate (PMS), and persulfate (PS), are being employed for oxidation. Free radicals, such as hydroxyl ($HO^{\bullet}$) and sulfate ($SO_4^{\bullet-}$) radicals, are generated to degrade the target pollutants. In order to boost the reaction rate, catalysts for efficient activation of the

superoxides are demanded. Metal-based and metal-free catalysts have been investigated in the past decades. In this section, MOFs-derived catalysts to initiate the AOPs are reviewed.

Large-pore Mn_3O_4 derived from Mn-MOF exhibited a high catalytic activity towards methylene blue degradation in the presence of H_2O_2 as the oxidant[217]. It was verified that the large mesopores and surface area facilitated the mass transfer during the catalytic reaction, and thus boosted the pollutant removal. Li *et al.* synthesized $Fe_xCo_{3-x}O_4$ nanocages templated by FeCo-PB for PMS activation, showing excellent catalytic degradation of bisphenol A (BPA) due to the generation of $SO_4^{\bullet-}$ and $OH^{\bullet}$ radicals[218]. The catalytic reaction performed on the surface of the catalyst and octahedral (B-site) Co^{II} was considered to be the main contributor to the outstanding catalytic effect. The reaction principle is shown as Equations (2.8-2.12): B-site Co^{II} was oxidized into Co^{III} by the HSO_5^- species adsorbing on the surface of the catalyst, and subsequently reduced to Co^{II} by accepting electrons from the lattice oxygen (O_β) in order to maintain the charge balance; finally, the $SO_4^{\bullet-}$ and $OH^{\bullet}$ radicals produced during the redox reactions degraded BPA into small organic intermediates or CO_2.

$$\equiv Co^{II} + HSO_5^- \rightarrow \equiv Co^{III} + SO_4^{\bullet-} + OH^- \quad (2.8)$$

$$SO_4^{\bullet-} + OH^- \rightarrow SO_4^{2-} + OH^{\bullet} \quad (2.9)$$

$$\equiv Co^{III} + HSO_5^- \rightarrow \equiv Co^{II} + SO_5^{\bullet-} + H_2O \quad (2.10)$$

$$SO_5^{\bullet-} + O_\beta \rightarrow SO_4^{\bullet-} + O_2 \quad (2.11)$$

$$SO_4^{\bullet-}/\ OH^{\bullet} + BPA \rightarrow CO_2 + \text{intermediates} \quad (2.12)$$

In order to protect the metal-based catalysts from leaching and improve the cycling performance, then incorporation of carbon in the catalysts is proposed. Li *et al.* synthesized graphene-encapsulated transition-metal nitrides ($Fe_xMn_{6-x}Co_4$-N@C) by one-step carbonization of FeMnCo-PB for PMS activation[219]. The catalyst showed superb effect on the

removal of BPA in the presence of PMS, due to the production of $SO_4^{\bullet-}$ and $OH^{\bullet}$ radicals. The Mn_4N was the main contributor for the high performance by lowering the adsorption energy and boosting the electron transfer. The high stability of $Fe_xMn_{6-x}Co_4$-N@C on BPA degradation was attributed to the well-developed graphene shells. They also proposed the catalytic activity of Fe_xCo_y@C derived from FeCo-PB on BPA degradation, showing good cycling performance due to the protection of graphene shell encapsulating metals[220]. Lin *et al.* synthesized magnetic cobalt-graphene (MPG) derived from ZIF-67/GO for peroxymonosulfate (PMS) activation, showing the enhanced catalytic effect on the decolorization of acid yellow (AY) dye in water which was attributed to the synergistic effect of cobalt and RGO[221]. High and stable regeneration efficiency (97.6%) over 50 cycles was obtained, suggesting excellent long-term recyclability of MPG.

In our previous work, we discussed the activities of carbonaceous catalysts derived from MOFs for wastewater treatment. Nitrogen-doped graphene was synthesized by pyrolysis of MIL-100 (Fe) and nitrogen sources (DCDA, melamine and urea) followed by acid washing, showing an excellent catalytic effect on organic pollutants (phenol and *p*-Hydroxylbenzoic acid) degradation[222, 223]. The nitrogen doping, as well as surface area and graphitic degree of carbon, imposed the significant influence on the efficiency of pollutant removal. Besides $SO_4^{\bullet-}$ and $OH^{\bullet}$ radicals, singlet oxygen was also found during the PMS activation attributed to the defective edge and nitrogen doping, and played the dominating role on the pollutant degradation. Previously, singlet oxygen was reported to be generated during PMS activation by homogeneous catalysis in alkaline solutions, such as ketone, cyclohexanone and benzoquinone as the catalysts[224, 225, 226]. Nonradical pathway was proposed besides the generation of hydroxyl and sulfate radicals, but the active species were not specified[227]. Therefore, singlet oxygen was firstly observed to be generated, and work during heterogeneous catalysis. The active sites on the catalysts which were responsible for the generation of singlet

oxygen were also clarified. Unlike the unselective property of hydroxyl and sulfate radicals, singlet oxygen could selectively degrade a variety of pollutants in the presence of background matters. The finding has the great significance for the development of PMS oxidations by carbon-based materials in environmental science, such as contaminant removal, soil and wastewater remediation, and bacterial inactivation.

2.4. Summary and perspectives

Functional materials are always the research hotspot in various fields. Metal-organic frameworks (MOFs) are fascinating precursors or templates for a rational design of functional materials, due to the reasonable compositions and tuneable structures. Apart from pristine MOFs, the modified MOFs by in-situ or post treatment are also explored as the precursors.

In this review, the recent progress from synthesis to the applications of MOFs-derived materials in electrochemical and environmental fields has been summarized. Metal-based materials, including (mixed) metal oxides, metal nitride, metal carbide, metal sulfide and so on, are fabricated using pristine MOFs, multi-metallic MOFs, and MOFs modified as the additional precursors. The as-derived metallic materials reveal abundant morphologies and structures, as well as the controllable components. The MOFs-derived carbon materials, such as amorphous carbon, graphene, carbon nanotubes, carbon wires and carbon sheets, exhibit various advantages such as high specific areas, rich porosity, high graphitic degree in comparison with the nanocarbons synthesized by other methods. In addition, heteroatoms (N, P, S and B) doping into carbon is also realized, as the rich porosity and open channels of MOFs enable the alien molecules to access. The carbon and metal oxide composites derived from MOFs are developed, in which the aggregation of metal oxides is suppressed. Furthermore, strategies for modulating the morphology, structure and components are reported.

The applications in electrochemical energy storage of the MOFs-derived materials are

reviewed from the points of fuel cells, batteries and supercapacitors. The factors, such as specific surface area, pore volume and size distribution, graphitic degree, heteroatom doping, and inner structures, determine the electrochemical efficiency. Therefore, the efficiency-oriented MOFs-derived functional materials are synthesized, showing excellent electrochemical performances. Furthermore, the applications in environmental remediation by means of adsorption, photocatalytic reaction and advanced oxidation processes are also summarized. The pollutants are effectively removed by physical and chemical processes.

Despite the rapid and great progress has been made in the derivatives of MOFs during the past few decades, challenges in materials synthesis are still existing, such as the precise control on the structure and composition of the derivatives, despite that the removal of templates is avoided and the synthetic ways are facile. In the future, the changes of structures during pyrolysis and the relationship between structures and synthesis parameters (like temperature, atmosphere, time, routes, *etc.*) should be clarified. In addition, modification of precursors is another direction. More MOFs precursors with reasonable structures, components and morphologies are still needed to be further explored.

Apart from materials synthesis, the applications of MOFs-derived materials also need the in-depth and in-width study. The active sites, as well as the influences of structures on the electrochemical activity, should be further investigated. Moreover, the stability of catalysts, especially under harsh environment, needs more attention in the future. Furthermore, the application of MOFs-derived materials in environment field is less reported previously. As the components and structures of MOFs-derived materials are various and relatively controllable, the catalytic activities of the derivatives and mechanisms in environmental remediation are worthy of study.

Table 2.1. ORR, OER and HER performances of MOFs-derived materials.

Samples	Precursors	SSA ($m^2 g^{-1}$)	N, P, S (at.%)	Loading (mg cm^{-2})	Electrolyte	ORR (V)		OER (V)		HER (mV)		References
						E_{onset}	$E_{1/2}$	E_{onset}	$E_{j=10}$	E_{onset}	$E_{j=10}$	
Fe-NC	FeIM/ZIF-8	572	N:4.5	0.4	0.1 M $HClO_4$	0.915						132
Fe-NC	Fe-doped ZIF-8	969	N:4.2	0.56	0.1 M $HClO_4$	0.95	0.82					116
N-Fe/Fe_3C@C/RGO	PB/GO	64	N:3.7	0.7	0.1 M KOH	1	0.93					126
Fe-N/C-CNT	Fe-ZIF-8 /FA/CNT	507.66	N:8.8	0.5	0.1 M $HClO_4$		0.8					133
Fe/N-CNT	Zn-Fe-ZIF /DCDA	151	N:12.27 wt.%	0.57	0.1 M KOH		-0.183 *vs.* [a]SCE					98
Co-NC	ZIF-67	501.7		0.36	0.1 M KOH	0.93						134
Co-NC	ZnCo-MOF	484	N:8.5 wt.%	0.283	0.1 M KOH	0.982	0.871					111
				0.6	0.1 M phosphate buffer		0.731					
				0.6	0.1 M $HClO_4$		0.761					
N,P-Co/C	ZnCo-ZIF /TPP[b]		N:2.8 P:0.25	0.1	0.1 M KOH	0.93	0.85					135
Co_3O_4@NC	Co-I-MOF			0.85	0.1 M KOH	0.95						136
Co-NC	ZIF-67 /CoAl-LDH	220	N:4.81	0.2	0.1 M KOH	0.94						131
CoZn-C	CoZn-ZIF-8/ CoAl-LDH	429	N:6.94	0.2	0.1 M KOH	0.976	0.849					85
Co-N/CNF	ZnCo-ZIF @$mSiO_2$	1170	N:7.807	0.12	0.1 M KOH	0.883	0.8103					113
Co-NC microtubes	ZIF-67/cobalt oxalate microtubes	520	N:2.64	0.1	0.1 M KOH	0.973	0.871					121

Table 2.1. ORR, OER and HER performances of MOFs-derived materials (continued).

Samples	Precursors	SSA ($m^2 g^{-1}$)	N, P, S (at.%)	Loading (mg cm^{-2})	Electrolyte	ORR (V)		OER (V)		HER (mV)		References
						E_{onset}	$E_{1/2}$	E_{onset}	$E_{j=10}$	E_{onset}	$E_{j=10}$	
CoFe-NC	PANI[c]/PB	701.6	N:2.7	0.36	0.1 M KOH		0.85					137
Cu-NC	Cu-ZIF-8	1071	N:4.07	0.2	0.1 M KOH	-0.067 *vs.* SCE	-0.156 *vs.* SCE					138
Graphene/ graphene tube	Co-MOF/ DCDA/iron acetate	449	N:2.69	1	0.1 M KOH		0.88					99
Carbon framework	ZIF-8/PVP	396	N:8.49	0.25	0.1 M KOH	0.83	0.752					92
P-carbon nanofiber	Te-ZIF-8/TPP	1417	P:0.51	0.1	0.1 M KOH	0.881	0.79					104
Graphene/carbon sheet	ZIF-8/GO	911	N:4.38	0.2	0.1 M KOH	0.957						102
Graphene/NC	ZIF-8@GO	917	N:6.12	0.25	0.1 M KOH	0.88	0.75					103
NC/CNT	MOF-5/ urea/nickel formate	1053	N:5.04 wt.%	0.1	0.1 M KOH	-0.051 *vs.* Ag/AgCl	-0.172 *vs.* Ag/AgCl					101
Zn-doped $CeSe_2$	ZnCo-ZIF/selenium on CFC				1 M KOH			1.347	1.586			130
CoNi-hydroxide	CoNi-MOF			0.2	1 M KOH			1.48	1.554			139
$Co_3O_4/NiCo_2O_4$	ZIF- 67/ NiCo-LDH	46		1	1 M KOH			1.53	1.57			78
Ni-Co mixed metal oxides	NiCo-PBA	30.8			1 M KOH				1.61			73
$Fe_{0.5}Ni_{0.5}O_x$	FeNi-MOF	38.4		0.35	0.1 M KOH			1.63	1.814			140
$Co_{0.85}Se$@C	ZIF-67/ NaHSe	13.56	N:3.44	0.136	1 M KOH			1.52	1.59			141

Table 2.1. ORR, OER and HER performances of MOFs-derived materials (continued).

Samples	Precursors	SSA ($m^2 g^{-1}$)	N, P, S (at.%)	Loading (mg cm^{-2})	Electrolyte	ORR (V)		OER (V)		HER (mV)		References
						E_{onset}	$E_{1/2}$	E_{onset}	$E_{j=10}$	E_{onset}	$E_{j=10}$	
FeNi/$NiFe_2O_4$@NC	FeNi-MOF	26.7		0.13	1 M KOH				1.546			142
CoFe-P	CoFe-MOF/NaH_2PO_2			0.424	1 M KOH			1.43	1.49			143
CoFe-NC	Co-doped NH_2-MIL-53	235.37		0.071	0.1 M KOH				1.62			144
Ni-P	NiNi-PBA/ NaH_2PO_2	35	P:21.33	0.2	1 M KOH			1.48	1.53			145
NiS@N, S-C	Ni-MOF		N:11.11 S:5.33	0.2	1 M KOH			1.54	1.647			146
$Co_{0.59}Fe_{0.41}P$	CoFe-PBA/ NaH_2PO_2	11.5		0.35	1 M KOH					-39	-92	147
					0.5 M H_2SO_4					-31	-72	
$Zn_{0.30}Co_{2.70}S_4$	ZnCo-MOF /thioacetamide	125		0.285	1 M KOH						-85	83
					0.1 M phosphate buffer						-90	
					0.5 M H_2SO_4						-80	
Co@N,B-C	ZIF-67/H_3BO_3	191.25	N:3 B:0.7		0.5 M H_2SO_4					~0	-96	127
					1 M KOH						-183	
Ni-Co-P	NiCo-PBA/ NaH_2PO_2	22		0.286	1 M KOH						-150	148
FeCo@ NG	$Fe_3[Co(CN)_6]_2$	66.2	N:8.2	0.285	0.5 M H_2SO_4					-88	-262	149
PdCo@NC	Pd_xCo_{3-x} $[Co(CN)_6]_2$	57.13		0.285	0.5 M H_2SO_4						-80	150
$CoSe_2$@CNT	Se-ZIF-67		N:4.4	0.357	0.5 M H_2SO_4					-40	-132	151
Co_3O_4C-NA	Co-MOF on Cu foil	251		0.2	0.1 M KOH		0.78	1.47	1.52			128

Table 2.1. ORR, OER and HER performances of MOFs-derived materials (continued).

Samples	Precursors	SSA ($m^2 g^{-1}$)	N, P, S (at.%)	Loading (mg cm^{-2})	Electrolyte	ORR (V)		OER (V)		HER (mV)		References
						E_{onset}	$E_{1/2}$	E_{onset}	$E_{j=10}$	E_{onset}	$E_{j=10}$	
Co@Co_3O_4/CNT-NC	ZIF-67	111	N:1.26	0.21	0.1 M KOH		0.8	1.56	1.65			119
Co@NC	Co-MOF	110.8	N:1.62	0.407	0.1 M KOH	0.88			1.61			152
$Ni_xCo_yO_4$/Co-NG	Ni-ZIF-67/GO	480.8	N:6.04	0.2	0.1 M KOH		0.804		1.629			153
NC/graphene	ZIF-8/GO	1094.3	N:4.42	0.4	0.1 M KOH	1.01	0.8		1.63			154
NCNTFs	ZIF-67	513	N:2.4	0.2	0.1 M KOH	0.97	0.87		1.6			100
NC@GC	ZIF-8@ ZIF-67			0.25	0.1 M KOH 1 M KOH	1	0.93		1.57			155
N,B-co-doped carbon	Zn-MOF	1348	N:7.29 wt.% B:5 wt.%	0.4	0.1 M KOH	0.894	0.793	1.38				156
Co-P/NC	ZIF-67/ NaH_2PO_2	183		0.283	1 M KOH			1.5	1.584		-191	157
CoP/RGO	ZIF-67/ GO/NaH_2PO_2			0.28	1 M KOH				1.57		-150	158
CoP	ZIF-67/ NaH_2PO_2	46.9		0.102	0.5 M H_2SO_4 1 M KOH			1.53	1.63	-35	-159	159
Co/Co_9S_8@SNGS	Co-MOF/GO	246.9	N:1.9 S:1.46	0.305	0.1 M KOH				1.52	-150		116

[a]SCE: saturated calomel electrode

[b]TPP: triphenylphosphine

[c]PANI: polyanilin

Table 2.2. The performances of MOFs-derived anode materials.

Samples	**Precursors**	**Battery**	**SSA** ($m^2 g^{-1}$)	**Current density** ($mA g^{-1}$)	**Capacity** ($mA h g^{-1}$)	**Cycle life**	**Reference**
ZnO QDs/C	IRMOF-1	LIB	513	75	1200	50	107
ZnO/C	ZIF-8@chitosan	LIB	90	50	750	50	164
ZnO@ZnO QDs/C	ZnO@ZIF-8 on CC	LIB		500	699	100	129
NiO@C	Ni-MOF	LIB	182.65	1 C	960	200	165
NiSb/C	Ni-MOF/$SbCl_3$	LIB	116.9	100	497.3	100	166
ZnO/$ZnFe_2O_4$/C	Fe^{III}-modified MOF-5	LIB	140	500	1390	100	43
ZnO/$ZnFe_2O_4$/C	ZnCo-MOF	LIB	27.9	500	669	250	167
CuO/Cu_2O/C	Cu-MOF	LIB	6.387	60	887.3	200	168
		SIB		50	302.9		
SnO_2@C	Sn-HKUST-1	LIB	64	100	900	50	169
MnO@$ZnMn_2O_4$/NC	α-MnO_2/ZIF-8	LIB	21.78	50	803	100	170
Fe_3O_4/VO_x@C	PB/$NaVO_4$/polydopamine	LIB	94	500	742	400	171
Fe_3O_4@C/NG	GO/NH_2-MIL-88-Fe	LIB	86.4	10000	458	1000	125
Fe-Fe_3C/NG	MIL-100/DCDA	LIB		1000	607	100	172
Fe_2O_3/3DGN	MIL-88-Fe/3DGN	LIB		200	863	50	122
CoO/NC	ZIF-67	LIB	364	100	1383	200	118
graphene/Co_3O_4	GO/ZIF-67	LIB		200	908	100	123
RGO/MnO_2-Co_3O_4	GO/MnO_2-ZIF-67	LIB		500	577.4	400	173
CoZnS@NSC-CNT	CoZn-ZIF-67/S	LIB	75	100	941	250	120
NC	ZIF-8	LIB	634.6	500	1147	200	174
NC/graphene	ZIF-8@GO	LIB	872	500	1070	100	148
TiO_2	MIL-125 (Ti)	LIB	220	1 C	166.2	500	175
Co_3O_4	MOF-71	LIB	59	200	913	60	176
Co_3O_4	ZIF-67	LIB	45	100	1335	100	58
Co_3O_4	ZIF-67	LIB	54.5	100	780	100	59
Co_3O_4	Co-MOF	LIB	20.1	100	1370	30	60
Co_3O_4/3DNF	ZIF-67/3DNF	LIB		5000	976	500	177
CoS_2	ZIF-67/thioacetamide	LIB	28.1	1000	737	200	82
$Zn_xCo_{3-x}O_4$	ZnCo-ZIF	LIB	65.58	100	990	50	66
ZnO/$ZnCo_2O_4$	ZnCo-MOF	LIB	20	2000	1016	250	68

Table 2.2. The performances of MOFs-derived anode materials (continued).

Samples	**Precursors**	**Battery**	**SSA** ($m^2 g^{-1}$)	**Current density** ($mA g^{-1}$)	**Capacity** ($mA h g^{-1}$)	**Cycle life**	**Reference**
$Co_3V_2O_8$	Co-V-MOF	LIB	8	200	980	140	178
α-Fe_2O_3	MIL-88-Fe	LIB	75	200	911	50	54
β-Fe_2O_3/γ-Fe_2O_3	PB	LIB	25.4	200	945	30	55
Fe_2O_3/SnO_2	PB/K_2SnO_3	LIB	43	200	500	100	56
$NiFe_2O_4$/Fe_2O_3	Fe_2Ni MIL-88/Fe MIL-88	LIB	39.2	100	936.9	100	179
Fe_2O_3@$NiCo_2O_4$	$Co_3[Fe(CN)_6]_2$@ $Ni_3[Co(CN)_6]_2$	LIB	12.72	100	1079.6	100	72
$NiCo_2O_4$/NiO	ZIF-67/$Ni(NO_3)_2$	LIB	126.3	200	1497	100	79
$NiCo_2O_4$	PB/nickel acetate	LIB		1000	841	100	79
CuO	Cu-MOF	LIB		100	484.2	40	61
CuO	Cu-MOF	LIB	49.6	100	470	100	62
CuO@NiO	CuNi-MOF	LIB	16.3	100	1061	200	76
CuO/Cu_2O	Cu-MOF	LIB	9	100	740	250	63
Mn_2O_3	Mn-MOF	LIB		1000	819.8	1200	65
ACN/ZnO	ZIF-8	SIB	427	1670	175	2000	180
CuO/Cu_2O	Cu-MOF	SIB	10.65	50	415	50	181
CuO/Cu_2O/RGO	Cu-MOF/GO	LIB		200	1490	220	182
		SIB		500	~250	3400	
G-NC@TiO_2	GO@NH_2-MIL-125 (Ti)	SIB	154.8	1000	120	5000	183
NiO/Ni/graphene	Ni-MOF	LIB	104	2000	962	1000	184
		SIB		1000	248	190	
CoSe/NC	ZIF-67/Se	SIB	154.2	500	531.6	50	185
Co_3ZnC/CNT-NCCP	ZnCo-ZIF	LIB	87	500	754	200	186
		SIB		200	500		
CPC	MOF-5	SIB	2316	100	240	100	187

Table 2.3. The performances of MOF-derived cathode materials on LSBs.

Samples	**Precursors**	**SSA** ($m^2 g^{-1}$)	**Current density** (mA g^{-1})	**Capacity** (mA h g^{-1})	**Cycle life**	**Reference**
Microporous carbon	ZIF-8	849	100	210	100	188
NC	ZIF-8	1104.5	335	936.5	100	189
Carbon	Zn-MOF	4793	400	662.3	40	190
Multi-wall CNT@Meso-C	Multi-wall CNT@MOF-5		0.5 C	540	50	191
GO@Meso-C	GO@MOF-5	394	0.2 C	820	100	192
TiO_2	MIL-125 (Ti)	20	1000	675	500	193
Co-N-GC	ZIF-67	308.89	0.2 C	850	200	194
Co-NC	ZIF-67		0.5 C	702	250	195
C-Co-N	ZIF-67	282.6	0.2 C	929.6	300	196
GO@C-Co	GO@ZIF-67	292.6	300	949	300	127
$Ti_3C_2T_x$@Meso-C	$Ti_3C_2T_x$@Meso-MOF-5	1531.9	0.5 C	704.6	300	197

Table 2.4. The performances of MOFs-derived materials on supercapacitors.

Samples	**Precursors**	**SSA** (m^2g^{-1})	**Electrolyte**	**Electrode number**	**Current density** ($A\ g^{-1}$)	**Specific capacitance** ($F\ g^{-1}$)	**Reference**
HPC	ZIF-8	2972	1 M H_2SO_4	2	50	204	198
NPC	ZIF-8	1523	1 M H_2SO_4	2	0.5	98	199
NPC	ZIF-8	1075	0.5 M H_2SO_4	3	5 mV/s	214	88
HPC	ZIF-8	1056	6 M KOH	3	0.5	332	200
NPC	ZIF-67	943	0.5 M H_2SO_4	2	2	62	96
NC	ZIF-8/sucrose	934	6 M KOH	3	0.1	285.8	89
C-GMOF	MOF-5/GO	979	6 M KOH	3	2 mV/s	345	201
Carbon	Al-PCP	1103	30 wt.% KOH	3	0.1	232.8	202
Carbon	Cu@NH_2-Al-MIL-101	1397	1 M H_2SO_4	2	10 mV/s	185	95
NC@GC	ZIF-8@ZIF-67	1276	1 M H_2SO_4	3	2	270	97
Graphene nanoribbon	MOF-74 Rod	1492	1 M H_2SO_4	2	0.05	198	105
CeO_2	Ce-MOF	77	3 M KOH + 0.1 M $K_4Fe(CN)_6$	3	0.2	1204	203
Co_3O_4	Co-MOF	21.5	6 M KOH	3	1	208	204
$Co_3O_4/ZnFe_2O_4$	Co_3O_4/Fe^{III}-MOF-5	46.2	6 M KOH	3	1	326.7	77
$Co_3O_4/NiCo_2O_4$ DSNC	ZIF-67/Ni-Co LDH	46	2 M KOH	3	5	972	78
$Ni_xP_yO_z$	Ni-MOF/NaH_2PO_4	142.24	2 M KOH	3	1	1627	84
3DGN/Mn_2O_3	3DGN/Mn-MOF		0.5 M Na_2SO_4	3	0.2	471.1	124
Fe_3O_4/C	NH_2-Fe-MIL-88B	37.7	1 M KOH	3	0.5	139	205
$Cu_{1.96}S$-C	HKUST-1	140.4	1 M H_2SO_4	3	0.5	200	206

2.5. References

1. S. Kitagawa, R. Kitaura and S.I. Noro, Angew. Chem., Int. Ed., 2004, **43**, 2334-2375.
2. J. R. Long and O. M. Yaghi, *Chem. Soc. Rev.*, 2009, **38**, 1213-1214.
3. A. M. Spokoyny, D. Kim, A. Sumrein and C. A. Mirkin, *Chem. Soc. Rev.*, 2009, **38**, 1218-1227.
4. S. T. Meek, J. A. Greathouse and M. D. Allendorf, *Adv. Mater.*, 2011, **23**, 249-267.
5. H. L. Jiang and Q. Xu, *Chem. Commun.*, 2011, **47**, 3351-3370.
6. M. O'Keeffe, *Chem. Soc. Rev.*, 2009, **38**, 1215-1217.
7. D. J. Tranchemontagne, J. L. Mendoza-Cortes, M. O'Keeffe and O. M. Yaghi, *Chem. Soc. Rev.*, 2009, **38**, 1257-1283.
8. J. J. t. Perry, J. A. Perman and M. J. Zaworotko, *Chem. Soc. Rev.*, 2009, **38**, 1400-1417.
9. H. Furukawa, N. Ko, Y. B. Go, N. Aratani, S. B. Choi, E. Choi, A. O.Yazaydin, R. Q. Snurr, M. O'Keeffe, J. Kim and O. M. Yaghi, *Science*, 2010, **329**, 424-428.
10. O. K. Farha, A. Özgür Yazaydın, I. Eryazici, C. D. Malliakas, B. G. Hauser, M. G. Kanatzidis, S. T. Nguyen, R. Q. Snurr and J. T. Hupp, *Nat. Chem.*, 2010, **2**, 944-948.
11. O. K. Farha, I. Eryazici, N. C. Jeong, B. G. Hauser, C. E. Wilmer, A. A. Sarjeant, R. Q. Snurr, S. T. Nguyen, A. Ö. Yazaydın and J. T. Hupp, *J. Am. Chem. Soc.*, 2012, **134**, 15016-15021.
12. J. R. Li, J. Sculley and H. C. Zhou, *Chem. Rev.*, 2012, **112**, 869-932.
13. D. Zhao, D. Yuan and H.-C. Zhou, *Energy Environ. Sci.*, 2008, **1**, 222-235.
14. N. C. Burtch, H. Jasuja and K. S. Walton, *Chem. Rev.*, 2014, **114**, 10575-10612.
15. J. Canivet, A. Fateeva, Y. Guo, B. Coasne and D. Farrusseng, *Chem. Soc. Rev.*, 2014, **43**, 5594-5617.
16. L. E. Kreno, K. Leong, O. K. Farha, M. Allendorf, R. P. Van Duyne and J. T. Hupp, *Chem. Rev.*, 2012, **112**, 1105-1125.

17. B. Chen, Y. Yang, F. Zapata, G. Lin, G. Qian and E. B. Lobkovsky, *Adv. Mater.*, 2007, **19**, 1693-1696.

18. S. Achmann, G. Hagen, J. Kita, I. M. Malkowsky, C. Kiener and R. Moos, *Sens.*, 2009, **9**, 1574-1589.

19. P. Horcajada, R. Gref, T. Baati, P. K. Allan, G. Maurin, P. Couvreur, G. Férey, R. E. Morris and C. Serre, *Chem. Rev.*, 2012, **112**, 1232-1268.

20. P. Horcajada, T. Chalati, C. Serre, B. Gillet, C. Sebrie, T. Baati, J. F. Eubank, D. Heurtaux, P. Clayette, C. Kreuz, J.-S. Chang, Y. K. Hwang, V. Marsaud, P.-N. Bories, L. Cynober, S. Gil, G. Ferey, P. Couvreur and R. Gref, *Nat. Mater.*, 2010, **9**, 172-178.

21. J. Della Rocca, D. Liu and W. Lin, *Acc. Chem. Res.*, 2011, **44**, 957-968.

22. L. Ai, C. Zhang, L. Li and J. Jiang, *Appl. Catal., B*, 2014, **148-149**, 191-200.

23. L. Chen, Y. Peng, H. Wang, Z. Gu and C. Duan, *Chem. Commun.*, 2014, **50**, 8651-8654.

24. L. Hamidipour and F. Farzaneh, *React. Kinet., Mech. Catal.*, 2013, **109**, 67-75.

25. J. H. Wang, M. Li and D. Li, *Chem. Eur. J.*, 2014, **20**, 12004-12008.

26. B. Liu, F. Yang, Y. Zou and Y. Peng, *J. Chem. Eng. Data*, 2014, **59**, 1476-1482.

27. R. Ameloot, L. Stappers, J. Fransaer, L. Alaerts, B. F. Sels and D. E. De Vos, *Chem. Mater.*, 2009, **21**, 2580-2582.

28. R. Ameloot, L. Pandey, M. V. d. Auweraer, L. Alaerts, B. F. Sels and D. E. De Vos, *Chem. Commun.*, 2010, **46**, 3735-3737.

29. R. Ranjan and M. Tsapatsis, *Chem. Mater.*, 2009, **21**, 4920-4924.

30. Y. Hu, X. Dong, J. Nan, W. Jin, X. Ren, N. Xu and Y. M. Lee, *Chem. Commun.*, 2011, **47**, 737-739.

31. P. Falcaro, A. J. Hill, K. M. Nairn, J. Jasieniak, J. I. Mardel, T. J. Bastow, S. C. Mayo, M. Gimona, D. Gomez, H. J. Whitfield, R. Riccò, A. Patelli, B. Marmiroli, H. Amenitsch, T. Colson, L. Villanova and D. Buso, *Nat. Commun.*, 2011, **2**, 237.

32. R. Ricco, L. Malfatti, M. Takahashi, A. J. Hill and P. Falcaro, *J. Mater. Chem. A*, 2013, **1**, 13033-13045.

33. K. Khaletskaya, J. Reboul, M. Meilikhov, M. Nakahama, S. Diring, M. Tsujimoto, S. Isoda, F. Kim, K. I. Kamei, R. A. Fischer, S. Kitagawa and S. Furukawa, *J. Am. Chem. Soc.*, 2013, **135**, 10998-11005.

34. Y. Wei, S. Han, D. A. Walker, P. E. Fuller and B. A. Grzybowski, *Angew. Chem., Int. Ed.*, 2012, **51**, 7435-7439.

35. Q. L. Zhu and Q. Xu, *Chem. Soc. Rev.*, 2014, **43**, 5468-5512.

36. J. Cravillon, S. Munzer, S. J. Lohmeier, A. Feldhoff, K. Huber and M. Wiebcke, *Chem. Mater.*, 2009, **21**, 1410-1412.

37. Y. K. Seo, J. W. Yoon, J. S. Lee, U. H. Lee, Y. K. Hwang, C. H. Jun, P. Horcajada, C. Serre and J. S. Chang, *Microporous Mesoporous Mater.*, 2012, **157**, 137-145.

38. S. H. Jhung, J. H. Lee, J. W. Yoon, C. Serre, G. Férey and J. S. Chang, *Adv. Mater.*, 2007, **19**, 121-124.

39. T. Friscic, *J. Mater. Chem.*, 2010, **20**, 7599-7605.

40. M. A. Alavi, A. Morsali, S. W. Joo and B. K. Min, *Ultrason. Sonochem.*, 2015, **22**, 349-358.

41. B. Liu, H. Shioyama, H. Jiang, X. Zhang and Q. Xu, *Carbon*, 2010, **48**, 456-463.

42. T. K. Kim, K. J. Lee, J. Y. Cheon, J. H. Lee, S. H. Joo and H. R. Moon, *J. Am. Chem. Soc.*, 2013, **135**, 8940-8946.

43. F. Zou, X. Hu, Z. Li, L. Qie, C. Hu, R. Zeng, Y. Jiang and Y. Huang, *Adv. Mater.*, 2014, **26**, 6622-6628.

44. M. Tiemann, *Chem. Mater.*, 2008, **20**, 961-971.

45. Y. Ren, Z. Ma and P. G. Bruce, *Chem. Soc. Rev.*, 2012, **41**, 4909-4927.

46. J. Ba, J. Polleux, M. Antonietti and M. Niederberger, *Adv. Mater.*, 2005, **17**, 2509-2512.

47. J. Y. Chane Ching, F. Cobo, D. Aubert, H. G. Harvey, M. Airiau and A. Corma, *Chem.*, 2005, **11**, 979-987.

48. P. M. Ajayan, J. M. Lambert, P. Bernier, L. Barbedette, C. Colliex and J. M. Planeix, *Chem. Phys. Lett.*, 1993, **215**, 509-517.

49. T. Yamada, T. Namai, K. Hata, D. N. Futaba, K. Mizuno, J. Fan, M. Yudasaka, M. Yumura and S. Iijima, *Nat. Nanotechnol.*, 2006, **1**, 131-136.

50. H. C. Zhou, J. R. Long and O. M. Yaghi, *Chem. Rev.*, 2012, **112**, 673-674.

51. N. Stock and S. Biswas, *Chem. Rev.*, 2012, **112**, 933-969.

52. W. Xia, A. Mahmood, R. Zou and Q. Xu, *Energy Environ. Sci.*, 2015, **8**, 1837-1866.

53. M. Hu, J. S. Jiang and Y. Zeng, *Chem. Commun.*, 2010, **46**, 1133-1135.

54. X. Xu, R. Cao, S. Jeong and J. Cho, *Nano Lett.*, 2012, **12**, 4988-4991.

55. L. Zhang, H. B. Wu, S. Madhavi, H. H. Hng and X. W. Lou, *J. Am. Chem. Soc.*, 2012, **134**, 17388-17391.

56. L. Zhang, H. B. Wu and X. W. Lou, *J. Am. Chem. Soc.*, 2013, **135**, 10664-10672.

57. B. Kong, J. Tang, Z. Wu, J. Wei, H. Wu, Y. Wang, G. Zheng and D. Zhao, *Angew. Chem., Int. Ed.*, 2014, **53**, 2888-2892.

58. J. Shao, Z. Wan, H. Liu, H. Zheng, T. Gao, M. Shen, Q. Qu and H. Zheng, *J. Mater. Chem., A*, 2014, **2**, 12194.

59. R. Wu, X. Qian, X. Rui, H. Liu, B. Yadian, K. Zhou, J. Wei, Q. Yan, X. Q. Feng, Y. Long, L. Wang and Y. Huang, *Small*, 2014, **10**, 1932-1938.

60. P. Su, S. Liao, F. Rong, F. Wang, J. Chen, C. Li and Q. Yang, *J. Mater. Chem. A*, 2014, **2**, 17408-17414.

61. A. Banerjee, U. Singh, V. Aravindan, M. Srinivasan and S. Ogale, *Nano Energy*, 2013, **2**, 1158-1163.

62. R. Wu, X. Qian, F. Yu, H. Liu, K. Zhou, J. Wei and Y. Huang, *J. Mater. Chem. A*, 2013, **1**, 11126.

63. L. Hu, Y. Huang, F. Zhang and Q. Chen, *Nanoscale*, 2013, **5**, 4186-4190.

64. G. Zhan and H. C. Zeng, *Adv. Funct. Mater.*, 2016, **26**, 3268-3281.

65. K. Cao, L. Jiao, H. Xu, H. Liu, H. Kang, Y. Zhao, Y. Liu, Y. Wang and H. Yuan, *Adv. Sci.*, 2016, **3**, 1500185.

66. R. Wu, X. Qian, K. Zhou, J. Wei, J. Lou and P. M. Ajayan, *ACS Nano*, 2014, **8**, 6297-6303.

67. T. Wang, L. Shi, J. Tang, V. Malgras, S. Asahina, G. Liu, H. Zhang, X. Meng, K. Chang, J. He, O. Terasaki, Y. Yamauchi and J. Ye, *Nanoscale*, 2016, **8**, 6712-6720.

68. X. Xu, K. Cao, Y. Wang and L. Jiao, *J. Mater. Chem. A*, 2016, **4**, 6042-6047.

69. L. Hu, P. Zhang, H. Zhong, X. Zheng, N. Yan and Q. Chen, *Chem. Eur. J.*, 2012, **18**, 15049-15056.

70. C. J. Du, F. X. Bu, D. M. Jiang, Q. H. Zhang and J. S. Jiang, *CrystEngComm*, 2013, **15**, 10597.

71. L. Hu, P. Zhang, Y. Sun, S. Bao and Q. Chen, *Chemphyschem*, 2013, **14**, 3953-3959.

72. G. Huang, L. Zhang, F. Zhang and L. Wang, *Nanoscale*, 2014, **6**, 5509-5515.

73. L. Han, X. Y. Yu and X. W. Lou, *Adv. Mater.*, 2016, **28**, 4601-4605.

74. H. Shi and G. Zhao, *J. Phys. Chem. C*, 2014, **118**, 25939-25946.

75. J. Wang, T. Qiu, X. Chen, Y. Lu and W. Yang, *J. Power Sources*, 2014, **268**, 341-348.

76. W. Guo, W. Sun and Y. Wang, *ACS Nano*, 2015, **9**, 11462-11471.

77. X. W. Hu, S. Liu, B. T. Qu and X. Z. You, *ACS Appl. Mater. Interfaces*, 2015, **7**, 9972-9981.

78. H. Hu, B. Guan, B. Xia and X. W. Lou, *J. Am. Chem. Soc.*, 2015, **137**, 5590-5595.

79. C. Sun, J. Yang, X. Rui, W. Zhang, Q. Yan, P. Chen, F. Huo, W. Huang and X. Dong, *J. Mater. Chem. A*, 2015, **3**, 8483-8488.

80. F. Qu, H. Jiang and M. Yang, *Nanoscale*, 2016, **8**, 16349-16356.

81. R. Wu, D. P. Wang, J. Han, H. Liu, K. Zhou, Y. Huang, R. Xu, J. Wei, X. Chen and Z. Chen, *Nanoscale*, 2015, **7**, 965-974.

82. L. Yu, J. F. Yang and X. W. Lou, *Angew. Chem., Int. Ed.*, 2016, **55**, 13422-13426.

83. Z. F. Huang, J. Song, K. Li, M. Tahir, Y. T. Wang, L. Pan, L. Wang, X. Zhang and J. J. Zou, *J. Am. Chem. Soc.*, 2016, **138**, 1359-1365.

84. R. Bendi, V. Kumar, V. Bhavanasi, K. Parida and P. S. Lee, *Adv. Energy Mater.*, 2016, **6**, 1501833.

85. P. Wang, J. Feng, Y. Zhao, S. Wang and J. Liu, *ACS Appl. Mater. Interfaces*, 2016, **8**, 23755-23762.

86. X. Wang, S. Zhao, Y. Zhang, Z. Wang, J. Feng, S. Song and H. Zhang, *Chem. Sci.*, 2016, **7**, 1109-1114.

87. J. Hu, H. Wang, Q. Gao and H. Guo, *Carbon*, 2010, **48**, 3599-3606.

88. W. Chaikittisilp, M. Hu, H. Wang, H. S. Huang, T. Fujita, K. C. W. Wu, L. C. Chen, Y. Yamauchi and K. Ariga, *Chem. Commun.*, 2012, **48**, 7259-7261.

89. S. Zhong, C. Zhan and D. Cao, *Carbon*, 2015, **85**, 51-59.

90. B. Ding, J. Wang, Z. Chang, G. Xu, X. Hao, L. Shen, H. Dou and X. Zhang, *ChemElectroChem*, 2016, **3**, 668-674.

91. R. Zhao, W. Xia, C. Lin, J. Sun, A. Mahmood, Q. Wang, B. Qiu, H. Tabassum and R. Zou, *Carbon*, 2017, **114**, 284-290.

92. Q. Lai, Y. Zhao, Y. Liang, J. He and J. Chen, *Adv. Funct. Mater.*, 2016, **26**, 8334-8344.

93. H. J. Lee, S. Choi and M. Oh, *Chem. Commun.*, 2014, **50**, 4492-4495.

94. A. Aijaz, J. K. Sun, P. Pachfule, T. Uchida and Q. Xu, *Chem. Commun.*, 2015, **51**, 13945-13948.

95. J. K. Sun and Q. Xu, *Chem. Commun.*, 2014, **50**, 13502-13505.

96. N. L. Torad, R. R. Salunkhe, Y. Li, H. Hamoudi, M. Imura, Y. Sakka, C. C. Hu and Y. Yamauchi, *Chem. Eur. J.*, 2014, **20**, 7895-7900.

97. J. Tang, R. R. Salunkhe, J. Liu, N. L. Torad, M. Imura, S. Furukawa and Y. Yamauchi, *J. Am. Chem. Soc.*, 2015, **137**, 1572-1580.

98. P. Su, H. Xiao, J. Zhao, Y. Yao, Z. Shao, C. Li and Q. Yang, *Chem. Sci.*, 2013, **4**, 2941.

99. Q. Li, P. Xu, W. Gao, S. Ma, G. Zhang, R. Cao, J. Cho, H. L. Wang and G. Wu, *Adv. Mater.*, 2014, **26**, 1378-1386.

100. B. Y. Xia, Y. Yan, N. Li, H. B. Wu, X. W. Lou and X. Wang, *Nat. Energy*, 2016, **1**, 15006.

101. L. Zhang, X. Wang, R. Wang and M. Hong, *Chem. Mater.*, 2015, **27**, 7610-7618.

102. H. X. Zhong, J. Wang, Y. W. Zhang, W. L. Xu, W. Xing, D. Xu, Y. F. Zhang and X. B. Zhang, *Angew. Chem., Int. Ed.*, 2014, **53**, 14235-14239.

103. M. Thomas, R. Illathvalappil, S. Kurungot, B. N. Nair, A. A. P. Mohamed, G. M. Anilkumar, T. Yamaguchi and U. S. Hareesh, *ACS Appl. Mater. Interfaces*, 2016, **8**, 29373-29382.

104. W. Zhang, Z. Y. Wu, H. L. Jiang and S. H. Yu, *J. Am. Chem. Soc.*, 2014, **136**, 14385-14388.

105. P. Pachfule, D. Shinde, M. Majumder and Q. Xu, *Nat. Chem.*, 2016, **8**, 718-724.

106. X. Xu, M. Wang, Y. Liu, T. Lu and L. Pan, *J. Mater. Chem. A*, 2016, **4**, 5467-5473.

107. S. J. Yang, S. Nam, T. Kim, J. H. Im, H. Jung, J. H. Kang, S. Wi, B. Park and C. R. Park, *J. Am. Chem. Soc.*, 2013, **135**, 7394-7397.

108. J. Kim, G. T. Neumann, N. D. McNamara and J. C. Hicks, *J. Mater. Chem. A*, 2014, **2**, 14014.

109. B. Chen, G. Ma, D. Kong, Y. Zhu and Y. Xia, *Carbon*, 2015, **95**, 113-124.

110. V. P. Santos, T. A. Wezendonk, J. J. Jaen, A. I. Dugulan, M. A. Nasalevich, H. U. Islam, A. Chojecki, S. Sartipi, X. Sun, A. A. Hakeem, A. C. Koeken, M. Ruitenbeek, T. Davidian, G. R. Meima, G. Sankar, F. Kapteijn, M. Makkee and J. Gascon, *Nat. Commun.*, 2015, **6**, 6451.

111. B. You, N. Jiang, M. Sheng, W. S. Drisdell, J. Yano and Y. Sun, *ACS Catal.*, 2015, **5**, 7068-7076.

112. L. Shang, T. Bian, B. Zhang, D. Zhang, L.-Z. Wu, C.-H. Tung, Y. Yin and T. Zhang, *Angew. Chem., Int. Ed.*, 2014, **53**, 250-254.

113. L. Shang, H. Yu, X. Huang, T. Bian, R. Shi, Y. Zhao, G. I. Waterhouse, L. Z. Wu, C. H. Tung and T. Zhang, *Adv. Mater.*, 2016, **28**, 1668-1674.

114. S. Wang, L. Shang, L. Li, Y. Yu, C. Chi, K. Wang, J. Zhang, R. Shi, H. Shen, G. I. N. Waterhouse, S. Liu, J. Tian, T. Zhang and H. Liu, *Adv. Mater.*, 2016, **28**, 8379-8387.

115. H. Yang, S. J. Bradley, A. Chan, G. I. N. Waterhouse, T. Nann, P. E. Kruger and S. G. Telfer, *J. Am. Chem. Soc.*, 2016, **138**, 11872-11881.

116. X. Wang, H. Zhang, H. Lin, S. Gupta, C. Wang, Z. Tao, H. Fu, T. Wang, J. Zheng, G. Wu and X. Li, *Nano Energy*, 2016, **25**, 110-119.

117. W. Chaikittisilp, N. L. Torad, C. Li, M. Imura, N. Suzuki, S. Ishihara, K. Ariga and Y. Yamauchi, *Chem. Eur. J.*, 2014, **20**, 4217-4221.

118. S. Wang, M. Chen, Y. Xie, Y. Fan, D. Wang, J. J. Jiang, Y. Li, H. Grutzmacher and C. Y. Su, *Small*, 2016, **12**, 2365-2375.

119. A. Aijaz, J. Masa, C. Rosler, W. Xia, P. Weide, A. J. Botz, R. A. Fischer, W. Schuhmann and M. Muhler, *Angew. Chem., Int. Ed.*, 2016, **55**, 4087-4091.

120. H. Li, Y. Su, W. Sun and Y. Wang, *Adv. Funct. Mater.*, 2016, **26**, 8345-8353.

121. S. H. Ahn and A. Manthiram, *Small*, 2017, **13**, 1603437-1-8.

122. X. Cao, B. Zheng, X. Rui, W. Shi, Q. Yan and H. Zhang, *Angew. Chem., Int. Ed.*, 2014, **53**, 1404-1409.

123. Q. Qu, T. Gao, H. Zheng, X. Li, H. Liu, M. Shen, J. Shao and H. Zheng, *Carbon*, 2015, **92**, 119-125.

124. D. Ji, H. Zhou, J. Zhang, Y. Dan, H. Yang and A. Yuan, *J. Mater. Chem. A*, 2016, **4**, 8283-8290.

125. L. Qi, Y. Xin, Z. Zuo, C. Yang, K. Wu, B. Wu and H. Zhou, *ACS Appl. Mater. Interfaces*, 2016, **8**, 17245-17252.

126. Y. Hou, T. Huang, Z. Wen, S. Mao, S. Cui and J. Chen, *Adv. Energy Mater.*, 2014, **4,** 1400337-1-8.

127. Z. Li, C. Li, X. Ge, J. Ma, Z. Zhang, Q. Li, C. Wang and L. Yin, *Nano Energy*, 2016, **23**, 15-26.

128. T. Y. Ma, S. Dai, M. Jaroniec and S. Z. Qiao, *J. Am. Chem. Soc.*, 2014, **136**, 13925-13931.

129. G. Zhang, S. Hou, H. Zhang, W. Zeng, F. Yan, C. C. Li and H. Duan, *Adv. Mater.*, 2015, **27**, 2400-2405.

130. Q. Dong, Q. Wang, Z. Dai, H. Qiu and X. Dong, *ACS Appl. Mater. Interfaces*, 2016, **8**, 26902-26907.

131. Z. Li, M. Shao, Z. Lei, R. Zhang, C. Zhang, M. Wei, D. Evans and X. Duan, *Adv. Mater.*, 2016, **28**, 2337-2344.

132. D. Zhao, J. L. Shui, C. Chen, X. Chen, B. M. Reprogle, D. Wang and D. J. Liu, *Chem. Sci.*, 2012, **3**, 3200-3205.

133. C. Zhang, Y. C. Wang, B. An, R. Huang, C. Wang, Z. Zhou and W. Lin, *Adv. Mater.*, 2017, **29**, 1604556-1-7.

134. X. Wang, J. Zhou, H. Fu, W. Li, X. Fan, G. Xin, J. Zheng and X. Li, *J. Mater. Chem. A*, 2014, **2**, 14064-14070.

135. Y. Z. Chen, C. Wang, Z. Y. Wu, Y. Xiong, Q. Xu, S. H. Yu and H. L. Jiang, *Adv. Mater.*, 2015, **27**, 5010-5016.

136. G. Zhang, C. Li, J. Liu, L. Zhou, R. Liu, X. Han, H. Huang, H. Hu, Y. Liu and Z. Kang, *J. Mater. Chem. A*, 2014, **2**, 8184.

137. X. Wang, L. Zou, H. Fu, Y. Xiong, Z. Tao, J. Zheng and X. Li, *ACS Appl. Mater. Interfaces*, 2016, **8**, 8436-8444.

138. H. Yu, A. Fisher, D. Cheng and D. Cao, *ACS Appl. Mater. Interfaces*, 2016, **8**, 21431-21439.

139. K. He, Z. Cao, R. Liu, Y. Miao, H. Ma and Y. Ding, *Nano Res.*, 2016, **9**, 1856-1865.

140. J. Jiang, C. Zhang and L. Ai, *Electrochim. Acta*, 2016, **208**, 17-24.

141. Y. Liang, J. Wei, X. Zhang, J. Zhang, S. P. Jiang and H. Wang, *ChemCatChem*, 2016, **8**, 1901-1904.

142. Y. Ma, X. Dai, M. Liu, J. Yong, H. Qiao, A. Jin, Z. Li, X. Huang, H. Wang and X. Zhang, *ACS Appl. Mater. Interfaces*, 2016, **8**, 34396-34404.

143. T. Zhang, J. Du, P. Xi and C. Xu, *ACS Appl. Mater. Interfaces*, 2017, **9**, 362-370.

144. Y. Han, J. Zhai, L. Zhang and S. Dong, *Nanoscale*, 2016, **8**, 1033-1039.

145. X.-Y. Yu, Y. Feng, B. Guan, X. W. Lou and U. Paik, *Energy Environ. Sci.*, 2016, **9**, 1246-1250.

146. L. Yang, M. Gao, B. Dai, X. Guo, Z. Liu and B. Peng, *Electrochim. Acta*, 2016, **191**, 813-820.

147. J. Hao, W. Yang, Z. Zhang and J. Tang, *Nanoscale*, 2015, **7**, 11055-11062.

148. Z. Xie, Z. He, X. Feng, W. Xu, X. Cui, J. Zhang, C. Yan, M. A. Carreon, Z. Liu and Y. Wang, *ACS Appl. Mater. Interfaces*, 2016, **8**, 10324-10333.

149. Y. Yang, Z. Lun, G. Xia, F. Zheng, M. He and Q. Chen, *Energy Environ. Sci.*, 2015, **8**, 3563-3571.

150. J. Chen, G. Xia, P. Jiang, Y. Yang, R. Li, R. Shi, J. Su and Q. Chen, *ACS Appl. Mater. Interfaces*, 2016, **8**, 13378-13383.

151. W. Zhou, J. Lu, K. Zhou, L. Yang, Y. Ke, Z. Tang and S. Chen, *Nano Energy*, 2016, **28**, 143-150.

152. H. S. Lu, H. Zhang, R. Liu, X. Zhang, H. Zhao and G. Wang, *Appl. Surf. Sci.*, 2017, **392**, 402-409.

153. Y. Hao, Y. Xu, J. Liu and X. Sun, *J. Mater. Chem. A*, 2017, **5**, 5594-5600.

154. S. Liu, H. Zhang, Q. Zhao, X. Zhang, R. Liu, X. Ge, G. Wang, H. Zhao and W. Cai, *Carbon*, 2016, **106**, 74-83.

155. J. Tang, S. Wu, T. Wang, H. Gong, H. Zhang, S. M. Alshehri, T. Ahamad, H. Zhou and Y. Yamauchi, *ACS Appl. Mater. Interfaces*, 2016, **8**, 2796-2804.

156. Y. Qian, Z. Hu, X. Ge, S. Yang, Y. Peng, Z. Kang, Z. Liu, J. Y. Lee and D. Zhao, *Carbon*, 2017, **111**, 641-650.

157. B. You, N. Jiang, M. Sheng, S. Gul, J. Yano and Y. Sun, *Chem. Mater.*, 2015, **27**, 7636-7642.

158. L. Jiao, Y. X. Zhou and H. L. Jiang, *Chem. Sci.*, 2016, **7**, 1690-1695.

159. M. Liu and J. Li, *ACS Appl. Mater. Interfaces*, 2016, **8**, 2158-2165.

160. V. Armel, S. Hindocha, F. Salles, S. Bennett, D. Jones and F. Jaouen, *J. Am. Chem. Soc.*, 2017, **139**, 453-464.

161. S. You, X. Gong, W. Wang, D. Qi, X. Wang, X. Chen and N. Ren, *Adv. Energy Mater.*, 2016, **6**, 1501497-1-9.

162. Y. Yang, Z. Lin, S. Gao, J. Su, Z. Lun, G. Xia, J. Chen, R. Zhang and Q. Chen, *ACS Catal.*, 2017, **7**, 469-479.

163. S. Gadipelli, T. Zhao, S. A. Shevlin and Z. Guo, *Energy Environ. Sci.*, 2016, **9**, 1661-1667.

164. Y. Han, P. Qi, S. Li, X. Feng, J. Zhou, H. Li, S. Su, X. Li and B. Wang, *Chem. Commun.*, 2014, **50**, 8057-8060.

165. L. Liu, H. Guo, J. Liu, F. Qian, C. Zhang, T. Li, W. Chen, X. Yang and Y. Guo, *Chem. Commun.*, 2014, **50**, 9485-9488.

166. L. Yu, J. Liu, X. Xu, L. Zhang, R. Hu, J. Liu, L. Yang and M. Zhu, *ACS Appl. Mater. Interfaces*, 2017, **9**, 2516-2525.

167. X. Ge, Z. Li, C. Wang and L. Yin, *ACS Appl. Mater. Interfaces*, 2015, **7**, 26633-26642.

168. A. Y. Kim, M. K. Kim, K. Cho, J. Y. Woo, Y. Lee, S. H. Han, D. Byun, W. Choi and J. K. Lee, *ACS Appl. Mater. Interfaces*, 2016, **8**, 19514-19523.

169. M. Wang, H. Yang, X. Zhou, W. Shi, Z. Zhou and P. Cheng, *Chem. Commun.*, 2016, **52**, 717-720.

170. M. Zhong, D. Yang, C. Xie, Z. Zhang, Z. Zhou and X. H. Bu, *Small*, 2016, **12**, 5564-5571.

171. Z. W. Zhao, T. Wen, K. Liang, Y. F. Jiang, X. Zhou, C. C. Shen and A. W. Xu, *ACS Appl. Mater. Interfaces*, 2017, **9**, 3757-3765.

172. Y. Tan, K. Zhu, D. Li, F. Bai, Y. Wei and P. Zhang, *Chem. Eng. J.*, 2014, **258**, 93-100.

173. Q. Zhu, Y. Li, Y. Gao, X. Wang and S. Song, *Chem. Eur. J.*, 2016, **22**, 6876-6880.

174. F. Zheng, Y. Yang and Q. Chen, *Nat. Commun.*, 2014, **5**, 5261-1-10.

175. Z. Wang, X. Li, H. Xu, Y. Yang, Y. Cui, H. Pan, Z. Wang, B. Chen and G. Qian, *J. Mater. Chem. A*, 2014, **2**, 12571-12575.

176. C. Li, T. Chen, W. Xu, X. Lou, L. Pan, Q. Chen and B. Hu, *J. Mater. Chem. A*, 2015, **3**, 5585-5591.

177. Guozhao Fang, Jiang Zhou, Caiwu Liang, Anqiang Pan, Cheng Zhang, Yan Tang, Xiaoping Tan, Jun Liu and S. Liang, *Nano Energy*, 2016, **26**, 57-65.

178. V. Soundharrajan, B. Sambandam, J. Song, S. Kim, J. Jo, S. Kim, S. Lee, V. Mathew and J. Kim, *ACS Appl. Mater. Interfaces*, 2016, **8**, 8546-8553.

179. G. Huang, F. Zhang, L. Zhang, X. Du, J. Wang and L. Wang, *J. Mater. Chem. A*, 2014, **2**, 8048-8053.

180. J. M. Fan, J. J. Chen, Q. Zhang, B. B. Chen, J. Zang, M. S. Zheng and Q. F. Dong, *ChemSusChem*, 2015, **8**, 1856-1861.

181. X. Zhang, W. Qin, D. Li, D. Yan, B. Hu, Z. Sun and L. Pan, *Chem. Commun.*, 2015, **51**, 16413-16416.

182. B. Ramaraju, C. H. Li, S. Prakash and C. C. Chen, *Chem. Commun.*, 2016, **52**, 946-949.

183. Z. Zhang, Y. An, X. Xu, C. Dong, J. Feng, L. Ci and S. Xiong, *Chem. Commun.*, 2016, **52**, 12810-12812.

184. F. Zou, Y. M. Chen, K. Liu, Z. Yu, W. Liang, S. M. Bhaway, M. Gao and Y. Zhu, *ACS Nano*, 2016, **10**, 377-386.

185. T. Chen, B. Cheng, R. Chen, Y. Hu, H. Lv, G. Zhu, Y. Wang, L. Ma, J. Liang, Z. Tie, Z. Jin and J. Liu, *ACS Appl. Mater. Interfaces*, 2016, **8**, 26834-26841.

186. G. Zou, X. Jia, Z. Huang, S. Li, H. Liao, H. Hou, L. Huang and X. Ji, *Electrochim. Acta*, 2016, **196**, 413-421.

187. Y. Zhang, A. Pan, L. Ding, Z. Zhou, Y. Wang, S. Niu, S. Liang and G. Cao, *ACS Appl. Mater. Interfaces*, 2017, **9**, 3624-3633.

188. H. B. Wu, S. Wei, L. Zhang, R. Xu, H. H. Hng and X. W. Lou, *Chem. Eur. J.*, 2013, **19**, 10804-10808.

189. Z. Yue, S. Liu and Y. Liu, *RSC Adv.*, 2015, **5**, 10619-10622.

190. K. Xi, S. Cao, X. Peng, C. Ducati, R. V. Kumar and A. K. Cheetham, *Chem. Commun.*, 2013, **49**, 2192-2194.

191. W. Bao, Z. Zhang, C. Zhou, Y. Lai and J. Lia, *J. Power Sources*, 2014, **248**, 570-576.

192. W. Bao, Z. Zhang, W. Chen, C. Zhou, Y. Lai and J. Li, *Electrochim. Acta*, 2014, **127**, 342-348.

193. C. Li, Z. Li, Q. Li, Z. Zhang, S. Dong and L. Yin, *Electrochim. Acta*, 2016, **215**, 689-698.

194. Y. Li, J. Fan, M. Zheng and Q. Dong, *Energy Environ. Sci.*, 2016, **9**, 1998-2004.

195. J. Zhou, N. Lin, W. Cai, C. Guo, K. Zhang, J. Zhou, Y. Zhu and Y. Qian, *Electrochim. Acta*, 2016, **218**, 243-251.

196. J. He, Y. Chen, W. Lv, K. Wen, C. Xu, W. Zhang, Y. Li, W. Qin and W. He, *ACS Nano*, 2016, **10**, 10981-10987.

197. W. Bao, D. Su, W. Zhang, X. Guo and G. Wang, *Adv. Funct. Mater.*, 2016, **26**, 8746-8756.

198. A. J. Amali, J. K. Sun and Q. Xu, *Chem. Commun.*, 2014, **50**, 1519-1522.

199. R. R. Salunkhe, Y. Kamachi, N. L. Torad, S. M. Hwang, Z. Sun, S. X. Dou, J. H. Kim and Y. Yamauchi, *J. Mater. Chem. A*, 2014, **2**, 19848-19854.

200. W. Bao, A. K. Mondal, J. Xu, C. Wang, D. Su and G. Wang, *J. Power Sources*, 2016, **325**, 286-291.

201. L. Wang, T. Wei, L. Sheng, L. Jiang, X. Wu, Q. Zhou, B. Yuan, J. Yue, Z. Liu and Z. Fan, *Nano Energy*, 2016, **30**, 84-92.

202. X. Yan, X. Li, Z. Yan and S. Komarneni, *Appl. Surf. Sci.*, 2014, **308**, 306-310.

203. S. Maiti, A. Pramanik and S. Mahanty, *Chem. Commun.*, 2014, **50**, 11717-11720.

204. F. Zhang, L. Hao, L. Zhang and X. Zhang, *Int. J. Electrochem. Sci.*, 2011, **6**, 2943-2954.

205. W. Meng, W. Chen, L. Zhao, Y. Huang, M. Zhu, Y. Huang, Y. Fu, F. Geng, J. Yu, X. Chen and C. Zhi, *Nano Energy*, 2014, **8**, 133-140.

206. R. Wu, D. P. Wang, V. Kumar, K. Zhou, A. W. Law, P. S. Lee, J. Lou and Z. Chen, *Chem. Commun.*, 2015, **51**, 3109-3112.

207. S. Li, X. Zhang and Y. Huang, *J. Hazard. Mater.*, 2017, **321**, 711-719.

208. A. Banerjee, R. Gokhale, S. Bhatnagar, J. Jog, M. Bhardwaj, B. Lefez, B. Hannoyer and S. Ogale, *J. Mater. Chem.*, 2012, **22**, 19694.

209. N. L. Torad, M. Hu, S. Ishihara, H. Sukegawa, A. A. Belik, M. Imura, K. Ariga, Y. Sakka and Y. Yamauchi, *Small*, 2014, **10**, 2096-2107.

210. C. W. Abney, J. C. Gilhula, K. Lu and W. Lin, *Adv. Mater.*, 2014, **26**, 7993-7997.

211. P. Liang, C. Zhang, H. Sun, S. Liu, M. Tade and S. Wang, *Energy Fuels*, 2016, **31**, 2138-2143.

212. P. Liang, C. Zhang, H. Sun, S. Liu, M. Tadé and S. Wang, *RSC Adv.*, 2016, **6**, 95903-95909.

213. S. J. Yang, J. H. Im, T. Kim, K. Lee and C. R. Park, *J. Hazard. Mater.*, 2011, **186**, 376-382.

214. G. Zhu, X. Li, H. Wang and L. Zhang, *Catal. Commun.*, 2017, **88**, 5-8.

215. Y. Zhang, L. Qiu, Y. Yuan, Y. Zhu, X. Jiang and J. Xiao, *Appl. Catal.*, B, 2014, **144**, 863-869.

216. S. Wu, X. Shen, G. Zhu, H. Zhou, Z. Ji, K. Chen and A. Yuan, *Appl. Catal., B*, 2016, **184**, 328-336.

217. L. Peng, J. Zhang, Z. Xue, B. Han, J. Li and G. Yang, *Chem. Commun.,* 2013, **49**, 11695-11697.

218. X. Li, Z. Wang, B. Zhang, A. I. Rykov, M. A. Ahmed and J. Wang, *Appl. Catal., B*, 2016, **181**, 788-799.

219. X. Li, Z. Ao, J. Liu, H. Sun, A. I. Rykov and J. Wang, *ACS Nano*, 2016, **10**, 11532-11540.

220. X. Li, A. I. Rykov, B. Zhang, Y. Zhang and J. Wang, *Catal. Sci. Technol.*, 2016, **6**, 7486-7494.

221. K. Y. Andrew Lin, F. K. Hsu and W. D. Lee, *J. Mater. Chem. A*, 2015, **3**, 9480-9490.

222. P. Liang, C. Zhang, X. Duan, H. Sun, S. Liu, M. O. Tade and S. Wang, *ACS Sustainable Chem. Eng.*, 2017, **5**, 2693-2701.

223. P. Liang, C. Zhang, X. Duan, H. Sun, S. Liu, M. O. Tade and S. Wang, *Environ. Sci.: Nano*, 2017, **4**, 315-324.

224. Montgomery, R. E., *J. Am. Chem. Soc.*, 1974, **96**, 7820−7821.

225. Edwards, J. O., Pater, R. H., Curclf, R. and Furia, F. D., *Photochem. Photobiol.*, 1979, **30**, 63−70.

226. Y. Zhou, J. Jiang, Y. Gao, J. Ma, S. Pang, J. Li, X. Lu and L. Yuan, *Environ. Sci. Technol.*, 2015, **49**, 12941−12950.

227. X. Duan, H. Sun, Y. Wang, J. Kang and S. Wang, *ACS Catal.*, 2015, **5**, 553−559.

Chapter 3: Solar photocatalytic water oxidation and purification on ZIF-8 derived C-N-ZnO composites

ABSTRACT

Photocatalytic water splitting and purification become more and more important to tackle the severe energy and environment challenges in modern society. In this study, carbon and nitrogen modified ZnO photocatalysts were prepared by the controlled thermal decomposition of Zeolitic Imidazolate Framework (ZIF)-8. ZIF-8 carbonization in nitrogen atmosphere confined highly dispersive Zn into the porous carbon and the followed calcination in air induced the formation of nanosized ZnO photocatalysts. The physicochemical properties of the photocatalysts were investigated by a variety of characterization techniques and the photocatalytic performances were evaluated in both oxygen evolution and degradation of dye under solar light. It was found that the two-step synthesis delivered better photocatalyst materials than that from one-step (directly annealing in nitrogen or air). The co-existence of nitrogen and carbon in ZnO was suggested to be favorable to enhanced photocatalysis.

The content of this chapter is published in RSC Advances, 2016, 6, 95903-95909.

3.1. Introduction

Semiconductor-based photocatalysis has been widely employed for water purification [1] and energy conversion (water splitting) [2, 3] due to the merits of non-selectivity, ambient condition and cost-effective operation. [4] Zinc oxide (ZnO) with versatile shapes and structures has been chosen as a photocatalyst or photoelectrode because it has a high electron mobility and is low cost. [5] However, ZnO has a wide band-gap (E_g = 3.37 eV) which can only be activated by ultraviolet (UV) light, [6] representing less than 5% solar spectrum energy.

It was reported that introduction of various carbon or nitrogen to ZnO lattices can lower down the band-gap energy, leading to the extended absorption edge to visible light region for the utilization of about 42% solar energy. [7, 8] Hybridization of carbonaceous materials such as C_{60} and graphene with ZnO has been demonstrated to be effective for enhanced photocatalysis, compared to the counterparts of pure metal oxides. [9-11] Yang *et al.* reported that nitrogen-doped ZnO nanowire arrays showed a promising photocatalytic activity.[12] Xie *et al.* synthesized carbon and nitrogen co-treated ZnO *via* a two-step method for hydrogen evolution, which showed a fascinating photostability. [13] However, not many attempts were made on ZnO for photocatalytic oxygen evolution reaction (OER).

Carbon or nitrogen can be introduced to ZnO via either *in situ* synthesis or post-treatment [14-18]. However, *in situ* doping generally requires a critical synthesis condition while post-treatment usually leads to random distribution along the profile from surface to the core of a particle. [19] Metal-organic frameworks (MOFs) are well-known crystalline porous materials constructed by metal clusters and organic ligands. [20] In recent years, advanced protocols have employed MOFs as templates or precursors to fabricate nanoporous carbon, [21, 22] metal oxides, [23-26] and hybrid composites, [27-29] for enhanced performances in gas adsorption, battery, and electrical chemistry,

etc. Compared to conventional templates, MOFs possess permanent nanoscaled pores and open channels for small alien molecules to access and can sacrifice themselves to form new materials. [22, 30] As a result, the chemical compositions and the nano-architectures can be rationally designed.

Zeolitic Imidazolate Framework (ZIF)-8, as a Zn-containing N-rich MOF, can be feasibly synthesized using a rapid room-temperature route without a stabilizing agent or activation processes such as heating, microwave or ultrasound irradiation. [31] It was reported that porous ZnO photocatalysts were prepared by the thermal treatment of ZIF-8, and enhanced photodegradation of methylene blue was achieved.[32] Further exploration of such a strategy would be made for heteroatoms doping and hybrid synthesis. The synthesis would be simpler than other *in situ* or post-treatment of carbon- and/or nitrogen-doping methods.

Herein, we report our systematic investigations on synthesis of carbon and nitrogen modified ZnO photocatalysts using ZIF-8 as a precursor through three pyrolysis-calcination synthesis routes. The characteristics of the obtained photocatalysts were analyzed and the photocatalytic performances were estimated in both photocatalytic OER and degradation of methylene blue (MB) in water under simulated sunlight irradiations.

3.2. Experimental Section

3.2.1. Materials and reagents

2-Methylimidazole (99%, Hmim), zinc nitrate hexahydrate (98%, $Zn(NO_3)_2 \cdot 6H_2O$), methanol (99.8%), and methylene blue (99.9%), silver nitrate (99.0%, $AgNO_3$), lanthanum oxide (La_2O_3, 99.9%) were purchased from Sigma-Aldrich. All the chemicals were used as received without further treatment or purification.

3.2.2. Synthesis of ZIF-8 and it derived catalyst materials

ZIF-8 was synthesized by dissolving $Zn(NO_3)_2 \cdot 6H_2O$ and Hmim in methanol at room temperature as reported elsewhere. [31] The C, N-ZnO photocatalysts were prepared in three different ways as shown in Scheme 3.1. In route (a), the prepared ZIF-8 was transferred into a furnace and heated in air at 450 °C for 120 min, and then cooled down to room temperature. The sample prepared was denoted as A120. In route (b), the synthesized ZIF-8 in an alumina boat was placed in a tube furnace and heated at 800 °C for 2 h in nitrogen atmosphere with a flow rate of 50 mL/min. The resulting black powders were designated as C800. In route (c), C800 was further annealed in air at 450 °C for 120 min, and then cooled down to room temperature. The obtained sample was denominated as 8C120. Two reference samples of ZnO were obtained by directly calcining $Zn(NO_3)_2 \cdot 6H_2O$ in air at 450 °C for 2 h and in N_2 at 800 °C for 2 h, labelled as ZnO-a and ZnO-b, respectively.

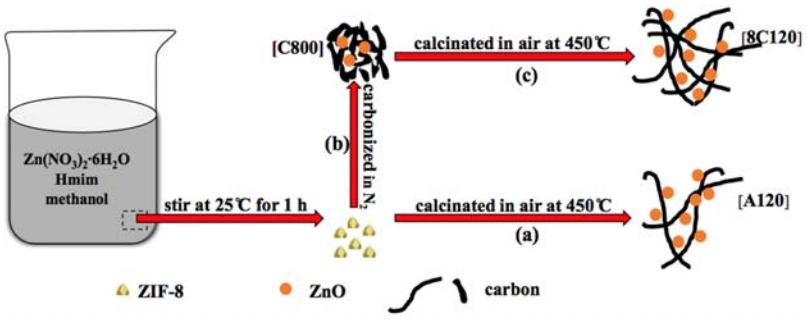

Scheme 3.1. Synthesis routes of ZIF-8-templated materials.

3.2.3. Characterization of materials

Powder X-ray diffraction (XRD) patterns were recorded on a Bruker D8-Advance X-ray diffractometer with Cu Kα radiation (λ = 1.5418 Å). The morphology and crystal structure were analyzed by field emission scanning electron microscopy (FE-SEM, Zeiss Neon 40 EsB) and high-resolution transmission electron microscopy (HRTEM, JEOL 2100). Element distribution was

obtained on an energy dispersive X-ray spectroscopy (EDX). X-ray photoelectron spectroscopy (XPS) was utilized to investigate the chemical states of the modified ZnO using a Kratos AXIS Ultra DLD system with Al-Kα X-ray. UV-visible diffuse reflectance spectra (UV-vis DRS) were acquired on a JASCO V-670 spectrophotometer with an Ø60 mm integrating sphere, using $BaSO_4$ as a reference. Thermogravimetric-differential thermal analysis (TG-DTA) was recorded on a TGA/DSC-1 thermogravimetric analyzer from Mettler-Toledo Instrument and the heating rate was set at 10 °C/min. N_2 adsorption/desorption was carried out on a Micromeritics Tristar 3020 to measure the Brunauer–Emmett–Teller (BET) specific surface area at liquid nitrogen temperature (-196 °C).

3.2.4. Photocatalytic OER and MB degradation

Photocatalytic reactions were carried out in a closed reactor connecting to a water bath for maintaining the reaction temperature at 25 °C. A Xenon lamp (300 W) provided simulated sunlight for water oxidation with $AgNO_3$ as an electron scavenger. Specifically, 0.5 g/L samples were added into $AgNO_3$ solution (0.03 M) with La_2O_3 (0.1 g/L) in it. Before light irradiation, degassing was conducted to remove oxygen in the reactor. The concentrations of oxygen produced in the reactor were measured with a NEOFOX O_2 probe.

Photodegradation of MB was performed under the simulated sunlight supplied by a MSR 575/2 metal halide lamp (575 W, Philips) at 25 °C. Typically, 0.25 g/L catalyst was dispersed into 200 mL of 10 ppm MB solution. Prior to the degradation, the solution was continuously stirred in dark for 30 min to achieve adsorption/desorption equilibrium, followed by switching on the lamp. Adsorption of MB was conducted similarly to photodegradation tests without light irradiation. The concentration of MB was determined by a UV-vis spectrometer at $\lambda = 664$ nm.

3.3. Results and Discussion

3.3.1. Characterization of the materials

TG-DTA curves of ZIF-8 in air showed that ZIF-8 experienced a steep mass loss at both 450 and 540 °C (Figure 3.1). The weight loss at around 450 °C was attributed to the removal of guest molecules (*e.g.* methanol and Hmim) in the cavity or on the surface of ZIF-8. Thus, we set the pyrolysis temperature at 450 °C. The second rapid mass decrease occurred at around 540 °C, due to the combustion of the organic linker molecules.[31]

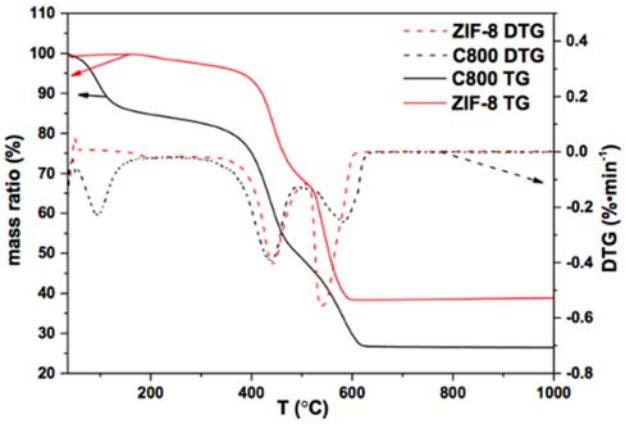

Figure 3.1. TG-DTG curves of ZIF-8 and C800 in air.

Figure 3.2 presents XRD patterns of various synthesized samples. ZIF-8 showed the same diffraction peaks observed in previous reports. [31] The XRD pattern of A120 was identified to be similar to crystalline ZnO. However, no ZIF-8 and ZnO peaks could be found on the XRD pattern of C800, because the framework of ZIF-8 collapsed and crystalline ZnO was not successfully formed or was enclosed in the carbon generating restraint for crystallization. On the other hand, the peaks ascribed to ZnO were observed on the sample of 8C120 derived from the two-step synthesis. The ZnO grain sizes of A120 and 8C120 were calculated to be 21.6 and 16.9 nm, respectively, according to the Scherrer equations.

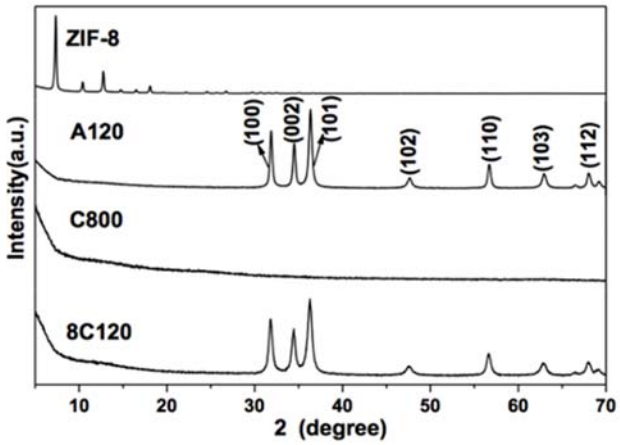

Figure 3.2. XRD patterns of ZIF-8 and the derived C, N-ZnO photocatalysts.

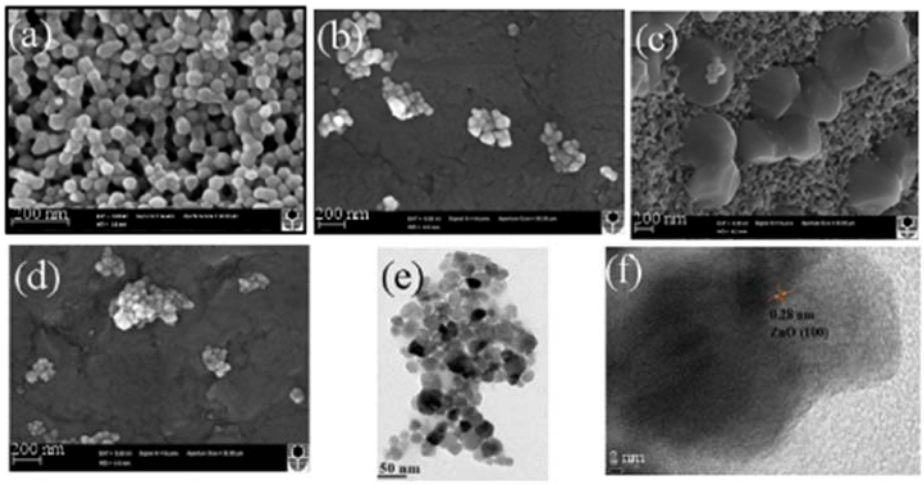

Figure 3.3. FE-SEM images of ZIF-8 (a), A120 (b), C800 (c), 8C120 (d), TEM image of 8C120 (d), and HRTEM image of 8C120.

Figure 3.3 shows FE-SEM and TEM images of the samples. ZIF-8 presented as dodecahedral nanoparticles (Figure 3.3a). After heat treatment, the framework of ZIF-8 collapsed down. A120 image displayed ellipse-like ZnO nanoparticles corresponding to XRD pattern (Figure 3.3b). C800 showed the dodecahedral carbon particles (Figure 3.3c). With further calcination in air, ZnO nanoparticles with significant aggregation were observed in 8C120 (Figure 3.3d), as confirmed by

XRD. The TEM image of 8C120 (Figure 3.3e) showed that the ZnO particles were uniform in size at around 16 nm, consistent with XRD results. The lattice spacing of 8C120 was 0.28 nm (Figure 3.3f), corresponding to the distance between the {100} planes in the ZnO crystal lattice.

The compositions and chemical states of A120 and 8C120 were investigated by XPS, confirming the elemental compositions of C, N, Zn and O (Figure 3.4). A120 contained 10.49 at.% C and no N, while C and N contents of 8C120 were 13.09 and 1.14 at.%, respectively, higher than those in A120 (Figure 3.4a). The lower contents of C and N on A120 could be explained by Figure 3.1: the combustion of C and N on ZIF-8 occurred at around 540 °C while at 580 °C on C800, and the combustion rate on ZIF-8 was much higher than that on C800. It indicated that C and N on C800 were more stable compared with ZIF-8, resulting in more C and N residues. The C in A120 and 8C120 distributed uniformly (Figure 3.5) while no N mapping was obtained because the content of N in 8C120 was too low beyond the detection limit. The N 1s spectrum for 8C120 showed two peaks at 398.7 and 400.2 eV, attributed to O-Zn-N and N-O, respectively, which formed during the pyrolysis (Figure 3.4b).[33, 34] It is revealed that N dopant was implanted substitutionally at O sites. C 1s peaks at 286.2, 287.2 and 288.5 eV were also observed on 8C120, assigned to C-O, C=O and O=C-O, respectively (Figure 3.4c). [35] A120 showed C 1s peaks at 286.1 and 288.9 eV, corresponding to C-O and O=C-O, respectively. [36] The peak centered at 284.6 eV was attributed to graphite and/or carbon from contaminations.[37] There were no peaks at around 281 eV, indicating no C-Zn bond formed. In the O 1s spectrum (Figure 3.4d), two peaks at 529.9 and 531.4 eV were observed on A120 and 8C120, assigned to the O^{2-} ions and oxygen vacancy on the surface of materials, respectively. [38] Zn 2p XPS spectrum contained two peaks at binding energy of 1021.2 and 1044.3 eV, ascribed to Zn $2p_{3/2}$ and $2p_{1/2}$, respectively (Figure 3.4e). The distance between the two lines was 23.1 eV, suggesting that Zn^{2+} ions existed in the two samples.

[39] Thus, XPS results suggested that 8C120 was N-doped ZnO embedded within carbon while A120 was ZnO modified by carbon but not N (Figure 3.4f).

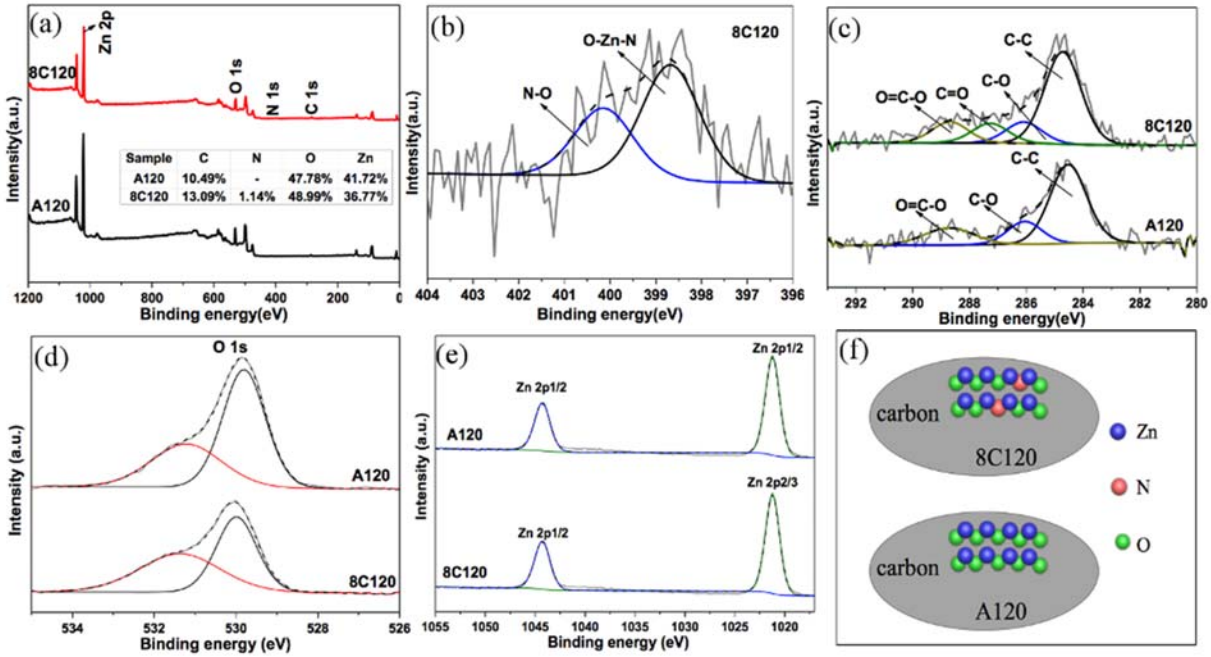

Figure 3.4. XPS wide-scans of A120 and 8C120 (a), high-resolution spectra of N 1s for 8C120 (b), C 1s (c) O 1s (d) and Zn 2p (e) for A120 and 8C120, and illustration (f) of 8C120 and A120.

Figure 3.6 exhibits UV-vis DRS and tauc plots of the prepared samples. As shown in Figure 3.6a, ZIF-8 could only absorb UV light at wavelengths below 240 nm. It was reported that it can show efficient photocatalytic MB degradation under UV light irradiation. [40] ZnO-a, A120 and 8C120 showed a strong absorption in the region of 200 to 400 nm. The light absorption of ZnO-a presented a sharp decline after 400 nm in the visible region, while A120 and 8C120 extended their absorption edge to the visible light region. It suggested that C and N doping could extend the light absorption thresholds. The band-gap energies of ZnO-a, A120 and 8C120 were estimated to be 3.01, 2.97 and 2.93 eV (Figure 3.6b), respectively, indicating that 8C120 owned the enhanced light absorption capability, compared with the other two samples in direct air calcination.

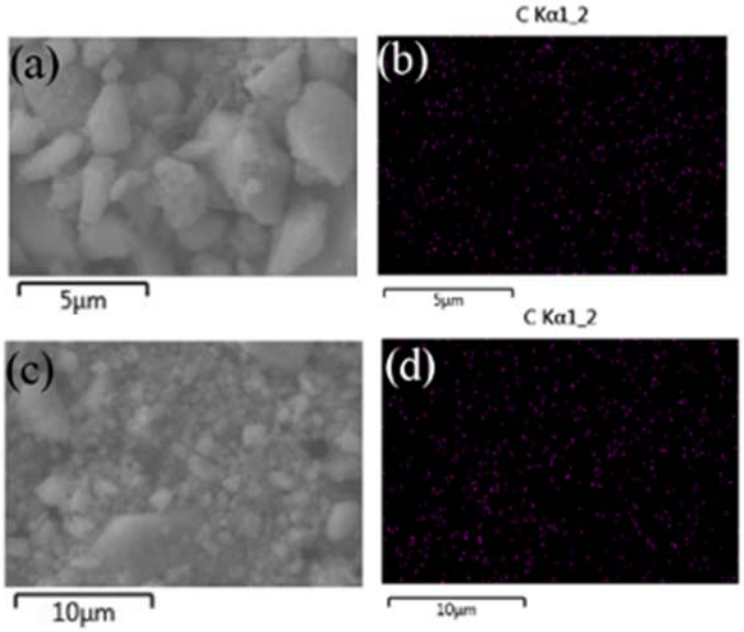

Figure 3.5. FE-SEM images of A120 (a) and 8C120 (c), carbon mapping of A120 (b) and 8C120 (d).

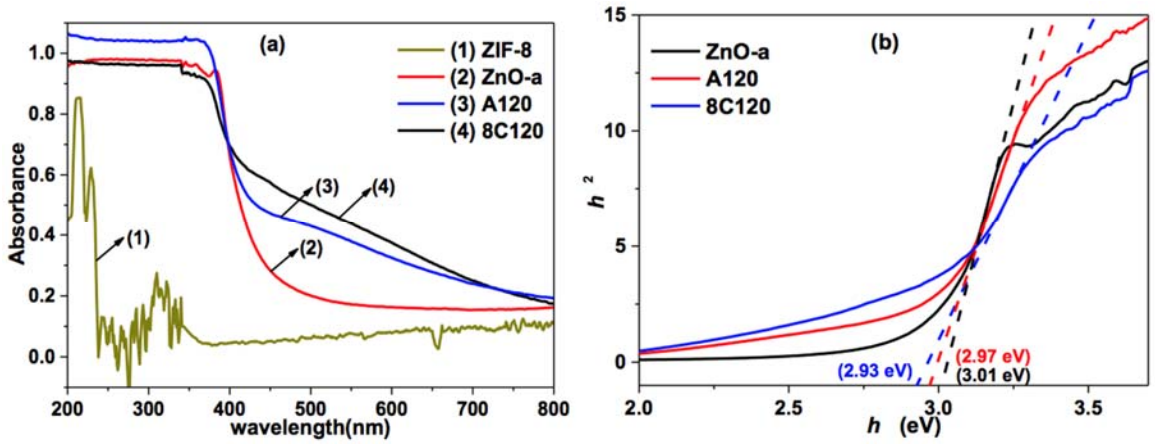

Figure 3.6. UV-vis DRS (a) and tauc plots (b) of ZIF-8, ZnO-a, A120 and 8C120.

3.3.2. Photocatalytic reactions

Photocatalytic O_2 evolution reactions (OER) on ZnO-a, A120, 8C120 and commercial ZnO under simulated sunlight irradiations were carried out and the results are shown in Figure 3.7. The

produced O_2 was observed and the amount increased rapidly in the initial 10 min, then it grew slowly with the time due to the consumption of electron acceptor Ag^+ in the solutions. The photocatalytic activity of 8C120 (8.22 μmol/min) for water oxidation in the initial 10 min was much higher than that of A120 (5.47 μmol/min), ZnO-a (1.85 μmol/min) and commercial ZnO (4.66 μmol/min). It could be concluded that narrower band-gap facilitated the better conversion from solar energy to chemical energy on ZnO-based materials. Meanwhile, the better performance of 8C120 could also be partly attributed to the higher BET surface area along with more active sites.[41, 42] In addition, the N dopant in the carbon matrix is able to enhance the OER activity as reported previously.[43, 44]

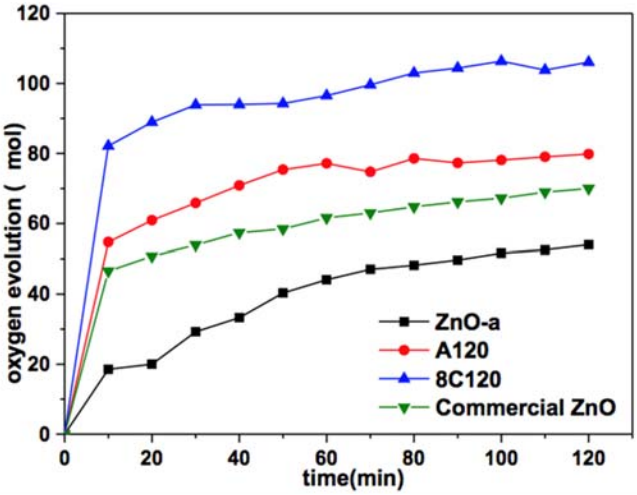

Figure 3.7. Oxygen evolution rates with ZnO-a, A120, 8C120 and commercial ZnO under simulated sunlight irradiations.

Figure 3.8 reveals the photodegradation of MB on synthesized samples. The photocatalytic efficiency of the samples followed an order of ZnO-a ≈ ZnO-b < A120 < 8C120. Self-decomposition of 60% MB in 150 min could be observed without catalysts under the solar-simulated light. About 72% MB was removed by ZIF-8 and C800 in 180 min, approximately 12%

higher than the photolysis without a catalyst ascribed to adsorption (Figure 3.9). It could be concluded that ZIF-8 and C800 were not effective for MB photodegradation, because ZIF-8 cannot absorb visible light while the crystallinity of ZnO was hindered by carbon in C800, as discussed above.

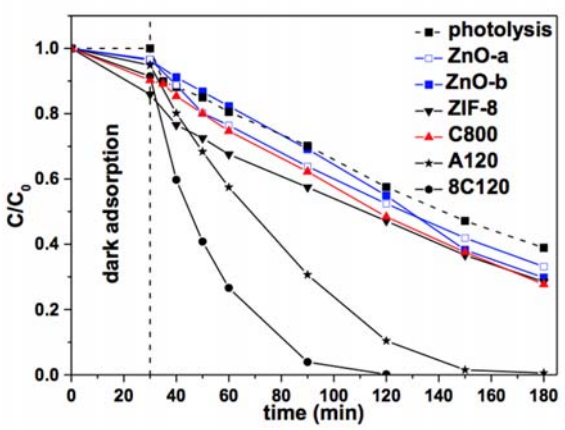

Figure 3.8. Photodegradation of MB on various materials [catalyst: 0.25 g/L (C800: 0.1 g/L); MB: 10 ppm; T: 25 °C].

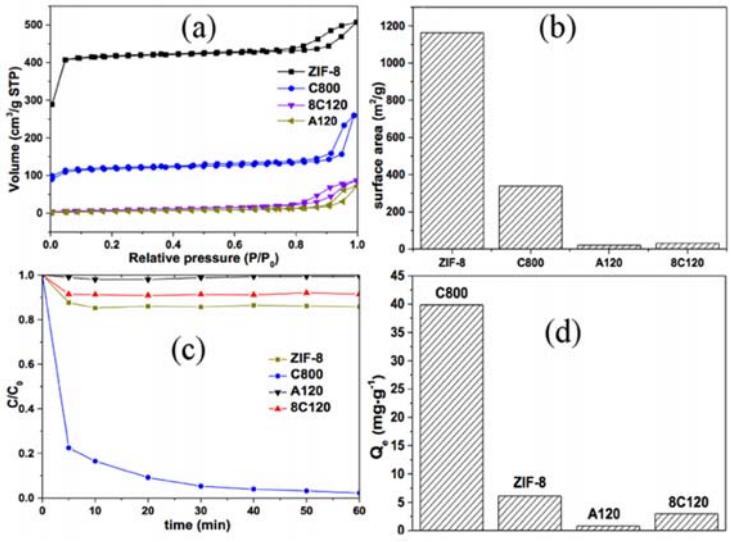

Figure 3.9. N_2 sorption isotherms (a), surface areas (b), and MB adsorption (c-d) on various materials [catalyst: 0.25 g/L; MB: 10 ppm; T: 25 °C].

ZnO-a showed weak absorption in the visible light region as depicted in Figure 3.6, so it exhibited a poor catalytic ability like ZnO-b. About 100% MB was decolorized in 150 min on A120 while 8C120 showed 100% MB degradation in 120 min, the best photocatalytic performance and the same as graphene-ZnO composites synthesized by post-treatment method.[45] The reactions of the materials conformed more to the first-order kinetics, according to R^2 in Figure 3.10. The first-order reaction rate constants of ZnO-a, A120 and 8C120 were found to be 0.0068, 0.021 and 0.053 min^{-1}, respectively, suggesting ZnO catalysts prepared from ZIF-8 *via* two-step synthesis route exhibited much better photocatalysis. The stability test (Figure 3.11) showed that the photocatalytic activity of 8C120 on MB degradation decreased slightly, due to the loss of catalysts and the adsorption of intermediates on the surface of catalysts [38, 45].

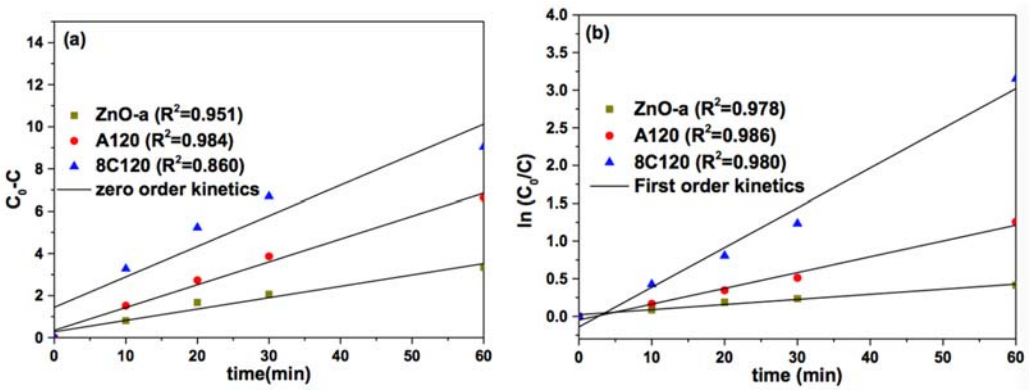

Figure 3.10. Zero-order (a) and first-order kinetics (b) of photocatalysis on different materials.

8C120 demonstrated the best performance for OER and MB degradation, which can be possibly attributed to multiple merits from the synthesis. Firstly, the higher dye adsorption on the surface of 8C120 (Figure 3.9) facilitated the interaction between the photocatalyst and MB. Secondly, the light absorption threshold was extended and the band-gap was lowered compared to ZnO-a and A120, inducing more photoinduced carriers for the enhanced photocatalytic efficiency. Noteworthy, the photocurrent density (Figure 3.12) did not follow the same order of the

photocatalytic activity. It could be explained by the varied carrier mobility. As reported elsewhere,[46] the carrier mobility of the composite would be improved while the materials combined with semiconductors were conductive or have a higher carrier mobility. However, the amorphous carbon doped in 8C120 was poorly conductive, inducing the lower carrier mobility and photocurrent.

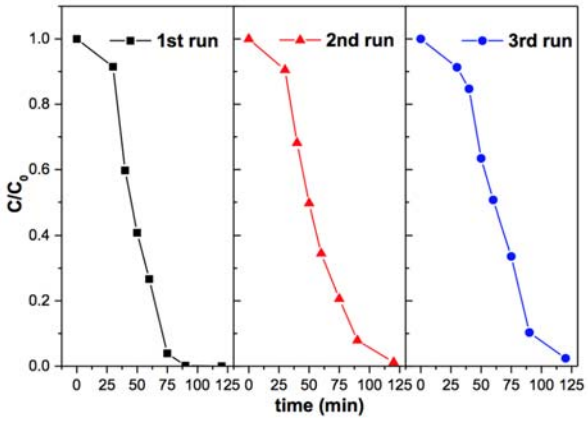

Figure 3.11. The stability of 8C120 on photodegradation of MB under solar-simulated light irradiations.

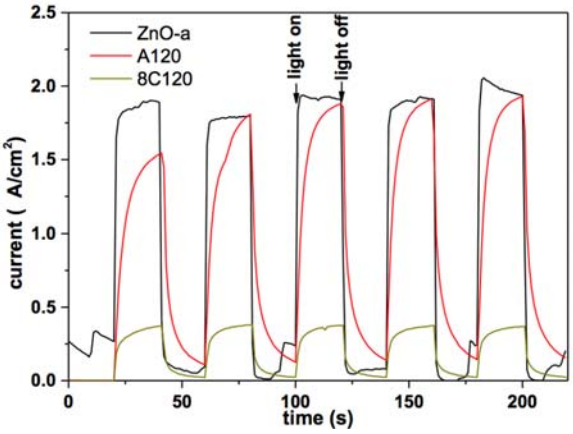

Figure 3.12. Photocurrent-time curves of photocatalytic materials under solar-simulated light ([$NaSO_4$] = 0.1 M).

3.4. Conclusions

Carbon and nitrogen modified ZnO hybrids derived from ZIF-8 were prepared through three different thermal transformation processes: single-step air combustion, N_2 annealing, and two-step N_2 annealing followed by air calcination. The photocatalytic activity of MOF-derived C, N-ZnO for the first time was systematically examined in water oxidation and photodegradation of dyes. It was also found that C, N-ZnO prepared from ZIF-8 by the two-step approach presented a much higher activity than those directly calcination of ZIF-8 from one-step method. This investigation introduces a facile synthesis of functionalized materials for oxygen evolution and catalytic remediation.

3.5. References

1. M. R. Hoffmann, S. T. Martin, W. Y. Choi and D. W. Bahnemannt, *Chem. Rev.*, 1995, **95**, 69-96.
2. J. Liu, X. Yu, Q. Liu, R. Liu, X. Shang, S. Zhang, W. Li, W. Zheng, G. Zhang, H. Cao and Z. Gu, *Appl. Catal., B*, 2014, **158-159**, 296-300.
3. H. M. Chen, C. K. Chen, Y. C. Chang, C. W. Tsai, R. S. Liu, S. F. Hu, W. S. Chang and K. H. Chen, *Angew. Chem. Int. Ed. Engl.*, 2010, **49**, 5966-5969.
4. S. G. Kumar and K. S. R. K. Rao, *RSC Adv.*, 2015, **5**, 3306-3351.
5. Q. Zhang, C. S. Dandeneau, X. Zhou and G. Cao, *Adv. Mater.*, 2009, **21**, 4087-4108.
6. H. Sun, G. Zhou, S. Liu, H. M. Ang, M. O. Tadé and S. Wang, *Chem. Eng. J.*, 2013, **231**, 18-25.
7. Z. Zhang, Y. Chen, S. He, J. Zhang, X. Xu, Y. Yang, F. Nosheen, F. Saleem, W. He and X. Wang, *Angew. Chem., Int. Ed. Engl.*, 2014, **53**, 12517-12521.
8. H. Zhang, G. Chen and D. W. Bahnemann, *J. Mater. Chem.*, 2009, **19**, 5089-5121.
9. H. Sun, S. Liu, S. Liu and S. Wang, *Appl. Catal., B*, 2014, **146**, 162-168.
10. T. Xu, L. Zhang, H. Cheng and Y. Zhu, *Appl. Catal., B*, 2011, **101**, 382-387.
11. O. Akhavan, *ACS nano*, 2010, **4**, 4177-4180.
12. X. Y. Yang, A. Wolcott, G. M. Wang, A. Sobo, R. C. Fitzmorris, F. Qian, J. Z. Zhang and Y. Li, *Nano Lett.*, 2009, **9**, 2331-2336.
13. S. Xie, X. Lu, T. Zhai, W. Li, M. Yu, C. Liang and Y. Tong, *J. Mater. Chem.*, 2012, **22**, 14272.
14. L. Sun, H. He, L. Hu and Z. Ye, *Phys. Chem. Chem. Phys.*, 2013, **15**, 1369-1373.
15. X. Zong, C. Sun, H. Yu, Z. G. Chen, Z. Xing, D. Ye, G. Q. Lu, X. Li and L. Wang, *J. Phys. Chem. C*, 2013, **117**, 4937-4942.
16. D. Li and H. Haneda, *J. Photochem. Photobiol., A*, 2003, **155**, 171-178.

17. J. Mu, C. Shao, Z. Guo, Z. Zhang, M. Zhang, P. Zhang, B. Chen and Y. Liu, *ACS Appl. Mater. Interfaces*, 2011, **3**, 590-596.

18. Y. Qiu, M. Yang, H. Fan, Y. Xu, Y. Shao, X. Yang and S. Yang, *Mater. Lett.*, 2013, **99**, 105-107.

19. G. Liu, L. Wang, C. Sun, X. Yan, X. Wang, Z. Chen, S. C. Smith, H.-M. Cheng and G. Q. Lu, *Chem. Mater.*, 2009, **21**, 1266-1274.

20. S. Kitagawa, R. Kitaura and S. Noro, *Angew. Chem., Int. Ed. Engl.*, 2004, **43**, 2334-2375.

21. O. K. Farha, I. Eryazici, N. C. Jeong, B. G. Hauser, C. E. Wilmer, A. A. Sarjeant, R. Q. Snurr, S. T. Nguyen, A. Ö. Yazaydın and J. T. Hupp, *J. Am. Chem. Soc.*, 2012, **134**, 15016-15021.

22. B. Liu, H. Shioyama, T. Akita and Q. Xu, *J. Am. Chem. Soc.*, 2008, **130**, 5390-5391.

23. L. Peng, J. Zhang, Z. Xue, B. Han, J. Li and G. Yang, *Chem. Commun.*, 2013, **49**, 11695-11697.

24. T. K. Kim, K. J. Lee, J. Y. Cheon, J. H. Lee, S. H. Joo and H. R. Moon, *J. Am. Chem. Soc.*, 2013, **135**, 8940-8946.

25. R. Wu, X. Qian, K. Zhou, J. Wei, J. Lou and P. M. Ajayan, *ACS Nano*, 2014, **8**, 6297-6303.

26. R. Wu, D. P. Wang, J. Han, H. Liu, K. Zhou, Y. Huang, R. Xu, J. Wei, X. Chen and Z. Chen, *Nanoscale*, 2015, **7**, 965-974.

27. R. Das, P. Pachfule, R. Banerjee and P. Poddar, *Nanoscale*, 2012, **4**, 591-599.

28. W. Chaikittisilp, N. L. Torad, C. Li, M. Imura, N. Suzuki, S. Ishihara, K. Ariga and Y. Yamauchi, *Chemistry*, 2014, **20**, 4217-4221.

29. R. Wu, D. P. Wang, X. Rui, B. Liu, K. Zhou, A. W. K. Law, Q. Yan, J. Wei and Z. Chen, *Adv. Mater.*, 2015, **27**, 3038-3044.

30. A. Aijaz, N. Fujiwara and Q. Xu, *J. Am. Chem. Soc.*, 2014, **136**, 6790-6793.

31. J. Cravillon, S. Münzer, S. J. Lohmeier, A. Feldhoff, K. Huber and M. Wiebcke, *Chem. Mater.*, 2009, **21**, 1410-1412.

32. Y. Du, R. Z. Chen, J. F. Yao and H. T. Wang, *J. Alloys Compd.*, 2013, **551**, 125-130.

33. S. Cho, J. W. Jang, K. j. Kong, E. S. Kim, K. H. Lee and J. S. Lee, *Adv. Funct. Mater.*, 2013, **23**, 2348-2356.

34. Y. Yan, S. B. Zhang and S. T. Pantelides, *Phys. Rev. Lett.*, 2001, **86**, 5723-5726.

35. D. Jiang, X. Du, Q. Liu, L. Zhou, J. Qian and K. Wang, *ACS Appl. Mater. Interfaces*, 2015, **7**, 3093-3100.

36. S. A. Wohlgemuth, R. J. White, M. G. Willinger, M. M. Titirici and M. Antonietti, *Green Chem.*, 2012, **14**, 1515.

37. H. Pan, J. B. Yi, L. Shen, R. Q. Wu, J. H. Yang, J. Y. Lin, Y. P. Feng, J. Ding, L. H. Van and J. H. Yin, *Phys. Rev. Lett.*, 2007, **99**, 127201.

38. M. Zhou, X. Gao, Y. Hu, J. Chen and X. Hu, *Appl. Catal., B*, 2013, **138-139**, 1-8.

39. F. Bai, Y. Xia, B. Chen, H. Su and Y. Zhu, *Carbon*, 2014, **79**, 213-226.

40. H. P. Jing, C. C. Wang, Y. W. Zhang, P. Wang and R. Li, *RSC Adv.*, 2014, **4**, 54454-54462.

41. Y. Qu, W. Zhou and H. Fu, *ChemCatChem*, 2014, **6**, 265-270.

42. H. Jin, J. Wang, D. Su, Z. Wei, Z. Pang and Y. Wang, *J. Am. Chem. Soc.*, 2015, **137**, 2688-2694.

43. Y. Zhao, R. Nakamura, K. Kamiya, S. Nakanishi and K. Hashimoto, *Nat. Commun.*, 2013, **4**, 2390.

44. J. Zhang, Z. Zhao, Z. Xia and L. Dai, *Nat. Nanotechnol.*, 2015, **10**, 444-452.

45. S. Liu, H. Sun, A. Suvorova and S. Wang, *Chem. Eng. J.*, 2013, **229**, 533-539.

46. Y. Liu, C. Xie, J. Li, T. Zou and D. Zeng, *Appl Catal., A*, 2012, **433-434**, 81-87.

Chapter 4: Photocatalysis of C, N-doped ZnO derived from ZIF-8 for dye degradation and water oxidation

ABSTRACT

The carbon and nitrogen co-doped ZnO was synthesized by a simple, two-step pyrolysis of a zinc-based metal organic framework (Zeolitic Imidazolate Framework-8, ZIF-8). ZIF-8 was firstly carbonized in the nitrogen atmosphere, followed by the pyrolysis in air forming the carbon and zinc oxide hybrids. The hybrids were evaluated by photocatalytic dye degradation and oxygen evolution reaction (OER). The contents of the dopants influenced the photocatalytic performances of the hybrids. The mechanism was illustrated and showed that hydroxyl radicals and photo-excited electrons contributed to the dye degradation. The carbon-zinc oxide hybrid also demonstrated a great potential for water oxidation because of the more active sites induced by dopants.

The content of this Chapter is published in Energy & Fuels, 2017, 31, 2138-2143.

4.1. Introduction

Zinc oxide (ZnO) is a promising heterogeneous photocatalyst for degradation of organic pollutants because of its environment- and economic-friendly nature and excellent photosensitivity[1]. However, the rapid recombination of light-induced electron-hole pairs and the narrow light-absorption range have restricted its wide applications. Hence, a variety of efforts were made to solve the problems, *e.g.* morphology control[2], metal or metal oxide doping[3, 4] and hybrid composites with other materials[5, 6]. It was reported that carbon and/or nitrogen doping could enhance the photocatalytic activity by the synergistic effect between the dopants and ZnO[7-10]. Many efforts on C/N-doped ZnO were also made for photocatalytic and photoelectrochemical applications [11-13]. Cho *et al.* synthesized carbon-doped ZnO using vitamin C and observed the visible photocatalytic activity of the resulting photocatalyst[14]. Cesano *et al.* reported the synthesis of ZnO-carbon composites by the pyrolysis of $ZnCl_2$-catalyzed furfuryl alcochol polymers[15]. Sun *et al.* prepared carbon and nitrogen doped ZnO by the vapor phase transport method using N_2O as the nitrogen source[16]. However, the conventional synthetic methods usually require critical conditions, complex synthesis procedures and high expenses.

Metal organic frameworks (MOFs), as porous crystalline materials, have been utilized as templates for synthesis of carbon, metal oxides and hybrid materials [17-19]. Using MOFs as precursors owns advantages over conventional routes, for example, the MOFs sacrifice themselves to the formation of materials to generate the uniform distributions of elements. Zeolitic Imidazolate Framework (ZIF)-8 is a N-rich Zn-containing MOF which could be synthesized through a facile way at room temperature[20]. It can be employed as carbon, nitrogen and zinc sources simultaneously, without extra functional precursors or post-synthesis treatment. Bai *et al.*[21] synthesized N-dope carbon derived from ZIF-8, showing excellent

carbon dioxide uptake capacity. However, direct synthesis of carbon-ZnO hybrid materials from a MOF as the sole precursor still needs further investigation.

Herein, we reported our study on a two-step synthesis route towards carbon and nitrogen modified ZnO. The resulting materials were evaluated by the photocatalytic oxygen evolution reaction and dye degradation under solar-simulated light. The mechanism of dye photodegradation was validated by quenching tests.

4.2. Experimental Section

4.2.1. Materials and reagents

2-Methylimidazole (99%, Hmim), zinc nitrate hexahydrate (98%, $Zn(NO_3)_2•6H_2O$), methanol (99.8%), methylene blue (99.9%, MB), silver nitrate (99.0%, $AgNO_3$), lanthanum oxide (99.9%, La_2O_3), tert-butyl alcohol (99.5%, TBA), potassium iodide (99.0%, KI), benzoquinone (98%, BQ), zinc oxide (99.0%, commercial ZnO) were purchased from Sigma-Aldrich.

4.2.2. Synthesis of materials

ZIF-8 was synthesized by mixing $Zn(NO_3)_2•6H_2O$ and Hmim in methanol at room temperature as reported elsewhere [20]. The photocatalysts were prepared *via* a two-step route as shown in Scheme 4.1. The synthesized ZIF-8 was carbonized at various temperatures (from 600 to 800 °C) for 2 h in nitrogen atmosphere (the samples were named as C600, C700 and C800), followed by pyrolysis in air at 450 °C for different durations (from 20 to 40 min), and then cooled down to room temperature. The obtained samples were denominated as *m*C*n* (*m* was the carbonization temperature in N_2 and *n* was the pyrolysis time in air). ZnO-R was obtained as above, employing $Zn(NO_3)_2•6H_2O$ as the precursor instead of ZIF-8.

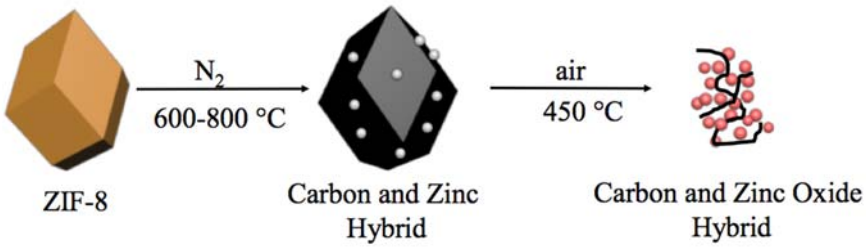

Scheme 4.1. The synthesis route of samples

4.2.3. Characterization of materials

Powder X-ray diffraction (XRD) patterns were recorded on a Bruker D8-Advance X-ray diffractometer with Cu Kα radiation (λ = 1.5418 Å). The morphology and particle size were analyzed by field emission scanning electron microscopy (FE-SEM, Zeiss Neon 40 EsB) and transmission electron microscopy (TEM, JEOL 2100). An energy dispersive X-ray spectroscopy (EDX) was used to estimate the chemical compositions. X-ray photoelectron spectroscopy (XPS) was utilized to investigate the chemical states of the modified ZnO using a Kratos AXIS Ultra DLD system with Al-Kα X-ray and C-C peak at 284.6 eV was used as a charge correction reference. UV-visible diffuse reflectance spectra (UV-vis DRS) were acquired on a JASCO V-670 spectrophotometer with an Ø60 mm integrating sphere, using $BaSO_4$ as a reference. The zinc ions were quantified using the inductively coupled plasma-mass spectroscopy (ICP-MS, model PerkinElmer NexION 350D). N_2 sorption isotherms and pore size distributions were obtained on a Tristar 3020 at -196°C according to Brunauer–Emmett–Teller (BET) equation and the Barrett-Joyner-Halenda (BJH) method.

4.2.4. Photocatalytic OER and MB degradation

Photocatalytic reactions were carried out in a closed reactor connecting to a water bath for maintaining the reaction temperature at 25 °C. A Xenon lamp (300 W) provided simulated sunlight for water oxidation with $AgNO_3$ as an electron scavenger. Specifically, 0.5 g/L samples were added into $AgNO_3$ solution (0.03 M) with La_2O_3 (0.1 g/L) in it. Before light

irradiation, degassing was conducted to dispel air in the reactor. The concentration of oxygen produced in the reactor was measured with a NEOFOX O_2 probe.

Photodegradation of MB was performed under the simulated sunlight at 25 °C. Typically, 0.25 g/L catalyst was dispersed into 10 ppm MB solution. Prior to the degradation, the solution was continuously stirred in dark for 30 min to achieve adsorption/desorption equilibrium, followed by switching on the lamp. The concentration of MB was determined by a UV-vis spectrometer at λ = 664 nm. Radical trapping experiments were conducted under the same conditions with the addition of radical scavengers: TBA, KI and BQ.

4.3. Results and Discussion

As shown in Scheme 4.1, the framework of ZIF-8 was supposed to collapse after the carbonization in nitrogen atmosphere and zinc oxide was reduced to zinc by carbon at a high temperature, generating carbon/nitrogen and zinc hybrid. After calcination in air, carbon/nitrogen was combusted to form CO_x/NO_x while zinc was oxidized into zinc oxide. It was envisioned that carbon/nitrogen-doped ZnO was finally obtained.

The TGA results (Figure 4.1a) showed that the residual weights were about 98.2%, 92.9% and 84.5% on 6C25, 7C25 and 8C25, respectively. It can be seen that the content of carbonaceous materials in 7C25 and 8C25 (7.1 wt.% and 15.5 wt.%, respectively) was much higher than 6C25 (1.8 wt.%), which was reconfirmed by the EDX results in Table 4.1. However, more carbonaceous materials were generally considered to be lost with the increase of carbonization temperature during the first step. The mass ratios of carbon in C600, C700 and C800 were 66.5 wt.%., 67.1 wt.%. and 73.5 wt.% (Figure 4.1b). In addition, the carbon combustion started at 401, 420 and 441°C for C600, C700 and C800, respectively, indicating that the carbonaceous materials were more stable with the increase of carbonization

temperature in N_2. At a low temperature, the functional groups in MOF might mainly undergo desorption and decomposition, thus successful carbonization cannot be obtained. On the contrary, a higher calcination temperature in N_2 might be beneficial to the formation of carbon hybrids while lower carbonization temperature would induce incomplete conversion of ZIF-8[21]. Consequently, more carbon was retained in 7C25 and 8C25 compared with 6C25. Similar result was reported elsewhere by Yamauchi *et al*.[19]

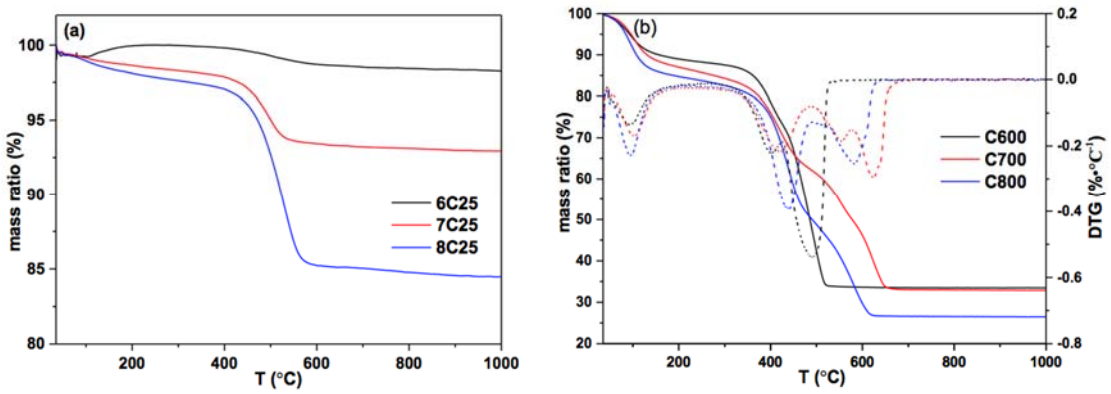

Figure 4.1. TGA of 6C25, 7C25 and 8C25 in air (a) and TGA/DTG of C600, C700 and C800 in air (b).

Table 4.1. Carbon and nitrogen contents of the samples obtained from EDX analysis.

samples	6C25	7C25	8C25	6C20	6C30	6C40
C (wt.%)	2.71	4.48	12.66	4.01	0.93	0.66
N (wt.%)	0.57	1.47	4.02	1.16	0.35	0.14

Figure 4.2 shows XRD patterns of 6C25, 7C25 and 8C25. The similar peaks of the three samples can be ascribed to crystalline ZnO with a wurtzite structure (JCPDS 36-1451). It is noted that the XRD patterns of 6C25 were strong and sharp, while those of 7C25 and 8C25 appeared to be weak, suggesting that ZnO in 6C25 has a high crystalline degree. The carbonaceous materials in 7C25 and 8C25 restrained the crystallinity of ZnO during the pyrolysis in air, because Zn species were covered by the matrix which would hinder the

interaction between Zn species and oxygen[21]. As a result, the amount and crystallinity of ZnO on 7C25 and 8C25 were inferior to 6C25.The particle sizes of ZnO in 6C25, 7C25 and 8C25 were calculated to be 16.1, 17.3 and 18.8 nm, according to the Scherrer equations. The lattice constants of 6C25 (a = 3.2505, c = 5.2111) were larger than those of pure ZnO (a = 3.2495, c = 5.2069), indicating that carbon/nitrogen substituted oxygen in the ZnO lattice inducing the change of the lattice constants [22].

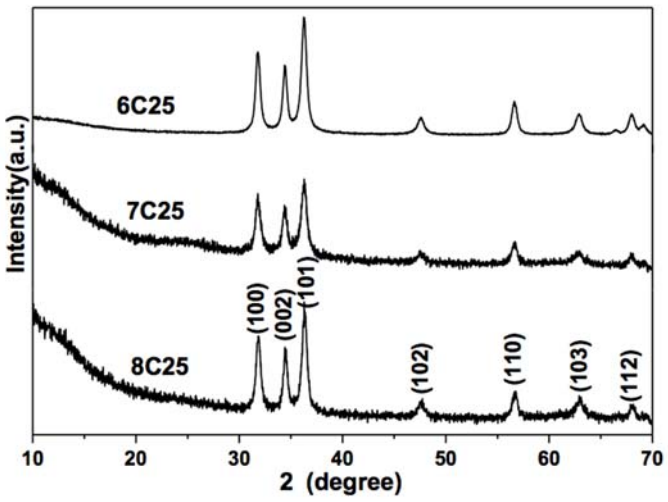

Figure 4.2. XRD patterns of 6C25, 7C25 and 8C25.

The morphologies of samples were shown in Figure 4.3. The carbon network decomposed and collapsed, inducing that ZnO particles agglomerated together densely for 6C25 (Figure 4.3a). The TEM image of 6C25 (Figure 4.3b) showed that the hexagonal ZnO particles were about 16 nm, conforming to the XRD result above. Much less nanoparticles scattered in the matrix for 7C25 (Figure 4.3c) and 8C25 (Figure 4.3d), which were proved to be poorly crystalline ZnO by XRD.

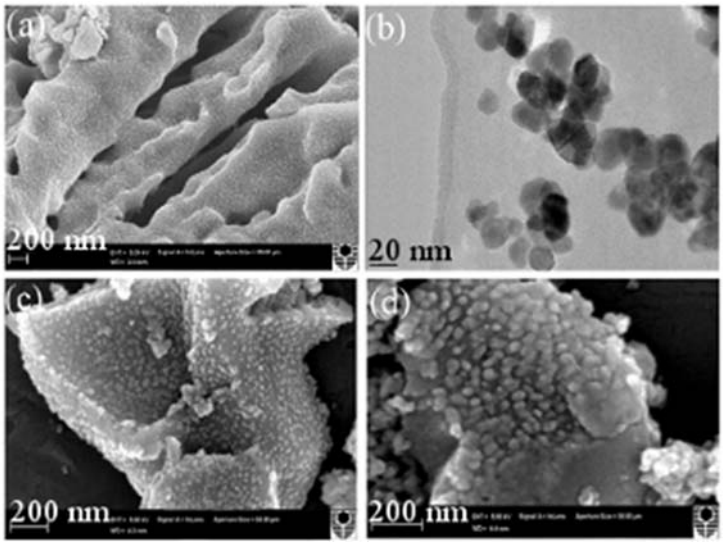

Figure 4.3. SEM (a) and TEM (b) of 6C25, SEM of 7C25 (c) and SEM of 8C25 (d).

The compositions and chemical status of 6C25 were investigated by XPS, as shown in Figure 4.4. The strong and sharp peaks of Zn 2p and O 1s could be found with weak peaks assigned to C 1s and N 1s (Figure 4.4a). The contents of C, N, O and Zn were 8.74 at.%, 1.80 at.%, 47.74 at.% and 41.72 at.%, respectively. Figure 4.4b shows the high-resolution C 1s spectra of 6C25. Four peaks centered at 283.6, 284.5, 286.2 and 288.5 eV were observed, which are corresponding to Zn-C, C-C, C-O and O=C-O, respectively [23-25]. The presence of Zn-C indicated that carbon was incorporated into the ZnO lattice by substituting for oxygen [14, 26]. The Zn-C bond would improve the lattice parameters of carbon-doped ZnO due to the larger size of C^{4-} (0.26 nm) compared with that of O^{2-} (0.14 nm), which was consistent with the XRD result above. In the N 1s spectrum (Figure 4.4c), only one peak at 398.3 eV was observed, which is located between the binding energy for metal nitride (396-397 eV)[27] and NO species (above400 eV)[28]. Thereby, the peak of N 1s was attributed to O-Zn-N, indicating that N dopant was incorporated at O sites in the synthesized structures[29, 30]. The XPS spectrum of oxygen was wide and asymmetrical, indicating that it can be de-convoluted into more than one peaks, as shown in Figure 4.4d. The peaks centered at 529.5 and 531.0 eV, assigned to O^{2-} in the ZnO

lattice and oxygen vacancies on the surface of 6C25 which resulted from pyrolysis in oxygen-poor condition (the first step in this study), respectively [22, 31-33]. The high-resolution spectra of Zn 2p (Figure 4.4e) showed two peaks at 1020.73 and 1043.81 eV, which are attributed to Zn^{2+} ions[21].

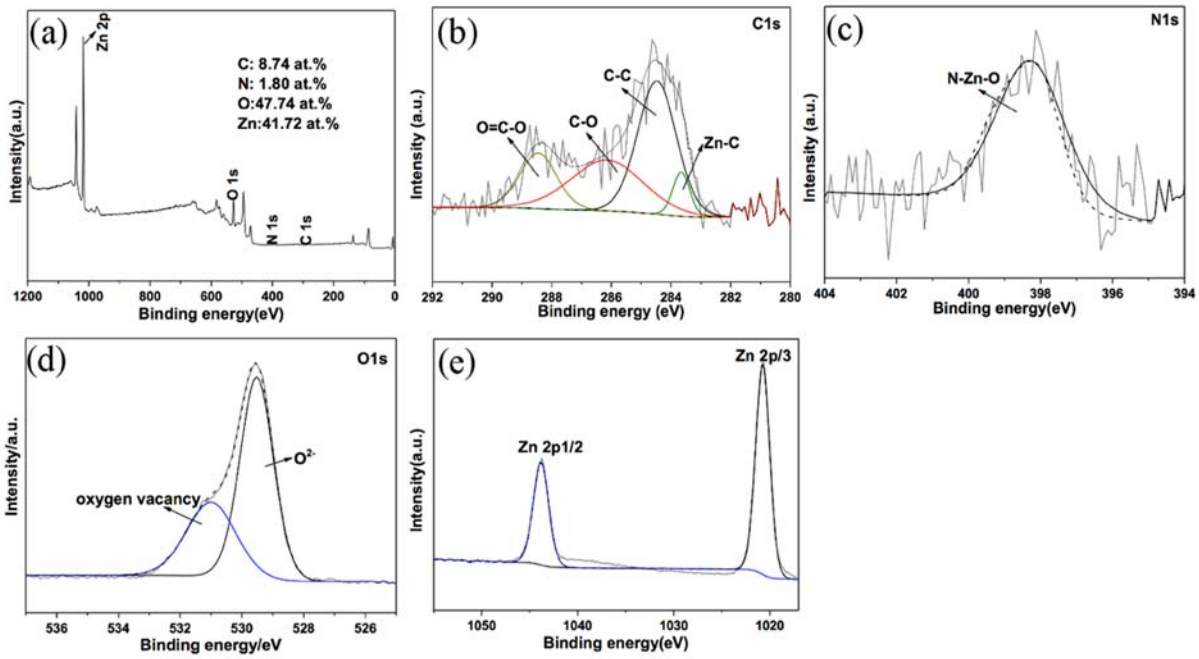

Figure 4.4. wide-scan XPS spectrum (a), the high-resolution spectra of C 1s (b), N 1s (c), O 1s (d) and Zn 2p (e) of 6C25.

Figure 4.5 reveals UV-vis diffuse reflectance spectra of 6C25, 7C25 and 8C25. 7C25 and 8C25 demonstrated strong absorption from 200 to 1500 nm, due to much carbon covering the ZnO, as confirmed in Figure 4.1. The absorption of 6C25 was strong below 400 nm and gradually decreased in the visible-light range. The tauc plot (inset) showed that the band-gap energy of 6C25 was 2.98 eV which was less than that of pure ZnO (3.20 eV)[34]. The narrowed bandgap was induced by oxygen vacancies confirmed by XPS above, which would generate new energy state under the conduction band [35-37].

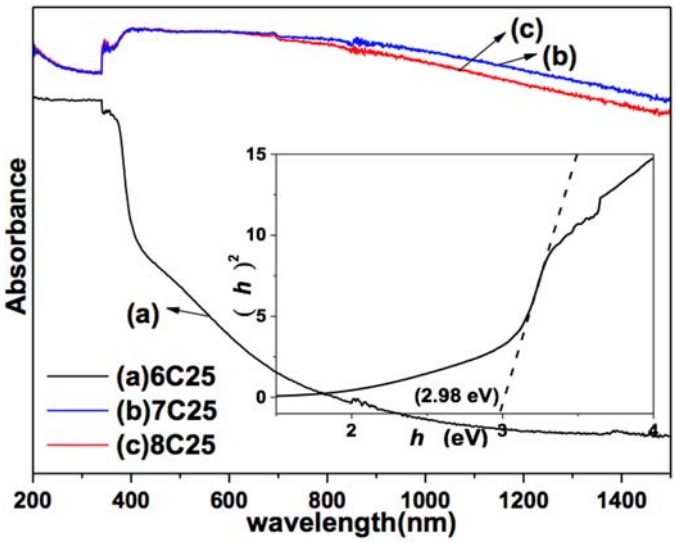

Figure 4.5. UV-vis DRS of 6C25, 7C25 and 8C25 and tauc plot of 6C25 (inset).

The N_2 sorption isotherm curves of 6C25, 7C25 and 8C25 in Figure 4.6a were classified to be type IV isotherm and H2 hysteresis loop, suggesting the existence of mesopores. The specific surface areas of 6C25, 7C25 and 8C25 were 40.9, 47.5 and 41.73 m^2g^{-1}, respectively. The pore size of 7C25 (Figure 4.6b) was about 2.2 and 3.4 nm while that of 8C25 was mainly 2.2 nm. The pore size of 6C25 was about 10.9 nm, much larger than that of 7C25 and 8C25.

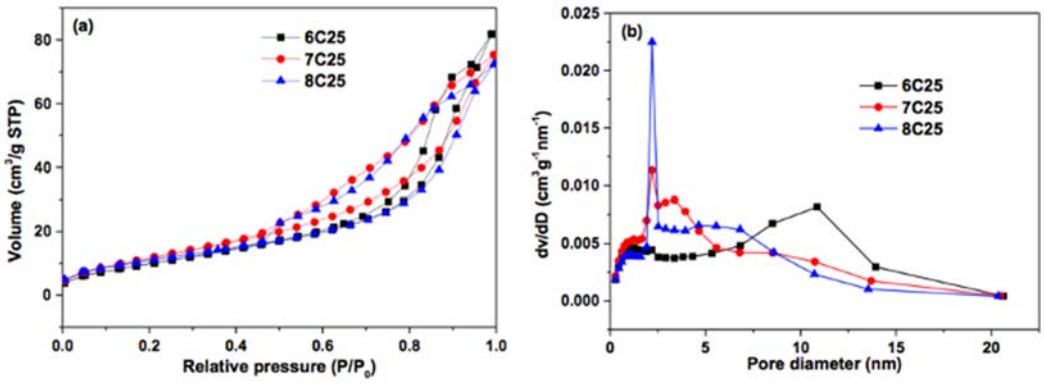

Figure 4.6. N_2 sorption isotherm (a) and pore size distribution (b) curves of 6C25, 7C25 and 8C25.

Figure 4.7 presents the photocatalytic activity of synthesized samples on degradation of MB

under the solar-simulated light. As shown in Figure 4.7a, the light could solely degrade about 53% of MB in 150 min. About 68% of MB was removed in 150 min on 7C25 and 92.5% of MB on 8C25, which was mainly attributed to the dark adsorption in the first 30 min and photolysis by solar-simulated light. The first-order kinetic reaction rate constants of 7C25 and 8C25 were calculated to be 0.006 and 0.01 min^{-1}, respectively. The poor photocatalytic activities of 7C25 and 8C25 were attributed to the poor crystalline and minor amount of ZnO covered by carbon, although the samples showed strong light absorption which could not be employed effectively. ZnO-R exhibited better photocatalytic performance, 100% of MB degradation in 150 min and the first-order kinetic rate was 0.049 min^{-1}. 6C25 showed the best photocatalytic effect, 100% of MB degradation in 90 min, and the first-order kinetic rate was 0.068 min^{-1}. Less than 10% of MB was adsorbed in the dark for 6C25, indicating that the decolorization of MB was mainly ascribed to photooxidation.

The influence of carbon and nitrogen fractions on photocatalytic performance was investigated in Figure 4.7b. It took 90 min to completely degrade MB on 6C25, while 120 min on 6C20, 6C30 and 6C40. The first-order kinetic rates of 6C20, 6C25, 6C30 and 6C40 were 0.039, 0.068, 0.050 and 0.028 min^{-1}, respectively (Figure 4.7c). It seems that calcination time in air exerted a great influence on the photocatalytic efficiency and had an optimum value towards the best effect. The carbon and nitrogen contents decreased with the extension of pyrolysis time in air as shown in Table 4.1. 6C20 showed an inferior photocataytic activity due to too much carbonaceous materials hindering the light absorption. The carbon and nitrogen were burned out in the form of CO_x and NO_x with the calcination time in air, which resulted in the decreased amount of carbon and nitrogen in 6C30 and 6C40 compared with 6C25. Consequently, the positive performances of carbon and nitrogen species (improving the adsorption of MB and hindering the recombination of holes and electrons) on photocatalysis were weakened, leading to the poorer efficiencies. Conclusively, the carbon and nitrogen

fractions were important in determining photocatalytic performance, as reported similarly elsewhere [13, 38].

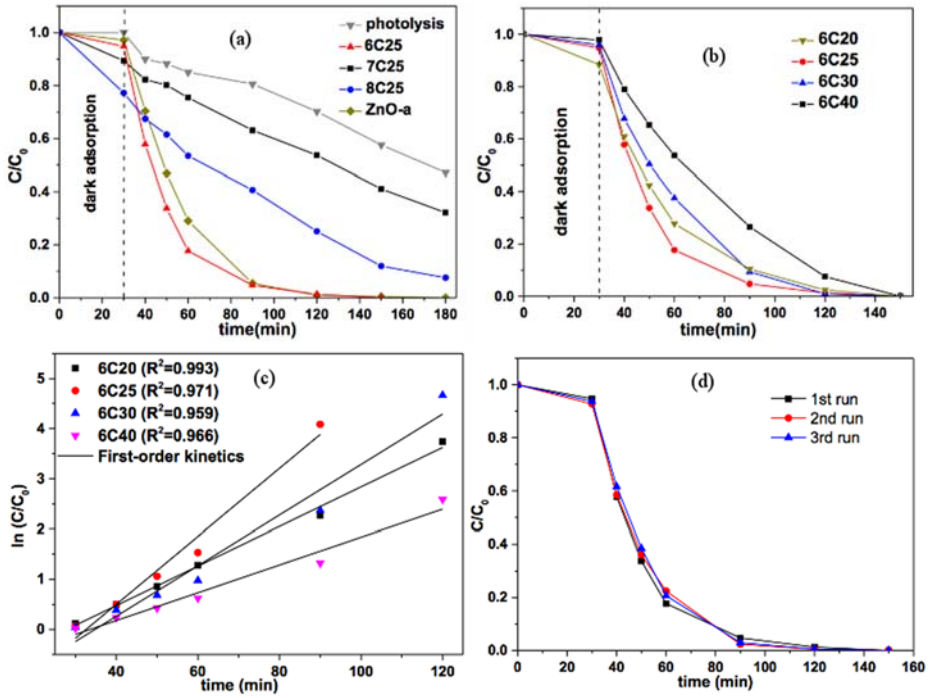

Figure 4.7. The photocatalytic activity of the synthesized samples (a) and influence of pyrolysis time in air (b) on degradation of MB under the solar-simulated light; First-order kinetic rates of 6C20, 6C25, 6C30 and 6C40 (c); Stability of 6C25 (d). Reaction condition: catalyst 0.25g/L, MB 10 ppm, T 25 °C.

The stability of the photocatalyst was investigated under solar-simulated light, as shown in Figure 4.7d. It can be seen that the photocatalytic activity decreased slightly after three runs, partially due to the coverage of intermediates on the catalyst, which would weaken the light absorption and electron transfer[39]. The concentrations of dissolved zinc ions in the reaction solutions after the 2nd and 3rd runs were 4 and 8.5 ppm, respectively, and thereby, the reduction of photocatalytic activity was also induced by the loss of zinc oxide *via* photo-corrosion.

The best photocatalytic activity of 6C25 could be attributed to the following reasons: (i) ZnO in 6C25 was well-crystalline and the dopants fraction was proper; (ii) the carbon can enhance the MB adsorption ability and improve the interaction between MB and the catalyst; (iii) 6C25 showed high UV absorption ability and narrowed bandgap, compared with ZnO; (iv) the synergetic effect between carbon/nitrogen and ZnO retarded the recombination of electrons and holes, as reported elsewhere[40]; (v) as mentioned previously[35], the oxygen vacancy facilitated the photocatalytic activity, due to the new-generated energy level below the conduction band which would inhibit the recombination of photo-excited electrons and holes.

To investigate the mechanism of dye degradation, quenching tests were conducted as shown in Figure 4.8. TBA as a typical hydroxyl ($^{\bullet}OH$) radicals scavenger was added into the reaction solution to verify the effect of $^{\bullet}OH$ radicals. The photocatalytic effect decreased with the addition of 0.01 M TBA. Assuming that $^{\bullet}OH$ radicals dominated the degradation, the degradation rate should drop greatly. The decrease indicated that dye degradation was attributed partially to $^{\bullet}OH$ radicals.

Iodide ion (I^-) was reported to be a scavenger of both $^{\bullet}OH$ radicals and positive holes (h^+) as reactions below[41, 42]:

$$2I^- + {}^{\bullet}OH \rightarrow I_2 + OH^- + e^- \qquad (4\text{-}1)$$

$$2I^- + 2h^+ \rightarrow I_2 \qquad (4\text{-}2)$$

Figure 4.8 showed that the photocatalytic effect increased nearly six times with the addition of KI as I^-. As discussed above, $^{\bullet}OH$ radicals acted slightly on dye degradation. Thereby, photo-excited holes would be attributed to the photocatalytic reaction. However, the reaction rate would decrease if the dye degradation was realized *via* holes. The discrepancy revealed that

photodegradation was not facilitated by holes. The consumption of holes caused by I^- inhibited the recombination of electrons and holes, inducing the increase of electrons amount. Therefore, the dye degradation could be ascribed to electrons. Similar conclusions were also reported by other groups [22, 43].

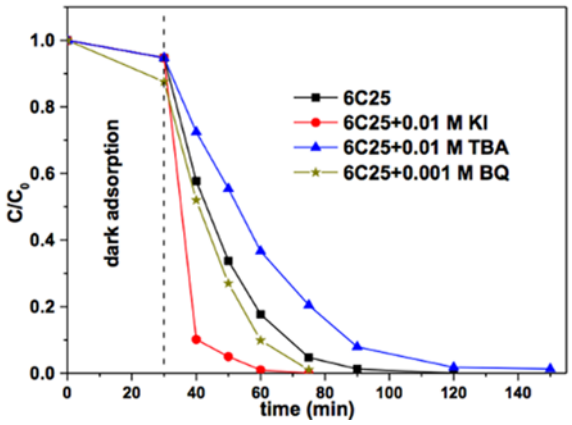

Figure 4.8. The quenching tests with the addition of TBA, KI and BQ.

As reported by other researchers, the carbon state lies deeply in the bandgap of ZnO while the reduction potential of superoxide radicals (-0.28 V *vs.* NHE) is just below the conductive band of ZnO[44]. Thereby, the electrons transferred to carbon could not be trapped by O_2 to produce superoxide radicals[22]. The addition of BQ in Figure 4.8 did not change the reaction rate compared with the absence of BQ excluding dark adsorption in the first 30 min. Li *et al.* reported that the reaction rate decreased dramatically after adding BQ in the system, confirming the effect of superoxide radicals[41]. The contrary results indicated that superoxide ions were not produced in this study. Conclusively, the dye degradation on 6C25 was attributed to hydroxyl radicals and photo-excited electrons.

The mechanism of 6C25 on photocatalytic degradation of the dye was proposed as shown in Figure 4.9. The electrons in the valence band (VB) were exited to the conduction band (CB)

with the generation of holes in the VB. The holes would oxide the water into •OH radicals which would contribute partially to the dye degradation as discussed above. Meanwhile, the electrons in the CB would transfer to the new electron donor state caused by oxygen vacancies which was below the conduction band. The carbon would accept the electrons and then finish the degradation of dye adsorbed on it. It could be seen that the existence of oxygen vacancies and carbon retarded the recombination of holes and electrons. MB was decomposed into CO_2 and H_2O eventually by •OH radicals and photo-excited electrons.

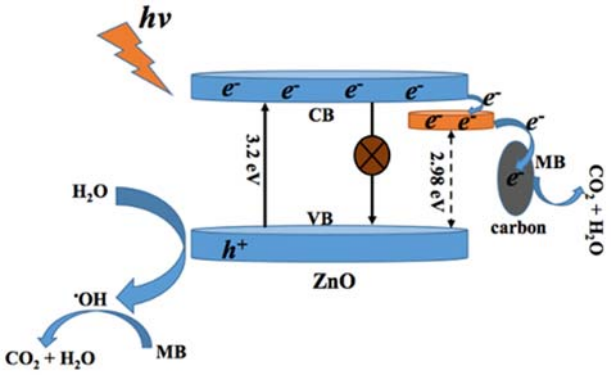

Figure 4.9. The proposed photocatalytic mechanism of 6C25 under solar-simulated light.

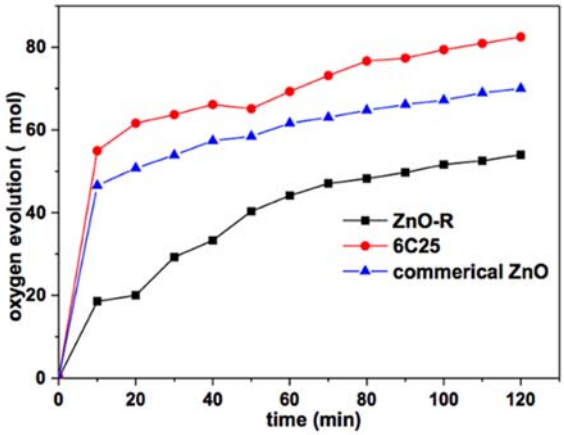

Figure 4.10. The amount of evolved O_2 on samples under solar-simulated light.

The photocatalytic water oxidation performances of samples were shown in Figure 4.10. It

could be seen that the oxygen evolution rate was the largest in the first 10 min and then decreased due to the consumption of electron acceptor Ag^+ and the block of light induced by the generation of Ag. The amount of O_2 evolved on ZnO-R, commercial ZnO and 6C25 were 1.85, 4.65 and 5.50 μmol/min, respectively, indicating that carbon and nitrogen dopants facilitated oxygen evolution reaction by lowering the bandgap energy and hindering the recombination of photo-excited electrons and holes.

4.4. Conclusions

In summary, carbon and nitrogen co-doped ZnO was prepared *via* a two-step route by thermal conversion of ZIF-8. 6C25 showed the best photocatalytic activity on dye degradation, due to the proper carbon/nitrogen dopants and oxygen vacancies. The mechanism investigation showed that hydroxyl radicals and photo-excited electrons act on the decomposition of methylene blue. 6C25 also showed a better photocatalytic oxygen evolution performance than commercial ZnO, due to more active sites introduced by dopants. This research provides a simple and effective way to obtain the photocatalysts for water decontamination and oxidation.

4.5. References

1. S. Xie, X. Lu, T. Zhai, W. Li, M. Yu, C. Liang and Y. Tong, *J. Mater. Chem.*, 2012, **22**, 14272.
2. S. Cho, S. H. Jung and K. H. Lee, *J. Phys. Chem. C*, 2008, **112**, 12769-12776.
3. R. Saleh and N. F. Djaja, *Spectrochim. Acta, Part A*, 2014, **130**, 581-590.
4. C. Cheng, A. Amini, C. Zhu, Z. Xu, H. Song and N. Wang, *Sci. Rep.*, 2014, **4**, 4181.
5. Y. J. Wang, R. Shi, J. Lin and Y. F. Zhu, *Energy Environ. Sci.*, 2011, **4**, 2922-2929.
6. H. Sun, S. Liu, G. Zhou, H. M. Ang, M. O. Tade and S. Wang, *ACS Appl. Mater. Interfaces*, 2012, **4**, 5466-5471.
7. H. Fu, T. Xu, S. Zhu and Y. Zhu, *Environ. Sci. Technol.*, 2008, **42**, 8064–8069.
8. H. Zhang, R. Zong and Y. Zhu, *J. Phys. Chem. C*, 2009, **113**, 4605–4611.
9. S. Z. Liu, H. Q. Sun, A. Suvorova and S. B. Wang, *Chem. Eng. J.*, 2013, **229**, 533-539.
10. Z. F. Shen, P. Liang, S. B. Wang, L. H. Liu and S. M. Liu, *ACS Sustainable Chem. Eng.*, 2015, **3**, 1010-1016.
11. M. Zhou, X. Gao, Y. Hu, J. Chen and X. Hu, *Appl. Catal., B*, 2013, **138-139**, 1-8.
12. X. Zong, C. Sun, H. Yu, Z. G. Chen, Z. Xing, D. Ye, G. Q. Lu, X. Li and L. Wang, *J. Phys. Chem. C*, 2013, **117**, 4937-4942.
13. S. Lian, H. Huang, J. Zhang, Z. Kang and Y. Liu, *Solid State Commun.*, 2013, **155**, 53-56.
14. S. Cho, J. W. Jang, J. S. Lee and K. H. Lee, *CrystEngComm*, 2010, **12**, 3929.
15. F. Cesano, D. Scarano, S. Bertarione, F. Bonino, A. Damin, S. Bordiga, C. Prestipino, C. Lamberti and A. Zecchina, *J. Photochem. Photobiol., A*, 2008, **196**, 143-153.
16. L. Sun, H. He, L. Hu and Z. Ye, *Phys. Chem. Chem. Phys.*, 2013, **15**, 1369-1373.
17. B. Liu, H. Shioyama, T. Akita and Q. Xu, *J. Am. Chem. Soc.*, 2008, **130**, 5390-5391.

18. K. E. deKrafft, C. Wang and W. Lin, *Adv. Mater.*, 2012, **24**, 2014-2018.

19. W. Chaikittisilp, N. L. Torad, C. Li, M. Imura, N. Suzuki, S. Ishihara, K. Ariga and Y. Yamauchi, *Chemistry*, 2014, **20**, 4217-4221.

20. J. Cravillon, S. Munzer, S. J. Lohmeier, A. Feldhoff, K. Huber and M. Wiebcke, *Chem. Mater.*, 2009, **21**, 1410-1412.

21. F. H. Bai, Y. D. Xia, B. L. Chen, H. Q. Su and Y. Q. Zhu, *Carbon*, 2014, **79**, 213-226.

22. M. Samadi, H. A. Shivaee, A. Pourjavadi and A. Z. Moshfegh, *Appl. Catal., A*, 2013, **466**, 153-160.

23. H. Pan, J. B. Yi, L. Shen, R. Q. Wu, J. H. Yang, J. Y. Lin, Y. P. Feng, J. Ding, L. H. Van and J. H. Yin, *Phys. Rev. Lett.*, 2007, **99**, 127201.

24. F. Ahimou, C. J. P. Boonaert, Y. Adriaensen, P. Jacques, P. Thonart, M. Paquot and P. G. Rouxhet, *J. Colloid Interface Sci.*, 2007, **309**, 49-55.

25. S. T. Tan, X. W. Sun, Z. G. Yu, P. Wu, G. Q. Lo and D. L. Kwong, *Appl. Phys. Lett.*, 2007, **91**, 072101.

26. S. Zhou, Q. Xu, K. Potzger, G. Talut, R. Grötzschel, J. r. Fassbender, M. Vinnichenko, J. r. Grenzer, M. Helm, H. Hochmuth, M. Lorenz, M. Grundmann and H. Schmidt, *Appl. Phys. Lett.*, 2008, **93**, 232507.

27. K. Toyoura, H. Tsujimura, T. Goto, K. Hachiya, R. Hagiwara and Y. Ito, *Thin Solid Films*, 2005, **492**, 88-92.

28. Y. Yan, S. B. Zhang and S. T. Pantelides, *Phys. Rev. Lett.*, 2001, **86**, 5723-5726.

29. J. M. Bian, X. M. Li, X. D. Gao, W. D. Yu and L. D. Chen, *Appl. Phys. Lett.*, 2004, **84**, 541.

30. S. Cho, J. W. Jang, K. j. Kong, E. S. Kim, K. H. Lee and J. S. Lee, *Adv. Funct. Mater.*, 2013, **23**, 2348-2356.

31. F. H. Wang, H. P. Chang, C. C. Tseng and C. C. Huang, *Surf. Coat. Technol.*, 2011, **205**, 5269-5277.

32. G. Wu, X. Tan, G. Li and C. Hu, *J. Alloys Compd.*, 2010, **504**, 371-376.

33. M. R. Bayati, J. Ding, Y. F. Lee, R. J. Narayan, J. Narayan, H. Zhou and S. J. Pennycook, *J. Phys.: Condens. Matter*, 2012, **24**, 395005.

34. H. Q. Sun, X. H. Feng, S. B. Wang, H. M. Ang and M. O. Tade, *Chem. Eng. J.*, 2011, **170**, 270-277.

35. Y. Lai, M. Meng, Y. Yu, X. Wang and T. Ding, *Appl. Catal., B*, 2011, **105**, 335-345.

36. U. N. Maiti, S. Maiti and K. K. Chattopadhyay, *CrystEngComm*, 2012, **14**, 640-647.

37. Yuanhui Zheng, Chongqi Chen, Yingying Zhan, Xingyi Lin, Qi Zheng, Kemei Wei, Jiefang Zhu and Y. Zhu, *Inorg. Chem.*, 2007, **46**, 6675-6682.

38. R. Liu, Y. Ren, Y. Shi, F. Zhang, L. Zhang, B. Tu and D. Zhao, *Chem. Mater.*, 2008, **20**, 1140-1146.

39. S. Liu, H. Sun, A. Suvorova and S. Wang, *Chem. Eng. J.*, 2013, **229**, 533-539.

40. Q. Zhang, T. P. Chou, B. Russo, S. A. Jenekhe and G. Cao, *Angew. Chem.*, 2008, **120**, 2436-2440.

41. Y. Li, J. Wang, H. Yao, L. Dang and Z. Li, *J. Mol. Catal. A: Chem.*, 2011, **334**, 116-122.

42. S. H. Yoon. and J. H. Lee, *Environ. Sci. Technol.*, 2005, **39**, 9695-9701.

43. Y. Wang and P. Zhang, *J. Hazard. Mater.*, 2011, **192**, 1869-1875.

44. S. Sakong and P. Kratzer, *Semicond. Sci. Technol.*, 2011, **26**, 014038.

Chapter 5: An insight to metal organic framework derived N-doped graphene towards oxidative degradation of persistent contaminants: Formation mechanism and generation of singlet oxygen from peroxymonosulfate

ABSTRACT

Synthesis of carbonaceous materials from metal organic framework (MIL-100), organic linker and N-precursor was comprehensively investigated and their structures were characterized. It was found that simple pyrolysis of MIL-100 (Fe) and dicyandiamide (DCDA) could produce nitrogen doped graphene (N-graphene). The N-graphene showed excellent performances in peroxymonosulfate (PMS) activation, superior to the counterparts of graphene, iron (II, III) oxide, manganese (IV) oxide and cobalt (II, III) oxide. With PMS activation, N-graphene exhibited efficient catalytic degradation of various organic pollutants such as phenol, 2,4,6-tricholophenol (TCP), sulfachloropyridazine (SCP) and p-hydroxybenzoic acid (PHBA). The electron paramagnetic resonance (EPR) and radical quenching tests were employed to investigate the PMS activation and organic degradation processes. It was found that singlet oxygen ($^1O_2$) was mainly produced during the activation of PMS by N-graphene and contributed to the catalytic oxidation instead of sulfate and/or hydroxyl radicals. These findings provided new insights into PMS activation by metal-free carboncatalysis.

The content of this Chapter is published in Environmental Science: Nano, 2017, 4, 315-324.

5.1. Introduction

The worldwide water shortage and pollution has been intriguing the development of remediation technologies for water treatment. Peroxymonosulfate (PMS), persulfate (PS) and hydrogen peroxide (H_2O_2) are generally used as oxidants for degradation of aqueous pollutants by advanced oxidation processes (AOPs) [1-3]. In the processes, complete degradation of organic pollutants can be achieved by generating sulfate and/or hydroxyl radicals [4, 5]. However, as acidic condition is usually required, metal-based catalysts tend to cause secondary contamination due to hazardous metal leaching [6]. Hence, metal-free materials are highly demanded as the catalysts for removal of organic pollutants.

Graphene is considered as a promising green catalyst owing to its high surface area, chemical stability and impressive electrical conductivity[7]. Sun *et al.* [3] firstly reported that reduced graphene oxide (rGO) could activate PMS for degradation of organic pollutants. It has been further proven that the electronic and chemical performances of graphene are sensitive to heteroatom (nitrogen, phosphorus, sulfur or boron) doping which would induce more active sites on the graphene surfaces [8-11]. Nitrogen doping has been widely demonstrated to be effective due to the resemblance of carbon and nitrogen atomic sizes and strong covalence between them [12]. N-graphene could be feasibly synthesized through routes such as chemical vapor deposition (CVD)[13], arc-discharge[14], segregation growth[15] and post-synthesis treatment[16]. However, the above methods are time-consuming and require critical synthesis conditions, thus a novel and facile route as an alternative is demanded [11, 17].

Metal-organic frameworks (MOFs), as promising crystalline porous materials, have been explored for many applications such as gas separation, catalysis and removal of pollutants by adsorption [18-21]. Given the good configuration of metal clusters and organic ligands as well as tuneable porous structures, MOFs were employed as self-sacrificial templates or precursors to fabricate carbon or hybrid composites *via* pyrolysis [22-24]. Graphene nanostructures were also

fabricated *via* the graphitization processes of heteroatom polymers in the presence of iron or cobalt species [25-27]. Li *et al.* [17, 28] synthesized the graphene/graphene tube nanocomposites templated by a cage-containing cobalt (II) MOF and the bamboo-like nitrogen-doped graphene tubes using MIL-100 (Fe) and dicyandiamide (DCDA) as the precursors, showing excellent performances in oxygen reduction reaction (ORR). Mao *et al.*[29] fabricated highly graphitized, nitrogen-doped carbon spheres with capsulation of iron nanoparticles using MIL-100 (Fe) and DCDA as the precursors for ORR. Lv *et al.*[30] constructed porous Co/carbon composites by thermal decomposition of ZIF-67 under an inert gas, obtaining splendid electromagnetic wave absorption properties. However, few attempts were made on the understanding of carbon formation from different precursors of MOFs and the application in activation of oxidants for removal of organic pollutants in water on MOF-templated N-graphene.

Herein, we synthesized N-graphene templated by MIL-100 with DCDA and other carbons from the precursors towards MIL-100. The catalytic performances were evaluated by degradation of various organic pollutants in aqueous solutions. Electron paramagnetic resonance (EPR) and radical quenching tests were carried out to investigate the mechanism of PMS activation on N-graphene. In our previous discussions [31, 32], nonradical reaction was generated during PMS activation on N-doped single-walled carbon nanotubes, reduced graphene oxide and annealed nanodiamond. However, the nonradical species was not specified. In this study, singlet oxygen ($^1O_2$) was identified for the first time to contribute to the activation of PMS on N-graphene instead of hydroxyl (•OH) and sulfate ($SO_4^{\bullet-}$) radicals, which provides new insight into the PMS activation mechanism towards organic oxidation.

5.2. Experimental Section

5.2.1. Materials and chemicals

Iron(III) nitrate nonahydrate ($Fe(NO_3)_3$•$9H_2O$, 100%), benzene trimesic acid (BTC, 95%), DCDA (99.9%), sulfuric acid (H_2SO_4, 98%), potassium peroxymonosulfate (Oxone® or PMS),

phenol (99.0%), sulfachloropyridazine (SCP, 99.9%), p-hydroxybenzoic acid (PHBA, 99%), 2,4,6-trichlorophenol (TCP, 99.9%), manganese (IV) oxide (MnO_2, 100%), iron (II, III) oxide (Fe_3O_4, 100%), 2,2,6,6-tetramethyl-4-piperidinol (TMP, 99%), 5,5-dimethyl-1-pyrroline N-oxide (DMPO, 99.0%), *tert*-butanol (TBA, 99.5%), ethanol (99.5%), methanol and acetonitrile of HPLC grade were purchased from Sigma-Aldrich. Sodium azide (NaN_3, 99.5%) was purchased from Rowe Scientific.

5.2.2. Preparation of samples

MIL-100 (Fe) was synthesized *via* a fluorine-free route by the hydrothermal reactions as reported elsewhere [33]. As shown in Scheme 5.1, 4 g of DCDA and 0.25 g of MIL-100 were mixed in ethanol and kept stirring at 80 °C for 8 h. The solvent was evaporated at 60 °C and then the solid was heated at 800 °C for 2 h in N_2. The resulting sample was labelled as N-C-Fe. The N-C-Fe was then washed by 0.5 M H_2SO_4 at 80 °C for 24 h to remove the unstable iron species, designated as N-G. MOF-C was prepared by the similar procedure without DCDA. BTC-C and C-N were obtained by pyrolysis of BTC and BTC/DCDA, respectively, under the same condition as N-C-Fe. The synthesis conditions of samples in this study were shown in Table 5.1. Cobalt (II, III) oxide (Co_3O_4) was obtained from a previous report [34].

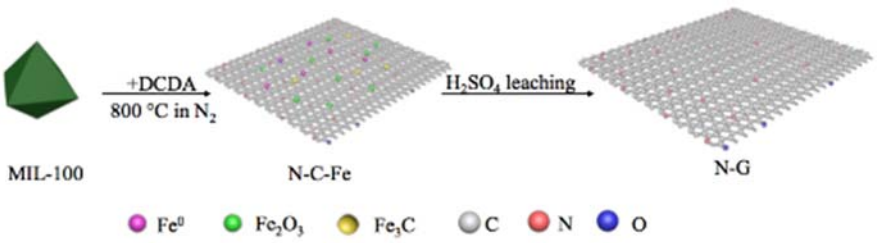

Scheme 5.1. Synthesis of N-doped graphene samples.

Table 5.1. The synthesis conditions of samples

Sample name	Precursors	Pyrolysis condition	Acid washing
BTC-C	BTC	800˚C for 2h under N_2	NO
C-N	BTC+DCDA	800˚C for 2h under N_2	NO
MOF-C	MIL-100	800˚C for 2h under N_2	YES
N-C-Fe	MIL-100+DCDA	800˚C for 2h under N_2	NO
N-G	MIL-100+DCDA	800˚C for 2h under N_2	YES

5.2.3. Characterization of the samples

Powder X-ray diffraction (XRD) patterns were obtained on a Bruker D8-Advance X-ray diffractometer with Cu Kα radiation (λ = 1.5418 Å). Field emission scanning electron microscopy (FE-SEM, Zeiss Neon 40 EsB) and transmission electron microscopy (TEM, JEOL 2100) were employed to investigate the morphologies of the samples. The composition and chemical states were studied on X-ray photoelectron spectroscopy (XPS) using a Kratos AXIS Ultra DLD system with Al-Kα X-ray. Thermogravimetric-differential thermal analysis (TG-DTA) was carried on a TGA/DSC-1 thermogravimetric analyzer from Mettler-Toledo Instrument in the inert atmosphere to acquire the mass loss of MIL-100. N_2 adsorption/desorption isotherms were acquired at -196 °C on a Tristar 3020 to obtain the specific surface area (SSA) and pore size distributions according to the Brunauer–Emmett–Teller (BET) equation and the Barrett-Joyner-Halenda (BJH) method, respectively.

5.2.4. Catalytic performances in degradation of organics

The experiments were conducted in a thermostatic water bath with the catalysts (0.1 g/L) and PMS (1 g/L) and target pollutants (e.g., phenol (50 ppm), SCP (20 ppm), TCP (50 ppm), and

PHBA (20 ppm)) in a glass reactor. At a given interval, 1 mL of solution was withdrawn by a syringe, filtered by a 0.45 μm Millipore film, and injected into a vial which held 0.5 mL of methanol as a quenching agent. The resulting solution was analyzed on a high performance liquid chromatograph (HPLC, Varian) with a C-18 column. For the stability tests, the samples were collected and washed several times by deionized water after 3 h reactions, and then dried in air at 60 °C.

5.2.5. Mechanistic studies

The contributors during the degradation of organics by the activation of PMS were detected by electron paramagnetic resonance (EPR). DMPO was selected to be the spin-trapping agent for $SO_4^{\bullet-}$ and $^{\bullet}OH$. TMP was used to capture singlet oxygen ($^1O_2$) which would oxidize TMP into 2,2,6,6-tetramethyl-4-piperidinol-N-oxyl radical (TMPN). The quantitative results and intensity of TMPN were obtained directly by Spin Fitting from Bruker Xenon Software package. The reactive radicals and nonradical reactions were identified by classical quenching tests. Specifically, ethanol and TBA were used as the quenching agents for hydroxyl and sulfate radicals, while sodium azide would verify the existence of singlet oxygen.

5.3. Results and Discussion

5.3.1. Characterization of the materials

XRD patterns of the resulting carbonaceous materials are shown in Figure 5.1a. BTC-C and C-N were identified as amorphous carbons containing low level of graphitized carbon by XRD [35]. The (002) peak at 26° (2θ) corresponding to graphene could be detected for MOF-C, N-C-Fe and N-G, due to the catalytic role of iron species in the precursor of MIL-100 [36]. The (002) peak shifted from 26.5 to 26.1° after N doping, indicating an increased interlayer spacing [13]. Zero-valent iron at the peak of 44.8° could not be eliminated by the post-treatment of acid washing for MOF-C, probably due to the capsulation by carbon. The peaks at 31.1, 35.6 and 43.1° of N-C-Fe were assigned to γ-Fe_2O_3 which was formed during the collapse of MIL-100

at around 470 °C (Figure 5.1b). The peaks at 43.7 and 44.8° corresponded to Fe_3C and α-Fe, respectively, forming after the annealing at about 600 °C (Figure 5.1b). After H_2SO_4 digestion, only the peak at 26.1° presented without peaks assigned to iron species for N-G, which differed from MOF-C as discussed above. However, the mass ratio of residue in Figure 5.1c (TGA result of N-G) was greater than zero, suggesting the existence of iron species in N-G. The discrepancy between XRD and TGA results may be attributed to the fact that quantity of the iron species was below the detection limit of XRD analysis.

Raman spectra of MOF-C and N-G in Figure 5.1d showed the vibration of the edges/defects (D band) at 1354 cm^{-1} and graphite lattice (G band) at ~ 1580 cm^{-1}. Specifically, the G band of N-G was broaden and shifted to a higher frequency compared with MOF-C (blue shift, 1581 *vs.* 1576 cm^{-1}). The I_D/I_G (the intensity ratio of D band and G band) of N-G increased to 0.90 from 0.71 for MOF-C, indicating that N doping increased the defectiveness of graphene. Meanwhile, the smaller I_{2D}/I_G of N-G compared to that of MOF-C (0.448 *vs.* 1.86) confirmed the conclusion above.

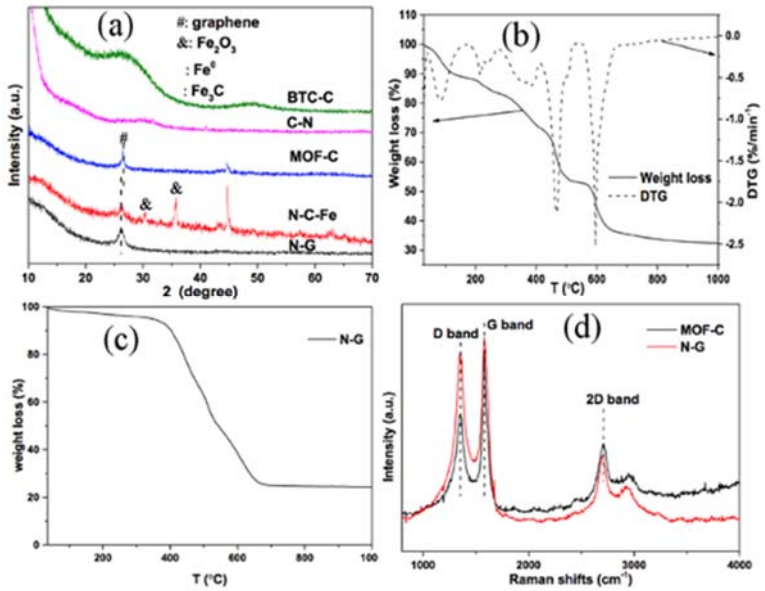

Figure 5.1. XRD patterns (a); TG-DTG curves of MIL-100 (Fe) in argon (b) and N-G in air (c); Raman spectra (d) of catalysts.

The particles of MIL-100 are mainly in polyhedral, as shown in Figure 5.2.

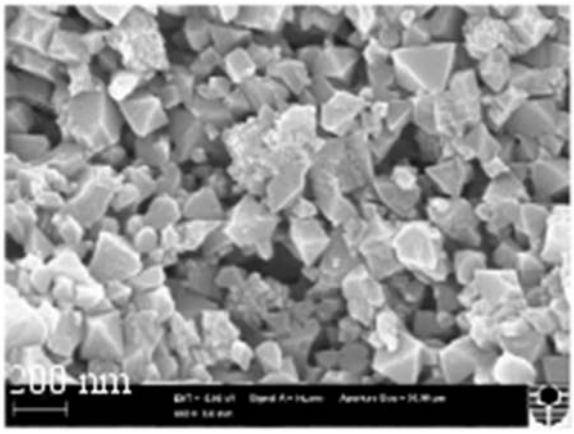

Figure 5.2. SEM image of MIL-100 (Fe).

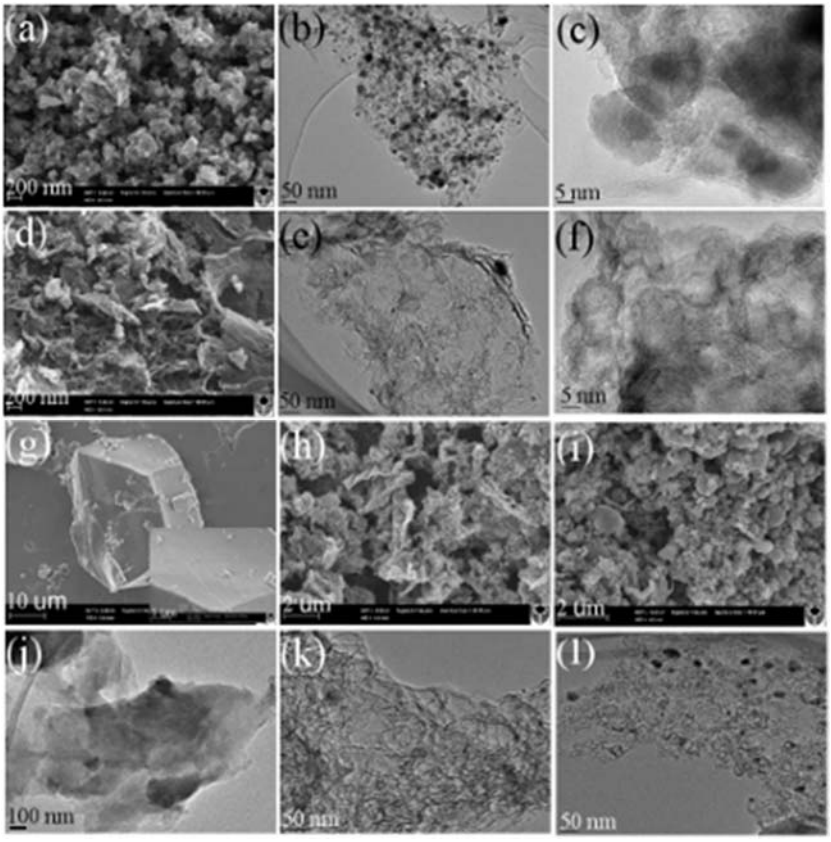

Figure 5.3. SEM images (a, d, g-i), TEM images (b, e, j-l) and HRTEM images (c, f) of N-C-Fe(a-c), N-G(d-f), BTC-C (g, j), C-N (h, k) and MOF-C (i, l).

After carbonizing MIL-100/DCDA at 800 °C, N-C-Fe was formed with the collapse of the polyhedral shape of MIL-100, showing iron-bearing nanoparticles embedded within

carbonaceous materials (Figure 5.3a). The iron species dispersed uniformly due to the separation of carbon materials (Figure 5.3b). The HRTEM in Figure 5.3c showed that iron species were surrounded by onion-like graphitic carbon. The nanoparticles were eliminated by acid digestion for the formation of N-G (Figure 5.3d). The TEM (Figure 5.3e) confirmed the removal of iron nanoparticles and a tiny amount of iron particles still remained, which escaped from acid wash. Figure 5.3f showed that N-G was hollow onion-like graphitic carbon. In addition, the monolith of BTC-C was amorphous carbon while some sheet-like ordered carbon appeared on C-N (Figure 5.3g-h, j-k). Similar to N-G, MOF-C also exhibited hollow onion-like shells with minimal iron particles left (Figure 5.3i, l).

The formation mechanisms of different carbonaceous materials from varying precursors were discussed. BTC molecules were linked by hydrogen bond C-O···H (Scheme 5.2a). At low pyrolysis temperature, water was driven off accompanied by the condensation of BTC. Upon further heating, carbon-carbon bonds were formed with the loss of oxygen *via* CO_x. With the increase of temperature, the six carbon phenyl rings broke and formed layered carbon network which was confirmed to be amorphous carbon. The formation mechanism of amorphous carbon in C-N was similar to that of BTC-C. In addition, DCDA would be decomposed to layered graphitic carbon nitride which confined the as-formed carbon intermediates to the interlayer gaps[37]. When the pyrolysis temperature went above 750 °C, carbon nitride was subjected to complete thermolysis and sheet-like ordered carbon formed (Scheme 5.2b). Therefore, ordered carbon could be formed in C-N besides the amorphous carbon. MIL-100 and DCDA were interconnected by hydrogen bonds N-H···O and O-H···N (Scheme 5.2c). Upon pyrolysis, the framework of MOF collapsed with the condensation of polymers, releasing water vapor, CO_x, NH_x and NO_x. The iron species were firstly decomposed to metallic oxides and then reduced to iron metals by the carbon surrounding them[38]. Liquid mobile iron-carbon particles could form at relatively low temperatures (600-670 °C) as reported by Krivoruchko *et al*.[39] Here, the

carbon and nitrogen species dissolved into iron particles at high pyrolysis temperatures and precipitated out as curved graphitic carbon when supersaturation was reached, named as in dissolution-precipitation dynamic equilibrium[40]. The released graphitic layers were rearranged into closed shells following the energy minimization principle and the van der Waals interactions between the shells stabilized the system[41, 42]. Conclusively, after the procedure of condensation, dissolution, precipitation and rearrangement, N-C-Fe exhibited metal-enclosed shell structure and N-G showed hollow onion-like shells after metal removal by acid wash. The formation mechanism of MOF-C was similar to N-G, without the addition of DCDA (Scheme 5.2d).

The compositions and chemical states of N-C-Fe and N-G were analyzed by XPS. As shown in Figure 5.4a, the oxygen content of N-C-Fe decreased from 4.10 at.% to 2.99 at.% after post-acid treatment, due to the loss of Fe_2O_3. N-C-Fe and N-G contained much lower oxygen levels than N-doped reduced graphene oxide (N-rGO, 11.53 at.%) and rGO (14.44 at.%)[34] , therefore, the oxygen groups in the samples contributed little to the catalytic oxidation[31]. N-C-Fe and N-G contained a similar N content, 2.91 at.% and 2.31 at.%, respectively. As shown in Figure 5.4b, three high-resolution N peaks of N-C-Fe and N-G were observed at 398.6, 401.1 and 403.9 eV, corresponding to pyridinic N, graphitic N and nitrogen oxide, respectively[17, 43]. The results suggested that nitrogen was successfully doped into graphene. As previously reported, the existence of Fe facilitated the formation of quaternary N in high temperature pyrolysis of carbon/nitrogen precursors[36, 44]. Both N-C-Fe and N-G showed a higher content of graphitic N (one specific type of quaternary N within graphene plane) than that of pyridinic N, suggesting that nitrogen atoms preferred to be doped into the basal plane instead of the edges of graphene sheets. The de-convoluted C1s XPS spectra of N-C-Fe and N-G (Figure 5.4c) centred at 284.6, 285.8, 286.7 and 290.1 eV, assigning to sp^2-C, C=N/C-O, C-N/C=O and π-π^* shake-up satellite, respectively [7, 45].

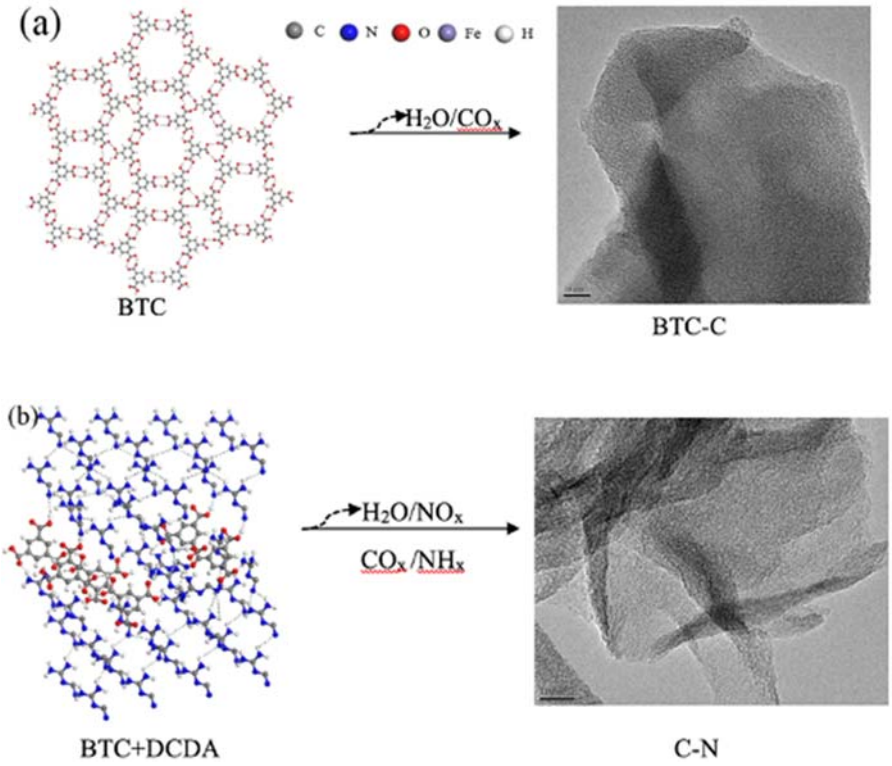
(a)
C
N
O
Fe
H
H_2O/CO_x
BTC
BTC-C
(b)
H_2O/NO_x
CO_x/NH_x
BTC+DCDA
C-N
(c)
H_2O/NH_3
CO_2/NO_x
$NH_3/CO_x/NO_x$
MIL-100+DCDA
FeO_x/N-C
Fe/N-C
precipitate
acid wash
N-G
N-C-Fe
(d)
H_2O
CO_x
CO_x
MIL-100
FeO_x/C
Fe/C
dissolve
precipitate
acid wash
MOF-C
MOF-C-Fe

Scheme 5.2. The formation mechanism of BTC-C (a), C-N (b), N-C-Fe and N-G (c), and MOF-C (d).

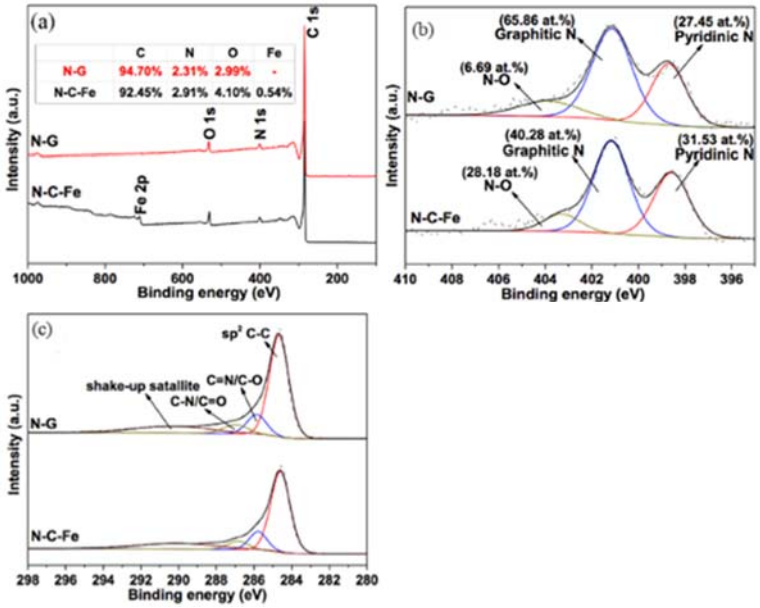

Figure 5.4. (a) XPS survey; (b) N 1s and (c) C 1s spectra of N-C-Fe and N-G.

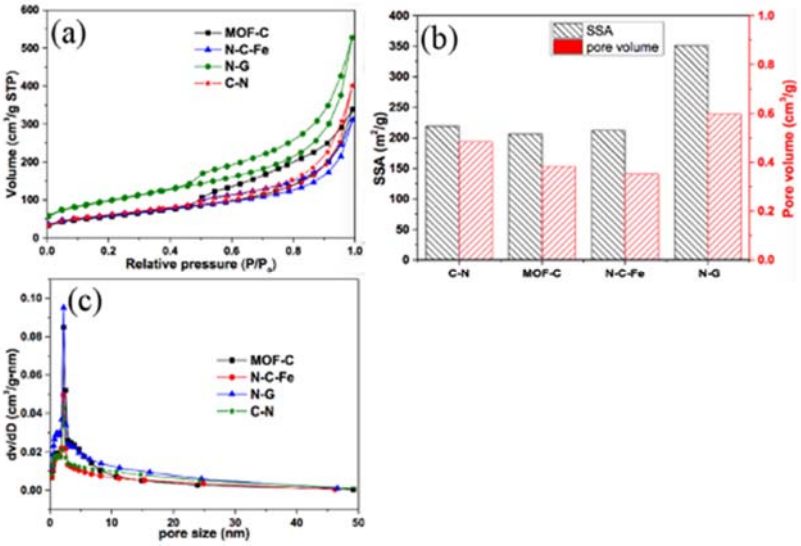

Figure 5.5. N_2 sorption isotherms (a), SSA/pore volumes (b) and pore size distribution (c) of the catalysts.

The SSA and pore size distribution of the samples were investigated through N_2 adsorption/desorption isotherms. The curves shown in Figure 5.5a agreed with a type IV

isotherm and H3 hysteresis loop. The SSA and pore volume of N-G (351.2 m^2/g and 0.597 cm^3/g, respectively) were much higher than those of C-N (219.2 m^2/g and 0.484 cm^3/g), MOF-C (206.1 m^2/g and 0.383 cm^3/g) and N-C-Fe (212.2 m^2/g and 0.351 cm^3/g) (Figure 5.5b). The addition of DCDA, the framework of MIL-100 as the template and the post-acid treatment for removal of unstable iron species induced more porous structures and higher surface areas. The pore size of the materials above mainly ranged from 0 to 5 nm (Figure 5.5c).

5.3.2. Catalytic oxidation of organic pollutants

The catalytic degradation of phenol solutions on various materials is shown in Figure 5.6a. PMS alone without a catalyst exhibited negligible oxidation of phenol. The catalytic oxidation can deliver more effective removal of organics. For BTC-C, less than 10% phenol was degraded within 180 min, while 80% phenol removal was achieved on C-N. It was suggested that N doping could significantly improve the catalytic effect by boosting the electron transfer [34]. About 90% phenol was decomposed within 180 min on MOF-C, which was superior to C-N, even though the C-N had a higher SSA and pore volume than MOF-C. This is because free electron flowing of graphene on MOF-C facilitated more effective catalytic oxidation, compared with amorphous carbon of C-N [3]. Almost 98% phenol was removed on N-C-Fe in 180 min. The XRD results in Figure 5.6b showed that the peaks assigned to Fe_2O_3 became weaker after the 1st run, indicating that Fe_2O_3 worked during PMS activation for N-C-Fe. N-G presented the greatest catalysis for phenol degradation, with 100% phenol removal within 30 min. Meanwhile, N-G showed minor adsorption of phenol. Thereby, the decomposition of phenol on N-G was mainly attributed to catalytic oxidation. It was noteworthy that C-N showed a higher content and the similar chemical states of N (Figure 5.6c-d) compared with N-G, while the catalytic efficiency was inferior to that of N-G. It could be explained by both the higher SSA/pore volume and graphene structure of N-G. It could be concluded that the fascinating metal-free catalysis on N-G was contributed by high SSA/pore volume, N doping and graphene

structure.

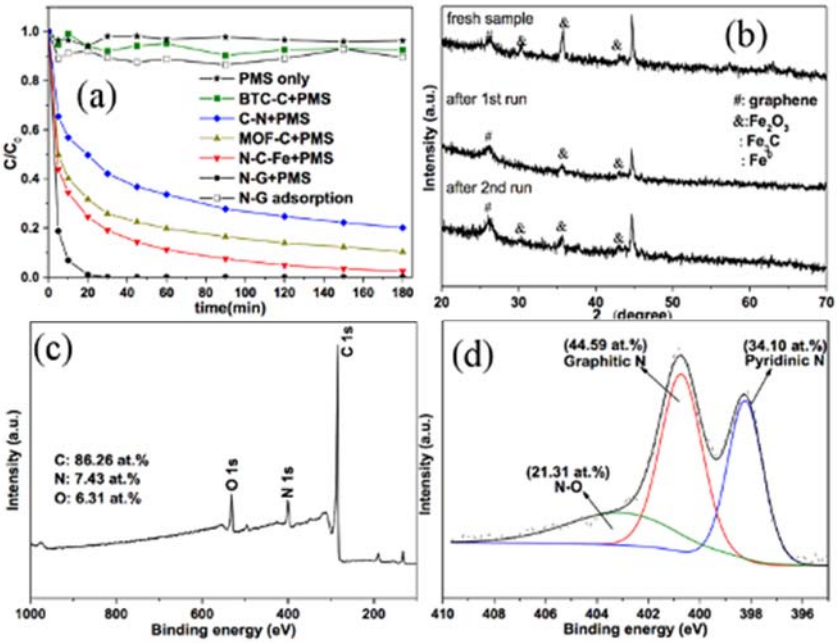

Figure 5.6. Phenol removal on various catalysts (a); XRD patterns of fresh and used N-C-Fe (b); XPS survey (c) and N 1s (d) spectra of C-N.

The reusability of N-G in catalytic degradation of phenol is shown in Figure 5.7a. About 100% and 61% phenol removals were achieved in 120 and 180 min for the second and third runs, respectively, indicating that N-G showed a much better stability than rGO [3] and N-rGO[34]. The deactivation of catalysts was attributed to the change of surface chemistry and structure by produced intermediates[46]. N-G showed weaker defectiveness (I_D/I_G=0.9), compared with rGO (I_D/I_G=1.48) and N-rGO (I_D/I_G=1.34). As a result, the surface chemistry of N-G here was more stable than the highly defective rGO and N-rGO, inducing excellent stability in catalytic performances.

The effect of reaction temperature on catalytic oxidation is shown in Figure 5.7b. The temperature exhibited a slight influence on phenol degradation. According to the Arrhenius equation, the activation energy on N-G was calculated to be 15.8 kJ/mol (the initial concentration of phenol 50 ppm, catalyst 100 mg/L), which was lower than the value of

materials previously reported such as graphene (84.0 kJ/mol), N-rGO (31.6 kJ/mol) and N-doped carbon nanotube (N-CNT, 39.2 kJ/mol) [3, 7, 47]. The lower activation energy of N-G could be attributed to the higher surface area (351.2 m^2/g) than others (<160 m^2/g) as well as N doping, inducing more active sites participating in the reactions and boosting the electron transfer.

The catalytic oxidation of phenol on N-G was also much better than the generally used metal-based catalysts such as Fe_3O_4, MnO_2 and Co_3O_4 (Figure 5.7c). Moreover, N-G also showed excellent degradation efficiencies of some other organic pollutants such as SCP, PHBA and TCP (Figure 5.7d).

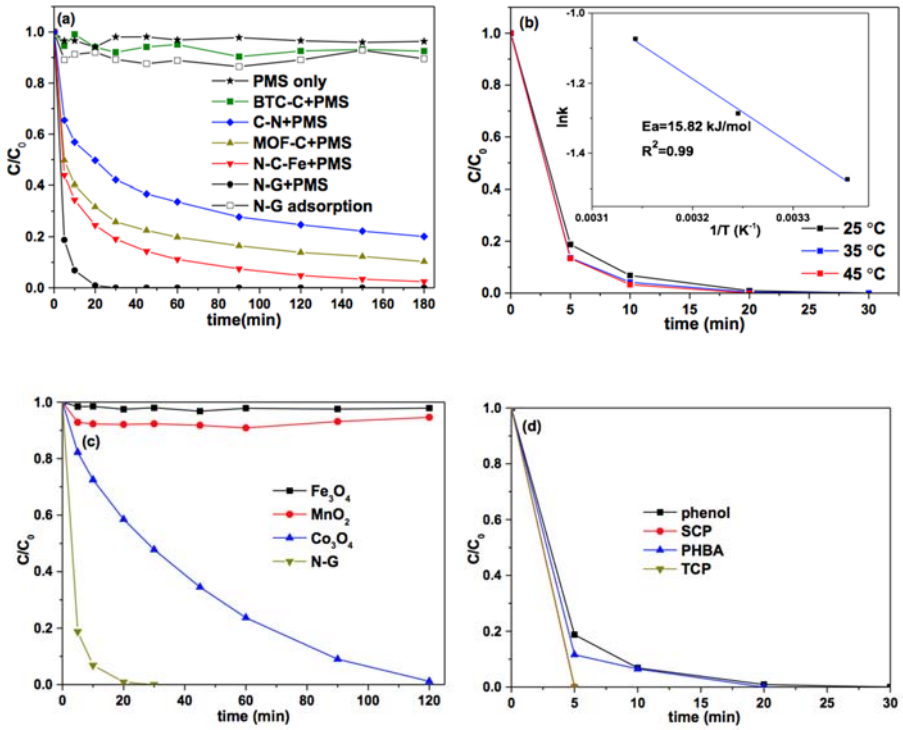

Figure 5.7. Stability test of N-G (a); effect of reaction temperature on phenol removal on N-G and activation energy (inset) (b); phenol removal on N-G and various metal-based catalysts (c); various pollutant removals on N-G (d). Reaction conditions: catalyst 100 mg/L, PMS 3.25 mM, phenol 50 ppm (phenol 20 ppm for stability test), SCP 20 ppm, PHBA 20 ppm, TCP 50 ppm, temperature 25 °C (if not mentioned specifically).

5.3.3. Mechanism of the catalytic oxidation

In the previous studies, hydroxyl and sulfate radicals were found to be produced during PMS activation by metal-based catalysts and N-rGO [7, 48]. Here, EPR was employed to examine free radicals generated during PMS activation using DMPO as a radical spin trapping agent. As shown in Figure 5.8a, DMPO-OH and DMPO-SO_4 peaks could be observed on MOF-C, N-C-Fe and N-G, indicating that •OH and $SO_4^{\bullet-}$ radicals were generated during PMS activation. Meanwhile, DMPO-OH peaks were greatly higher than DMPO-SO_4. In this study, the hydroxyl radicals' intensity from N-G catalysis was much lower than that of N-C-Fe. However, N-G exhibited a higher catalytic oxidation than N-C-Fe. Furthermore, Figure 5.8b reveals that the intensity of •OH radicals for N-G climbed fastest between 5 and 10 min while the degradation rate of phenol reached the maximum at the initial 5 min. Conclusively, hydroxyl radicals were not the dominating radicals during phenol oxidation *via* PMS activation on N-G.

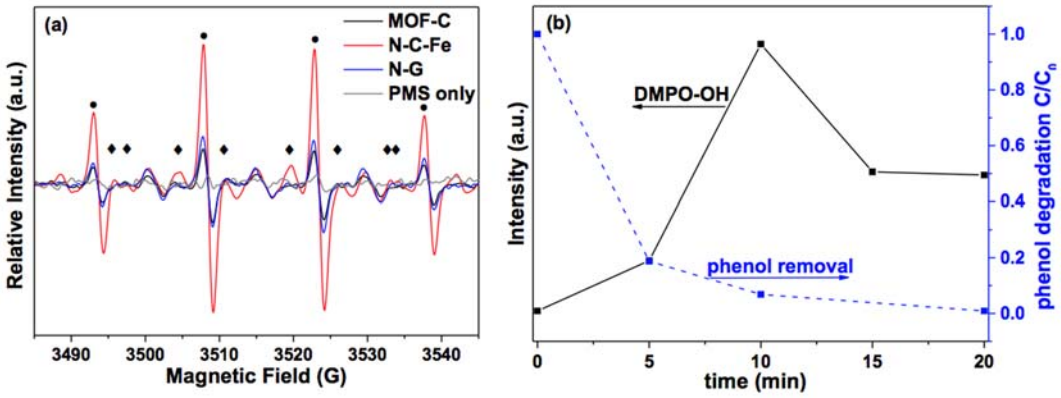

Figure 5.8. EPR spectra of PMS activation on various catalysts (a) and hydroxyl radicals evolution during PMS activation on N-G (b). Conditions: catalyst 100 mg/L, PMS 3.25 mM, phenol 50 ppm, temperature 25 °C, ●: DMPO-OH, ♦: DMPO-SO_4).

It was reported that $^1O_2$ can be generated during the self-decomposition of PMS and the rate constant κ is about 0.2 M^{-1} s^{-1} [49, 50], as shown in reaction (1).

$$HSO_5^- + SO_5^{2-} \rightarrow HSO_4^- + SO_4^{2-} + {}^1O_2 \qquad (5\text{-}1)$$

PMS could also be activated by ketones and benzoquinone to produce $^1O_2$ as previously reported [51, 52]. The carbonaceous materials synthesized in this research could boost the degradation of phenol by activating PMS. So it is likely that more $^1O_2$ would be generated during the activation of PMS. TMP was then selected to trap $^1O_2$ for EPR, forming the stable TMPN which can be detected by its typical three-line EPR spectrum with equal intensities (a_N=16.9 G, g=2.0054). As it is shown in Figure 5.9a, TMP used here was not oxidized and could not react with N-G due to no peaks detected. Three peaks assigned to TMPN could be seen for PMS only without any catalyst in phenol solution due to the self-decomposition of PMS. However, negligible effect on phenol degradation was found by PMS only, indicating that the phenol degradation in the system possibly occurred on the interface of catalysts and solution. Much more $^1O_2$ was generated in the catalysts/PMS system and N-G showed the greatest intensity of $^1O_2$, which could explain the best catalytic performance of N-G. It could be speculated that $^1O_2$ played a dominating role in degradation of phenol on N-G. In addition, the higher efficiency of phenol decomposition on N-C-Fe than MOF-C can be attributed to more •OH radicals, because the intensities of $^1O_2$ on N-C-Fe and MOF-C were almost equal. Moreover, the intensity of $^1O_2$ increased rapidly in the first 5 min and then at a slower rate, which was in accordance with the decomposition rate of phenol (Figure 5.9b), confirming that singlet oxygen dominated the phenol degradation on N-G. The reaction atmosphere (ambient condition, nitrogen gas and air purging) exerted no influence on phenol degradation as shown in Figure 5.9c, confirming that $^1O_2$ was originated from PMS rather than dissolved oxygen in the reaction solution. It was reported that only free radicals were generated during PMS activation by Co^{2+} [31, 53]. For comparison, TMP was then used as a trapping agent in Co_3O_4/PMS system (Figure 5.9d). The intensity of $^1O_2$ was lower than PMS only in the initial 5 min and disappeared after 10 min, which was totally different from that on N-G/PMS system.

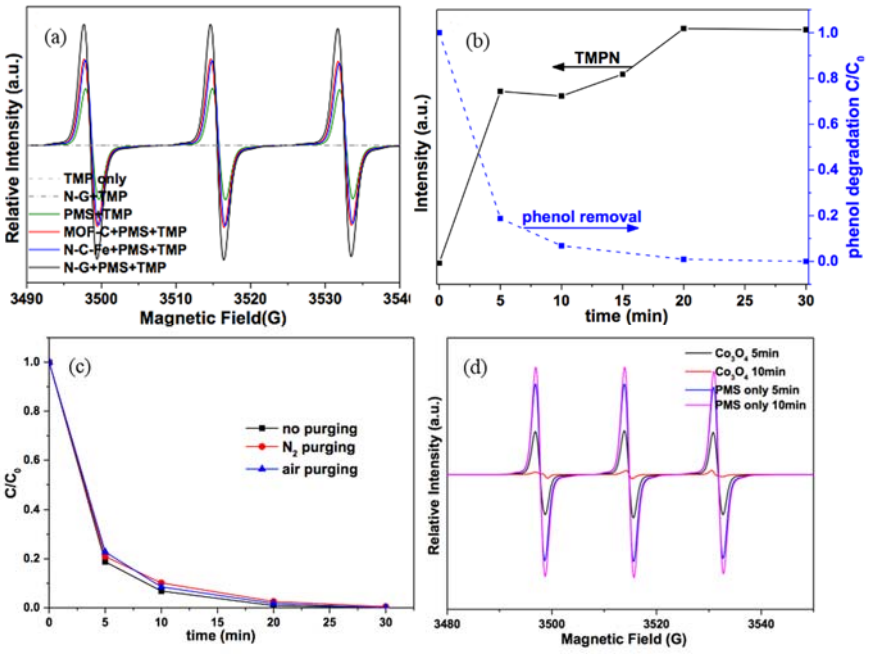

Figure 5.9. EPR spectra of TMPN on various catalysts (a); singlet oxygen evolution during PMS activation on N-G (b) (catalyst: 100 mg/L, PMS: 3.25 mM, phenol: 50 ppm, temperature: 25 °C, reaction time: 20 min; TMP: 1.16 g/L); phenol degradation in the N-G/PMS system under ambient condition, nitrogen gas purging and air purging (c) (catalyst: 100 mg/L, PMS: 3.25 mM, phenol: 50 ppm, temperature: 25 °C); EPR spectra of TMPN on Co_3O_4 (d) (catalyst: 200 mg/L, PMS: 6.5 mM, phenol: 50 ppm, temperature: 25 °C, reaction time: 5-10 min; TMP: 1.16 g/L).

To further verify the effects of •OH and $SO_4^{\bullet-}$ radicals as well as $^1O_2$, quenching tests were conducted. Ethanol and *tert*-butanol were used as the scavengers of •OH and $SO_4^{\bullet-}$ radicals. NaN_3 was chosen to quench $^1O_2$ according to the previous report [54]. Remarkably, $^1O_2$ could oxidize phenol with a high efficiency while trifle activity towards ethanol and *tert*-butanol[55]. The rate constants of quenching are shown in Table 5.2.

Table 5.2. Reaction rate constants of quenchers with radicals and $^1O_2$.

Quenching agents	Rate constants ($M^{-1}s^{-1}$)		
	•OH	$SO_4^{\bullet-}$	$^1O_2$
Ethanol	$(1.2\text{-}2.8)\times10^9$	$(1.6\text{-}7.8)\times10^7$	-
Tert-butanol	$(3.8\text{-}7.6)\times10^8$	$(4\text{-}9.1)\times10^5$	-
NaN_3	1.2×10^{10}	2.52×10^9	1×10^9

As shown in Figure 5.10a, the addition of ethanol and *tert*-butanol had no influence on phenol degradation, indicating that •OH and $SO_4^{\bullet-}$ radicals exhibited negligible effects on phenol oxidation. For comparison, the efficiencies of phenol degradation on MOF-C, C-N and N-C-Fe were inhibited at various degrees by ethanol (Figure 5.10b-d), suggesting that •OH and $SO_4^{\bullet-}$ radicals contributed to the decomposition of phenol on the above three catalysts.

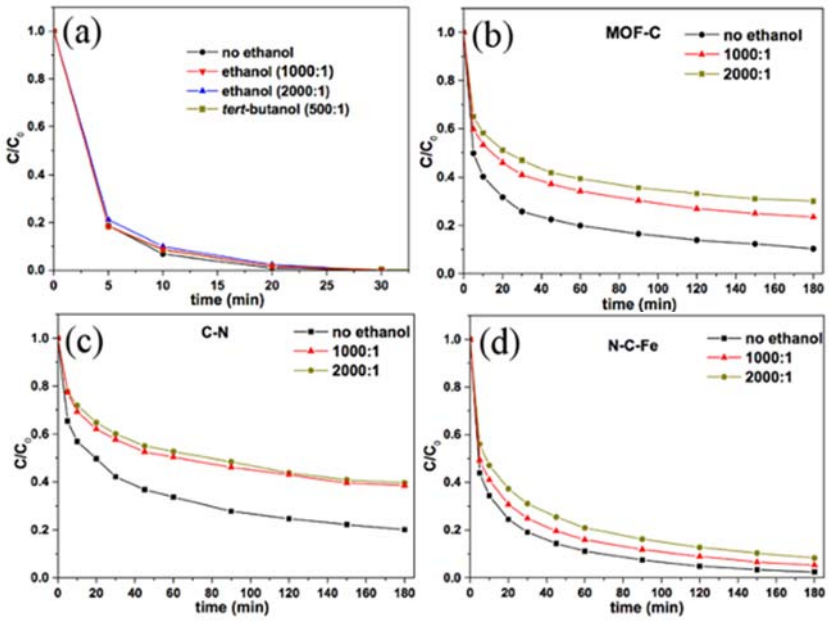

Figure 5.10. Effect of ethanol on phenol degradation: (a) N-G/PMS; (b) MOF-C/PMS; (c) C-N/PMS; (d) N-C-Fe/PMS. Reaction conditions: catalyst 100 mg/L, PMS 3.25 mM, phenol 50 ppm, temperature 25 °C, molar ratio (ethanol *vs.* PMS) 1000:1 (2000:1).

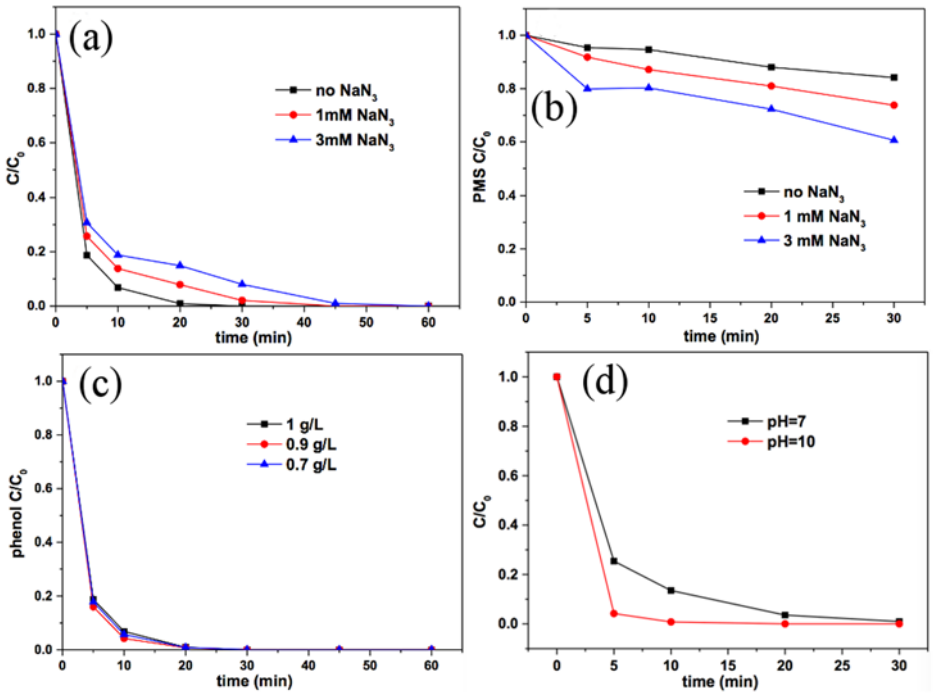

Figure 5.11. Effect of NaN_3 on phenol degradation (a); effect of NaN_3 on PMS decomposition in the phenol solution (b); phenol degradation with different PMS concentrations (c); influence of pH on phenol degradation (d). Reaction conditions: catalyst 100 mg/L, PMS 3.25 mM, phenol 50 ppm, temperature 25 °C, buffer (sodium borate) 20 mM.

The addition of NaN_3 could hinder the degradation of phenol effectively as shown in Figure 5.11a. Although NaN_3 could also quench •OH and $SO_4^{\bullet-}$ radicals, the scavenging ability of NaN_3 at 3 mM (3.6×10^7 and 3×10^6 s^{-1}, respectively) was weaker than that of ethanol (ethanol *vs.* PMS = 1000:1, 3.9×10^{12} and 2.5×10^{11} s^{-1}, respectively). Ethanol should be more effective in hindering phenol degradation than NaN_3 if •OH or $SO_4^{\bullet-}$ radicals played the dominant role during the catalytic oxidation. The contrary results indicated that $^1O_2$ was the contributor to phenol removal. The presence of NaN_3 (1 mM and 3 mM) would boost the decomposition of PMS by ~10% and 24%, respectively (Figure 5.11b). However, the degradation efficiency of phenol did not decrease when the concentrations of PMS in the reaction solution were 0.7 and 0.9 g/L compared with 1 g/L (Figure 5.11c). As a result, the decrease in degradation efficiency with the addition of NaN_3 was attributed to $^1O_2$ quenching. The influence of pH on phenol

degradation was also investigated (Figure 5.11d), showing that the alkaline condition could enhance the degradation of phenol. For one thing, the phenolate anion exhibits higher reactivity toward $^1O_2$ than neutral phenol [56-58]; in addition, alkaline environment facilitated the generation of SO_5^{2-}, inducing more singlet oxygen to be produced.

5.4. Conclusions

In this research, N-G was prepared using MIL-100(Fe) and DCDA as the precursors in combination with a post-acid treatment. N-G showed excellent phenol degradation by catalytic PMS activation, due to N doping, fast electron flowing of graphene and high SSA. The mechanism of PMS activation on N-G was investigated by means of both EPR and quenching tests. Singlet oxygen was observed during PMS activation on N-G and was determined to be the primary role in phenol degradation. The N-G/PMS system showed a better efficiency on phenol degradation in alkaline condition. This study opened a facile avenue to synthesize N-doped graphene for environmental remediation and provided a new insight into the catalytic reaction on N-doped graphene.

5.5. References

1. A. Dirany, I. Sires, N. Oturan, A. Ozcan and M. A. Oturan, *Environ. Sci. Technol.*, 2012, **46**, 4074-4082.
2. W. Tian, H. Zhang, X. Duan, H. Sun, M. O. Tade, H. M. Ang and S. Wang, *ACS Appl. Mater. Interfaces*, 2016, **8**, 7184-7193.
3. H. Sun, S. Liu, G. Zhou, H. M. Ang, M. O. Tade and S. Wang, *ACS Appl. Mater. Interfaces*, 2012, **4**, 5466-5471.
4. J. J. Pignatello, E. Oliveros and A. MacKay, *Crit. Rev. Environ. Sci. Technol.*, 2006, **36**, 1-84.
5. S. Wang, *Dyes Pigm.*, 2008, **76**, 714-720.
6. E. Saputra, S. Muhammad, H. Sun, H. M. Ang, M. O. Tade and S. Wang, *Environ. Sci. Technol.*, 2013, **47**, 5882-5887.
7. S. Indrawirawan, H. Q. Sun, X. G. Duan and S. B. Wang, *J. Mater. Chem. A*, 2015, **3**, 3432-3440.
8. B. Frank, J. Zhang, R. Blume, R. Schlogl and D. S. Su, *Angew. Chem., Int. Ed. Engl.*, 2009, **48**, 6913-6917.
9. Z. Yang, Z. Yao, G. F. Li, G. Y. Fang, H. G. Nie, Z. Liu, X. M. Zhou, X. A. Chen and S. M. Huang, *ACS nano*, 2012, **6**, 205-211.
10. C. Zhang, N. Mahmood, H. Yin, F. Liu and Y. Hou, *Adv. Mater.*, 2013, **25**, 4932-4937.
11. H. B. Wang, T. Maiyalagan and X. Wang, *ACS Catal.*, 2012, **2**, 781-794.
12. K. Parvez, S. B. Yang, Y. Hernandez, A. Winter, A. Turchanin, X. L. Feng and K. Mu¨llen, *ACS nano*, 2012, **6**, 9541-9550.
13. L. T. Qu, Y. Liu, J. B. Baek and L. M. Dai, *ACS nano*, 2010, **4**, 1321-1326.

14. N. Li, Z. Y. Wang, K. K. Zhao, Z. J. Shi, Z. N. Gu and S. K. Xu, *Carbon*, 2010, **48**, 255-259.

15. C. Zhang, L. Fu, N. Liu, M. Liu, Y. Wang and Z. Liu, *Adv. Mater.*, 2011, **23**, 1020-1024.

16. X. R. Wang, X. L. Li, L. Zhang, Y. K. Yoon, P. K. Weber, H. L. Wang, J. Guo and H. J. Dai, *Science*, 2009, **324**, 768-771.

17. Q. Li , H. Y. Pan , D. Higgins , R. G. Cao , G. Q. Zhang , H. F. Lv , K. B. Wu , J. Cho and G. Wu, *Small*, 2015, **11**, 1443–1452.

18. Z. H. Rada, H. R. Abid, H. Sun and S. Wang, *J. Chem. Eng. Data*, 2015, **60**, 2152-2161.

19. Z. H. Rada, H. R. Abid, J. Shang, Y. D. He, P. Webley, S. M. Liu, H. Q. Sun and S. B. Wang, *Fuel*, 2015, **160**, 318-327.

20. F. Wang, Z. S. Liu, H. Yang, Y. X. Tan and J. Zhang, *Angew. Chem., Int. Ed. Engl.*, 2011, **50**, 450-453.

21. L. H. Ai, C. H. Zhang, L. L. Li and J. Jiang, *Appl. Catal., B*, 2014, **148-149**, 191-200.

22. N. L. Torad, M. Hu, S. Ishihara, H. Sukegawa, A. A. Belik, M. Imura, K. Ariga, Y. Sakka and Y. Yamauchi, *Small*, 2014, **10**, 2096-2107.

23. H. L. Jiang, B. Liu, Y. Q. Lan, K. Kuratani, T. Akita, H. Shioyama, F. Zong and Q. Xu, *J. Am. Chem. Soc.*, 2011, **133**, 11854-11857.

24. H. Jin, J. Wang, D. Su, Z. Wei, Z. Pang and Y. Wang, *J. Am. Chem. Soc.*, 2015, **137**, 2688-2694.

25. G. Wu, H. T. Chunga, M. Nelsona, K. Artyushkovab, K. L. Morec, C. M. Johnstona and P. Zelenaya, *ECS Trans.*, 2011, **41**, 1709-1717.

26. G. Wu, N. H. Mack, W. Gao, S. G. Ma, R. Q. Zhong, J. T. Han, J. K. Baldwin and P. Zelenay, *ACS nano*, 2012, **6**, 9764–9776.

27. G. Wu, K. L. More, C. M. Johnston and P. Zelenay, *Science*, 2011, **332**, 443-447.

28. Q. Li, P. Xu, W. Gao, S. Ma, G. Zhang, R. Cao, J. Cho, H. L. Wang and G. Wu, *Adv. Mater.*, 2014, **26**, 1378-1386.

29. C. Mao, A. Kong, Y. Wang, X. Bu and P. Feng, *Nanoscale*, 2015, **7**, 10817-10822.

30. Y. Lu, Y. Wang, H. Li, Y. Lin, Z. Jiang, Z. Xie, Q. Kuang and L. Zheng, *ACS Appl. Mater. Interfaces*, 2015, **7**, 13604-13611.

31. X. G. Duan, H. Q. Sun, Y. X. Wang, J. Kang and S. B. Wang, *ACS Catal.*, 2015, **5**, 553-559.

32. X. Duan, Z. Ao, L. Zhou, H. Sun, G. Wang and S. Wang, *Appl. Catal., B*, 2016, **188**, 98-105.

33. Y. K. Seo, J. W. Yoon, J. S. Lee, U. H. Lee, Y. K. Hwang, C. H. Jun, P. Horcajada, C. Serre and J. S. Chang, *Microporous Mesoporous Mater.*, 2012, **157**, 137-145.

34. H. Sun, Y. Wang, S. Liu, L. Ge, L. Wang, Z. Zhu and S. Wang, *Chem. Commun. (Camb)*, 2013, **49**, 9914-9916.

35. Y. Xia, G. S. Walker, D. M. Grant and R. Mokaya, *J. Am. Chem. Soc.*, 2009, **131**, 16493-16499.

36. G. Wu and P. Zelenay, *Acc. Chem. Res.*, 2013, **46**, 1878–1889.

37. X. H. Li, S. Kurasch, U. Kaiser and M. Antonietti, *Angew. Chem., Int. Ed. Engl.*, 2012, **51**, 9689-9692.

38. M. Sevilla and A. B. Fuertes, *Carbon*, 2006, **44**, 468-474.

39. O. P. Krivoruchko and V. I. Zaikovskii, *Mendeleev Commun.*, 1998, **8**, 97-99.

40. G. Wu, M. Nelson, S. Ma, H. Meng, G. Cui and P. K. Shen, *Carbon*, 2011, **49**, 3972-3982.

41. A. Maiti, C. J. Brabec and J. Bernholc, *Mod. Phys. Lett. B*, 1993, **07**, 1883-1895.

42. M. Zhao, H. Song, X. Chen and W. Lian, *Acta Mater.*, 2007, **55**, 6144-6150.

43. L. F. Lai, J. R. Potts, D. Zhan, L. Wang, C. K. Poh, C. H. Tang, H. Gong, Z. X. Shen, L. Y. Jianyi and R. S. Ruoff, *Energy Environ. Sci.*, 2012, **5**, 7936-7942.

44. J. R. Pels, F. Kapteun, J. A. Moulun, Q. Zhu and K. M. Thomas, *Carbon*, 1995, **33**, 1641-1653.

45. G. Singh, D. S. Sutar, V. Divakar Botcha, P. K. Narayanam, S. S. Talwar, R. S. Srinivasa and S. S. Major, *Nanotechnology*, 2013, **24**, 1-8.

46. X. Duan, Z. Ao, H. Sun, S. Indrawirawan, Y. Wang, J. Kang, F. Liang, Z. H. Zhu and S. Wang, *ACS Appl. Mater. Interfaces*, 2015, **7**, 4169-4178.

47. H. Q. Sun, C. Kwan, A. Suvorova, H. M. Ang, M. O. Tade and S. B. Wang, *Appl. Catal., B*, 2014, **154**, 134-141.

48. Y. X. Wang, H. Q. Sun, X. G. Duan, H. M. Ang, M. O. Tade and S. B. Wang, *Appl. Catal., B*, 2015, **172-173**, 73-81.

49. D. F. Evans; and M. W. Upton, *J. Chem. Soc., Dalton Trans.*, 1985, **6**, 1151−1153.

50. D. L. Ball and J. O. Edwards, *J. Am. Chem. Soc.*, 1956, **78**, 1125-1129.

51. R. E. Montgomery, *J. Am. Chem. Soc.*, 1974, **96**, 7820-7821.

52. Y. Zhou, J. Jiang, Y. Gao, J. Ma, S. Y. Pang, J. Li, X. T. Lu and L. P. Yuan, *Environ. Sci. Technol.*, 2015, **49**, 12941-12950.

53. G. P. ANIPSITAKIS; and D. D. DIONYSIOU., *Environ. Sci. Technol.*, 2003, **37**, 4790-4797.

54. H. E. Gsponer, C. M. Previtali and N. A. García, *Toxicol. Environ. Chem.*, 1987, **16**, 23-37.

55. M. A. J. Rodgers, *J. Am. Chem. Soc.*, 1983, **105**, 6201-6205.

56. H. Kim, W. Kim, Y. Mackeyev, G. S. Lee, H. J. Kim, T. Tachikawa, S. Hong, S. Lee, J. Kim, L. J. Wilson, T. Majima, P. J. Alvarez, W. Choi and J. Lee, *Environ. Sci. Technol.*, 2012, **46**, 9606-9613.

57. P. G. Tratnyek; and J. Hoigne., *Environ. Sci. Technol.*, 1991, **25**, 1596-1604.

58. J. Lee, S. Hong, Y. Mackeyev, C. Lee, E. Chung, L. J. Wilson, J. H. Kim and P. J. Alvarez, *Environ. Sci. Technol.*, 2011, **45**, 10598-10604.

Chapter 6: N-doped graphene from metal organic frameworks for catalytic oxidation of *p*-hydroxylbenzoic acid: N functionality and mechanism

ABSTRACT

N-doped graphene has been considered as a promising catalyst with surface metal-free active sites for environmental remediation. Several MIL-100 (Fe)-templated N-doped graphene samples were synthesized using dicyandiamide, melamine and urea as the nitrogen precursors. Excellent catalytic oxidation of *p*-hydroxylbenzoic acid (PHBA) was observed on the as-synthesized samples *via* peroxymonosulfate (PMS) activation. The mechanism was investigated by both electron paramagnetic resonance (EPR, 5,5-dimethyl-1-pyrroline N-oxide and 2,2,6,6-tetramethyl-4-piperidinol as the trapping agents) and quenching tests (ethanol and sodium azide as the radical scavengers). Benzoic acid and furfuryl alcohol were also employed as probing reagents for hydroxyl/sulfate radicals and singlet oxygen, respectively. The results confirmed that singlet oxygen was generated and dominated the PHBA degradation on N-doped graphene other than hydroxyl/sulfate radicals. With the novel N-doped graphene, this study illustrates the formation mechanism of nitrogen functionalities for reactive radicals *via* PMS activation for removal of organic contaminants in water.

The content of this Chapter is published in ACS Sustainable Chemistry & Engineering, 2017, 5(3), 2693-2701.

6.1. Introduction

Toxic organic pollutants in wastewater have become a challenging issue in the development of a sustainable society. Adsorption and catalytic oxidation were considered to be effective methods for pollutant removal.[1-4] Compared with adsorption, advanced oxidation processes (AOPs) are able to degrade the pollutants completely other than phase transfer in physical processes.[5, 6] Some superoxides, such as hydrogen peroxide (H_2O_2), ozone, peroxymonosulfate (PMS), and persulfate (PS), have been used to initiate AOPs after proper activation using catalysts.[7-10] Traditional metal-based catalysts are toxic and might cause second contamination. Carbonaceous catalysts are eco-friendly, and therefore highly demanded for wastewater remediation to avoid secondary pollution.

Carbon-based catalysts, such as activated carbon (AC), carbon nanotube (CNT), reduced graphene oxide (rGO) and nanodiamond, have been demonstrated as effective catalysts for activation of PMS or PS.[11-14] Heteroatom doping such as nitrogen, phosphorus, sulphur and boron into sp^2-hybridized carbon frameworks would modify the carbon electronical properties and induce pronounced catalysis.[15-19] Nitrogen doping was preferential due to its comparable atom size and strong bond with carbon atoms.[20] The amount of N dopant, pyridinic N and graphitic N were reported to be effective in achieving enhanced catalytic activity.[21-23] The factors influencing catalytic performances and mechanism still need further investigations.

Nitrogen doping could be achieved *via* chemical vapor deposition (CVD), segregation growth or arc-discharge.[24] However, the conventional method like CVD was cost-intensive and demands complicated instrumentation. Metal-organic frameworks (MOFs) have been employed as precursors for synthesis of novel carbon materials or carbon-metal composites because of the following advantages: (a) carbon with a hierarchical pore structure could be obtained by thermal pyrolysis based on the highly ordered porous structure of MOFs; (b) alien

molecules would enter the pores and channels of MOFs, inducing a better elemental distribution.[25, 26]

Hydroxyl (•OH) and sulfate ($SO_4^{\bullet-}$) radicals have been observed in PMS activation processes by both metal-based and metal-free catalysis.[13, 27-32] Nonradical degradation pathway was introduced during PS activation by CuO through outer-sphere interaction.[33] PMS could also be activated by N-doped single-walled carbon nanotubes and rGO *via* nonradical process, as shown by previous reports.[12, 34] However, the reactive species during the nonradical process has not been fully specified. In this work, we focused on different reactive species from PMS activated by N-doped carbons for degradation of p-hydroxylbenzoic acid (PHBA). PHBA is very toxic and commonly presented in agroindustrial and pharmaceutical wastewaters.[35] The mineralization of PHBA was reported to be sensitive to •OH and $SO_4^{\bullet-}$ radicals, superoxide radical ($\bullet O_2^-$) as well as singlet oxygen ($^1O_2$).[8, 36, 37]

Here, we synthesized N-doped graphene templated by MIL-100 (Fe) in the presence of three different nitrogen-containing compounds (dicyandiamide, melamine and urea) *via* pyrolysis in nitrogen atmosphere followed by acid digestion to remove Fe. The catalytic oxidation of PHBA on the N-doped graphene was comprehensively studied and the N-functionality and degradation mechanism was investigated.

6.2. Materials and Methods

6.2.1. Materials and chemicals

Iron(III) nitrate nonahydrate ($Fe(NO_3)_3 \bullet 9H_2O$, 100%), benzene trimesic acid (BTC, 95%), dicyandiamide (DCDA, 99.9%), sulfuric acid (H_2SO_4, 98%), potassium peroxymonosulfate (Oxone® or PMS), ferric oxide (Fe_2O_3, 99%), ferrous chloride tetrahydrate ($FeCl_2 \cdot 4H_2O$, 98%), iron (II,III) oxide (Fe_3O_4, 95%), iron (Fe^0, 97%), phenol (99%), p-hydroxylbenzoic acid (PHBA, 99%), benzoic acid (BA, 99.5%), furfuryl alcohol (FFA, 98%), 2,2,6,6-tetramethyl-4-

piperidinol (TMP, 99%), 5,5-dimethyl-1-pyrroline N-oxide (DMPO, 99.0%), ethanol (99.5%), methanol and acetonitrile of HPLC grade were purchased from Sigma-Aldrich. Sodium azide (NaN_3, 99.5%) was obtained from Rowe Scientific.

6.2.2. Synthesis of MIL-100 (Fe) and its derived carbon samples

MIL-100 (Fe) was prepared *via* a fluorine-free route by hydrothermal reactions as reported elsewhere.[38] For synthesis of N-doped graphene, firstly, 4 g of DCDA and 0.20 g of MIL-100 (Fe) were mixed in ethanol and kept being stirred at 80 °C for 8 h, followed by solvent evaporation at 60 °C. The solid was then pyrolyzed at 800 °C for 2 h in N_2. After that, the sample was washed by 0.5 M H_2SO_4 at 80 °C overnight to remove the unstable iron species, labelled as N-G (D). N-G (M) and N-G (U) were synthesized by the same procedure above with melamine and urea as nitrogen sources, respectively. To investigate the influence of pyrolysis temperature, other two N-G (D) samples (D7 and D9) were also prepared at the thermal pyrolysis temperature of 700 and 900 °C, respectively. The as-synthesized carbon materials were summarized in Table 6.1.

Table 6.1. The names and conditions of the as-synthesized carbon materials.

Samples	Nitrogen sources	Pyrolysis temperature (°C)
N-G (D)	DCDA	800
N-G (M)	Melamine	800
N-G (U)	Urea	800
D7	DCDA	700
D9	DCDA	900

6.2.3. Characterization of the samples

Powder X-ray diffraction (XRD) patterns were achieved on a Bruker D8-Advance X-ray diffractometer with Cu Kα radiation (λ = 1.5418 Å). The morphologies of samples were investigated on field emission scanning electron microscopy (FE-SEM, Zeiss Neon 40 EsB),

transmission electron microscopy (TEM, JEOL 2100) and high-resolution TEM (HRTEM, JEOL 2100). The composition and chemical states were studied on X-ray photoelectron spectroscopy (XPS) using a Kratos AXIS Ultra DLD system with Al-Kα X-ray. The specific surface area (SSA) and pore size distributions were evaluated by N_2 sorption at -196 °C on a Tristar 3020 according to the Brunauer–Emmett–Teller (BET) equation and Barrett-Joyner-Halenda (BJH) method, respectively. The concentrations of leaching iron ions in the reaction solutions were measured by the inductively coupled plasma-mass spectroscopy (ICP-MS, PerkinElmer NexION 350D). Thermogravimetric analysis (TGA) was carried on a TGA/DSC-1 thermogravimetric analyzer from Mettler-Toledo Instrument to estimate the content of iron species in samples. Total organic carbon (TOC) was obtained on a Shimadzu TOC-vcph analyzer.

6.2.4. Catalytic performance of the catalysts for organic degradation

The experiments were carried out in a thermostatic water bath with catalysts (100 mg/L), PMS (3.25 mM) and the substrate solutions (*e.g.*, phenol (50 ppm), PHBA (20 ppm), FFA (1 mM), and BA (20 ppm)) in a glass reactor. At a given interval, 1 mL of solution was withdrawn by a syringe, filtered by a 0.45 μm Millipore film, and injected into a vial which held 0.5 mL of methanol as a quenching agent. The resulting solution was analyzed on an ultrahigh performance liquid chromatograph (UHPLC) with a C-18 column. The flow phases and detection wavelengths were set as follows: acetonitrile and water (30:70 v/v) with λ = 270 nm for phenol; methanol and 0.03 M acetic acid (40:60 v/v) with λ = 270 nm for PHBA; methanol and 0.03 M acetic acid solution (15:85 v/v) with λ = 220 nm for FFA; methanol and 0.03 M acetic acid (50:50 v/v) with λ = 270 nm for BA.

6.2.5. Mechanism of catalytic reactions

The mechanism of PMS activation on N-graphene was investigated by electron paramagnetic resonance (EPR). DMPO was selected as the spin-trapping agent for $SO_4^{\bullet-}$ and $^{\bullet}OH$. TMP was

used to mark $^1O_2$ which would oxidize TMP into 2,2,6,6-tetramethyl-4-piperidinol-N-oxyl radical (TMPN). The quantitative results were obtained by Spin Fitting from Bruker Xenon Software package. Quenching tests were conducted with ethanol and NaN_3 to verify the effects of $SO_4^{\bullet-}$, $^{\bullet}OH$ radicals and singlet oxygen. In addition, BA and FFA were chosen to be probe compounds for $SO_4^{\bullet-}$/$^{\bullet}OH$ and singlet oxygen, respectively.

6.3. Results and Discussion

6.3.1. Characterization of the materials

The (002) diffraction peak at 26.1° was found in XRD patterns of N-G(D), N-G(M) and N-G(U), suggesting the formation of graphitic carbon structure (Figure 6.1a). The weak peaks assigned to iron species indicated that iron particles were not completely removed by acid washing. The graphitic carbon and iron residue were confirmed by TEM (Figures 6.2b, e, and h) and HRTEM (Figures 6.2c, f, and i), respectively. In addition, SEM image of N-G(D) (Figure 6.2a) revealed a sheet-like structure while the graphene flakes of N-G(M) and N-G(U) tended to agglomerate together due to π-π interactions (Figures 6.2d and g), inducing the coverage of active sites on the surfaces.[39] A slight amount of carbon nanotubes and shells were found on the samples. The Raman spectra of N-G(D), N-G(M) and N-G(U) (Figure 6.1b) showed that the D and G bands appeared at about 1350 and 1580 cm^{-1}, respectively. Blue shifts occurred on N-G(D) and N-G(M) due to the increased defects, compared with N-G(U). I(D)/I(G) (the intensity ratio of D and G bands) represents the defect degree in the materials.[40] The I(D)/I(G) values of N-G(D), N-G(M) and N-G(U) were 0.90, 1.00 and 0.54, respectively, indicating that N-G(U) had much less defects than N-G(D) and N-G(M) (Table 6.2).

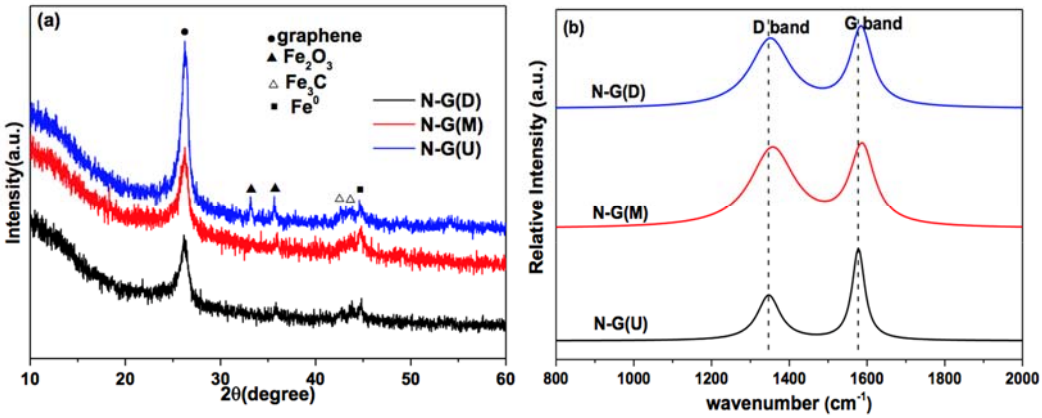

Figure 6.1. XRD patterns (a) and Raman spectra (b) of N-G(D), N-G(M) and N-G(U).

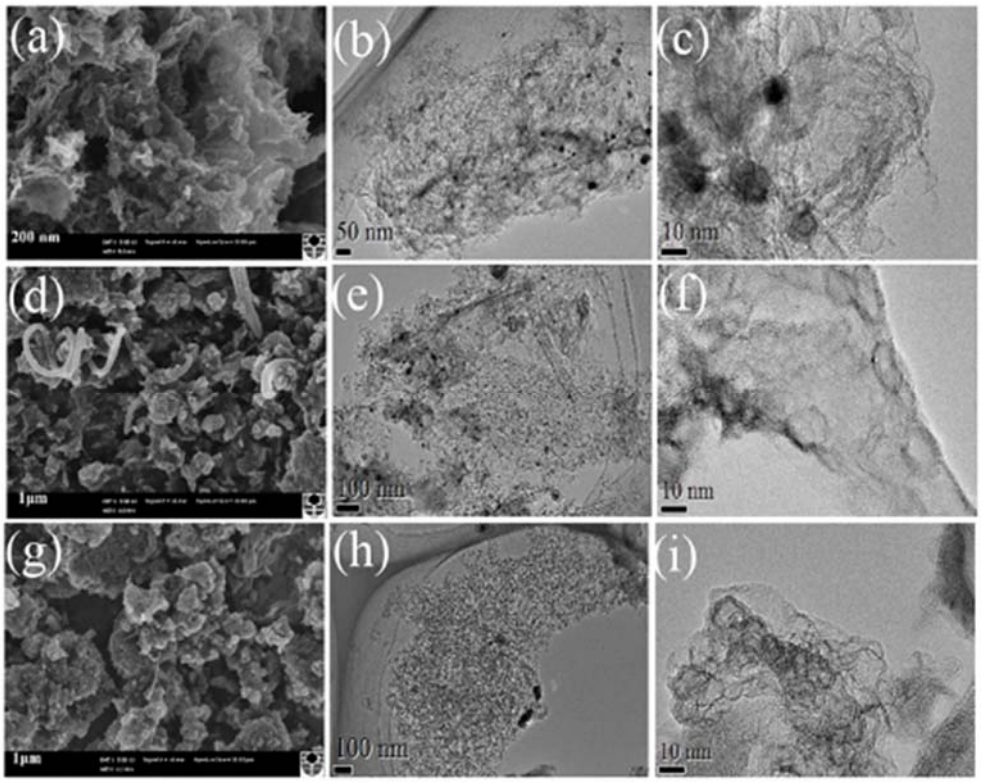

Figure 6.2. SEM images (a,d,g), TEM images (b,e,h) and HRTEM images (c,f,i) of N-G(D)(a-c), N-G(M)(d-f), N-G(U)(g-i).

Table 6.2. The microstructure and textual properties of N-G(D), N-G(M) and N-G(U).

Samples	D band (cm^{-1})	G band (cm^{-1})	I(D)/I(G)	SSA (m^2g^{-1})
N-G (D)	1354	1581	0.90	324.2
N-G (M)	1355	1586	1.00	242.9
N-G (U)	1346	1577	0.54	204.8

N_2 sorption isotherms and pore size distributions of as-synthesized samples are shown in Figure 6.3. The curves in Figure 6.3a were identified as a type IV isotherm and H3 hysteresis loop, due to the capillary condensation of nitrogen gas (N_2) in the mesopores.[41] The SSAs of N-G(D), N-G(M) and N-G(U) were 324.2, 242.9 and 204.8 $m^2 g^{-1}$ (Table 6.2), respectively. Duan *et al.* reported the synthesis of N-doped graphene by direct pyrolysis of GO and melamine at 800 °C, and the surface area of the as-obtained material was 104.9 $m^2 g^{-1}$.[23] N-doped graphene with a surface area of 165.8 $m^2 g^{-1}$ was reported by Wang *et al.*, using glucose, urea and ferric chloride as the precursors.[42] Choi *et al.* synthesized N-doped carbon by pyrolysis of ferric chloride and DCDA, exhibiting a surface area of 78 $m^2 g^{-1}$.[43] Compared with the MOF-free synthesis above, it indicated that the well-developed microporous structure of MIL-100 as a template facilitated the construction of porous structure of corresponding derived carbonaceous materials. N-G(D) possessed the largest SSA compared with the other two materials, possibly due to the higher exfoliation degree of graphene sheets.[44] The pore size of the three materials is mainly centred at about 2.2 nm (Figure 6.3b), suggesting that the nitrogen precursors were not the crucial factor determining the pore size distributions. The mesopores were primarily induced by the carbonization of precursors and removal of iron particles.

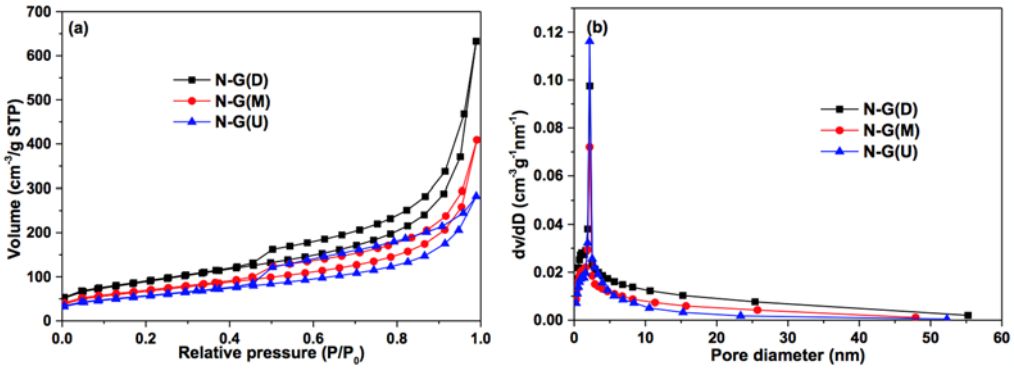

Figure 6.3. N_2 sorption isotherm (a) and pore size distribution (b) curves of N-G(D), N-G(M) and N-G(U).

The composition and chemical states of the as-synthesized N-graphene were evaluated by XPS (Figure 6.4). In the wide scan spectra of the materials (Figure 6.4a), C1s, N1s and O1s peaks clearly presented with negligible Fe 2p peak. N-G(D), N-G(M) and N-G(U) showed small Fe contents at 0.09, 0.1 and 0.08 at.%, respectively. The high-resolution Fe spectra (Figure 6.4b) revealed that Fe_2O_3 and Fe^0 mainly existed in the samples.[45] The C contents of N-G(D), N-G(M) and N-G(U) were 90.73, 90.73 and 93.09 at.%, respectively, and the C 1s spectrum could be deconvoluted into five components (Figure 6.4c-e): C=C (284.6 eV), C-C (285.6 eV), C-O/C=N (286.4 eV), C=O/C-N (287.4 eV) and π—π* shake-up satellite (290.0 eV)[46]. The oxygen contents of N-G(D), N-G(M) and N-G(U) were 6.12, 4.62 and 5.46 at.%, respectively, which originated from oxygen functional groups, adsorbed oxygen/water and Fe_2O_3 (Figure 6.4f-h).[27, 45, 47]

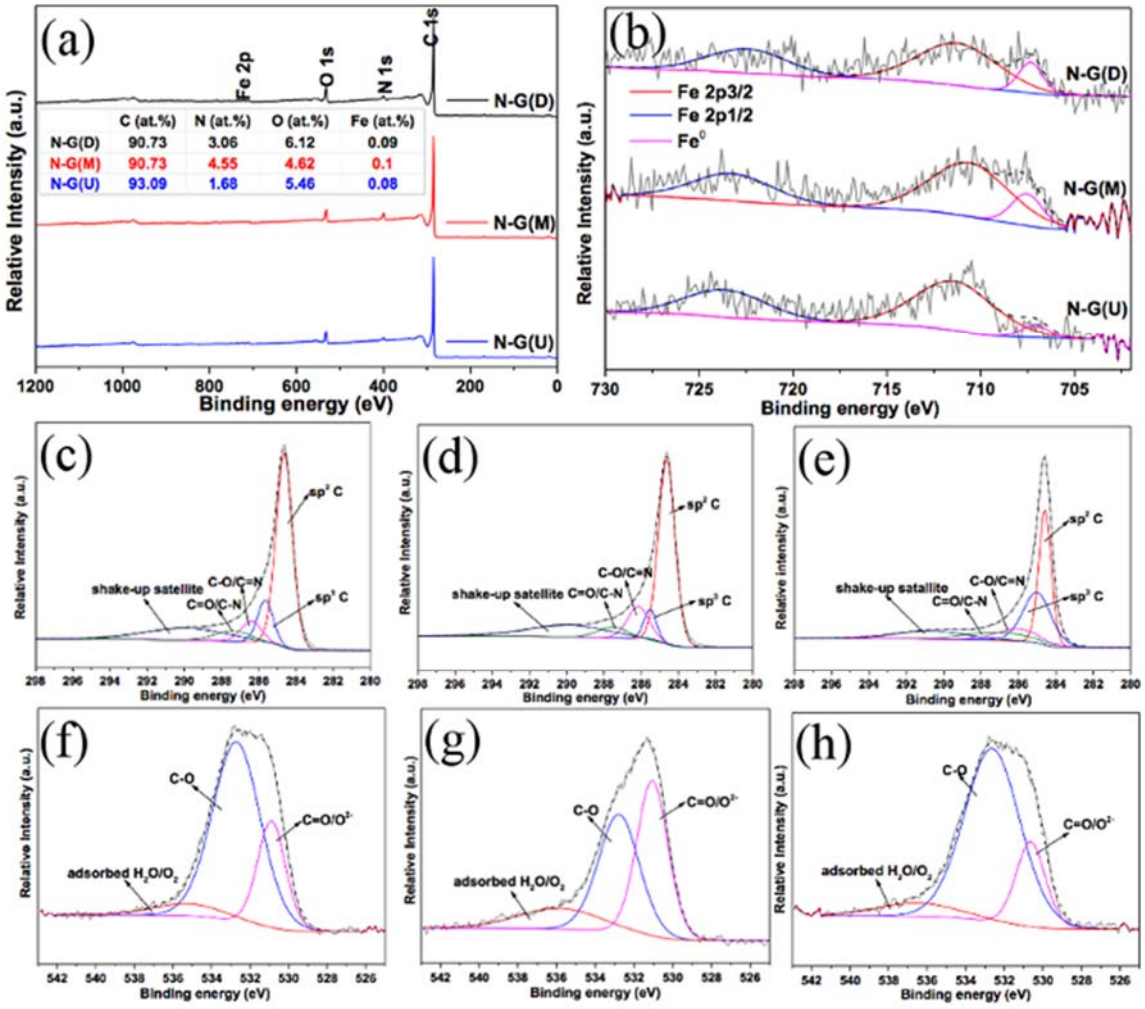

Figure 6.4. Wide scan spectra and elemental contents (inset) of N-graphene samples (a); the high-resolution Fe 2p (b), C1s (c-e) and O1s (f-h) spectra of N-G(D) (c, f), N-G(M) (d, g) and N-G(U) (e, h).

The total N content of N-G(D) was 3.06 at.%, which included pyridinic N (26.73 at.%), pyrrolic N (2.56 at.%), graphitic N (43.89 at.%) and N-O (26.81 at.%) (Figure 6.5a). N-G(M) contained more N (4.55 at.%) than N-G(D) and showed the similar components to N-G(D): pyridinic N (28.05 at.%), pyrrolic N (8.49 at.%), graphitic N (44.04 at.%) and N-O (19.42 at.%) (Figure 6.5b). In N-G(U), the overall N content (1.68 at.%) was the smallest and the high-resolution deconvoluted spectra were attributed to pyridinic N (18.78 at.%), pyrrolic N (15.58 at.%), graphitic N (56.83 at.%) and N-O (8.8 at.%) (Figure 6.5c). It was clearly shown that N

was successfully implanted into graphene sheets and graphitic N was the dominating component for the samples.

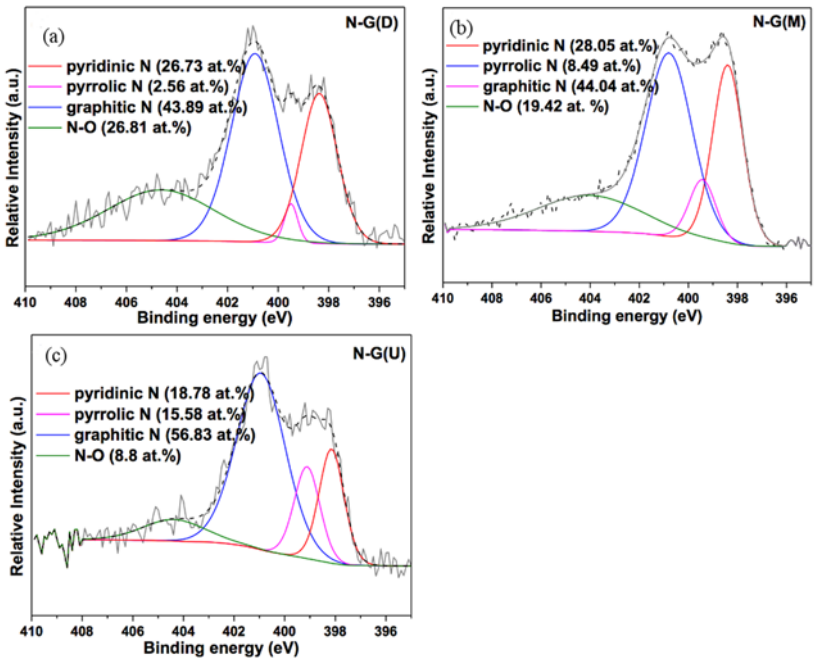

Figure 6.5. High-resolution N1s spectra of N-G(D) (a), N-G(M) (b) and N-G(U) (c).

The highest nitrogen content on N-G(M) was observed due to the following reasons: on one hand, melamine showed the best thermal stability compared with DCDA and urea (Figure 6.6a), resulting in a less nitrogen loss during pyrolysis; on the other hand, the pyridine nitrogen in the aromatic rings of melamine was reported to be more difficult to be eliminated than the non-aromatic nitrogen (Figure 6.6b), which would inhibit the gasification of melamine.[48, 49] Meanwhile, N-G(M) contained the least oxygen compared with N-G(D) and N-G(U), due to the competitive activity between nitrogen and oxygen atoms. More nitrogen atoms occupied the sites of oxygen atoms during carbonization for N-G(M). However, both nitrogen and oxygen contents on N-G(D) were higher than those of N-G(U), because more nitrogen was present as pyridinic N-oxide (Figure 6.5a).[50]

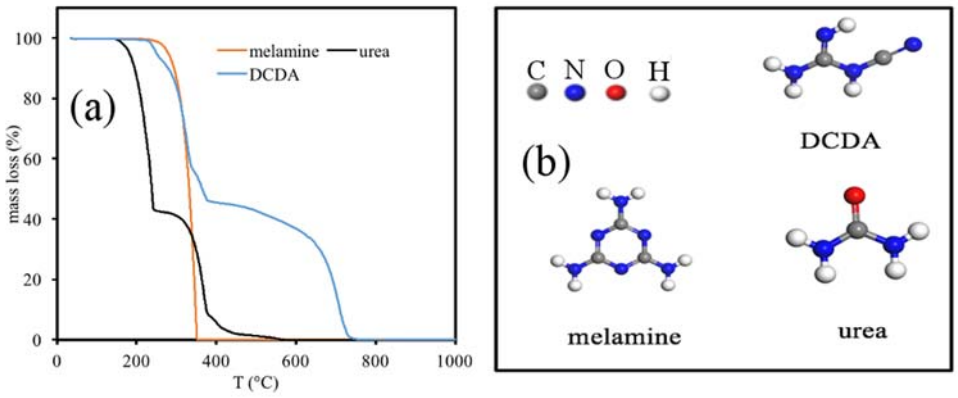

Figure 6.6. Mass loss of DCDA, melamine and urea in argon (a); the structures of DCDA, melamine and urea (b).

Graphitic N was the dominating components regardless of precursors in this study. The similar chemical state of nitrogen in the samples derived from different nitrogen precursors was attributed to the same pyrolysis temperature (800 °C). A similar conclusion was also reported by Sheng *et al*..[51] Nitrogen atoms preferred to substitute carbon atoms at the edge of carbon layers at low temperature. The nitrogen groups in the precursors like $–NH_2$, -C≡N, C-N=C, C=NH and C-NH-C would be rearranged in the forms of pyridinic and pyrrolic N. With the increased temperature, the unstable pyrrolic N and pyridinic N inclined to convert into high-temperature stable graphitic N, which could explain the dominated graphitic N in the samples here.[48, 52] Meanwhile, part of pyridinic N was oxidized into pyridinic N-oxide at high carbonization temperature. It is noteworthy that graphitic N was believed to adsorb PMS more easily, and thus more electrons were transferred from graphene to PMS for activation, which would present the excellent catalytic effect in this study.[23]

6.3.2. Catalytic oxidation of the organic pollutants

The catalytic oxidation of PHBA on the samples is shown in Figure 6.7a. Negligible PHBA degradation was found with PMS only. N-G(M) and N-G(U) could catalytically degrade PHBA completely within 30 and 90 min, respectively. N-G(D) showed the best catalytic efficiency in

PHBA removal, 100% in 20 min. Less than 20% of PHBA was adsorbed by N-G(D), N-G(M) and N-G(U) in 120 min. Conclusively, the removal of PHBA was mainly attributed to catalytic oxidation. The same conclusion was found in phenol degradation (Figure 6.7b), where N-G(D) showed the best catalytic effect on phenol removal while N-G(U) exhibited the worst performance.

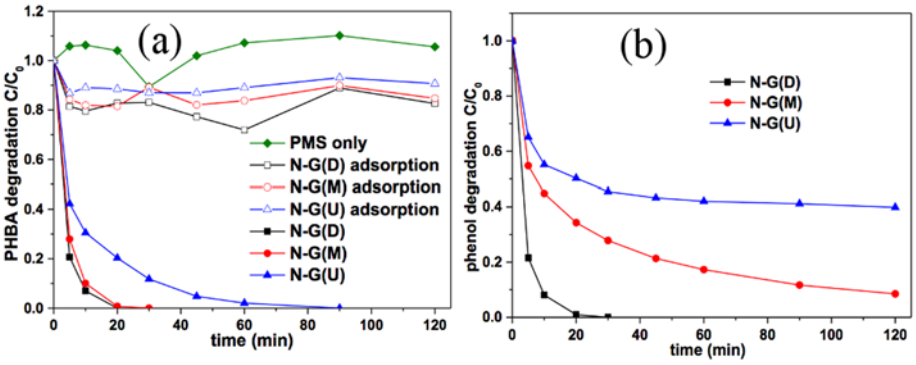

Figure 6.7. PHBA (a) and phenol (b) removal on various catalysts. Reaction conditions: catalyst 100 mg/L, PMS 3.25 mM, PHBA 20 ppm, phenol 50 ppm, temperature 25 °C.

As shown in the XRD and XPS results, the iron species in the catalysts were not completely washed out and possibly participated in the reaction. In order to clarify the catalytic effect of iron species in the catalysts, the leached iron ions in the solutions after the reaction for 120 min were tested by ICP-MS, exhibiting only 1.6, 1.8 and 1.0 ppm for N-G(D), N-G(M) and N-G(U), respectively. The catalytic effect of Fe_3O_4, Fe_2O_3, Fe^{2+} and Fe^0 (loading at 100 mg/L) on PHBA degradation (Figure 6.8a) was confirmed to be negligible. Meanwhile, the previous reports also validated that Fe_3O_4, Fe_2O_3, Fe^{2+} and Fe^0 showed poor performances on PMS activation.[53-55] We could conclude that the iron particles presented in N-G(D), N-G(M) and N-G(U) contributed a negligible catalytic effect. Oxygen groups were proved to be active in pollutant degradation, however, their impacts would be lowered down greatly under the coexistence with nitrogen dopants.[1, 28, 56] It was previously revealed that nitrogen dopant played the dominating role in catalytic oxidation of organic pollutants by changing the inertness of graphene, in terms

of total nitrogen and component contents excluding the non-effective NO_x groups.[21, 23, 28] N-G(U) showed inferior pollutant degradation compared with the other two samples, which could be explained by the low nitrogen dopant and component contents (Figure 6.8b). The effect of nitrogen dopant could also be elucidated in Figure 6.8c. The catalytic oxidation of PHBA weakened with the increase of carbonization temperature in N_2, due to the loss of nitrogen dopant in the form of NO_x. However, even though N-G(M) contained higher contents of total nitrogen and components, its catalytic oxidation efficiency still lagged behind N-G(D) due to the lower SSA (Figure 6.8b). The higher SSA and well-exfoliated graphene structures of N-G(D) induced more active sites to participate in the reactions, resulting in the best catalytic performance.

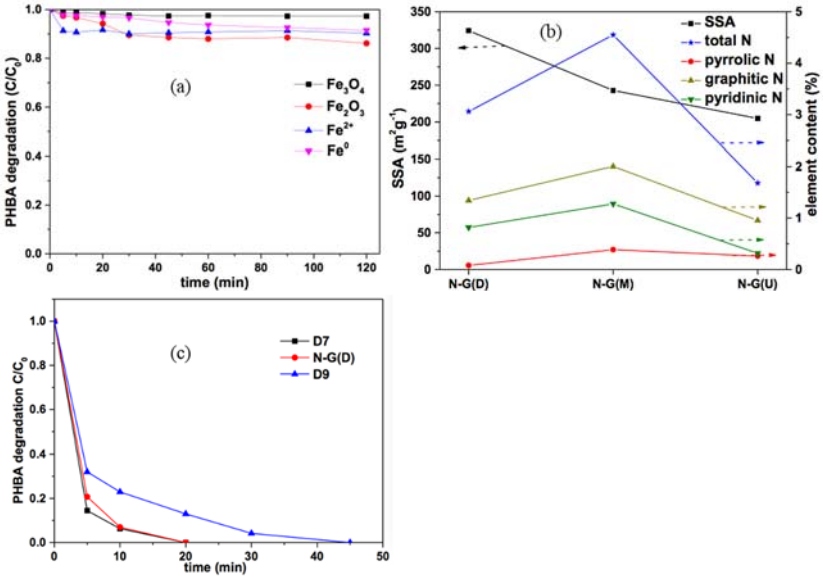

Figure 6.8. PHBA removal on iron-containing catalysts (a); the SSA and element contents of the different catalysts (b); the influence of carbonization temperature on PHBA removal (c). Reaction conditions: catalyst 100 mg/L, PMS 3.25 mM, PHBA 20 ppm, temperature 25 °C.

6.3.3. Mechanism of PMS activation

$SO_4^{\bullet-}$ and $^{\bullet}OH$ radicals have been found to be generated during PMS activation as reported previously.[13, 29] Here EPR was employed to screen the evolution of radicals using DMPO as

the trapping agent.

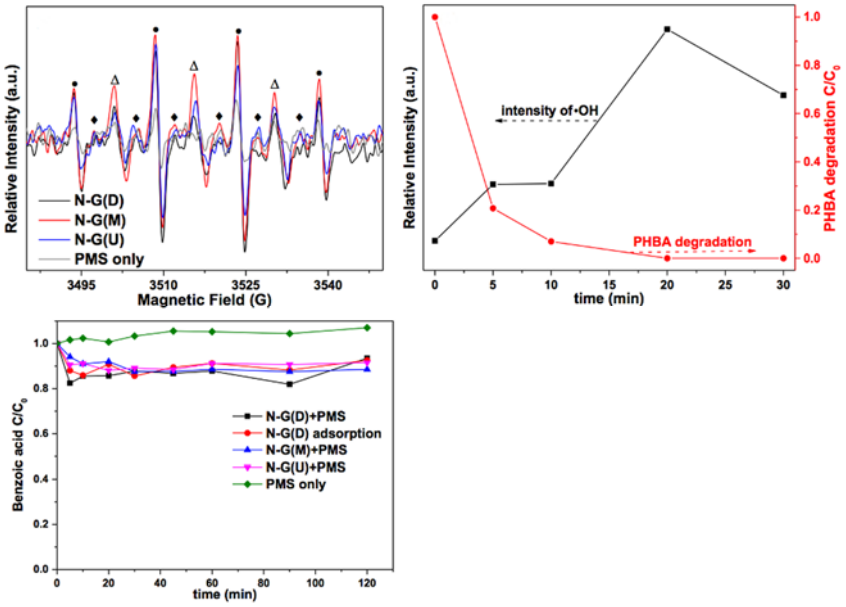

Figure 6.9. EPR spectra of PMS activation on various catalysts with DMPO as the trapping agent (a); hydroxyl radicals evolution during PMS activation on N-G(D) (b); benzoic acid removal on various catalysts (c). Conditions: catalyst 100 mg/L, PMS 3.25 mM, PHBA 20 ppm, BA 20 ppm, temperature 25 °C, DMPO 0.08 M. ●: DMPO-OH, ♦: DMPO-SO_4, Δ: DMPO-X.

As shown in Figure 6.9a, both $SO_4^{\bullet-}$ and $^{\bullet}OH$ radicals were produced on N-G(D), N-G(M) and N-G(U). The intensity of $^{\bullet}OH$ radicals on the catalysts was much higher than that of $SO_4^{\bullet-}$ radicals, indicating that $^{\bullet}OH$ radicals were selectively produced in the reactions compared with $SO_4^{\bullet-}$ radicals. In addition, the catalytic reactions produced much more $^{\bullet}OH$ radicals than PMS only, and the intensity of $^{\bullet}OH$ radicals on N-G(U) was lower than that on N-G(D) and N-G(M), which could explain the inferior efficiency of pollutant degradation on N-G(U). However, the intensity of $^{\bullet}OH$ radicals on N-G(D) and N-G(M) was similar while the catalytic effect of N-G(D) was superior to that of N-G(M). Meanwhile, the intensity of $^{\bullet}OH$ radicals on N-G(D) increased the fastest between 10 and 20 min, while the quickest catalytic degradation reaction occurred in the first 5 min (Figure 6.9b). In addition, as shown in Figure 6.9c, BA was used as

the probing compound of $SO_4^{\bullet-}$ and $^{\bullet}OH$ radicals. Less than 20% of BA was removed by the as-synthesized samples, attributed mainly to the adsorption. It indicated that $SO_4^{\bullet-}$ and $^{\bullet}OH$ radicals were not the dominating species in the catalytic oxidation reactions.

Singlet oxygen was found during the self-decomposition of PMS and PMS activation by benzoquinone and ketones under alkaline condition.[40, 57, 58] In this study, TMP was chosen as the trapping agent of $^1O_2$ and the typical three TMPN peaks with the equal intensity were found, as shown in Figure 6.10a. TMPN peaks were observed on PMS solely without any catalysts due to the self-decomposition of PMS and the intensity of singlet oxygen increased with the addition of the catalysts. FFA was further employed as the probing compound of singlet oxygen in this study as well, as shown in Figure 6.10b.[59, 60] Approximately 20% of FFA was removed by PMS only and 97% was degraded with the addition of the catalysts in 120 min. No adsorption of FFA was observed, so the removal of FFA was attributed to oxidation, confirming that more singlet oxygen was generated during PMS activation by the catalysts, compared with PMS only. The intensities of singlet oxygen produced on the catalysts were in the order: N-G(D) > N-G(M) > N-G(U) (Figure 6.10a), corresponding to the catalytic efficiency order of PHBA. In addition, the generation rate of singlet oxygen on N-G(D) rose the fastest in the first 5 min and then slowed down, which conformed to the degradation rate of PHBA (Figure 6.10c). It could be deduced that singlet oxygen was produced during PMS activation by the catalysts and acted as the dominating radical in the reactions.

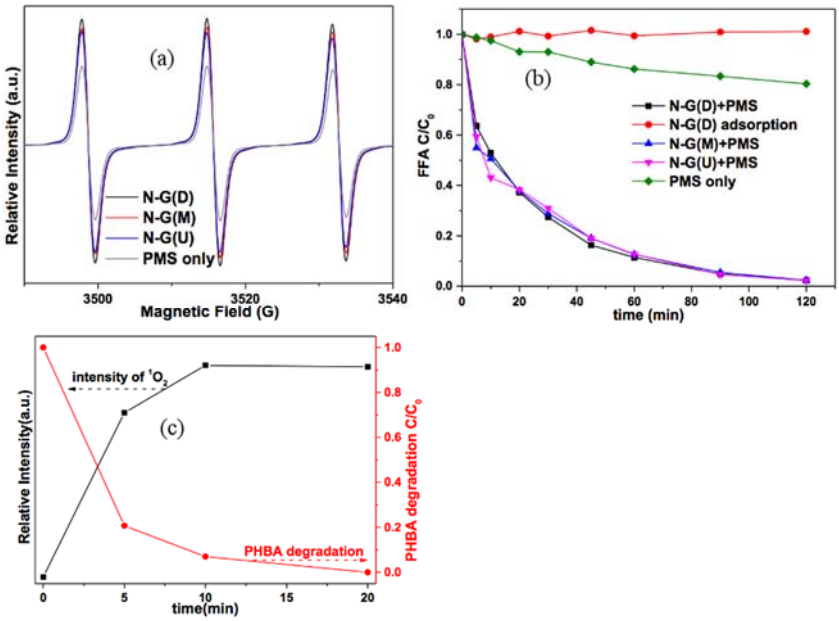

Figure 6.10. EPR spectra of PMS activation on various catalysts with TMP as the trapping agent (a); FFA removal on various catalysts (b); singlet oxygen evolution during PMS activation on N-G(D) (c). Conditions: catalyst 100 mg/L, PMS 3.25 mM, PHBA 20 ppm, FFA 1 mM, temperature: 25 °C, TMP: 1.16 g/L.

The quenching tests were also conducted in order to uncover the impact of the radicals. Ethanol was the classical scavenger for $SO_4^{\bullet-}$ and $^{\bullet}OH$ radicals ($k_{SO_4^{\bullet-}}$ = (1.6 – 7.8) × 10^7 $M^{-1}s^{-1}$, $k_{^{\bullet}OH}$ = (1.2 – 1.8) × 10^9 $M^{-1}s^{-1}$) while NaN_3 was for singlet oxygen ($k_{^1O_2}$ = 1 × 10^9 $M^{-1}s^{-1}$).[29, 61] However, ethanol was stubborn to singlet oxygen, and it was chosen as the radical scavenger together with NaN_3 in this study.[62] No more than 10% decrease in PHBA degradation was found with the addition of 1.625 M ethanol, especially on N-G(D) (Figure 6.11). The catalytic efficiency dropped more much after adding 3 mM NaN_3, suggesting that the inhibitory ability of 3 mM NaN_3 was stronger than that of 1.625 M ethanol. Noteworthily, NaN_3 would also react with $SO_4^{\bullet-}$ and $^{\bullet}OH$ radicals ($k_{SO_4^{\bullet-}}$ = 2.52 × 10^9 $M^{-1}s^{-1}$, $k_{^{\bullet}OH}$ = 1.2 × 10^{10} $M^{-1}s^{-1}$) besides singlet oxygen.[63] The reaction rates of 3 mM NaN_3 with $SO_4^{\bullet-}$ and $^{\bullet}OH$ radicals were calculated to be 7.56 ×10^6 and 3.6 ×10^7 s^{-1}, respectively, which were much smaller than those of 1.625 M

ethanol (1.27×10^8 and 2.9×10^9 s^{-1}, respectively). Assuming that $SO_4^{\bullet-}$ and $^{\bullet}OH$ radicals were the dominating radicals rather than singlet oxygen, the restrictive effect of 1.625 M ethanol on PHBA degradation must be higher than that of 3 mM NaN_3. The contrary results confirmed that singlet oxygen was the primary contributor instead of $SO_4^{\bullet-}$ and $^{\bullet}OH$ radicals.

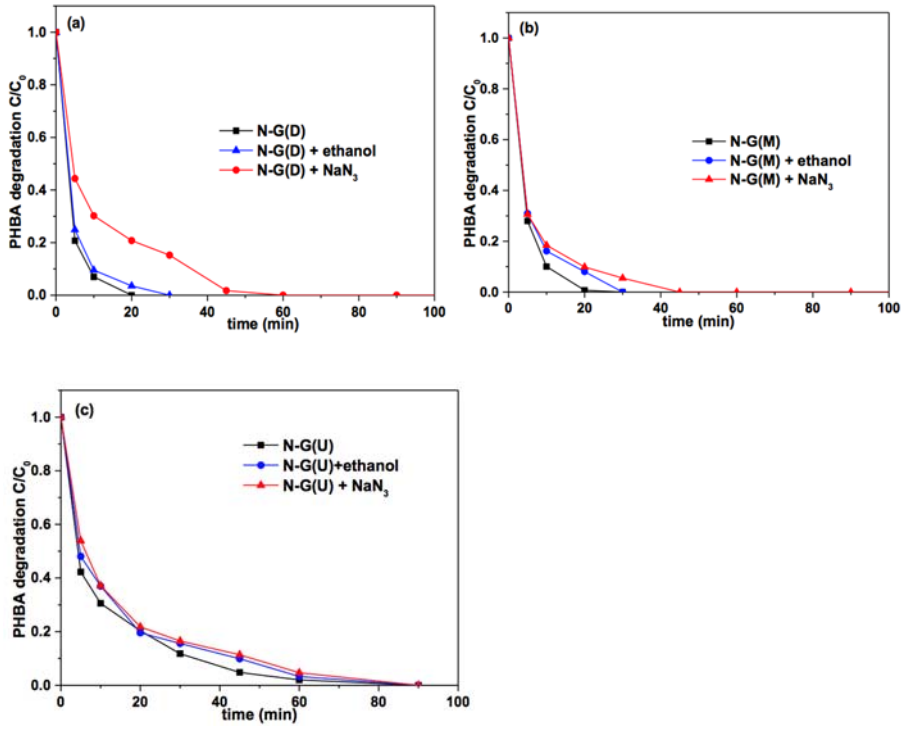

Figure 6.11. The quenching tests on N-G(D) (a), N-G(M) (b) and N-G(U) (c). Reaction conditions: catalyst: 100 mg/L, PMS: 3.25 mM, PHBA: 20 ppm, temperature: 25 °C, ethanol: 1.625 M, NaN_3: 3 mM.

Xiao *et al.* and Wang *et al.* proposed a similar degradation pathway of PHBA by photocatalysis and ozonation: PHBA was converted into dihydroxylbenzoic acid at first, followed by aromatic ring opening.[8, 64] With further oxidation, small molecular acids (*e.g.* maleic acid/fumaric acid, propionic acid, oxalic acid, acetic acid) were generated and eventually degraded into CO_2 and H_2O. In this study, the intermediates such as dihydroxylbenzoic acid, propionic acid, maleic acid and fumaric acid were found in UHPLC spectra (Figure 6.12). We supposed that PHBA here experienced the similar degradation route

as above (Figure 6.13). In addition, the TOC results (Figure 6.14) showed that approximately 50% TOC removal was achieved with the addition of catalysts while no PHBA was left, confirming the existence of intermediates.

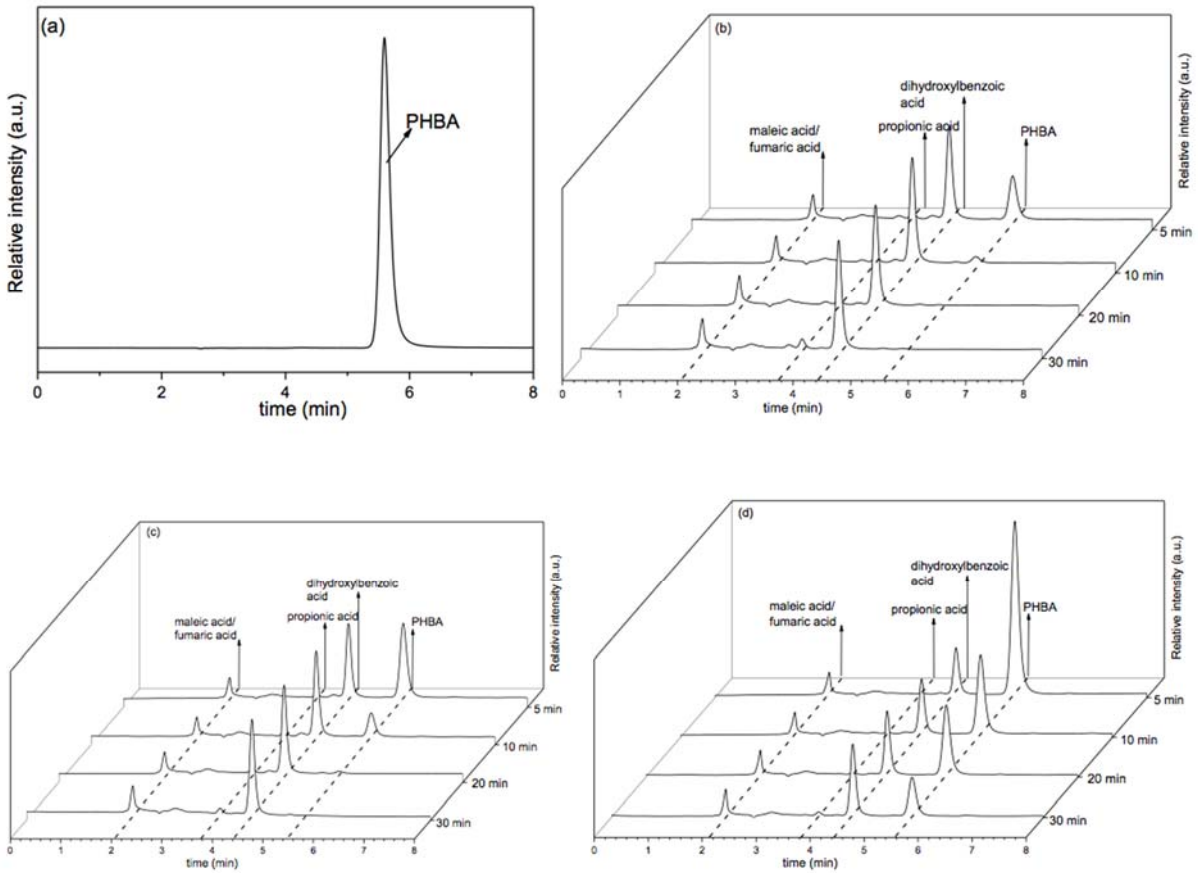

Figure 6.12. The UHPLC spectra of (a) pristine PHBA, and the intermediates detection in catalytic PHBA oxidation on (b) N-G(D), (c) N-G(M) and (c) N-G(U). Reaction conditions: C (PHBA) 20 ppm, catalyst 0.1 g/L, PMS 1 g/L, Temperature: 25 ºC.

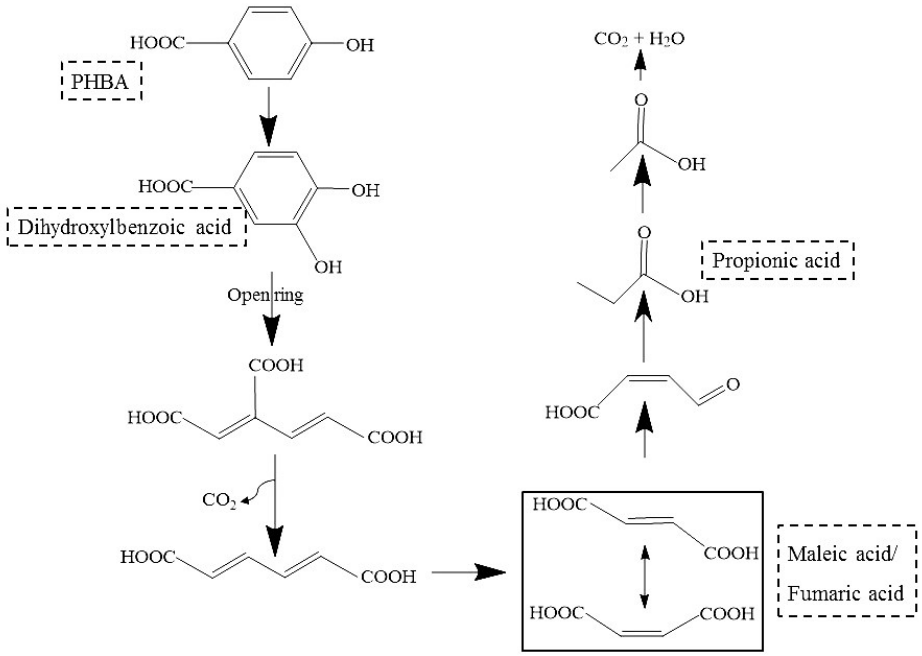

Figure 6.13. Proposed degradation pathway of PHBA by catalytic oxidation.

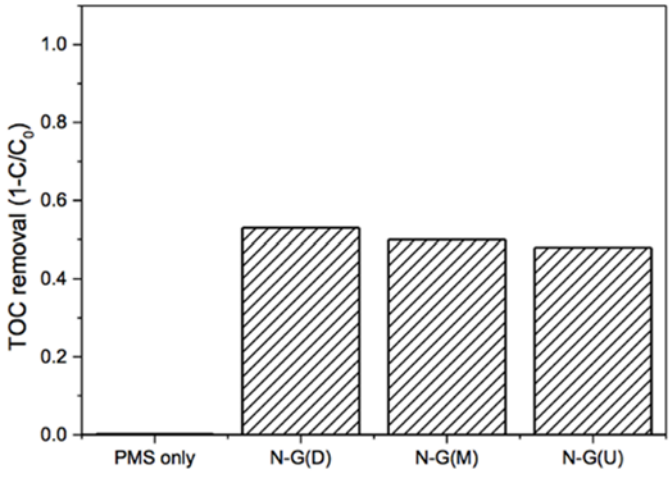

Figure 6.14. TOC removal for catalytic PHBA oxidation on various catalysts and PMS only. Reaction conditions: C (PHBA): 20 ppm, catalysts loading: 0.1 g/L, PMS loading: 1 g/L, Temperature: 25 ºC, reaction time: 120 min.

In terms of nanocarbons, it was reported that the defect edges, sp^2 carbon and oxygen groups acted as the active sites for PMS activation in advanced oxidation processes.[13, 65] In addition, doped heteroatoms like nitrogen or boron into nanocarbons would disrupt the carbon configuration and introduce new active sites.[66, 67] As reported by Duan *et al.*, the carbonyl

groups (C=O) and sp^2 hybridized carbon structure induced the generation of $SO_4^{\bullet-}$ and $^{\bullet}OH$ radicals by donating electrons to PMS, while nonradical reactions resulted from the defective edges.[12] Meanwhile, N doping would also induce nonradical pathway by drawing electrons from adjacent carbon atoms.[34, 68]

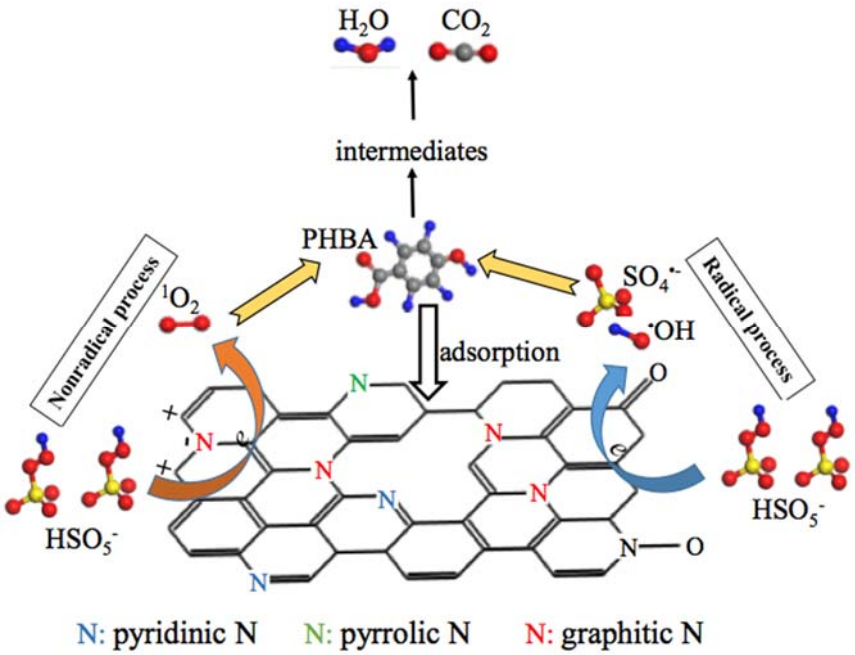

Figure 6.15. The proposed mechanism of catalytic PHBA oxidation on N-doped graphene catalysts.

In this study, the radical reaction occurred during the PMS activation by carbonyl group and sp^2 hybridized carbon lattice. Due to low defects degree confirmed by Raman spectra, the effect of defective edges should be excluded.[8] As a result, the doped N contributed to the generation of singlet oxygen here. A proposed mechanism is illustrated in Figure 6.15. On one hand, PMS was activated by carbonyl group and sp^2 hybridized carbon, generating $SO_4^{\bullet-}$ and $^{\bullet}OH$ radicals. On the other hand, HSO_5^- was adsorbed by positively charged carbon atoms adjacent to electron-withdrawing nitrogen atom, which facilitated the formation of $^1O_2$. PHBA adsorbed on catalysts was attacked by both radicals and singlet oxygen, and then degraded into CO_2 and H_2O.

6.4. Conclusions

In conclusion, N-doped graphene templated by MIL-100(Fe) was synthesized using dicyandiamide, melamine and urea as nitrogen sources *via* simple pyrolysis. The as-synthesized N-doped graphene showed excellent catalytic oxidation of organic pollutants (phenol, PHBA and FFA) by activation of PMS, especially N-G(D). The nitrogen dopant and specific surface area of catalysts were two key parameters influencing on the efficiency of pollutants removal. The mechanism investigation revealed that singlet oxygen contributed mainly to the pollutant degradation instead of hydroxyl or sulfate radicals on N-doped graphene regardless of nitrogen precursors. This study was important for the development of carbonaceous catalysts and mechanistic investigations on oxidants activation.

6.5. References

1. W. Peng, S. Liu, H. Sun, Y. Yao, L. Zhi and S. Wang, *J. Mater. Chem. A*, 2013, **1**, 5854-5859.
2. P. R. Shukla, S. Wang, H. Sun, H. M. Ang and M. O. Tadé, *Appl. Catal., B*, 2010, **100**, 529-534.
3. N. L. Torad, M. Hu, S. Ishihara, H. Sukegawa, A. A. Belik, M. Imura, K. Ariga, Y. Sakka and Y. Yamauchi, *Small*, 2014, **10**, 2096-2107.
4. W. Zhang, H. L. Tay, S. S. Lim, Y. Wang, Z. Zhong and R. Xu, *Appl. Catal., B*, 2010, **95**, 93-99.
5. Y. Yang, J. Jiang, X. Lu, J. Ma and Y. Liu, *Environ. Sci. Technol.*, 2015, **49**, 7330-7339.
6. Y. Yang, J. J. Pignatello, J. Ma and W. A. Mitch, *Environ. Sci. Technol.*, 2014, **48**, 2344-2351.
7. S. Indrawirawan, H. Sun, X. Duan and S. Wang, *J. Mater. Chem. A*, 2015, **3**, 3432-3440.
8. Y. Wang, Y. Xie, H. Sun, J. Xiao, H. Cao and S. Wang, *ACS Appl. Mater. Interfaces*, 2016, **8**, 9710-9720.
9. O. S. Furman, A. L. Teel and R. J. Watts, *Environ. Sci. Technol.*, 2010, **44**, 6423–6428.
10. A. W. Vermilyea and B. M. Voelker, *Environ. Sci. Technol.*, 2009, **43**, 6927–6933.
11. X. Duan, Z. Ao, D. Li, H. Sun, L. Zhou, A. Suvorova, M. Saunders, G. Wang and S. Wang, *Carbon*, 2016, **103**, 404-411.
12. X. Duan, Z. Ao, L. Zhou, H. Sun, G. Wang and S. Wang, *Appl. Catal., B*, 2016, **188**, 98-105.

13. H. Sun, S. Liu, G. Zhou, H. M. Ang, M. O. Tadé and S. Wang, *ACS Appl. Mater. Interfaces*, 2012, **4**, 5466-5471.

14. C. K. Chua and M. Pumera, *Chem. – Eur. J.*, 2015, **21**, 12550-12562.

15. Z. Yang, Z. Yao, G. Li, G. Fang, H. Nie, Z. Liu, X. Zhou, X. Chen and S. Huang, *ACS Nano*, 2012, **6**, 205–211.

16. Z. Liu, F. Peng, H. Wang, H. Yu, W. Zheng and J. Yang, *Angew. Chem., Int. Ed. Engl.*, 2011, **50**, 3257-3261.

17. X. Wang, Y. Qin, L. Zhu and H. Tang, *Environ. Sci. Technol.*, 2015, **49**, 6855-6864.

18. L. Yang, S. Jiang, Y. Zhao, L. Zhu, S. Chen, X. Wang, Q. Wu, J. Ma, Y. Ma and Z. Hu, *Angew. Chem., Int. Ed. Engl.*, 2011, **50**, 7132-7135.

19. X.X. Ma and X.Q. He, *Appl. Mater. Today*, 2016, **4**, 1-8.

20. M. Vikkisk, I. Kruusenberg, U. Joost, E. Shulga, I. Kink and K. Tammeveski, *Appl. Catal.,* 2014, **147**, 369-376.

21. H. Sun, Y. Wang, S. Liu, L. Ge, L. Wang, Z. Zhu and S. Wang, *Chem. Commun.*, 2013, **49**, 9914-9916.

22. O. S. G. P. Soares, R. P. Rocha, A. G. Gonçalves, J. L. Figueiredo, J. J. M. Órfão and M. F. R. Pereira, *Appl. Catal., B*, 2016, **192**, 296-303.

23. X. Duan, Z. Ao, H. Sun, S. Indrawirawan, Y. Wang, J. Kang, F. Liang, Z. Zhu and S. Wang, *ACS Appl. Mater. Interfaces*, 2015, **7**, 4169-4178.

24. H. Wang, T. Maiyalagan and X. Wang, *ACS Catal.*, 2012, **2**, 781-794.

25. A. Aijaz, N. Fujiwara and Q. Xu, *J. Am. Chem. Soc.*, 2014, **136**, 6790-6793.

26. T. K. Kim, K. J. Lee, J. Y. Cheon, J. H. Lee, S. H. Joo and H. R. Moon, *J. Am. Chem. Soc.*, 2013, **135**, 8940-8946.

27. S. Indrawirawan, H. Sun, X. Duan and S. Wang, *Appl. Catal., B*, 2015, **179**, 352-362.

28. H. Sun, C. Kwan, A. Suvorova, H. M. Ang, M. O. Tadé and S. Wang, *Appl. Catal., B*, 2014, **154-155**, 134-141.

29. G. P. Anipsitakis and D. D. Dionysiou, *Environ. Sci. Technol.*, 2003, **37**, 4790-4797.

30. J. E. Yang, H. Lan, X. Lin, B. Yuan and M. Fu, *Chem. Eng. J.*, 2016, **289**, 296-305.

31. C. Chen, W. Zuo, J. E. Yang, H. Cui and M. Fu, *RSC Adv.*, 2016, **6**, 101361-101364.

32. J. E. Yang, B. Yuan, H. Cui, S. Wang and M. Fu, *Appl. Catal., B*, 2017, **205**, 327-339.

33. T. Zhang, Y. Chen, Y. Wang, L. J. Roux, Y. Yang and J. Croué, *Environ. Sci. Technol.*, 2014, **48**, 5868-5875.

34. X. Duan, H. Sun, Y. Wang, J. Kang and S. Wang, *ACS Catal.*, 2015, **5**, 553-559.

35. B. H. Jesus, J. Torregrosa, J. R. Dominguez and J. A. Peres, *Chemosphere*, 2001, **42**, 351-359.

36. J. Criquet and N. K. V. Leitner, *Radiat. Phys. Chem.*, 2015, **106**, 307-314.

37. J. Xiao, Y. Xie, F. Nawaz, S. Jin, F. Duan, M. Li and H. Cao, *Appl. Catal., B*, 2016, **181**, 420-428.

38. Y. K. Seo, J. W. Yoon, J. S. Lee, U. H. Lee, Y. K. Hwang, C. H. Jun, P. Horcajada, C. Serre and J. S. Chang, *Microporous Mesoporous Mater.*, 2012, **157**, 137-145.

39. C. Zhu and S. Dong, *Nanoscale*, 2013, **5**, 1753-1767.

40. D. F. Evans and M. W. Upton, *J. Chem. Soc., Dalton Trans.*, 1985, **6**, 1151−1153.

41. J. Tang, R. R. Salunkhe, J. Liu, N. L. Torad, M. Imura, S. Furukawa and Y. Yamauchi, *J. Am. Chem. Soc.*, 2015, **137**, 1572-1580.

42. C. Wang, J. Kang, H. Sun, H. M. Ang, M. O. Tadé and S. Wang, *Carbon*, 2016, **102**, 279-287.

43. C. H. Choi, S. H. Park and S. I. Woo, *Appl. Catal., B*, 2012, **119–120**, 123-131.

44. S. Park, J. An, J. R. Potts, A. Velamakanni, S. Murali and R. S. Ruoff, *Carbon*, 2011, **49**, 3019-3023.

45. X. Li, D. W. Elliott and W. Zhang, *Crit. Rev. Solid State Mater. Sci.*, 2006, **31**, 111-122.

46. G. Singh, D. S. Sutar, V. D. Botchar, P. K. Narayanam, S. S. Talwar, R. S. Srinivasa and S. S. Major, *Nanotechnology*, 2013, **24**, 355704-1-8.

47. H. Darmstadta, C. Roya, S. Kaliaguinea, S. J. Choib and R. Ryoob, *Carbon*, 2002, **40**, 2673-2683.

48. K. Stańczyk, R. Dziembaj, Z. Piwowarska and S. Witkowski, *Carbon*, 1995, **33**, 1383-1392.

49. D. Mang, H. P. Boehm, K. Stanczyk and H. Marsh, *Carbon*, 1992, **30**, 391-398.

50. K. A. Grant, Q. Zhu and K. M. Thomas, *Carbon*, 1994, **32**, 883-895.

51. Z. Sheng, L. Shao, J. Chen, W. Bao, F. Wang and X. Xia, *ACS Nano*, 2011, **5**, 4350-4358.

52. J. R. Pels, F. Kapteijn, J. A. Moulijn, Q. Zhu and K. M. Thomas, *Carbon*, 1995, **33**, 1641-1653.

53. H. Sun, G. Zhou, S. Liu, H. M. Ang, M. O. Tadé and S. Wang, *ACS Appl. Mater. Interfaces*, 2012, **4**, 6235-6241.

54. J. Lu, Q. Liu, Z. Xiong, Z. Xu, Y. Cai and Q. Wang, *J. Chem. Technol. Biotechnol.*, 2016, DOI: 10.1002/jctb.5153.

55. Q. Yang, H. Choi, S. R. Al-Abed and D. D. Dionysiou, *Appl. Catal., B*, 2009, **88**, 462-469.

56. Y. Wang, Z. Ao, H. Sun, X. Duan and S. Wang, *Appl. Catal., B*, 2016, **198**, 295-302.

57. Y. Zhou, J. Jiang, Y. Gao, J. Ma, S. Y. Pang, J. Li, X. T. Lu and L. P. Yuan, *Environ. Sci. Technol.*, 2015, **49**, 12941-12950.

58. R. E. Montgomery, *J. Am. Chem. Soc.*, 1974, **96**, 7820-7821.

59. W. R. Haag, J. Hoigné , E. Gassman and A. M. Braun, *Chemosphere*, 1984, **13**, 631-640.

60. A. D. Bokare and W. Choi, *Environ. Sci. Technol.*, 2015, **49**, 14392-14400.

61. H. E. Gsponer, C. M. Previtali and N. A. García, *Toxicol. Environ. Chem.*, 1987, **16**, 23-37.

62. M. A. J. Rodgers, *J. Am. Chem. Soc.*, 1983, **105**, 6201-6205.

63. R. E. Huie and C. L. Clifton, *J. Phys. Chem.*, 1990, **94**, 8561-8567.

64. J. Xiao, Y. Xie, F. Nawaz, Y. Wang, P. Du and H. Cao, *Appl. Catal., B*, 2016, **183**, 417-425.

65. S. Liu, W. Peng, H. Sun and S. Wang, *Nanoscale*, 2014, **6**, 766-771.

66. D. Su , J. Zhang, B. Frank, A. Thomas, X. Wang, J. Paraknowitsch and R. Schlögl, *ChemSusChem*, 2010, **3**, 169-180.

67. H. Liu, Y. Liu and D. Zhu, *J. Mater. Chem.*, 2011, **21**, 3335-3345.

68. C. H. Choi, S. H. Park and S. I. Woo, *ACS Nano*, 2012, **6**, 7084-7091.

Chapter 7: Conclusions and perspectives

7.1. Conclusions

In this thesis, MOFs-derived materials for wastewater treatment are investigated through adsorption, photocatalytic reaction and advanced oxidation. Specifically, carbon and nitrogen co-doped zinc oxide samples were synthesized by the controllable pyrolysis of ZIF-8, and the photocatalytic effect on dye degradation and water oxidation of the as-synthesized materials were evaluated. The influences of pyrolysis procedure, carbonization temperature and pyrolysis time were tested. Meanwhile, the mechanistic investigation revealed that the photo-excited electrons and hydroxyl radicals contributed to the dye degradation. Nitrogen-doped graphene derived from MIL-100 (Fe) was also synthesized by using different nitrogen sources like DCDA, melamine and urea, and the catalytic effect on the degradation of organic pollutants was investigated in the presence of peroxymonosulfate. The mechanism of peroxymonosulfate activation by N-doped graphene was deeply studied with the assistance of EPR and quenching tests. Singlet oxygen was firstly observed and found to play the dominating role in the degradation of organic pollutants instead of hydroxyl and sulfate radicals. In addition, the conversion from MOF to N-doped graphene and degradation pathway of the different organic pollutants were also revealed.

7.1.1. Solar Photocatalytic Water Oxidation and Purification on ZIF-8 Derived C-N-ZnO Composites

1) Carbon and nitrogen modified ZnO hybrids derived from ZIF-8 were prepared through three different thermal transformation processes: single-step air combustion, N_2 annealing, and two-step N_2 annealing followed by air calcination.
2) The photocatalytic activity of MOF-derived C, N-ZnO was systematically evaluated in water oxidation and photodegradation of methylene blue. It was also found that C, N-

ZnO prepared from ZIF-8 by the two-step approach presented a much higher activity than those directly calcination of ZIF-8 from one-step method.

7.1.2. Photocatalysis of C, N-doped ZnO derived from ZIF-8 for dye degradation and water oxidation

1) Carbon and nitrogen co-doped ZnO was prepared *via* a two-step route (carbonization under N_2 followed by pyrolysis in air) by thermal conversion of ZIF-8.
2) The carbonization temperature and pyrolysis time exerted great influences on the photocatalytic activity of the as-obtained materials for methylene blue degradation, due to the various carbon/nitrogen dopants and oxygen vacancies.
3) The mechanistic investigation showed that hydroxyl radicals and photo-excited electrons act on the decomposition of methylene blue.
4) The carbon and nitrogen co-doped ZnO showed a better photocatalytic oxygen evolution performance than commercial ZnO, due to more active sites introduced by dopants.

7.1.3. An insight to metal organic framework derived N-doped graphene towards oxidative degradation of persistent contaminants: Formation mechanism and generation of singlet oxygen from peroxymonosulfate

1) Nitrogen-doped graphene was prepared using MIL-100(Fe) and DCDA as the precursors *via* pyrolysis at 800 °C under inert atmosphere followed by a post-acid treatment.
2) The transformation from MOF to the target carbonaceous materials was revealed.
3) The as-synthesized N-doped graphene showed excellent organic pollutants degradation in the presence of peroxymonosulfate, due to N doping, fast electron flowing of graphene and high specific surface area.

4) The mechanism of PMS activation on N-G was investigated by means of both EPR and quenching tests. Singlet oxygen was observed during PMS activation on N-G and was determined to be the primary role in phenol degradation.
5) The N-G/PMS system showed a better efficiency on phenol degradation in alkaline condition.

7.1.4. N-doped graphene from metal organic frameworks for catalytic oxidation of *p*-hydroxylbenzoic acid: N functionality and mechanism

1) N-doped graphene templated by MIL-100(Fe) was synthesized using dicyandiamide, melamine and urea as nitrogen sources *via* simple pyrolysis and post-acid washing. The texture and component characterizations of the as-synthesized materials were performed.
2) The N-doped graphene showed excellent catalytic oxidation of organic pollutants like phenol and *p*-hydroxylbenzoic acid by activation of PMS, especially the N-doped graphene with DCDA as the nitrogen source.
3) The nitrogen dopant and specific surface area of catalysts were two key parameters influencing on the efficiency of pollutant removals.
4) The mechanistic investigation revealed that singlet oxygen contributed mainly to the pollutant degradation instead of hydroxyl or sulfate radicals on N-doped graphene regardless of nitrogen precursors.
5) The degradation pathway of *p*-hydroxylbenzoic acid was studied.

7.2. Future perspectives

- The morphology control has considerable influences on the catalytic effect and adsorption capacity, and materials with various morphologies and structures by using MOFs as the precursors are reported to be fabricated by controlling the synthetic conditions. However, such MOFs-derived materials are mainly employed in the

electrochemical field to date and not mentioned in this thesis. Thus, tunning the morphologies of as-derived materials for the environmental remediation is inspiring.

- The photocatalytic experiments were carried out under solar-simulation lights. In consideration of cost, modifying the as-derived catalysts to improve the photocatalytic effect under visible light should be encouraged.
- The wastewater treatment *via* adsorption by MOFs-derived materials is insufficiently studied. In addition, the adsorption capacity and kinetics of the adsorbents are still needed to be improved.
- The mechanisms of oxidant activation like H_2O_2, PMS, persulfate and ozone by carbon materials as well as the metallic catalysts are still needed to be deeply investigated. The active sites and the reaction between the catalysts and oxidants should be clarified by means of experimental and simulation methods.
- The environmentally friendly carbonaceous catalysts for wastewater remediation are promising and widely studied. However, most of the work are accomplished in the lab scale and not suitable for the industrial applications. As the practical environment is complicated, exploring products for use outside the lab is an important issue to be addressed.

Appendix

The copyright licenses for some references in Chapter 2 (literature review) are attached below:

1. Ref. 55 (Figure 2.1)
2. Ref. 66 (Figure 2.3a)
3. Ref. 73 (Figure 2.3b)
4. Ref. 76 (Figure 2.3c)
5. Ref. 77 (Figure 2.4a, b)
6. Ref. 78 (Figure 2.4c, d)
7. Ref. 92 (Figure 2.5)
8. Ref. 97 (Figure 2.6)
9. Ref. 104 (Figure 2.7a)
10. Ref. 105 (Figure 2.7b, c, e)
11. Ref. 113 (Figure 2.8a-d)
12. Ref. 115 (Figure 2.8e-i)
13. Ref. 119 (Figure 2.9)
14. Ref. 122 (Figure 2.10a-e)
15. Ref. 127 (Figure 2.10f, g)
16. Ref. 128 (Figure 2.11a)
17. Ref. 129 (Figure 2.11b)
18. Ref. 131 (Figure 2.11c)
19. Ref. 135 (Figure 2.12)
20. Ref. 126 (Figure 2.13)
21. Ref. 83 (Figure 2.15)
22. Ref. 100 (Figure 2.16)
23. Ref. 43 (Figure 2.17)
24. Ref. 82 (Figure 2.18)
25. Ref. 197 (Figure 2.20)
26. Ref. 201 (Figure 2.22)
27. Ref. 215 (Figure 2.23a)
28. Ref. 216 (Figure 2.23b)

Title: Formation of Fe2O3 Microboxes with Hierarchical Shell Structures from Metal–Organic Frameworks and Their Lithium Storage Properties

Author: Lei Zhang, Hao Bin Wu, Srinivasan Madhavi, et al

Publication: Journal of the American Chemical Society

Publisher: American Chemical Society

Date: Oct 1, 2012

PERMISSION/LICENSE IS GRANTED FOR YOUR ORDER AT NO CHARGE

This type of permission/license, instead of the standard Terms & Conditions, is sent to you because no fee is being charged for your order. Please note the following:

- Permission is granted for your request in both print and electronic formats, and translations.
- If figures and/or tables were requested, they may be adapted or used in part.
- Please print this page for your records and send a copy of it to your publisher/graduate school.
- Appropriate credit for the requested material should be given as follows: "Reprinted (adapted) with permission from (COMPLETE REFERENCE CITATION). Copyright (YEAR) American Chemical Society." Insert appropriate information in place of the capitalized words.
- One-time permission is granted only for the use specified in your request. No additional uses are granted (such as derivative works or other editions). For any other uses, please submit a new request.

If credit is given to another source for the material you requested, permission must be obtained from that source.

BACK CLOSE WINDOW

Title: Porous Spinel ZnxCo3–xO4 Hollow Polyhedra Templated for High-Rate Lithium-Ion Batteries

Author: Renbing Wu, Xukun Qian, Kun Zhou, et al

Publication: ACS Nano

Publisher: American Chemical Society

Date: Jun 1, 2014

PERMISSION/LICENSE IS GRANTED FOR YOUR ORDER AT NO CHARGE

This type of permission/license, instead of the standard Terms & Conditions, is sent to you because no fee is being charged for your order. Please note the following:

- Permission is granted for your request in both print and electronic formats, and translations.
- If figures and/or tables were requested, they may be adapted or used in part.
- Please print this page for your records and send a copy of it to your publisher/graduate school.
- Appropriate credit for the requested material should be given as follows: "Reprinted (adapted) with permission from (COMPLETE REFERENCE CITATION). Copyright (YEAR) American Chemical Society." Insert appropriate information in place of the capitalized words.
- One-time permission is granted only for the use specified in your request. No additional uses are granted (such as derivative works or other editions). For any other uses, please submit a new request.

If credit is given to another source for the material you requested, permission must be obtained from that source.

JOHN WILEY AND SONS LICENSE TERMS AND CONDITIONS

May 23, 2017

This Agreement between Ms. Ping Liang ("You") and John Wiley and Sons ("John Wiley and Sons") consists of your license details and the terms and conditions provided by John Wiley and Sons and Copyright Clearance Center.

License Number	4114631043084
License date	May 23, 2017
Licensed Content Publisher	John Wiley and Sons
Licensed Content Publication	Advanced Materials
Licensed Content Title	Formation of Prussian-Blue-Analog Nanocages via a Direct Etching Method and their Conversion into Ni–Co-Mixed Oxide for Enhanced Oxygen Evolution
Licensed Content Author	Lei Han,Xin-Yao Yu,Xiong Wen (David) Lou
Licensed Content Date	Mar 23, 2016
Licensed Content Pages	5
Type of use	Dissertation/Thesis
Requestor type	University/Academic
Format	Print and electronic
Portion	Figure/table
Number of figures/tables	1
Original Wiley figure/table number(s)	1
Will you be translating?	No
Title of your thesis / dissertation	Synthesis and Evaluation of Nanostructured Membrane Catalytic Systems for Water Treatment
Expected completion date	Jun 2017
Expected size (number of pages)	200
Requestor Location	Ms. Ping Liang 4-31 nottingham street, east vic park perth, WA 6101 Australia Attn: Ms. Ping Liang
Publisher Tax ID	EU826007151
Billing Type	Invoice
Billing Address	Ms. Ping Liang 4-31 nottingham street, east vic park

perth, Australia 6101
Attn: Ms. Ping Liang

Total 0.00 AUD

Terms and Conditions

TERMS AND CONDITIONS

This copyrighted material is owned by or exclusively licensed to John Wiley & Sons, Inc. or one of its group companies (each a"Wiley Company") or handled on behalf of a society with which a Wiley Company has exclusive publishing rights in relation to a particular work (collectively "WILEY"). By clicking "accept" in connection with completing this licensing transaction, you agree that the following terms and conditions apply to this transaction (along with the billing and payment terms and conditions established by the Copyright Clearance Center Inc., ("CCC's Billing and Payment terms and conditions"), at the time that you opened your RightsLink account (these are available at any time at http://myaccount.copyright.com).

Terms and Conditions

- The materials you have requested permission to reproduce or reuse (the "Wiley Materials") are protected by copyright.

- You are hereby granted a personal, non-exclusive, non-sub licensable (on a stand-alone basis), non-transferable, worldwide, limited license to reproduce the Wiley Materials for the purpose specified in the licensing process. This license, **and any CONTENT (PDF or image file) purchased as part of your order,** is for a one-time use only and limited to any maximum distribution number specified in the license. The first instance of republication or reuse granted by this license must be completed within two years of the date of the grant of this license (although copies prepared before the end date may be distributed thereafter). The Wiley Materials shall not be used in any other manner or for any other purpose, beyond what is granted in the license. Permission is granted subject to an appropriate acknowledgement given to the author, title of the material/book/journal and the publisher. You shall also duplicate the copyright notice that appears in the Wiley publication in your use of the Wiley Material. Permission is also granted on the understanding that nowhere in the text is a previously published source acknowledged for all or part of this Wiley Material. Any third party content is expressly excluded from this permission.

- With respect to the Wiley Materials, all rights are reserved. Except as expressly granted by the terms of the license, no part of the Wiley Materials may be copied, modified, adapted (except for minor reformatting required by the new Publication), translated, reproduced, transferred or distributed, in any form or by any means, and no derivative works may be made based on the Wiley Materials without the prior permission of the respective copyright owner.**For STM Signatory Publishers clearing permission under the terms of the STM Permissions Guidelines only, the terms of the license are extended to include subsequent editions and for editions in other languages, provided such editions are for the work as a whole in situ and does not involve the separate exploitation of the permitted figures or extracts,** You may not alter, remove or suppress in any manner any copyright, trademark or other notices displayed by the Wiley Materials. You may not license, rent, sell, loan, lease, pledge, offer as security, transfer or assign the Wiley Materials on a stand-alone basis, or any of the rights granted to you hereunder to any other person.

- The Wiley Materials and all of the intellectual property rights therein shall at all times remain the exclusive property of John Wiley & Sons Inc, the Wiley Companies, or their respective licensors, and your interest therein is only that of having possession of and the right to reproduce the Wiley Materials pursuant to Section 2 herein during the continuance of this Agreement. You agree that you own no right, title or interest in or to the Wiley Materials or any of the intellectual property rights therein. You shall have no rights hereunder other than the license as provided for above in Section 2. No right, license or interest to any trademark, trade name, service mark or other branding ("Marks") of WILEY or its licensors is granted hereunder, and you agree that you shall not assert any such right, license or interest with respect thereto

- NEITHER WILEY NOR ITS LICENSORS MAKES ANY WARRANTY OR REPRESENTATION OF ANY KIND TO YOU OR ANY THIRD PARTY, EXPRESS, IMPLIED OR STATUTORY, WITH RESPECT TO THE MATERIALS OR THE ACCURACY OF ANY INFORMATION CONTAINED IN THE MATERIALS, INCLUDING, WITHOUT LIMITATION, ANY IMPLIED WARRANTY OF MERCHANTABILITY, ACCURACY, SATISFACTORY QUALITY, FITNESS FOR A PARTICULAR PURPOSE, USABILITY, INTEGRATION OR NON-INFRINGEMENT AND ALL SUCH WARRANTIES ARE HEREBY EXCLUDED BY WILEY AND ITS LICENSORS AND WAIVED BY YOU.

- WILEY shall have the right to terminate this Agreement immediately upon breach of this Agreement by you.

- You shall indemnify, defend and hold harmless WILEY, its Licensors and their respective directors, officers, agents and employees, from and against any actual or threatened claims, demands, causes of action or proceedings arising from any breach of this Agreement by you.

- IN NO EVENT SHALL WILEY OR ITS LICENSORS BE LIABLE TO YOU OR ANY OTHER PARTY OR ANY OTHER PERSON OR ENTITY FOR ANY SPECIAL, CONSEQUENTIAL, INCIDENTAL, INDIRECT, EXEMPLARY OR PUNITIVE DAMAGES, HOWEVER CAUSED, ARISING OUT OF OR IN CONNECTION WITH THE DOWNLOADING, PROVISIONING, VIEWING OR USE OF THE MATERIALS REGARDLESS OF THE FORM OF ACTION, WHETHER FOR BREACH OF CONTRACT, BREACH OF WARRANTY, TORT, NEGLIGENCE, INFRINGEMENT OR OTHERWISE (INCLUDING, WITHOUT LIMITATION, DAMAGES BASED ON LOSS OF PROFITS, DATA, FILES, USE, BUSINESS OPPORTUNITY OR CLAIMS OF THIRD PARTIES), AND WHETHER OR NOT THE PARTY HAS BEEN ADVISED OF THE POSSIBILITY OF SUCH DAMAGES. THIS LIMITATION SHALL APPLY NOTWITHSTANDING ANY FAILURE OF ESSENTIAL PURPOSE OF ANY LIMITED REMEDY PROVIDED HEREIN.

- Should any provision of this Agreement be held by a court of competent jurisdiction to be illegal, invalid, or unenforceable, that provision shall be deemed amended to achieve as nearly as possible the same economic effect as the original provision, and the legality, validity and enforceability of the remaining provisions of this Agreement

shall not be affected or impaired thereby.

- The failure of either party to enforce any term or condition of this Agreement shall not constitute a waiver of either party's right to enforce each and every term and condition of this Agreement. No breach under this agreement shall be deemed waived or excused by either party unless such waiver or consent is in writing signed by the party granting such waiver or consent. The waiver by or consent of a party to a breach of any provision of this Agreement shall not operate or be construed as a waiver of or consent to any other or subsequent breach by such other party.

- This Agreement may not be assigned (including by operation of law or otherwise) by you without WILEY's prior written consent.

- Any fee required for this permission shall be non-refundable after thirty (30) days from receipt by the CCC.

- These terms and conditions together with CCC's Billing and Payment terms and conditions (which are incorporated herein) form the entire agreement between you and WILEY concerning this licensing transaction and (in the absence of fraud) supersedes all prior agreements and representations of the parties, oral or written. This Agreement may not be amended except in writing signed by both parties. This Agreement shall be binding upon and inure to the benefit of the parties' successors, legal representatives, and authorized assigns.

- In the event of any conflict between your obligations established by these terms and conditions and those established by CCC's Billing and Payment terms and conditions, these terms and conditions shall prevail.

- WILEY expressly reserves all rights not specifically granted in the combination of (i) the license details provided by you and accepted in the course of this licensing transaction, (ii) these terms and conditions and (iii) CCC's Billing and Payment terms and conditions.

- This Agreement will be void if the Type of Use, Format, Circulation, or Requestor Type was misrepresented during the licensing process.

- This Agreement shall be governed by and construed in accordance with the laws of the State of New York, USA, without regards to such state's conflict of law rules. Any legal action, suit or proceeding arising out of or relating to these Terms and Conditions or the breach thereof shall be instituted in a court of competent jurisdiction in New York County in the State of New York in the United States of America and each party hereby consents and submits to the personal jurisdiction of such court, waives any objection to venue in such court and consents to service of process by registered or certified mail, return receipt requested, at the last known address of such party.

WILEY OPEN ACCESS TERMS AND CONDITIONS

Wiley Publishes Open Access Articles in fully Open Access Journals and in Subscription journals offering Online Open. Although most of the fully Open Access journals publish open access articles under the terms of the Creative Commons Attribution (CC BY) License only, the subscription journals and a few of the Open Access Journals offer a choice of

Creative Commons Licenses. The license type is clearly identified on the article.

The Creative Commons Attribution License

The Creative Commons Attribution License (CC-BY) allows users to copy, distribute and transmit an article, adapt the article and make commercial use of the article. The CC-BY license permits commercial and non-

Creative Commons Attribution Non-Commercial License

The Creative Commons Attribution Non-Commercial (CC-BY-NC)License permits use, distribution and reproduction in any medium, provided the original work is properly cited and is not used for commercial purposes.(see below)

Creative Commons Attribution-Non-Commercial-NoDerivs License

The Creative Commons Attribution Non-Commercial-NoDerivs License (CC-BY-NC-ND) permits use, distribution and reproduction in any medium, provided the original work is properly cited, is not used for commercial purposes and no modifications or adaptations are made. (see below)

Use by commercial "for-profit" organizations

Use of Wiley Open Access articles for commercial, promotional, or marketing purposes requires further explicit permission from Wiley and will be subject to a fee.

Further details can be found on Wiley Online Library

http://olabout.wiley.com/WileyCDA/Section/id-410895.html

Other Terms and Conditions:

v1.10 Last updated September 2015

Questions? customercare@copyright.com or +1-855-239-3415 (toll free in the US) or +1-978-646-2777.

Title: Multilayer CuO@NiO Hollow Spheres: Microwave-Assisted Metal–Organic-Framework Derivation and Highly Reversible Structure-Matched Stepwise Lithium Storage

Author: Wenxiang Guo, Weiwei Sun, Yong Wang

Publication: ACS Nano

Publisher: American Chemical Society

Date: Nov 1, 2015

PERMISSION/LICENSE IS GRANTED FOR YOUR ORDER AT NO CHARGE

This type of permission/license, instead of the standard Terms & Conditions, is sent to you because no fee is being charged for your order. Please note the following:

- Permission is granted for your request in both print and electronic formats, and translations.
- If figures and/or tables were requested, they may be adapted or used in part.
- Please print this page for your records and send a copy of it to your publisher/graduate school.
- Appropriate credit for the requested material should be given as follows: "Reprinted (adapted) with permission from (COMPLETE REFERENCE CITATION). Copyright (YEAR) American Chemical Society." Insert appropriate information in place of the capitalized words.
- One-time permission is granted only for the use specified in your request. No additional uses are granted (such as derivative works or other editions). For any other uses, please submit a new request.

If credit is given to another source for the material you requested, permission must be obtained from that source.

Title: Starfish-shaped $Co_3O_4/ZnFe_2O_4$ Hollow Nanocomposite: Synthesis, Supercapacity, and Magnetic Properties

Author: Xiao-Wei Hu, Sheng Liu, Bo-Tao Qu, et al

Publication: Applied Materials

Publisher: American Chemical Society

Date: May 1, 2015

PERMISSION/LICENSE IS GRANTED FOR YOUR ORDER AT NO CHARGE

This type of permission/license, instead of the standard Terms & Conditions, is sent to you because no fee is being charged for your order. Please note the following:

- Permission is granted for your request in both print and electronic formats, and translations.
- If figures and/or tables were requested, they may be adapted or used in part.
- Please print this page for your records and send a copy of it to your publisher/graduate school.
- Appropriate credit for the requested material should be given as follows: "Reprinted (adapted) with permission from (COMPLETE REFERENCE CITATION). Copyright (YEAR) American Chemical Society." Insert appropriate information in place of the capitalized words.
- One-time permission is granted only for the use specified in your request. No additional uses are granted (such as derivative works or other editions). For any other uses, please submit a new request.

If credit is given to another source for the material you requested, permission must be obtained from that source.

BACK CLOSE WINDOW

Title: Designed Formation of Co3O4/NiCo2O4 Double-Shelled Nanocages with Enhanced Pseudocapacitive and Electrocatalytic Properties

Author: Han Hu, Buyuan Guan, Baoyu Xia, et al

Publication: Journal of the American Chemical Society

Publisher: American Chemical Society

Date: Apr 1, 2015

PERMISSION/LICENSE IS GRANTED FOR YOUR ORDER AT NO CHARGE

This type of permission/license, instead of the standard Terms & Conditions, is sent to you because no fee is being charged for your order. Please note the following:

- Permission is granted for your request in both print and electronic formats, and translations.
- If figures and/or tables were requested, they may be adapted or used in part.
- Please print this page for your records and send a copy of it to your publisher/graduate school.
- Appropriate credit for the requested material should be given as follows: "Reprinted (adapted) with permission from (COMPLETE REFERENCE CITATION). Copyright (YEAR) American Chemical Society." Insert appropriate information in place of the capitalized words.
- One-time permission is granted only for the use specified in your request. No additional uses are granted (such as derivative works or other editions). For any other uses, please submit a new request.

If credit is given to another source for the material you requested, permission must be obtained from that source.

JOHN WILEY AND SONS LICENSE TERMS AND CONDITIONS

May 23, 2017

This Agreement between Ms. Ping Liang ("You") and John Wiley and Sons ("John Wiley and Sons") consists of your license details and the terms and conditions provided by John Wiley and Sons and Copyright Clearance Center.

License Number	4114781446911
License date	May 23, 2017
Licensed Content Publisher	John Wiley and Sons
Licensed Content Publication	Advanced Functional Materials
Licensed Content Title	In Situ Confinement Pyrolysis Transformation of ZIF-8 to Nitrogen-Enriched Meso-Microporous Carbon Frameworks for Oxygen Reduction
Licensed Content Author	Qingxue Lai,Yingxuan Zhao,Yanyu Liang,Jianping He,Junhong Chen
Licensed Content Date	Oct 6, 2016
Licensed Content Pages	11
Type of use	Dissertation/Thesis
Requestor type	University/Academic
Format	Print and electronic
Portion	Figure/table
Number of figures/tables	2
Original Wiley figure/table number(s)	Figure 3
Will you be translating?	No
Title of your thesis / dissertation	Synthesis and Evaluation of Nanostructured Membrane Catalytic Systems for Water Treatment
Expected completion date	Jun 2017
Expected size (number of pages)	200
Requestor Location	Ms. Ping Liang 4-31 nottingham street, east vic park perth, WA 6101 Australia Attn: Ms. Ping Liang
Publisher Tax ID	EU826007151
Billing Type	Invoice
Billing Address	Ms. Ping Liang 4-31 nottingham street, east vic park

perth, Australia 6101
Attn: Ms. Ping Liang

Total 0.00 AUD

Terms and Conditions

TERMS AND CONDITIONS

This copyrighted material is owned by or exclusively licensed to John Wiley & Sons, Inc. or one of its group companies (each a"Wiley Company") or handled on behalf of a society with which a Wiley Company has exclusive publishing rights in relation to a particular work (collectively "WILEY"). By clicking "accept" in connection with completing this licensing transaction, you agree that the following terms and conditions apply to this transaction (along with the billing and payment terms and conditions established by the Copyright Clearance Center Inc., ("CCC's Billing and Payment terms and conditions"), at the time that you opened your RightsLink account (these are available at any time at http://myaccount.copyright.com).

Terms and Conditions

- The materials you have requested permission to reproduce or reuse (the "Wiley Materials") are protected by copyright.

- You are hereby granted a personal, non-exclusive, non-sub licensable (on a stand-alone basis), non-transferable, worldwide, limited license to reproduce the Wiley Materials for the purpose specified in the licensing process. This license, **and any CONTENT (PDF or image file) purchased as part of your order,** is for a one-time use only and limited to any maximum distribution number specified in the license. The first instance of republication or reuse granted by this license must be completed within two years of the date of the grant of this license (although copies prepared before the end date may be distributed thereafter). The Wiley Materials shall not be used in any other manner or for any other purpose, beyond what is granted in the license. Permission is granted subject to an appropriate acknowledgement given to the author, title of the material/book/journal and the publisher. You shall also duplicate the copyright notice that appears in the Wiley publication in your use of the Wiley Material. Permission is also granted on the understanding that nowhere in the text is a previously published source acknowledged for all or part of this Wiley Material. Any third party content is expressly excluded from this permission.

- With respect to the Wiley Materials, all rights are reserved. Except as expressly granted by the terms of the license, no part of the Wiley Materials may be copied, modified, adapted (except for minor reformatting required by the new Publication), translated, reproduced, transferred or distributed, in any form or by any means, and no derivative works may be made based on the Wiley Materials without the prior permission of the respective copyright owner.**For STM Signatory Publishers clearing permission under the terms of the STM Permissions Guidelines only, the terms of the license are extended to include subsequent editions and for editions in other languages, provided such editions are for the work as a whole in situ and does not involve the separate exploitation of the permitted figures or extracts,** You may not alter, remove or suppress in any manner any copyright, trademark or other notices displayed by the Wiley Materials. You may not license, rent, sell, loan, lease, pledge, offer as security, transfer or assign the Wiley Materials on a stand-alone basis, or any of the rights granted to you hereunder to any other person.

- The Wiley Materials and all of the intellectual property rights therein shall at all times remain the exclusive property of John Wiley & Sons Inc, the Wiley Companies, or their respective licensors, and your interest therein is only that of having possession of and the right to reproduce the Wiley Materials pursuant to Section 2 herein during the continuance of this Agreement. You agree that you own no right, title or interest in or to the Wiley Materials or any of the intellectual property rights therein. You shall have no rights hereunder other than the license as provided for above in Section 2. No right, license or interest to any trademark, trade name, service mark or other branding ("Marks") of WILEY or its licensors is granted hereunder, and you agree that you shall not assert any such right, license or interest with respect thereto

- NEITHER WILEY NOR ITS LICENSORS MAKES ANY WARRANTY OR REPRESENTATION OF ANY KIND TO YOU OR ANY THIRD PARTY, EXPRESS, IMPLIED OR STATUTORY, WITH RESPECT TO THE MATERIALS OR THE ACCURACY OF ANY INFORMATION CONTAINED IN THE MATERIALS, INCLUDING, WITHOUT LIMITATION, ANY IMPLIED WARRANTY OF MERCHANTABILITY, ACCURACY, SATISFACTORY QUALITY, FITNESS FOR A PARTICULAR PURPOSE, USABILITY, INTEGRATION OR NON-INFRINGEMENT AND ALL SUCH WARRANTIES ARE HEREBY EXCLUDED BY WILEY AND ITS LICENSORS AND WAIVED BY YOU.

- WILEY shall have the right to terminate this Agreement immediately upon breach of this Agreement by you.

- You shall indemnify, defend and hold harmless WILEY, its Licensors and their respective directors, officers, agents and employees, from and against any actual or threatened claims, demands, causes of action or proceedings arising from any breach of this Agreement by you.

- IN NO EVENT SHALL WILEY OR ITS LICENSORS BE LIABLE TO YOU OR ANY OTHER PARTY OR ANY OTHER PERSON OR ENTITY FOR ANY SPECIAL, CONSEQUENTIAL, INCIDENTAL, INDIRECT, EXEMPLARY OR PUNITIVE DAMAGES, HOWEVER CAUSED, ARISING OUT OF OR IN CONNECTION WITH THE DOWNLOADING, PROVISIONING, VIEWING OR USE OF THE MATERIALS REGARDLESS OF THE FORM OF ACTION, WHETHER FOR BREACH OF CONTRACT, BREACH OF WARRANTY, TORT, NEGLIGENCE, INFRINGEMENT OR OTHERWISE (INCLUDING, WITHOUT LIMITATION, DAMAGES BASED ON LOSS OF PROFITS, DATA, FILES, USE, BUSINESS OPPORTUNITY OR CLAIMS OF THIRD PARTIES), AND WHETHER OR NOT THE PARTY HAS BEEN ADVISED OF THE POSSIBILITY OF SUCH DAMAGES. THIS LIMITATION SHALL APPLY NOTWITHSTANDING ANY FAILURE OF ESSENTIAL PURPOSE OF ANY LIMITED REMEDY PROVIDED HEREIN.

- Should any provision of this Agreement be held by a court of competent jurisdiction to be illegal, invalid, or unenforceable, that provision shall be deemed amended to achieve as nearly as possible the same economic effect as the original provision, and the legality, validity and enforceability of the remaining provisions of this Agreement

shall not be affected or impaired thereby.

- The failure of either party to enforce any term or condition of this Agreement shall not constitute a waiver of either party's right to enforce each and every term and condition of this Agreement. No breach under this agreement shall be deemed waived or excused by either party unless such waiver or consent is in writing signed by the party granting such waiver or consent. The waiver by or consent of a party to a breach of any provision of this Agreement shall not operate or be construed as a waiver of or consent to any other or subsequent breach by such other party.

- This Agreement may not be assigned (including by operation of law or otherwise) by you without WILEY's prior written consent.

- Any fee required for this permission shall be non-refundable after thirty (30) days from receipt by the CCC.

- These terms and conditions together with CCC's Billing and Payment terms and conditions (which are incorporated herein) form the entire agreement between you and WILEY concerning this licensing transaction and (in the absence of fraud) supersedes all prior agreements and representations of the parties, oral or written. This Agreement may not be amended except in writing signed by both parties. This Agreement shall be binding upon and inure to the benefit of the parties' successors, legal representatives, and authorized assigns.

- In the event of any conflict between your obligations established by these terms and conditions and those established by CCC's Billing and Payment terms and conditions, these terms and conditions shall prevail.

- WILEY expressly reserves all rights not specifically granted in the combination of (i) the license details provided by you and accepted in the course of this licensing transaction, (ii) these terms and conditions and (iii) CCC's Billing and Payment terms and conditions.

- This Agreement will be void if the Type of Use, Format, Circulation, or Requestor Type was misrepresented during the licensing process.

- This Agreement shall be governed by and construed in accordance with the laws of the State of New York, USA, without regards to such state's conflict of law rules. Any legal action, suit or proceeding arising out of or relating to these Terms and Conditions or the breach thereof shall be instituted in a court of competent jurisdiction in New York County in the State of New York in the United States of America and each party hereby consents and submits to the personal jurisdiction of such court, waives any objection to venue in such court and consents to service of process by registered or certified mail, return receipt requested, at the last known address of such party.

WILEY OPEN ACCESS TERMS AND CONDITIONS

Wiley Publishes Open Access Articles in fully Open Access Journals and in Subscription journals offering Online Open. Although most of the fully Open Access journals publish open access articles under the terms of the Creative Commons Attribution (CC BY) License only, the subscription journals and a few of the Open Access Journals offer a choice of

Creative Commons Licenses. The license type is clearly identified on the article.

The Creative Commons Attribution License

The Creative Commons Attribution License (CC-BY) allows users to copy, distribute and transmit an article, adapt the article and make commercial use of the article. The CC-BY license permits commercial and non-

Creative Commons Attribution Non-Commercial License

The Creative Commons Attribution Non-Commercial (CC-BY-NC)License permits use, distribution and reproduction in any medium, provided the original work is properly cited and is not used for commercial purposes.(see below)

Creative Commons Attribution-Non-Commercial-NoDerivs License

The Creative Commons Attribution Non-Commercial-NoDerivs License (CC-BY-NC-ND) permits use, distribution and reproduction in any medium, provided the original work is properly cited, is not used for commercial purposes and no modifications or adaptations are made. (see below)

Use by commercial "for-profit" organizations

Use of Wiley Open Access articles for commercial, promotional, or marketing purposes requires further explicit permission from Wiley and will be subject to a fee.

Further details can be found on Wiley Online Library

http://olabout.wiley.com/WileyCDA/Section/id-410895.html

Other Terms and Conditions:

v1.10 Last updated September 2015

Questions? customercare@copyright.com or +1-855-239-3415 (toll free in the US) or +1-978-646-2777.

RightsLink®

Home | Account Info | Help

Title: Thermal Conversion of Core–Shell Metal–Organic Frameworks: A New Method for Selectively Functionalized Nanoporous Hybrid Carbon

Author: Jing Tang, Rahul R. Salunkhe, Jian Liu, et al

Publication: Journal of the American Chemical Society

Publisher: American Chemical Society

Date: Feb 1, 2015

Logged in as:
Ping Liang
Account #:
3001154658

LOGOUT

PERMISSION/LICENSE IS GRANTED FOR YOUR ORDER AT NO CHARGE

This type of permission/license, instead of the standard Terms & Conditions, is sent to you because no fee is being charged for your order. Please note the following:

- Permission is granted for your request in both print and electronic formats, and translations.
- If figures and/or tables were requested, they may be adapted or used in part.
- Please print this page for your records and send a copy of it to your publisher/graduate school.
- Appropriate credit for the requested material should be given as follows: "Reprinted (adapted) with permission from (COMPLETE REFERENCE CITATION). Copyright (YEAR) American Chemical Society." Insert appropriate information in place of the capitalized words.
- One-time permission is granted only for the use specified in your request. No additional uses are granted (such as derivative works or other editions). For any other uses, please submit a new request.

If credit is given to another source for the material you requested, permission must be obtained from that source.

BACK CLOSE WINDOW

Title: Nanowire-Directed Templating Synthesis of Metal–Organic Framework Nanofibers and Their Derived Porous Doped Carbon Nanofibers for Enhanced Electrocatalysis

Author: Wang Zhang, Zhen-Yu Wu, Hai-Long Jiang, et al

Publication: Journal of the American Chemical Society

Publisher: American Chemical Society

Date: Oct 1, 2014

PERMISSION/LICENSE IS GRANTED FOR YOUR ORDER AT NO CHARGE

This type of permission/license, instead of the standard Terms & Conditions, is sent to you because no fee is being charged for your order. Please note the following:

- Permission is granted for your request in both print and electronic formats, and translations.
- If figures and/or tables were requested, they may be adapted or used in part.
- Please print this page for your records and send a copy of it to your publisher/graduate school.
- Appropriate credit for the requested material should be given as follows: "Reprinted (adapted) with permission from (COMPLETE REFERENCE CITATION). Copyright (YEAR) American Chemical Society." Insert appropriate information in place of the capitalized words.
- One-time permission is granted only for the use specified in your request. No additional uses are granted (such as derivative works or other editions). For any other uses, please submit a new request.

If credit is given to another source for the material you requested, permission must be obtained from that source.

BACK CLOSE WINDOW

NATURE PUBLISHING GROUP LICENSE TERMS AND CONDITIONS

May 23, 2017

This Agreement between Ms. Ping Liang ("You") and Nature Publishing Group ("Nature Publishing Group") consists of your license details and the terms and conditions provided by Nature Publishing Group and Copyright Clearance Center.

License Number	4115040015092
License date	May 23, 2017
Licensed Content Publisher	Nature Publishing Group
Licensed Content Publication	Nature Chemistry
Licensed Content Title	Fabrication of carbon nanorods and graphene nanoribbons from a metal–organic framework
Licensed Content Author	Pradip Pachfule, Dhanraj Shinde, Mainak Majumder, Qiang Xu
Licensed Content Date	May 9, 2016
Licensed Content Volume	8
Licensed Content Issue	7
Type of Use	reuse in a dissertation / thesis
Requestor type	academic/educational
Format	print and electronic
Portion	figures/tables/illustrations
Number of figures/tables/illustrations	3
High-res required	no
Figures	Figure 1, Figure 2
Author of this NPG article	no
Your reference number	
Title of your thesis / dissertation	Synthesis and Evaluation of Nanostructured Membrane Catalytic Systems for Water Treatment
Expected completion date	Jun 2017
Estimated size (number of pages)	200
Requestor Location	Ms. Ping Liang 4-31 nottingham street, east vic park perth, WA 6101 Australia Attn: Ms. Ping Liang
Billing Type	Invoice
Billing Address	Ms. Ping Liang 4-31 nottingham street, east vic park

perth, Australia 6101
Attn: Ms. Ping Liang

Total 0.00 AUD

Terms and Conditions

Terms and Conditions for Permissions

Nature Publishing Group hereby grants you a non-exclusive license to reproduce this material for this purpose, and for no other use,subject to the conditions below:

1. NPG warrants that it has, to the best of its knowledge, the rights to license reuse of this material. However, you should ensure that the material you are requesting is original to Nature Publishing Group and does not carry the copyright of another entity (as credited in the published version). If the credit line on any part of the material you have requested indicates that it was reprinted or adapted by NPG with permission from another source, then you should also seek permission from that source to reuse the material.

2. Permission granted free of charge for material in print is also usually granted for any electronic version of that work, provided that the material is incidental to the work as a whole and that the electronic version is essentially equivalent to, or substitutes for, the print version.Where print permission has been granted for a fee, separate permission must be obtained for any additional, electronic re-use (unless, as in the case of a full paper, this has already been accounted for during your initial request in the calculation of a print run).NB: In all cases, web-based use of full-text articles must be authorized separately through the 'Use on a Web Site' option when requesting permission.

3. Permission granted for a first edition does not apply to second and subsequent editions and for editions in other languages (except for signatories to the STM Permissions Guidelines, or where the first edition permission was granted for free).

4. Nature Publishing Group's permission must be acknowledged next to the figure, table or abstract in print. In electronic form, this acknowledgement must be visible at the same time as the figure/table/abstract, and must be hyperlinked to the journal's homepage.

5. The credit line should read:
   Reprinted by permission from Macmillan Publishers Ltd: [JOURNAL NAME] (reference citation), copyright (year of publication)
   For AOP papers, the credit line should read:
   Reprinted by permission from Macmillan Publishers Ltd: [JOURNAL NAME], advance online publication, day month year (doi: 10.1038/sj.[JOURNAL ACRONYM].XXXXX)

   Note: For republication from the *British Journal of Cancer,* the following credit lines apply.
   Reprinted by permission from Macmillan Publishers Ltd on behalf of Cancer Research UK: [JOURNAL NAME] (reference citation), copyright (year of publication)For AOP papers, the credit line should read:
   Reprinted by permission from Macmillan Publishers Ltd on behalf of Cancer Research UK: [JOURNAL NAME], advance online publication, day month year (doi: 10.1038/sj.[JOURNAL ACRONYM].XXXXX)

6. Adaptations of single figures do not require NPG approval. However, the adaptation should be credited as follows:

   Adapted by permission from Macmillan Publishers Ltd: [JOURNAL NAME] (reference citation), copyright (year of publication)

Note: For adaptation from the *British Journal of Cancer,* the following credit line applies.
Adapted by permission from Macmillan Publishers Ltd on behalf of Cancer Research UK: [JOURNAL NAME] (reference citation), copyright (year of publication)

7. Translations of 401 words up to a whole article require NPG approval. Please visit http://www.macmillanmedicalcommunications.com for more information.Translations of up to a 400 words do not require NPG approval. The translation should be credited as follows:

   Translated by permission from Macmillan Publishers Ltd: [JOURNAL NAME] (reference citation), copyright (year of publication).

   Note: For translation from the *British Journal of Cancer,* the following credit line applies.
   Translated by permission from Macmillan Publishers Ltd on behalf of Cancer Research UK: [JOURNAL NAME] (reference citation), copyright (year of publication)

We are certain that all parties will benefit from this agreement and wish you the best in the use of this material. Thank you.
Special Terms:
v1.1

Questions? customercare@copyright.com or +1-855-239-3415 (toll free in the US) or +1-978-646-2777.

JOHN WILEY AND SONS LICENSE TERMS AND CONDITIONS

May 23, 2017

This Agreement between Ms. Ping Liang ("You") and John Wiley and Sons ("John Wiley and Sons") consists of your license details and the terms and conditions provided by John Wiley and Sons and Copyright Clearance Center.

License Number	4115071508436
License date	May 23, 2017
Licensed Content Publisher	John Wiley and Sons
Licensed Content Publication	Advanced Materials
Licensed Content Title	Well-Dispersed ZIF-Derived Co,N-Co-doped Carbon Nanoframes through Mesoporous-Silica-Protected Calcination as Efficient Oxygen Reduction Electrocatalysts
Licensed Content Author	Lu Shang,Huijun Yu,Xing Huang,Tong Bian,Run Shi,Yufei Zhao,Geoffrey I. N. Waterhouse,Li-Zhu Wu,Chen-Ho Tung,Tierui Zhang
Licensed Content Date	Dec 16, 2015
Licensed Content Pages	7
Type of use	Dissertation/Thesis
Requestor type	University/Academic
Format	Print and electronic
Portion	Figure/table
Number of figures/tables	1
Original Wiley figure/table number(s)	Figure 1
Will you be translating?	No
Title of your thesis / dissertation	Synthesis and Evaluation of Nanostructured Membrane Catalytic Systems for Water Treatment
Expected completion date	Jun 2017
Expected size (number of pages)	200
Requestor Location	Ms. Ping Liang 4-31 nottingham street, east vic park perth, WA 6101 Australia Attn: Ms. Ping Liang
Publisher Tax ID	EU826007151
Billing Type	Invoice
Billing Address	Ms. Ping Liang 4-31 nottingham street, east vic park

perth, Australia 6101
Attn: Ms. Ping Liang

Total 0.00 AUD

Terms and Conditions

TERMS AND CONDITIONS

This copyrighted material is owned by or exclusively licensed to John Wiley & Sons, Inc. or one of its group companies (each a"Wiley Company") or handled on behalf of a society with which a Wiley Company has exclusive publishing rights in relation to a particular work (collectively "WILEY"). By clicking "accept" in connection with completing this licensing transaction, you agree that the following terms and conditions apply to this transaction (along with the billing and payment terms and conditions established by the Copyright Clearance Center Inc., ("CCC's Billing and Payment terms and conditions"), at the time that you opened your RightsLink account (these are available at any time at http://myaccount.copyright.com).

Terms and Conditions

- The materials you have requested permission to reproduce or reuse (the "Wiley Materials") are protected by copyright.

- You are hereby granted a personal, non-exclusive, non-sub licensable (on a stand-alone basis), non-transferable, worldwide, limited license to reproduce the Wiley Materials for the purpose specified in the licensing process. This license, **and any CONTENT (PDF or image file) purchased as part of your order,** is for a one-time use only and limited to any maximum distribution number specified in the license. The first instance of republication or reuse granted by this license must be completed within two years of the date of the grant of this license (although copies prepared before the end date may be distributed thereafter). The Wiley Materials shall not be used in any other manner or for any other purpose, beyond what is granted in the license. Permission is granted subject to an appropriate acknowledgement given to the author, title of the material/book/journal and the publisher. You shall also duplicate the copyright notice that appears in the Wiley publication in your use of the Wiley Material. Permission is also granted on the understanding that nowhere in the text is a previously published source acknowledged for all or part of this Wiley Material. Any third party content is expressly excluded from this permission.

- With respect to the Wiley Materials, all rights are reserved. Except as expressly granted by the terms of the license, no part of the Wiley Materials may be copied, modified, adapted (except for minor reformatting required by the new Publication), translated, reproduced, transferred or distributed, in any form or by any means, and no derivative works may be made based on the Wiley Materials without the prior permission of the respective copyright owner.**For STM Signatory Publishers clearing permission under the terms of the STM Permissions Guidelines only, the terms of the license are extended to include subsequent editions and for editions in other languages, provided such editions are for the work as a whole in situ and does not involve the separate exploitation of the permitted figures or extracts,** You may not alter, remove or suppress in any manner any copyright, trademark or other notices displayed by the Wiley Materials. You may not license, rent, sell, loan,

lease, pledge, offer as security, transfer or assign the Wiley Materials on a stand-alone basis, or any of the rights granted to you hereunder to any other person.

- The Wiley Materials and all of the intellectual property rights therein shall at all times remain the exclusive property of John Wiley & Sons Inc, the Wiley Companies, or their respective licensors, and your interest therein is only that of having possession of and the right to reproduce the Wiley Materials pursuant to Section 2 herein during the continuance of this Agreement. You agree that you own no right, title or interest in or to the Wiley Materials or any of the intellectual property rights therein. You shall have no rights hereunder other than the license as provided for above in Section 2. No right, license or interest to any trademark, trade name, service mark or other branding ("Marks") of WILEY or its licensors is granted hereunder, and you agree that you shall not assert any such right, license or interest with respect thereto

- NEITHER WILEY NOR ITS LICENSORS MAKES ANY WARRANTY OR REPRESENTATION OF ANY KIND TO YOU OR ANY THIRD PARTY, EXPRESS, IMPLIED OR STATUTORY, WITH RESPECT TO THE MATERIALS OR THE ACCURACY OF ANY INFORMATION CONTAINED IN THE MATERIALS, INCLUDING, WITHOUT LIMITATION, ANY IMPLIED WARRANTY OF MERCHANTABILITY, ACCURACY, SATISFACTORY QUALITY, FITNESS FOR A PARTICULAR PURPOSE, USABILITY, INTEGRATION OR NON-INFRINGEMENT AND ALL SUCH WARRANTIES ARE HEREBY EXCLUDED BY WILEY AND ITS LICENSORS AND WAIVED BY YOU.

- WILEY shall have the right to terminate this Agreement immediately upon breach of this Agreement by you.

- You shall indemnify, defend and hold harmless WILEY, its Licensors and their respective directors, officers, agents and employees, from and against any actual or threatened claims, demands, causes of action or proceedings arising from any breach of this Agreement by you.

- IN NO EVENT SHALL WILEY OR ITS LICENSORS BE LIABLE TO YOU OR ANY OTHER PARTY OR ANY OTHER PERSON OR ENTITY FOR ANY SPECIAL, CONSEQUENTIAL, INCIDENTAL, INDIRECT, EXEMPLARY OR PUNITIVE DAMAGES, HOWEVER CAUSED, ARISING OUT OF OR IN CONNECTION WITH THE DOWNLOADING, PROVISIONING, VIEWING OR USE OF THE MATERIALS REGARDLESS OF THE FORM OF ACTION, WHETHER FOR BREACH OF CONTRACT, BREACH OF WARRANTY, TORT, NEGLIGENCE, INFRINGEMENT OR OTHERWISE (INCLUDING, WITHOUT LIMITATION, DAMAGES BASED ON LOSS OF PROFITS, DATA, FILES, USE, BUSINESS OPPORTUNITY OR CLAIMS OF THIRD PARTIES), AND WHETHER OR NOT THE PARTY HAS BEEN ADVISED OF THE POSSIBILITY OF SUCH DAMAGES. THIS LIMITATION SHALL APPLY NOTWITHSTANDING ANY FAILURE OF ESSENTIAL PURPOSE OF ANY LIMITED REMEDY PROVIDED HEREIN.

- Should any provision of this Agreement be held by a court of competent jurisdiction to be illegal, invalid, or unenforceable, that provision shall be deemed amended to

achieve as nearly as possible the same economic effect as the original provision, and the legality, validity and enforceability of the remaining provisions of this Agreement shall not be affected or impaired thereby.

- The failure of either party to enforce any term or condition of this Agreement shall not constitute a waiver of either party's right to enforce each and every term and condition of this Agreement. No breach under this agreement shall be deemed waived or excused by either party unless such waiver or consent is in writing signed by the party granting such waiver or consent. The waiver by or consent of a party to a breach of any provision of this Agreement shall not operate or be construed as a waiver of or consent to any other or subsequent breach by such other party.

- This Agreement may not be assigned (including by operation of law or otherwise) by you without WILEY's prior written consent.

- Any fee required for this permission shall be non-refundable after thirty (30) days from receipt by the CCC.

- These terms and conditions together with CCC's Billing and Payment terms and conditions (which are incorporated herein) form the entire agreement between you and WILEY concerning this licensing transaction and (in the absence of fraud) supersedes all prior agreements and representations of the parties, oral or written. This Agreement may not be amended except in writing signed by both parties. This Agreement shall be binding upon and inure to the benefit of the parties' successors, legal representatives, and authorized assigns.

- In the event of any conflict between your obligations established by these terms and conditions and those established by CCC's Billing and Payment terms and conditions, these terms and conditions shall prevail.

- WILEY expressly reserves all rights not specifically granted in the combination of (i) the license details provided by you and accepted in the course of this licensing transaction, (ii) these terms and conditions and (iii) CCC's Billing and Payment terms and conditions.

- This Agreement will be void if the Type of Use, Format, Circulation, or Requestor Type was misrepresented during the licensing process.

- This Agreement shall be governed by and construed in accordance with the laws of the State of New York, USA, without regards to such state's conflict of law rules. Any legal action, suit or proceeding arising out of or relating to these Terms and Conditions or the breach thereof shall be instituted in a court of competent jurisdiction in New York County in the State of New York in the United States of America and each party hereby consents and submits to the personal jurisdiction of such court, waives any objection to venue in such court and consents to service of process by registered or certified mail, return receipt requested, at the last known address of such party.

WILEY OPEN ACCESS TERMS AND CONDITIONS

Wiley Publishes Open Access Articles in fully Open Access Journals and in Subscription journals offering Online Open. Although most of the fully Open Access journals publish

open access articles under the terms of the Creative Commons Attribution (CC BY) License only, the subscription journals and a few of the Open Access Journals offer a choice of Creative Commons Licenses. The license type is clearly identified on the article.

The Creative Commons Attribution License

The Creative Commons Attribution License (CC-BY) allows users to copy, distribute and transmit an article, adapt the article and make commercial use of the article. The CC-BY license permits commercial and non-

Creative Commons Attribution Non-Commercial License

The Creative Commons Attribution Non-Commercial (CC-BY-NC)License permits use, distribution and reproduction in any medium, provided the original work is properly cited and is not used for commercial purposes.(see below)

Creative Commons Attribution-Non-Commercial-NoDerivs License

The Creative Commons Attribution Non-Commercial-NoDerivs License (CC-BY-NC-ND) permits use, distribution and reproduction in any medium, provided the original work is properly cited, is not used for commercial purposes and no modifications or adaptations are made. (see below)

Use by commercial "for-profit" organizations

Use of Wiley Open Access articles for commercial, promotional, or marketing purposes requires further explicit permission from Wiley and will be subject to a fee.

Further details can be found on Wiley Online Library

http://olabout.wiley.com/WileyCDA/Section/id-410895.html

Other Terms and Conditions:

v1.10 Last updated September 2015

Questions? customercare@copyright.com or +1-855-239-3415 (toll free in the US) or +1-978-646-2777.

RightsLink®

Home | Account Info | Help

Title:	Catalytically Active Bimetallic Nanoparticles Supported on Porous Carbon Capsules Derived From Metal–Organic Framework Composites
Author:	Hui Yang, Siobhan J. Bradley, Andrew Chan, et al
Publication:	Journal of the American Chemical Society
Publisher:	American Chemical Society
Date:	Sep 1, 2016

Logged in as:
Ping Liang
Account #:
3001154658

LOGOUT

PERMISSION/LICENSE IS GRANTED FOR YOUR ORDER AT NO CHARGE

This type of permission/license, instead of the standard Terms & Conditions, is sent to you because no fee is being charged for your order. Please note the following:

- Permission is granted for your request in both print and electronic formats, and translations.
- If figures and/or tables were requested, they may be adapted or used in part.
- Please print this page for your records and send a copy of it to your publisher/graduate school.
- Appropriate credit for the requested material should be given as follows: "Reprinted (adapted) with permission from (COMPLETE REFERENCE CITATION). Copyright (YEAR) American Chemical Society." Insert appropriate information in place of the capitalized words.
- One-time permission is granted only for the use specified in your request. No additional uses are granted (such as derivative works or other editions). For any other uses, please submit a new request.

If credit is given to another source for the material you requested, permission must be obtained from that source.

BACK CLOSE WINDOW

JOHN WILEY AND SONS LICENSE TERMS AND CONDITIONS

May 23, 2017

This Agreement between Ms. Ping Liang ("You") and John Wiley and Sons ("John Wiley and Sons") consists of your license details and the terms and conditions provided by John Wiley and Sons and Copyright Clearance Center.

License Number	4115100388185
License date	May 23, 2017
Licensed Content Publisher	John Wiley and Sons
Licensed Content Publication	Angewandte Chemie International Edition
Licensed Content Title	Co@Co3O4 Encapsulated in Carbon Nanotube-Grafted Nitrogen-Doped Carbon Polyhedra as an Advanced Bifunctional Oxygen Electrode
Licensed Content Author	Arshad Aijaz,Justus Masa,Christoph Rösler,Wei Xia,Philipp Weide,Alexander J. R. Botz,Roland A. Fischer,Wolfgang Schuhmann,Martin Muhler
Licensed Content Date	Feb 23, 2016
Licensed Content Pages	5
Type of use	Dissertation/Thesis
Requestor type	University/Academic
Format	Print and electronic
Portion	Figure/table
Number of figures/tables	1
Original Wiley figure/table number(s)	Figure 1
Will you be translating?	No
Title of your thesis / dissertation	Synthesis and Evaluation of Nanostructured Membrane Catalytic Systems for Water Treatment
Expected completion date	Jun 2017
Expected size (number of pages)	200
Requestor Location	Ms. Ping Liang 4-31 nottingham street, east vic park perth, WA 6101 Australia Attn: Ms. Ping Liang
Publisher Tax ID	EU826007151
Billing Type	Invoice
Billing Address	Ms. Ping Liang 4-31 nottingham street, east vic park

perth, Australia 6101
Attn: Ms. Ping Liang

Total 0.00 AUD

Terms and Conditions

TERMS AND CONDITIONS

This copyrighted material is owned by or exclusively licensed to John Wiley & Sons, Inc. or one of its group companies (each a"Wiley Company") or handled on behalf of a society with which a Wiley Company has exclusive publishing rights in relation to a particular work (collectively "WILEY"). By clicking "accept" in connection with completing this licensing transaction, you agree that the following terms and conditions apply to this transaction (along with the billing and payment terms and conditions established by the Copyright Clearance Center Inc., ("CCC's Billing and Payment terms and conditions"), at the time that you opened your RightsLink account (these are available at any time at http://myaccount.copyright.com).

Terms and Conditions

- The materials you have requested permission to reproduce or reuse (the "Wiley Materials") are protected by copyright.

- You are hereby granted a personal, non-exclusive, non-sub licensable (on a stand-alone basis), non-transferable, worldwide, limited license to reproduce the Wiley Materials for the purpose specified in the licensing process. This license, **and any CONTENT (PDF or image file) purchased as part of your order,** is for a one-time use only and limited to any maximum distribution number specified in the license. The first instance of republication or reuse granted by this license must be completed within two years of the date of the grant of this license (although copies prepared before the end date may be distributed thereafter). The Wiley Materials shall not be used in any other manner or for any other purpose, beyond what is granted in the license. Permission is granted subject to an appropriate acknowledgement given to the author, title of the material/book/journal and the publisher. You shall also duplicate the copyright notice that appears in the Wiley publication in your use of the Wiley Material. Permission is also granted on the understanding that nowhere in the text is a previously published source acknowledged for all or part of this Wiley Material. Any third party content is expressly excluded from this permission.

- With respect to the Wiley Materials, all rights are reserved. Except as expressly granted by the terms of the license, no part of the Wiley Materials may be copied, modified, adapted (except for minor reformatting required by the new Publication), translated, reproduced, transferred or distributed, in any form or by any means, and no derivative works may be made based on the Wiley Materials without the prior permission of the respective copyright owner.**For STM Signatory Publishers clearing permission under the terms of the STM Permissions Guidelines only, the terms of the license are extended to include subsequent editions and for editions in other languages, provided such editions are for the work as a whole in situ and does not involve the separate exploitation of the permitted figures or extracts,** You may not alter, remove or suppress in any manner any copyright, trademark or other notices displayed by the Wiley Materials. You may not license, rent, sell, loan,

lease, pledge, offer as security, transfer or assign the Wiley Materials on a stand-alone basis, or any of the rights granted to you hereunder to any other person.

- The Wiley Materials and all of the intellectual property rights therein shall at all times remain the exclusive property of John Wiley & Sons Inc, the Wiley Companies, or their respective licensors, and your interest therein is only that of having possession of and the right to reproduce the Wiley Materials pursuant to Section 2 herein during the continuance of this Agreement. You agree that you own no right, title or interest in or to the Wiley Materials or any of the intellectual property rights therein. You shall have no rights hereunder other than the license as provided for above in Section 2. No right, license or interest to any trademark, trade name, service mark or other branding ("Marks") of WILEY or its licensors is granted hereunder, and you agree that you shall not assert any such right, license or interest with respect thereto

- NEITHER WILEY NOR ITS LICENSORS MAKES ANY WARRANTY OR REPRESENTATION OF ANY KIND TO YOU OR ANY THIRD PARTY, EXPRESS, IMPLIED OR STATUTORY, WITH RESPECT TO THE MATERIALS OR THE ACCURACY OF ANY INFORMATION CONTAINED IN THE MATERIALS, INCLUDING, WITHOUT LIMITATION, ANY IMPLIED WARRANTY OF MERCHANTABILITY, ACCURACY, SATISFACTORY QUALITY, FITNESS FOR A PARTICULAR PURPOSE, USABILITY, INTEGRATION OR NON-INFRINGEMENT AND ALL SUCH WARRANTIES ARE HEREBY EXCLUDED BY WILEY AND ITS LICENSORS AND WAIVED BY YOU.

- WILEY shall have the right to terminate this Agreement immediately upon breach of this Agreement by you.

- You shall indemnify, defend and hold harmless WILEY, its Licensors and their respective directors, officers, agents and employees, from and against any actual or threatened claims, demands, causes of action or proceedings arising from any breach of this Agreement by you.

- IN NO EVENT SHALL WILEY OR ITS LICENSORS BE LIABLE TO YOU OR ANY OTHER PARTY OR ANY OTHER PERSON OR ENTITY FOR ANY SPECIAL, CONSEQUENTIAL, INCIDENTAL, INDIRECT, EXEMPLARY OR PUNITIVE DAMAGES, HOWEVER CAUSED, ARISING OUT OF OR IN CONNECTION WITH THE DOWNLOADING, PROVISIONING, VIEWING OR USE OF THE MATERIALS REGARDLESS OF THE FORM OF ACTION, WHETHER FOR BREACH OF CONTRACT, BREACH OF WARRANTY, TORT, NEGLIGENCE, INFRINGEMENT OR OTHERWISE (INCLUDING, WITHOUT LIMITATION, DAMAGES BASED ON LOSS OF PROFITS, DATA, FILES, USE, BUSINESS OPPORTUNITY OR CLAIMS OF THIRD PARTIES), AND WHETHER OR NOT THE PARTY HAS BEEN ADVISED OF THE POSSIBILITY OF SUCH DAMAGES. THIS LIMITATION SHALL APPLY NOTWITHSTANDING ANY FAILURE OF ESSENTIAL PURPOSE OF ANY LIMITED REMEDY PROVIDED HEREIN.

- Should any provision of this Agreement be held by a court of competent jurisdiction to be illegal, invalid, or unenforceable, that provision shall be deemed amended to

achieve as nearly as possible the same economic effect as the original provision, and the legality, validity and enforceability of the remaining provisions of this Agreement shall not be affected or impaired thereby.

- The failure of either party to enforce any term or condition of this Agreement shall not constitute a waiver of either party's right to enforce each and every term and condition of this Agreement. No breach under this agreement shall be deemed waived or excused by either party unless such waiver or consent is in writing signed by the party granting such waiver or consent. The waiver by or consent of a party to a breach of any provision of this Agreement shall not operate or be construed as a waiver of or consent to any other or subsequent breach by such other party.

- This Agreement may not be assigned (including by operation of law or otherwise) by you without WILEY's prior written consent.

- Any fee required for this permission shall be non-refundable after thirty (30) days from receipt by the CCC.

- These terms and conditions together with CCC's Billing and Payment terms and conditions (which are incorporated herein) form the entire agreement between you and WILEY concerning this licensing transaction and (in the absence of fraud) supersedes all prior agreements and representations of the parties, oral or written. This Agreement may not be amended except in writing signed by both parties. This Agreement shall be binding upon and inure to the benefit of the parties' successors, legal representatives, and authorized assigns.

- In the event of any conflict between your obligations established by these terms and conditions and those established by CCC's Billing and Payment terms and conditions, these terms and conditions shall prevail.

- WILEY expressly reserves all rights not specifically granted in the combination of (i) the license details provided by you and accepted in the course of this licensing transaction, (ii) these terms and conditions and (iii) CCC's Billing and Payment terms and conditions.

- This Agreement will be void if the Type of Use, Format, Circulation, or Requestor Type was misrepresented during the licensing process.

- This Agreement shall be governed by and construed in accordance with the laws of the State of New York, USA, without regards to such state's conflict of law rules. Any legal action, suit or proceeding arising out of or relating to these Terms and Conditions or the breach thereof shall be instituted in a court of competent jurisdiction in New York County in the State of New York in the United States of America and each party hereby consents and submits to the personal jurisdiction of such court, waives any objection to venue in such court and consents to service of process by registered or certified mail, return receipt requested, at the last known address of such party.

WILEY OPEN ACCESS TERMS AND CONDITIONS

Wiley Publishes Open Access Articles in fully Open Access Journals and in Subscription journals offering Online Open. Although most of the fully Open Access journals publish

open access articles under the terms of the Creative Commons Attribution (CC BY) License only, the subscription journals and a few of the Open Access Journals offer a choice of Creative Commons Licenses. The license type is clearly identified on the article.

The Creative Commons Attribution License

The Creative Commons Attribution License (CC-BY) allows users to copy, distribute and transmit an article, adapt the article and make commercial use of the article. The CC-BY license permits commercial and non-

Creative Commons Attribution Non-Commercial License

The Creative Commons Attribution Non-Commercial (CC-BY-NC)License permits use, distribution and reproduction in any medium, provided the original work is properly cited and is not used for commercial purposes.(see below)

Creative Commons Attribution-Non-Commercial-NoDerivs License

The Creative Commons Attribution Non-Commercial-NoDerivs License (CC-BY-NC-ND) permits use, distribution and reproduction in any medium, provided the original work is properly cited, is not used for commercial purposes and no modifications or adaptations are made. (see below)

Use by commercial "for-profit" organizations

Use of Wiley Open Access articles for commercial, promotional, or marketing purposes requires further explicit permission from Wiley and will be subject to a fee.

Further details can be found on Wiley Online Library

http://olabout.wiley.com/WileyCDA/Section/id-410895.html

Other Terms and Conditions:

v1.10 Last updated September 2015

Questions? customercare@copyright.com or +1-855-239-3415 (toll free in the US) or +1-978-646-2777.

JOHN WILEY AND SONS LICENSE TERMS AND CONDITIONS

May 23, 2017

This Agreement between Ms. Ping Liang ("You") and John Wiley and Sons ("John Wiley and Sons") consists of your license details and the terms and conditions provided by John Wiley and Sons and Copyright Clearance Center.

License Number	4115110332623
License date	May 23, 2017
Licensed Content Publisher	John Wiley and Sons
Licensed Content Publication	Angewandte Chemie
Licensed Content Title	Metal Oxide-Coated Three-Dimensional Graphene Prepared by the Use of Metal–Organic Frameworks as Precursors
Licensed Content Author	Xiehong Cao,Bing Zheng,Xianhong Rui,Wenhui Shi,Qingyu Yan,Hua Zhang
Licensed Content Date	Dec 20, 2013
Licensed Content Pages	6
Type of use	Dissertation/Thesis
Requestor type	University/Academic
Format	Print and electronic
Portion	Figure/table
Number of figures/tables	1
Original Wiley figure/table number(s)	Figure 1
Will you be translating?	No
Title of your thesis / dissertation	Synthesis and Evaluation of Nanostructured Membrane Catalytic Systems for Water Treatment
Expected completion date	Jun 2017
Expected size (number of pages)	200
Requestor Location	Ms. Ping Liang 4-31 nottingham street, east vic park perth, WA 6101 Australia Attn: Ms. Ping Liang
Publisher Tax ID	EU826007151
Billing Type	Invoice
Billing Address	Ms. Ping Liang 4-31 nottingham street, east vic park

perth, Australia 6101
Attn: Ms. Ping Liang

Total 0.00 AUD

Terms and Conditions

TERMS AND CONDITIONS

This copyrighted material is owned by or exclusively licensed to John Wiley & Sons, Inc. or one of its group companies (each a"Wiley Company") or handled on behalf of a society with which a Wiley Company has exclusive publishing rights in relation to a particular work (collectively "WILEY"). By clicking "accept" in connection with completing this licensing transaction, you agree that the following terms and conditions apply to this transaction (along with the billing and payment terms and conditions established by the Copyright Clearance Center Inc., ("CCC's Billing and Payment terms and conditions"), at the time that you opened your RightsLink account (these are available at any time at http://myaccount.copyright.com).

Terms and Conditions

- The materials you have requested permission to reproduce or reuse (the "Wiley Materials") are protected by copyright.

- You are hereby granted a personal, non-exclusive, non-sub licensable (on a stand-alone basis), non-transferable, worldwide, limited license to reproduce the Wiley Materials for the purpose specified in the licensing process. This license, **and any CONTENT (PDF or image file) purchased as part of your order,** is for a one-time use only and limited to any maximum distribution number specified in the license. The first instance of republication or reuse granted by this license must be completed within two years of the date of the grant of this license (although copies prepared before the end date may be distributed thereafter). The Wiley Materials shall not be used in any other manner or for any other purpose, beyond what is granted in the license. Permission is granted subject to an appropriate acknowledgement given to the author, title of the material/book/journal and the publisher. You shall also duplicate the copyright notice that appears in the Wiley publication in your use of the Wiley Material. Permission is also granted on the understanding that nowhere in the text is a previously published source acknowledged for all or part of this Wiley Material. Any third party content is expressly excluded from this permission.

- With respect to the Wiley Materials, all rights are reserved. Except as expressly granted by the terms of the license, no part of the Wiley Materials may be copied, modified, adapted (except for minor reformatting required by the new Publication), translated, reproduced, transferred or distributed, in any form or by any means, and no derivative works may be made based on the Wiley Materials without the prior permission of the respective copyright owner.**For STM Signatory Publishers clearing permission under the terms of the STM Permissions Guidelines only, the terms of the license are extended to include subsequent editions and for editions in other languages, provided such editions are for the work as a whole in situ and does not involve the separate exploitation of the permitted figures or extracts,** You may not alter, remove or suppress in any manner any copyright, trademark or other notices displayed by the Wiley Materials. You may not license, rent, sell, loan, lease, pledge, offer as security, transfer or assign the Wiley Materials on a stand-alone basis, or any of the rights granted to you hereunder to any other person.

- The Wiley Materials and all of the intellectual property rights therein shall at all times remain the exclusive property of John Wiley & Sons Inc, the Wiley Companies, or their respective licensors, and your interest therein is only that of having possession of and the right to reproduce the Wiley Materials pursuant to Section 2 herein during the continuance of this Agreement. You agree that you own no right, title or interest in or to the Wiley Materials or any of the intellectual property rights therein. You shall have no rights hereunder other than the license as provided for above in Section 2. No right, license or interest to any trademark, trade name, service mark or other branding ("Marks") of WILEY or its licensors is granted hereunder, and you agree that you shall not assert any such right, license or interest with respect thereto

- NEITHER WILEY NOR ITS LICENSORS MAKES ANY WARRANTY OR REPRESENTATION OF ANY KIND TO YOU OR ANY THIRD PARTY, EXPRESS, IMPLIED OR STATUTORY, WITH RESPECT TO THE MATERIALS OR THE ACCURACY OF ANY INFORMATION CONTAINED IN THE MATERIALS, INCLUDING, WITHOUT LIMITATION, ANY IMPLIED WARRANTY OF MERCHANTABILITY, ACCURACY, SATISFACTORY QUALITY, FITNESS FOR A PARTICULAR PURPOSE, USABILITY, INTEGRATION OR NON-INFRINGEMENT AND ALL SUCH WARRANTIES ARE HEREBY EXCLUDED BY WILEY AND ITS LICENSORS AND WAIVED BY YOU.

- WILEY shall have the right to terminate this Agreement immediately upon breach of this Agreement by you.

- You shall indemnify, defend and hold harmless WILEY, its Licensors and their respective directors, officers, agents and employees, from and against any actual or threatened claims, demands, causes of action or proceedings arising from any breach of this Agreement by you.

- IN NO EVENT SHALL WILEY OR ITS LICENSORS BE LIABLE TO YOU OR ANY OTHER PARTY OR ANY OTHER PERSON OR ENTITY FOR ANY SPECIAL, CONSEQUENTIAL, INCIDENTAL, INDIRECT, EXEMPLARY OR PUNITIVE DAMAGES, HOWEVER CAUSED, ARISING OUT OF OR IN CONNECTION WITH THE DOWNLOADING, PROVISIONING, VIEWING OR USE OF THE MATERIALS REGARDLESS OF THE FORM OF ACTION, WHETHER FOR BREACH OF CONTRACT, BREACH OF WARRANTY, TORT, NEGLIGENCE, INFRINGEMENT OR OTHERWISE (INCLUDING, WITHOUT LIMITATION, DAMAGES BASED ON LOSS OF PROFITS, DATA, FILES, USE, BUSINESS OPPORTUNITY OR CLAIMS OF THIRD PARTIES), AND WHETHER OR NOT THE PARTY HAS BEEN ADVISED OF THE POSSIBILITY OF SUCH DAMAGES. THIS LIMITATION SHALL APPLY NOTWITHSTANDING ANY FAILURE OF ESSENTIAL PURPOSE OF ANY LIMITED REMEDY PROVIDED HEREIN.

- Should any provision of this Agreement be held by a court of competent jurisdiction to be illegal, invalid, or unenforceable, that provision shall be deemed amended to achieve as nearly as possible the same economic effect as the original provision, and the legality, validity and enforceability of the remaining provisions of this Agreement

shall not be affected or impaired thereby.

- The failure of either party to enforce any term or condition of this Agreement shall not constitute a waiver of either party's right to enforce each and every term and condition of this Agreement. No breach under this agreement shall be deemed waived or excused by either party unless such waiver or consent is in writing signed by the party granting such waiver or consent. The waiver by or consent of a party to a breach of any provision of this Agreement shall not operate or be construed as a waiver of or consent to any other or subsequent breach by such other party.

- This Agreement may not be assigned (including by operation of law or otherwise) by you without WILEY's prior written consent.

- Any fee required for this permission shall be non-refundable after thirty (30) days from receipt by the CCC.

- These terms and conditions together with CCC's Billing and Payment terms and conditions (which are incorporated herein) form the entire agreement between you and WILEY concerning this licensing transaction and (in the absence of fraud) supersedes all prior agreements and representations of the parties, oral or written. This Agreement may not be amended except in writing signed by both parties. This Agreement shall be binding upon and inure to the benefit of the parties' successors, legal representatives, and authorized assigns.

- In the event of any conflict between your obligations established by these terms and conditions and those established by CCC's Billing and Payment terms and conditions, these terms and conditions shall prevail.

- WILEY expressly reserves all rights not specifically granted in the combination of (i) the license details provided by you and accepted in the course of this licensing transaction, (ii) these terms and conditions and (iii) CCC's Billing and Payment terms and conditions.

- This Agreement will be void if the Type of Use, Format, Circulation, or Requestor Type was misrepresented during the licensing process.

- This Agreement shall be governed by and construed in accordance with the laws of the State of New York, USA, without regards to such state's conflict of law rules. Any legal action, suit or proceeding arising out of or relating to these Terms and Conditions or the breach thereof shall be instituted in a court of competent jurisdiction in New York County in the State of New York in the United States of America and each party hereby consents and submits to the personal jurisdiction of such court, waives any objection to venue in such court and consents to service of process by registered or certified mail, return receipt requested, at the last known address of such party.

WILEY OPEN ACCESS TERMS AND CONDITIONS

Wiley Publishes Open Access Articles in fully Open Access Journals and in Subscription journals offering Online Open. Although most of the fully Open Access journals publish open access articles under the terms of the Creative Commons Attribution (CC BY) License only, the subscription journals and a few of the Open Access Journals offer a choice of

Creative Commons Licenses. The license type is clearly identified on the article.

The Creative Commons Attribution License

The Creative Commons Attribution License (CC-BY) allows users to copy, distribute and transmit an article, adapt the article and make commercial use of the article. The CC-BY license permits commercial and non-

Creative Commons Attribution Non-Commercial License

The Creative Commons Attribution Non-Commercial (CC-BY-NC)License permits use, distribution and reproduction in any medium, provided the original work is properly cited and is not used for commercial purposes.(see below)

Creative Commons Attribution-Non-Commercial-NoDerivs License

The Creative Commons Attribution Non-Commercial-NoDerivs License (CC-BY-NC-ND) permits use, distribution and reproduction in any medium, provided the original work is properly cited, is not used for commercial purposes and no modifications or adaptations are made. (see below)

Use by commercial "for-profit" organizations

Use of Wiley Open Access articles for commercial, promotional, or marketing purposes requires further explicit permission from Wiley and will be subject to a fee.

Further details can be found on Wiley Online Library

http://olabout.wiley.com/WileyCDA/Section/id-410895.html

Other Terms and Conditions:

v1.10 Last updated September 2015

Questions? customercare@copyright.com or +1-855-239-3415 (toll free in the US) or +1-978-646-2777.

ELSEVIER LICENSE
TERMS AND CONDITIONS

May 23, 2017

This Agreement between Ms. Ping Liang ("You") and Elsevier ("Elsevier") consists of your license details and the terms and conditions provided by Elsevier and Copyright Clearance Center.

License Number	4115120565586
License date	May 23, 2017
Licensed Content Publisher	Elsevier
Licensed Content Publication	Nano Energy
Licensed Content Title	Reduced graphene oxide wrapped MOFs-derived cobalt-doped porous carbon polyhedrons as sulfur immobilizers as cathodes for high performance lithium sulfur batteries
Licensed Content Author	Zhaoqiang Li,Caixia Li,Xiaoli Ge,Jingyun Ma,Zhiwei Zhang,Qun Li,Chengxiang Wang,Longwei Yin
Licensed Content Date	May 1, 2016
Licensed Content Volume	23
Licensed Content Issue	n/a
Licensed Content Pages	12
Start Page	15
End Page	26
Type of Use	reuse in a thesis/dissertation
Intended publisher of new work	other
Portion	figures/tables/illustrations
Number of figures/tables/illustrations	1
Format	both print and electronic
Are you the author of this Elsevier article?	No
Will you be translating?	No
Order reference number	
Original figure numbers	Figure 2
Title of your thesis/dissertation	Synthesis and Evaluation of Nanostructured Membrane Catalytic Systems for Water Treatment
Expected completion date	Jun 2017
Estimated size (number of pages)	200
Elsevier VAT number	GB 494 6272 12
Requestor Location	Ms. Ping Liang

4-31 nottingham street, east vic park

perth, WA 6101
Australia
Attn: Ms. Ping Liang

Total 0.00 USD

Terms and Conditions

INTRODUCTION

1. The publisher for this copyrighted material is Elsevier. By clicking "accept" in connection with completing this licensing transaction, you agree that the following terms and conditions apply to this transaction (along with the Billing and Payment terms and conditions established by Copyright Clearance Center, Inc. ("CCC"), at the time that you opened your Rightslink account and that are available at any time at http://myaccount.copyright.com).

GENERAL TERMS

2. Elsevier hereby grants you permission to reproduce the aforementioned material subject to the terms and conditions indicated.
3. Acknowledgement: If any part of the material to be used (for example, figures) has appeared in our publication with credit or acknowledgement to another source, permission must also be sought from that source. If such permission is not obtained then that material may not be included in your publication/copies. Suitable acknowledgement to the source must be made, either as a footnote or in a reference list at the end of your publication, as follows:
"Reprinted from Publication title, Vol /edition number, Author(s), Title of article / title of chapter, Pages No., Copyright (Year), with permission from Elsevier [OR APPLICABLE SOCIETY COPYRIGHT OWNER]." Also Lancet special credit - "Reprinted from The Lancet, Vol. number, Author(s), Title of article, Pages No., Copyright (Year), with permission from Elsevier."
4. Reproduction of this material is confined to the purpose and/or media for which permission is hereby given.
5. Altering/Modifying Material: Not Permitted. However figures and illustrations may be altered/adapted minimally to serve your work. Any other abbreviations, additions, deletions and/or any other alterations shall be made only with prior written authorization of Elsevier Ltd. (Please contact Elsevier at permissions@elsevier.com). No modifications can be made to any Lancet figures/tables and they must be reproduced in full.
6. If the permission fee for the requested use of our material is waived in this instance, please be advised that your future requests for Elsevier materials may attract a fee.
7. Reservation of Rights: Publisher reserves all rights not specifically granted in the combination of (i) the license details provided by you and accepted in the course of this licensing transaction, (ii) these terms and conditions and (iii) CCC's Billing and Payment terms and conditions.
8. License Contingent Upon Payment: While you may exercise the rights licensed immediately upon issuance of the license at the end of the licensing process for the transaction, provided that you have disclosed complete and accurate details of your proposed use, no license is finally effective unless and until full payment is received from you (either by publisher or by CCC) as provided in CCC's Billing and Payment terms and conditions. If full payment is not received on a timely basis, then any license preliminarily granted shall be deemed automatically revoked and shall be void as if never granted. Further, in the event that you breach any of these terms and conditions or any of CCC's Billing and Payment

terms and conditions, the license is automatically revoked and shall be void as if never granted. Use of materials as described in a revoked license, as well as any use of the materials beyond the scope of an unrevoked license, may constitute copyright infringement and publisher reserves the right to take any and all action to protect its copyright in the materials.
9. Warranties: Publisher makes no representations or warranties with respect to the licensed material.
10. Indemnity: You hereby indemnify and agree to hold harmless publisher and CCC, and their respective officers, directors, employees and agents, from and against any and all claims arising out of your use of the licensed material other than as specifically authorized pursuant to this license.
11. No Transfer of License: This license is personal to you and may not be sublicensed, assigned, or transferred by you to any other person without publisher's written permission.
12. No Amendment Except in Writing: This license may not be amended except in a writing signed by both parties (or, in the case of publisher, by CCC on publisher's behalf).
13. Objection to Contrary Terms: Publisher hereby objects to any terms contained in any purchase order, acknowledgment, check endorsement or other writing prepared by you, which terms are inconsistent with these terms and conditions or CCC's Billing and Payment terms and conditions. These terms and conditions, together with CCC's Billing and Payment terms and conditions (which are incorporated herein), comprise the entire agreement between you and publisher (and CCC) concerning this licensing transaction. In the event of any conflict between your obligations established by these terms and conditions and those established by CCC's Billing and Payment terms and conditions, these terms and conditions shall control.
14. Revocation: Elsevier or Copyright Clearance Center may deny the permissions described in this License at their sole discretion, for any reason or no reason, with a full refund payable to you. Notice of such denial will be made using the contact information provided by you. Failure to receive such notice will not alter or invalidate the denial. In no event will Elsevier or Copyright Clearance Center be responsible or liable for any costs, expenses or damage incurred by you as a result of a denial of your permission request, other than a refund of the amount(s) paid by you to Elsevier and/or Copyright Clearance Center for denied permissions.

LIMITED LICENSE

The following terms and conditions apply only to specific license types:
15. **Translation**: This permission is granted for non-exclusive world **English** rights only unless your license was granted for translation rights. If you licensed translation rights you may only translate this content into the languages you requested. A professional translator must perform all translations and reproduce the content word for word preserving the integrity of the article.
16. **Posting licensed content on any Website**: The following terms and conditions apply as follows: Licensing material from an Elsevier journal: All content posted to the web site must maintain the copyright information line on the bottom of each image; A hyper-text must be included to the Homepage of the journal from which you are licensing at http://www.sciencedirect.com/science/journal/xxxxx or the Elsevier homepage for books at http://www.elsevier.com; Central Storage: This license does not include permission for a scanned version of the material to be stored in a central repository such as that provided by Heron/XanEdu.
Licensing material from an Elsevier book: A hyper-text link must be included to the Elsevier homepage at http://www.elsevier.com . All content posted to the web site must maintain the copyright information line on the bottom of each image.

Posting licensed content on Electronic reserve: In addition to the above the following clauses are applicable: The web site must be password-protected and made available only to bona fide students registered on a relevant course. This permission is granted for 1 year only. You may obtain a new license for future website posting.

17. **For journal authors:** the following clauses are applicable in addition to the above:

Preprints:

A preprint is an author's own write-up of research results and analysis, it has not been peer-reviewed, nor has it had any other value added to it by a publisher (such as formatting, copyright, technical enhancement etc.).

Authors can share their preprints anywhere at any time. Preprints should not be added to or enhanced in any way in order to appear more like, or to substitute for, the final versions of articles however authors can update their preprints on arXiv or RePEc with their Accepted Author Manuscript (see below).

If accepted for publication, we encourage authors to link from the preprint to their formal publication via its DOI. Millions of researchers have access to the formal publications on ScienceDirect, and so links will help users to find, access, cite and use the best available version. Please note that Cell Press, The Lancet and some society-owned have different preprint policies. Information on these policies is available on the journal homepage.

Accepted Author Manuscripts: An accepted author manuscript is the manuscript of an article that has been accepted for publication and which typically includes author-incorporated changes suggested during submission, peer review and editor-author communications.

Authors can share their accepted author manuscript:

- immediately
    - via their non-commercial person homepage or blog
    - by updating a preprint in arXiv or RePEc with the accepted manuscript
    - via their research institute or institutional repository for internal institutional uses or as part of an invitation-only research collaboration work-group
    - directly by providing copies to their students or to research collaborators for their personal use
    - for private scholarly sharing as part of an invitation-only work group on commercial sites with which Elsevier has an agreement
- After the embargo period
    - via non-commercial hosting platforms such as their institutional repository
    - via commercial sites with which Elsevier has an agreement

In all cases accepted manuscripts should:

- link to the formal publication via its DOI
- bear a CC-BY-NC-ND license - this is easy to do
- if aggregated with other manuscripts, for example in a repository or other site, be shared in alignment with our hosting policy not be added to or enhanced in any way to appear more like, or to substitute for, the published journal article.

Published journal article (JPA): A published journal article (PJA) is the definitive final record of published research that appears or will appear in the journal and embodies all value-adding publishing activities including peer review co-ordination, copy-editing, formatting, (if relevant) pagination and online enrichment.

Policies for sharing publishing journal articles differ for subscription and gold open access

articles:
Subscription Articles: If you are an author, please share a link to your article rather than the full-text. Millions of researchers have access to the formal publications on ScienceDirect, and so links will help your users to find, access, cite, and use the best available version.
Theses and dissertations which contain embedded PJAs as part of the formal submission can be posted publicly by the awarding institution with DOI links back to the formal publications on ScienceDirect.
If you are affiliated with a library that subscribes to ScienceDirect you have additional private sharing rights for others' research accessed under that agreement. This includes use for classroom teaching and internal training at the institution (including use in course packs and courseware programs), and inclusion of the article for grant funding purposes.
Gold Open Access Articles: May be shared according to the author-selected end-user license and should contain a CrossMark logo, the end user license, and a DOI link to the formal publication on ScienceDirect.
Please refer to Elsevier's posting policy for further information.
18. **For book authors** the following clauses are applicable in addition to the above:
Authors are permitted to place a brief summary of their work online only. You are not allowed to download and post the published electronic version of your chapter, nor may you scan the printed edition to create an electronic version. **Posting to a repository:** Authors are permitted to post a summary of their chapter only in their institution's repository.
19. **Thesis/Dissertation**: If your license is for use in a thesis/dissertation your thesis may be submitted to your institution in either print or electronic form. Should your thesis be published commercially, please reapply for permission. These requirements include permission for the Library and Archives of Canada to supply single copies, on demand, of the complete thesis and include permission for Proquest/UMI to supply single copies, on demand, of the complete thesis. Should your thesis be published commercially, please reapply for permission. Theses and dissertations which contain embedded PJAs as part of the formal submission can be posted publicly by the awarding institution with DOI links back to the formal publications on ScienceDirect.

Elsevier Open Access Terms and Conditions
You can publish open access with Elsevier in hundreds of open access journals or in nearly 2000 established subscription journals that support open access publishing. Permitted third party re-use of these open access articles is defined by the author's choice of Creative Commons user license. See our open access license policy for more information.
Terms & Conditions applicable to all Open Access articles published with Elsevier:
Any reuse of the article must not represent the author as endorsing the adaptation of the article nor should the article be modified in such a way as to damage the author's honour or reputation. If any changes have been made, such changes must be clearly indicated.
The author(s) must be appropriately credited and we ask that you include the end user license and a DOI link to the formal publication on ScienceDirect.
If any part of the material to be used (for example, figures) has appeared in our publication with credit or acknowledgement to another source it is the responsibility of the user to ensure their reuse complies with the terms and conditions determined by the rights holder.
Additional Terms & Conditions applicable to each Creative Commons user license:
CC BY: The CC-BY license allows users to copy, to create extracts, abstracts and new works from the Article, to alter and revise the Article and to make commercial use of the Article (including reuse and/or resale of the Article by commercial entities), provided the user gives appropriate credit (with a link to the formal publication through the relevant DOI), provides a link to the license, indicates if changes were made and the licensor is not

represented as endorsing the use made of the work. The full details of the license are available at http://creativecommons.org/licenses/by/4.0.
CC BY NC SA: The CC BY-NC-SA license allows users to copy, to create extracts, abstracts and new works from the Article, to alter and revise the Article, provided this is not done for commercial purposes, and that the user gives appropriate credit (with a link to the formal publication through the relevant DOI), provides a link to the license, indicates if changes were made and the licensor is not represented as endorsing the use made of the work. Further, any new works must be made available on the same conditions. The full details of the license are available at http://creativecommons.org/licenses/by-nc-sa/4.0.
CC BY NC ND: The CC BY-NC-ND license allows users to copy and distribute the Article, provided this is not done for commercial purposes and further does not permit distribution of the Article if it is changed or edited in any way, and provided the user gives appropriate credit (with a link to the formal publication through the relevant DOI), provides a link to the license, and that the licensor is not represented as endorsing the use made of the work. The full details of the license are available at http://creativecommons.org/licenses/by-nc-nd/4.0.
Any commercial reuse of Open Access articles published with a CC BY NC SA or CC BY NC ND license requires permission from Elsevier and will be subject to a fee.
Commercial reuse includes:

- Associating advertising with the full text of the Article
- Charging fees for document delivery or access
- Article aggregation
- Systematic distribution via e-mail lists or share buttons

Posting or linking by commercial companies for use by customers of those companies.

20. **Other Conditions**:

v1.9

Questions? customercare@copyright.com or +1-855-239-3415 (toll free in the US) or +1-978-646-2777.

Title: Metal–Organic Framework Derived Hybrid Co3O4-Carbon Porous Nanowire Arrays as Reversible Oxygen Evolution Electrodes

Author: Tian Yi Ma, Sheng Dai, Mietek Jaroniec, et al

Publication: Journal of the American Chemical Society

Publisher: American Chemical Society

Date: Oct 1, 2014

PERMISSION/LICENSE IS GRANTED FOR YOUR ORDER AT NO CHARGE

This type of permission/license, instead of the standard Terms & Conditions, is sent to you because no fee is being charged for your order. Please note the following:

- Permission is granted for your request in both print and electronic formats, and translations.
- If figures and/or tables were requested, they may be adapted or used in part.
- Please print this page for your records and send a copy of it to your publisher/graduate school.
- Appropriate credit for the requested material should be given as follows: "Reprinted (adapted) with permission from (COMPLETE REFERENCE CITATION). Copyright (YEAR) American Chemical Society." Insert appropriate information in place of the capitalized words.
- One-time permission is granted only for the use specified in your request. No additional uses are granted (such as derivative works or other editions). For any other uses, please submit a new request.

If credit is given to another source for the material you requested, permission must be obtained from that source.

JOHN WILEY AND SONS LICENSE TERMS AND CONDITIONS

May 23, 2017

This Agreement between Ms. Ping Liang ("You") and John Wiley and Sons ("John Wiley and Sons") consists of your license details and the terms and conditions provided by John Wiley and Sons and Copyright Clearance Center.

License Number	4115131023911
License date	May 23, 2017
Licensed Content Publisher	John Wiley and Sons
Licensed Content Publication	Advanced Materials
Licensed Content Title	High-Performance and Ultra-Stable Lithium-Ion Batteries Based on MOF-Derived ZnO@ZnO Quantum Dots/C Core–Shell Nanorod Arrays on a Carbon Cloth Anode
Licensed Content Author	Guanhua Zhang,Sucheng Hou,Hang Zhang,Wei Zeng,Feilong Yan,Cheng Chao Li,Huigao Duan
Licensed Content Date	Feb 27, 2015
Licensed Content Pages	6
Type of use	Dissertation/Thesis
Requestor type	University/Academic
Format	Print and electronic
Portion	Figure/table
Number of figures/tables	1
Original Wiley figure/table number(s)	Figure 2
Will you be translating?	No
Title of your thesis / dissertation	Synthesis and Evaluation of Nanostructured Membrane Catalytic Systems for Water Treatment
Expected completion date	Jun 2017
Expected size (number of pages)	200
Requestor Location	Ms. Ping Liang 4-31 nottingham street, east vic park perth, WA 6101 Australia Attn: Ms. Ping Liang
Publisher Tax ID	EU826007151
Billing Type	Invoice
Billing Address	Ms. Ping Liang 4-31 nottingham street, east vic park

perth, Australia 6101
Attn: Ms. Ping Liang

Total 0.00 AUD

Terms and Conditions

TERMS AND CONDITIONS

This copyrighted material is owned by or exclusively licensed to John Wiley & Sons, Inc. or one of its group companies (each a"Wiley Company") or handled on behalf of a society with which a Wiley Company has exclusive publishing rights in relation to a particular work (collectively "WILEY"). By clicking "accept" in connection with completing this licensing transaction, you agree that the following terms and conditions apply to this transaction (along with the billing and payment terms and conditions established by the Copyright Clearance Center Inc., ("CCC's Billing and Payment terms and conditions"), at the time that you opened your RightsLink account (these are available at any time at http://myaccount.copyright.com).

Terms and Conditions

- The materials you have requested permission to reproduce or reuse (the "Wiley Materials") are protected by copyright.

- You are hereby granted a personal, non-exclusive, non-sub licensable (on a stand-alone basis), non-transferable, worldwide, limited license to reproduce the Wiley Materials for the purpose specified in the licensing process. This license, **and any CONTENT (PDF or image file) purchased as part of your order,** is for a one-time use only and limited to any maximum distribution number specified in the license. The first instance of republication or reuse granted by this license must be completed within two years of the date of the grant of this license (although copies prepared before the end date may be distributed thereafter). The Wiley Materials shall not be used in any other manner or for any other purpose, beyond what is granted in the license. Permission is granted subject to an appropriate acknowledgement given to the author, title of the material/book/journal and the publisher. You shall also duplicate the copyright notice that appears in the Wiley publication in your use of the Wiley Material. Permission is also granted on the understanding that nowhere in the text is a previously published source acknowledged for all or part of this Wiley Material. Any third party content is expressly excluded from this permission.

- With respect to the Wiley Materials, all rights are reserved. Except as expressly granted by the terms of the license, no part of the Wiley Materials may be copied, modified, adapted (except for minor reformatting required by the new Publication), translated, reproduced, transferred or distributed, in any form or by any means, and no derivative works may be made based on the Wiley Materials without the prior permission of the respective copyright owner.**For STM Signatory Publishers clearing permission under the terms of the STM Permissions Guidelines only, the terms of the license are extended to include subsequent editions and for editions in other languages, provided such editions are for the work as a whole in situ and does not involve the separate exploitation of the permitted figures or extracts,** You may not alter, remove or suppress in any manner any copyright, trademark or other notices displayed by the Wiley Materials. You may not license, rent, sell, loan, lease, pledge, offer as security, transfer or assign the Wiley Materials on a stand-alone

basis, or any of the rights granted to you hereunder to any other person.

- The Wiley Materials and all of the intellectual property rights therein shall at all times remain the exclusive property of John Wiley & Sons Inc, the Wiley Companies, or their respective licensors, and your interest therein is only that of having possession of and the right to reproduce the Wiley Materials pursuant to Section 2 herein during the continuance of this Agreement. You agree that you own no right, title or interest in or to the Wiley Materials or any of the intellectual property rights therein. You shall have no rights hereunder other than the license as provided for above in Section 2. No right, license or interest to any trademark, trade name, service mark or other branding ("Marks") of WILEY or its licensors is granted hereunder, and you agree that you shall not assert any such right, license or interest with respect thereto

- NEITHER WILEY NOR ITS LICENSORS MAKES ANY WARRANTY OR REPRESENTATION OF ANY KIND TO YOU OR ANY THIRD PARTY, EXPRESS, IMPLIED OR STATUTORY, WITH RESPECT TO THE MATERIALS OR THE ACCURACY OF ANY INFORMATION CONTAINED IN THE MATERIALS, INCLUDING, WITHOUT LIMITATION, ANY IMPLIED WARRANTY OF MERCHANTABILITY, ACCURACY, SATISFACTORY QUALITY, FITNESS FOR A PARTICULAR PURPOSE, USABILITY, INTEGRATION OR NON-INFRINGEMENT AND ALL SUCH WARRANTIES ARE HEREBY EXCLUDED BY WILEY AND ITS LICENSORS AND WAIVED BY YOU.

- WILEY shall have the right to terminate this Agreement immediately upon breach of this Agreement by you.

- You shall indemnify, defend and hold harmless WILEY, its Licensors and their respective directors, officers, agents and employees, from and against any actual or threatened claims, demands, causes of action or proceedings arising from any breach of this Agreement by you.

- IN NO EVENT SHALL WILEY OR ITS LICENSORS BE LIABLE TO YOU OR ANY OTHER PARTY OR ANY OTHER PERSON OR ENTITY FOR ANY SPECIAL, CONSEQUENTIAL, INCIDENTAL, INDIRECT, EXEMPLARY OR PUNITIVE DAMAGES, HOWEVER CAUSED, ARISING OUT OF OR IN CONNECTION WITH THE DOWNLOADING, PROVISIONING, VIEWING OR USE OF THE MATERIALS REGARDLESS OF THE FORM OF ACTION, WHETHER FOR BREACH OF CONTRACT, BREACH OF WARRANTY, TORT, NEGLIGENCE, INFRINGEMENT OR OTHERWISE (INCLUDING, WITHOUT LIMITATION, DAMAGES BASED ON LOSS OF PROFITS, DATA, FILES, USE, BUSINESS OPPORTUNITY OR CLAIMS OF THIRD PARTIES), AND WHETHER OR NOT THE PARTY HAS BEEN ADVISED OF THE POSSIBILITY OF SUCH DAMAGES. THIS LIMITATION SHALL APPLY NOTWITHSTANDING ANY FAILURE OF ESSENTIAL PURPOSE OF ANY LIMITED REMEDY PROVIDED HEREIN.

- Should any provision of this Agreement be held by a court of competent jurisdiction to be illegal, invalid, or unenforceable, that provision shall be deemed amended to achieve as nearly as possible the same economic effect as the original provision, and

the legality, validity and enforceability of the remaining provisions of this Agreement shall not be affected or impaired thereby.

- The failure of either party to enforce any term or condition of this Agreement shall not constitute a waiver of either party's right to enforce each and every term and condition of this Agreement. No breach under this agreement shall be deemed waived or excused by either party unless such waiver or consent is in writing signed by the party granting such waiver or consent. The waiver by or consent of a party to a breach of any provision of this Agreement shall not operate or be construed as a waiver of or consent to any other or subsequent breach by such other party.

- This Agreement may not be assigned (including by operation of law or otherwise) by you without WILEY's prior written consent.

- Any fee required for this permission shall be non-refundable after thirty (30) days from receipt by the CCC.

- These terms and conditions together with CCC's Billing and Payment terms and conditions (which are incorporated herein) form the entire agreement between you and WILEY concerning this licensing transaction and (in the absence of fraud) supersedes all prior agreements and representations of the parties, oral or written. This Agreement may not be amended except in writing signed by both parties. This Agreement shall be binding upon and inure to the benefit of the parties' successors, legal representatives, and authorized assigns.

- In the event of any conflict between your obligations established by these terms and conditions and those established by CCC's Billing and Payment terms and conditions, these terms and conditions shall prevail.

- WILEY expressly reserves all rights not specifically granted in the combination of (i) the license details provided by you and accepted in the course of this licensing transaction, (ii) these terms and conditions and (iii) CCC's Billing and Payment terms and conditions.

- This Agreement will be void if the Type of Use, Format, Circulation, or Requestor Type was misrepresented during the licensing process.

- This Agreement shall be governed by and construed in accordance with the laws of the State of New York, USA, without regards to such state's conflict of law rules. Any legal action, suit or proceeding arising out of or relating to these Terms and Conditions or the breach thereof shall be instituted in a court of competent jurisdiction in New York County in the State of New York in the United States of America and each party hereby consents and submits to the personal jurisdiction of such court, waives any objection to venue in such court and consents to service of process by registered or certified mail, return receipt requested, at the last known address of such party.

WILEY OPEN ACCESS TERMS AND CONDITIONS

Wiley Publishes Open Access Articles in fully Open Access Journals and in Subscription journals offering Online Open. Although most of the fully Open Access journals publish open access articles under the terms of the Creative Commons Attribution (CC BY) License

only, the subscription journals and a few of the Open Access Journals offer a choice of Creative Commons Licenses. The license type is clearly identified on the article.

The Creative Commons Attribution License

The Creative Commons Attribution License (CC-BY) allows users to copy, distribute and transmit an article, adapt the article and make commercial use of the article. The CC-BY license permits commercial and non-

Creative Commons Attribution Non-Commercial License

The Creative Commons Attribution Non-Commercial (CC-BY-NC)License permits use, distribution and reproduction in any medium, provided the original work is properly cited and is not used for commercial purposes.(see below)

Creative Commons Attribution-Non-Commercial-NoDerivs License

The Creative Commons Attribution Non-Commercial-NoDerivs License (CC-BY-NC-ND) permits use, distribution and reproduction in any medium, provided the original work is properly cited, is not used for commercial purposes and no modifications or adaptations are made. (see below)

Use by commercial "for-profit" organizations

Use of Wiley Open Access articles for commercial, promotional, or marketing purposes requires further explicit permission from Wiley and will be subject to a fee.
Further details can be found on Wiley Online Library
http://olabout.wiley.com/WileyCDA/Section/id-410895.html

Other Terms and Conditions:

v1.10 Last updated September 2015

Questions? customercare@copyright.com or +1-855-239-3415 (toll free in the US) or +1-978-646-2777.

JOHN WILEY AND SONS LICENSE TERMS AND CONDITIONS

May 24, 2017

This Agreement between Ms. Ping Liang ("You") and John Wiley and Sons ("John Wiley and Sons") consists of your license details and the terms and conditions provided by John Wiley and Sons and Copyright Clearance Center.

License Number	4115251418852
License date	May 24, 2017
Licensed Content Publisher	John Wiley and Sons
Licensed Content Publication	Advanced Materials
Licensed Content Title	Directed Growth of Metal-Organic Frameworks and Their Derived Carbon-Based Network for Efficient Electrocatalytic Oxygen Reduction
Licensed Content Author	Zhenhua Li,Mingfei Shao,Lei Zhou,Ruikang Zhang,Cong Zhang,Min Wei,David G. Evans,Xue Duan
Licensed Content Date	Jan 25, 2016
Licensed Content Pages	8
Type of use	Dissertation/Thesis
Requestor type	University/Academic
Format	Print and electronic
Portion	Figure/table
Number of figures/tables	1
Original Wiley figure/table number(s)	Figure 1
Will you be translating?	No
Title of your thesis / dissertation	Synthesis and Evaluation of Nanostructured Membrane Catalytic Systems for Water Treatment
Expected completion date	Jun 2017
Expected size (number of pages)	200
Requestor Location	Ms. Ping Liang 4-31 nottingham street, east vic park perth, WA 6101 Australia Attn: Ms. Ping Liang
Publisher Tax ID	EU826007151
Billing Type	Invoice
Billing Address	Ms. Ping Liang 4-31 nottingham street, east vic park

perth, Australia 6101
Attn: Ms. Ping Liang

Total 0.00 AUD

Terms and Conditions

TERMS AND CONDITIONS

This copyrighted material is owned by or exclusively licensed to John Wiley & Sons, Inc. or one of its group companies (each a"Wiley Company") or handled on behalf of a society with which a Wiley Company has exclusive publishing rights in relation to a particular work (collectively "WILEY"). By clicking "accept" in connection with completing this licensing transaction, you agree that the following terms and conditions apply to this transaction (along with the billing and payment terms and conditions established by the Copyright Clearance Center Inc., ("CCC's Billing and Payment terms and conditions"), at the time that you opened your RightsLink account (these are available at any time at http://myaccount.copyright.com).

Terms and Conditions

- The materials you have requested permission to reproduce or reuse (the "Wiley Materials") are protected by copyright.

- You are hereby granted a personal, non-exclusive, non-sub licensable (on a stand-alone basis), non-transferable, worldwide, limited license to reproduce the Wiley Materials for the purpose specified in the licensing process. This license, **and any CONTENT (PDF or image file) purchased as part of your order,** is for a one-time use only and limited to any maximum distribution number specified in the license. The first instance of republication or reuse granted by this license must be completed within two years of the date of the grant of this license (although copies prepared before the end date may be distributed thereafter). The Wiley Materials shall not be used in any other manner or for any other purpose, beyond what is granted in the license. Permission is granted subject to an appropriate acknowledgement given to the author, title of the material/book/journal and the publisher. You shall also duplicate the copyright notice that appears in the Wiley publication in your use of the Wiley Material. Permission is also granted on the understanding that nowhere in the text is a previously published source acknowledged for all or part of this Wiley Material. Any third party content is expressly excluded from this permission.

- With respect to the Wiley Materials, all rights are reserved. Except as expressly granted by the terms of the license, no part of the Wiley Materials may be copied, modified, adapted (except for minor reformatting required by the new Publication), translated, reproduced, transferred or distributed, in any form or by any means, and no derivative works may be made based on the Wiley Materials without the prior permission of the respective copyright owner.**For STM Signatory Publishers clearing permission under the terms of the STM Permissions Guidelines only, the terms of the license are extended to include subsequent editions and for editions in other languages, provided such editions are for the work as a whole in situ and does not involve the separate exploitation of the permitted figures or extracts,** You may not alter, remove or suppress in any manner any copyright, trademark or other notices displayed by the Wiley Materials. You may not license, rent, sell, loan, lease, pledge, offer as security, transfer or assign the Wiley Materials on a stand-alone

basis, or any of the rights granted to you hereunder to any other person.

- The Wiley Materials and all of the intellectual property rights therein shall at all times remain the exclusive property of John Wiley & Sons Inc, the Wiley Companies, or their respective licensors, and your interest therein is only that of having possession of and the right to reproduce the Wiley Materials pursuant to Section 2 herein during the continuance of this Agreement. You agree that you own no right, title or interest in or to the Wiley Materials or any of the intellectual property rights therein. You shall have no rights hereunder other than the license as provided for above in Section 2. No right, license or interest to any trademark, trade name, service mark or other branding ("Marks") of WILEY or its licensors is granted hereunder, and you agree that you shall not assert any such right, license or interest with respect thereto

- NEITHER WILEY NOR ITS LICENSORS MAKES ANY WARRANTY OR REPRESENTATION OF ANY KIND TO YOU OR ANY THIRD PARTY, EXPRESS, IMPLIED OR STATUTORY, WITH RESPECT TO THE MATERIALS OR THE ACCURACY OF ANY INFORMATION CONTAINED IN THE MATERIALS, INCLUDING, WITHOUT LIMITATION, ANY IMPLIED WARRANTY OF MERCHANTABILITY, ACCURACY, SATISFACTORY QUALITY, FITNESS FOR A PARTICULAR PURPOSE, USABILITY, INTEGRATION OR NON-INFRINGEMENT AND ALL SUCH WARRANTIES ARE HEREBY EXCLUDED BY WILEY AND ITS LICENSORS AND WAIVED BY YOU.

- WILEY shall have the right to terminate this Agreement immediately upon breach of this Agreement by you.

- You shall indemnify, defend and hold harmless WILEY, its Licensors and their respective directors, officers, agents and employees, from and against any actual or threatened claims, demands, causes of action or proceedings arising from any breach of this Agreement by you.

- IN NO EVENT SHALL WILEY OR ITS LICENSORS BE LIABLE TO YOU OR ANY OTHER PARTY OR ANY OTHER PERSON OR ENTITY FOR ANY SPECIAL, CONSEQUENTIAL, INCIDENTAL, INDIRECT, EXEMPLARY OR PUNITIVE DAMAGES, HOWEVER CAUSED, ARISING OUT OF OR IN CONNECTION WITH THE DOWNLOADING, PROVISIONING, VIEWING OR USE OF THE MATERIALS REGARDLESS OF THE FORM OF ACTION, WHETHER FOR BREACH OF CONTRACT, BREACH OF WARRANTY, TORT, NEGLIGENCE, INFRINGEMENT OR OTHERWISE (INCLUDING, WITHOUT LIMITATION, DAMAGES BASED ON LOSS OF PROFITS, DATA, FILES, USE, BUSINESS OPPORTUNITY OR CLAIMS OF THIRD PARTIES), AND WHETHER OR NOT THE PARTY HAS BEEN ADVISED OF THE POSSIBILITY OF SUCH DAMAGES. THIS LIMITATION SHALL APPLY NOTWITHSTANDING ANY FAILURE OF ESSENTIAL PURPOSE OF ANY LIMITED REMEDY PROVIDED HEREIN.

- Should any provision of this Agreement be held by a court of competent jurisdiction to be illegal, invalid, or unenforceable, that provision shall be deemed amended to achieve as nearly as possible the same economic effect as the original provision, and

the legality, validity and enforceability of the remaining provisions of this Agreement shall not be affected or impaired thereby.

- The failure of either party to enforce any term or condition of this Agreement shall not constitute a waiver of either party's right to enforce each and every term and condition of this Agreement. No breach under this agreement shall be deemed waived or excused by either party unless such waiver or consent is in writing signed by the party granting such waiver or consent. The waiver by or consent of a party to a breach of any provision of this Agreement shall not operate or be construed as a waiver of or consent to any other or subsequent breach by such other party.

- This Agreement may not be assigned (including by operation of law or otherwise) by you without WILEY's prior written consent.

- Any fee required for this permission shall be non-refundable after thirty (30) days from receipt by the CCC.

- These terms and conditions together with CCC's Billing and Payment terms and conditions (which are incorporated herein) form the entire agreement between you and WILEY concerning this licensing transaction and (in the absence of fraud) supersedes all prior agreements and representations of the parties, oral or written. This Agreement may not be amended except in writing signed by both parties. This Agreement shall be binding upon and inure to the benefit of the parties' successors, legal representatives, and authorized assigns.

- In the event of any conflict between your obligations established by these terms and conditions and those established by CCC's Billing and Payment terms and conditions, these terms and conditions shall prevail.

- WILEY expressly reserves all rights not specifically granted in the combination of (i) the license details provided by you and accepted in the course of this licensing transaction, (ii) these terms and conditions and (iii) CCC's Billing and Payment terms and conditions.

- This Agreement will be void if the Type of Use, Format, Circulation, or Requestor Type was misrepresented during the licensing process.

- This Agreement shall be governed by and construed in accordance with the laws of the State of New York, USA, without regards to such state's conflict of law rules. Any legal action, suit or proceeding arising out of or relating to these Terms and Conditions or the breach thereof shall be instituted in a court of competent jurisdiction in New York County in the State of New York in the United States of America and each party hereby consents and submits to the personal jurisdiction of such court, waives any objection to venue in such court and consents to service of process by registered or certified mail, return receipt requested, at the last known address of such party.

WILEY OPEN ACCESS TERMS AND CONDITIONS

Wiley Publishes Open Access Articles in fully Open Access Journals and in Subscription journals offering Online Open. Although most of the fully Open Access journals publish open access articles under the terms of the Creative Commons Attribution (CC BY) License

only, the subscription journals and a few of the Open Access Journals offer a choice of Creative Commons Licenses. The license type is clearly identified on the article.

The Creative Commons Attribution License

The Creative Commons Attribution License (CC-BY) allows users to copy, distribute and transmit an article, adapt the article and make commercial use of the article. The CC-BY license permits commercial and non-

Creative Commons Attribution Non-Commercial License

The Creative Commons Attribution Non-Commercial (CC-BY-NC)License permits use, distribution and reproduction in any medium, provided the original work is properly cited and is not used for commercial purposes.(see below)

Creative Commons Attribution-Non-Commercial-NoDerivs License

The Creative Commons Attribution Non-Commercial-NoDerivs License (CC-BY-NC-ND) permits use, distribution and reproduction in any medium, provided the original work is properly cited, is not used for commercial purposes and no modifications or adaptations are made. (see below)

Use by commercial "for-profit" organizations

Use of Wiley Open Access articles for commercial, promotional, or marketing purposes requires further explicit permission from Wiley and will be subject to a fee.
Further details can be found on Wiley Online Library
http://olabout.wiley.com/WileyCDA/Section/id-410895.html

Other Terms and Conditions:

v1.10 Last updated September 2015

Questions? customercare@copyright.com or +1-855-239-3415 (toll free in the US) or +1-978-646-2777.

JOHN WILEY AND SONS LICENSE TERMS AND CONDITIONS

May 24, 2017

This Agreement between Ms. Ping Liang ("You") and John Wiley and Sons ("John Wiley and Sons") consists of your license details and the terms and conditions provided by John Wiley and Sons and Copyright Clearance Center.

License Number	4115250493225
License date	May 24, 2017
Licensed Content Publisher	John Wiley and Sons
Licensed Content Publication	Advanced Materials
Licensed Content Title	From Bimetallic Metal-Organic Framework to Porous Carbon: High Surface Area and Multicomponent Active Dopants for Excellent Electrocatalysis
Licensed Content Author	Yu-Zhen Chen,Chengming Wang,Zhen-Yu Wu,Yujie Xiong,Qiang Xu,Shu-Hong Yu,Hai-Long Jiang
Licensed Content Date	Jul 20, 2015
Licensed Content Pages	7
Type of use	Dissertation/Thesis
Requestor type	University/Academic
Format	Print and electronic
Portion	Figure/table
Number of figures/tables	2
Original Wiley figure/table number(s)	Figure 2, Figure 3
Will you be translating?	No
Title of your thesis / dissertation	Synthesis and Evaluation of Nanostructured Membrane Catalytic Systems for Water Treatment
Expected completion date	Jun 2017
Expected size (number of pages)	200
Requestor Location	Ms. Ping Liang 4-31 nottingham street, east vic park perth, WA 6101 Australia Attn: Ms. Ping Liang
Publisher Tax ID	EU826007151
Billing Type	Invoice
Billing Address	Ms. Ping Liang 4-31 nottingham street, east vic park

perth, Australia 6101
Attn: Ms. Ping Liang

Total 0.00 AUD

Terms and Conditions

TERMS AND CONDITIONS

This copyrighted material is owned by or exclusively licensed to John Wiley & Sons, Inc. or one of its group companies (each a"Wiley Company") or handled on behalf of a society with which a Wiley Company has exclusive publishing rights in relation to a particular work (collectively "WILEY"). By clicking "accept" in connection with completing this licensing transaction, you agree that the following terms and conditions apply to this transaction (along with the billing and payment terms and conditions established by the Copyright Clearance Center Inc., ("CCC's Billing and Payment terms and conditions"), at the time that you opened your RightsLink account (these are available at any time at http://myaccount.copyright.com).

Terms and Conditions

- The materials you have requested permission to reproduce or reuse (the "Wiley Materials") are protected by copyright.

- You are hereby granted a personal, non-exclusive, non-sub licensable (on a stand-alone basis), non-transferable, worldwide, limited license to reproduce the Wiley Materials for the purpose specified in the licensing process. This license, **and any CONTENT (PDF or image file) purchased as part of your order,** is for a one-time use only and limited to any maximum distribution number specified in the license. The first instance of republication or reuse granted by this license must be completed within two years of the date of the grant of this license (although copies prepared before the end date may be distributed thereafter). The Wiley Materials shall not be used in any other manner or for any other purpose, beyond what is granted in the license. Permission is granted subject to an appropriate acknowledgement given to the author, title of the material/book/journal and the publisher. You shall also duplicate the copyright notice that appears in the Wiley publication in your use of the Wiley Material. Permission is also granted on the understanding that nowhere in the text is a previously published source acknowledged for all or part of this Wiley Material. Any third party content is expressly excluded from this permission.

- With respect to the Wiley Materials, all rights are reserved. Except as expressly granted by the terms of the license, no part of the Wiley Materials may be copied, modified, adapted (except for minor reformatting required by the new Publication), translated, reproduced, transferred or distributed, in any form or by any means, and no derivative works may be made based on the Wiley Materials without the prior permission of the respective copyright owner.**For STM Signatory Publishers clearing permission under the terms of the STM Permissions Guidelines only, the terms of the license are extended to include subsequent editions and for editions in other languages, provided such editions are for the work as a whole in situ and does not involve the separate exploitation of the permitted figures or extracts,** You may not alter, remove or suppress in any manner any copyright, trademark or other notices displayed by the Wiley Materials. You may not license, rent, sell, loan, lease, pledge, offer as security, transfer or assign the Wiley Materials on a stand-alone

basis, or any of the rights granted to you hereunder to any other person.

- The Wiley Materials and all of the intellectual property rights therein shall at all times remain the exclusive property of John Wiley & Sons Inc, the Wiley Companies, or their respective licensors, and your interest therein is only that of having possession of and the right to reproduce the Wiley Materials pursuant to Section 2 herein during the continuance of this Agreement. You agree that you own no right, title or interest in or to the Wiley Materials or any of the intellectual property rights therein. You shall have no rights hereunder other than the license as provided for above in Section 2. No right, license or interest to any trademark, trade name, service mark or other branding ("Marks") of WILEY or its licensors is granted hereunder, and you agree that you shall not assert any such right, license or interest with respect thereto

- NEITHER WILEY NOR ITS LICENSORS MAKES ANY WARRANTY OR REPRESENTATION OF ANY KIND TO YOU OR ANY THIRD PARTY, EXPRESS, IMPLIED OR STATUTORY, WITH RESPECT TO THE MATERIALS OR THE ACCURACY OF ANY INFORMATION CONTAINED IN THE MATERIALS, INCLUDING, WITHOUT LIMITATION, ANY IMPLIED WARRANTY OF MERCHANTABILITY, ACCURACY, SATISFACTORY QUALITY, FITNESS FOR A PARTICULAR PURPOSE, USABILITY, INTEGRATION OR NON-INFRINGEMENT AND ALL SUCH WARRANTIES ARE HEREBY EXCLUDED BY WILEY AND ITS LICENSORS AND WAIVED BY YOU.

- WILEY shall have the right to terminate this Agreement immediately upon breach of this Agreement by you.

- You shall indemnify, defend and hold harmless WILEY, its Licensors and their respective directors, officers, agents and employees, from and against any actual or threatened claims, demands, causes of action or proceedings arising from any breach of this Agreement by you.

- IN NO EVENT SHALL WILEY OR ITS LICENSORS BE LIABLE TO YOU OR ANY OTHER PARTY OR ANY OTHER PERSON OR ENTITY FOR ANY SPECIAL, CONSEQUENTIAL, INCIDENTAL, INDIRECT, EXEMPLARY OR PUNITIVE DAMAGES, HOWEVER CAUSED, ARISING OUT OF OR IN CONNECTION WITH THE DOWNLOADING, PROVISIONING, VIEWING OR USE OF THE MATERIALS REGARDLESS OF THE FORM OF ACTION, WHETHER FOR BREACH OF CONTRACT, BREACH OF WARRANTY, TORT, NEGLIGENCE, INFRINGEMENT OR OTHERWISE (INCLUDING, WITHOUT LIMITATION, DAMAGES BASED ON LOSS OF PROFITS, DATA, FILES, USE, BUSINESS OPPORTUNITY OR CLAIMS OF THIRD PARTIES), AND WHETHER OR NOT THE PARTY HAS BEEN ADVISED OF THE POSSIBILITY OF SUCH DAMAGES. THIS LIMITATION SHALL APPLY NOTWITHSTANDING ANY FAILURE OF ESSENTIAL PURPOSE OF ANY LIMITED REMEDY PROVIDED HEREIN.

- Should any provision of this Agreement be held by a court of competent jurisdiction to be illegal, invalid, or unenforceable, that provision shall be deemed amended to achieve as nearly as possible the same economic effect as the original provision, and

the legality, validity and enforceability of the remaining provisions of this Agreement shall not be affected or impaired thereby.

- The failure of either party to enforce any term or condition of this Agreement shall not constitute a waiver of either party's right to enforce each and every term and condition of this Agreement. No breach under this agreement shall be deemed waived or excused by either party unless such waiver or consent is in writing signed by the party granting such waiver or consent. The waiver by or consent of a party to a breach of any provision of this Agreement shall not operate or be construed as a waiver of or consent to any other or subsequent breach by such other party.

- This Agreement may not be assigned (including by operation of law or otherwise) by you without WILEY's prior written consent.

- Any fee required for this permission shall be non-refundable after thirty (30) days from receipt by the CCC.

- These terms and conditions together with CCC's Billing and Payment terms and conditions (which are incorporated herein) form the entire agreement between you and WILEY concerning this licensing transaction and (in the absence of fraud) supersedes all prior agreements and representations of the parties, oral or written. This Agreement may not be amended except in writing signed by both parties. This Agreement shall be binding upon and inure to the benefit of the parties' successors, legal representatives, and authorized assigns.

- In the event of any conflict between your obligations established by these terms and conditions and those established by CCC's Billing and Payment terms and conditions, these terms and conditions shall prevail.

- WILEY expressly reserves all rights not specifically granted in the combination of (i) the license details provided by you and accepted in the course of this licensing transaction, (ii) these terms and conditions and (iii) CCC's Billing and Payment terms and conditions.

- This Agreement will be void if the Type of Use, Format, Circulation, or Requestor Type was misrepresented during the licensing process.

- This Agreement shall be governed by and construed in accordance with the laws of the State of New York, USA, without regards to such state's conflict of law rules. Any legal action, suit or proceeding arising out of or relating to these Terms and Conditions or the breach thereof shall be instituted in a court of competent jurisdiction in New York County in the State of New York in the United States of America and each party hereby consents and submits to the personal jurisdiction of such court, waives any objection to venue in such court and consents to service of process by registered or certified mail, return receipt requested, at the last known address of such party.

WILEY OPEN ACCESS TERMS AND CONDITIONS

Wiley Publishes Open Access Articles in fully Open Access Journals and in Subscription journals offering Online Open. Although most of the fully Open Access journals publish open access articles under the terms of the Creative Commons Attribution (CC BY) License

only, the subscription journals and a few of the Open Access Journals offer a choice of Creative Commons Licenses. The license type is clearly identified on the article.

The Creative Commons Attribution License

The Creative Commons Attribution License (CC-BY) allows users to copy, distribute and transmit an article, adapt the article and make commercial use of the article. The CC-BY license permits commercial and non-

Creative Commons Attribution Non-Commercial License

The Creative Commons Attribution Non-Commercial (CC-BY-NC)License permits use, distribution and reproduction in any medium, provided the original work is properly cited and is not used for commercial purposes.(see below)

Creative Commons Attribution-Non-Commercial-NoDerivs License

The Creative Commons Attribution Non-Commercial-NoDerivs License (CC-BY-NC-ND) permits use, distribution and reproduction in any medium, provided the original work is properly cited, is not used for commercial purposes and no modifications or adaptations are made. (see below)

Use by commercial "for-profit" organizations

Use of Wiley Open Access articles for commercial, promotional, or marketing purposes requires further explicit permission from Wiley and will be subject to a fee.
Further details can be found on Wiley Online Library
http://olabout.wiley.com/WileyCDA/Section/id-410895.html

Other Terms and Conditions:

v1.10 Last updated September 2015

Questions? customercare@copyright.com or +1-855-239-3415 (toll free in the US) or +1-978-646-2777.

JOHN WILEY AND SONS LICENSE TERMS AND CONDITIONS

May 24, 2017

This Agreement between Ms. Ping Liang ("You") and John Wiley and Sons ("John Wiley and Sons") consists of your license details and the terms and conditions provided by John Wiley and Sons and Copyright Clearance Center.

License Number	4115260923132
License date	May 24, 2017
Licensed Content Publisher	John Wiley and Sons
Licensed Content Publication	Advanced Energy Materials
Licensed Content Title	Metal−Organic Framework-Derived Nitrogen-Doped Core-Shell-Structured Porous Fe/Fe3C@C Nanoboxes Supported on Graphene Sheets for Efficient Oxygen Reduction Reactions
Licensed Content Author	Yang Hou,Taizhong Huang,Zhenhai Wen,Shun Mao,Shumao Cui,Junhong Chen
Licensed Content Date	Apr 4, 2014
Licensed Content Pages	1
Type of use	Dissertation/Thesis
Requestor type	University/Academic
Format	Print and electronic
Portion	Figure/table
Number of figures/tables	1
Original Wiley figure/table number(s)	Figure 4
Will you be translating?	No
Title of your thesis / dissertation	Synthesis and Evaluation of Nanostructured Membrane Catalytic Systems for Water Treatment
Expected completion date	Jun 2017
Expected size (number of pages)	200
Requestor Location	Ms. Ping Liang 4-31 nottingham street, east vic park perth, WA 6101 Australia Attn: Ms. Ping Liang
Publisher Tax ID	EU826007151
Billing Type	Invoice
Billing Address	Ms. Ping Liang 4-31 nottingham street, east vic park

perth, Australia 6101
Attn: Ms. Ping Liang

Total 0.00 AUD

Terms and Conditions

TERMS AND CONDITIONS

This copyrighted material is owned by or exclusively licensed to John Wiley & Sons, Inc. or one of its group companies (each a"Wiley Company") or handled on behalf of a society with which a Wiley Company has exclusive publishing rights in relation to a particular work (collectively "WILEY"). By clicking "accept" in connection with completing this licensing transaction, you agree that the following terms and conditions apply to this transaction (along with the billing and payment terms and conditions established by the Copyright Clearance Center Inc., ("CCC's Billing and Payment terms and conditions"), at the time that you opened your RightsLink account (these are available at any time at http://myaccount.copyright.com).

Terms and Conditions

- The materials you have requested permission to reproduce or reuse (the "Wiley Materials") are protected by copyright.

- You are hereby granted a personal, non-exclusive, non-sub licensable (on a stand-alone basis), non-transferable, worldwide, limited license to reproduce the Wiley Materials for the purpose specified in the licensing process. This license, **and any CONTENT (PDF or image file) purchased as part of your order,** is for a one-time use only and limited to any maximum distribution number specified in the license. The first instance of republication or reuse granted by this license must be completed within two years of the date of the grant of this license (although copies prepared before the end date may be distributed thereafter). The Wiley Materials shall not be used in any other manner or for any other purpose, beyond what is granted in the license. Permission is granted subject to an appropriate acknowledgement given to the author, title of the material/book/journal and the publisher. You shall also duplicate the copyright notice that appears in the Wiley publication in your use of the Wiley Material. Permission is also granted on the understanding that nowhere in the text is a previously published source acknowledged for all or part of this Wiley Material. Any third party content is expressly excluded from this permission.

- With respect to the Wiley Materials, all rights are reserved. Except as expressly granted by the terms of the license, no part of the Wiley Materials may be copied, modified, adapted (except for minor reformatting required by the new Publication), translated, reproduced, transferred or distributed, in any form or by any means, and no derivative works may be made based on the Wiley Materials without the prior permission of the respective copyright owner.**For STM Signatory Publishers clearing permission under the terms of the STM Permissions Guidelines only, the terms of the license are extended to include subsequent editions and for editions in other languages, provided such editions are for the work as a whole in situ and does not involve the separate exploitation of the permitted figures or extracts,** You may not alter, remove or suppress in any manner any copyright, trademark or other notices displayed by the Wiley Materials. You may not license, rent, sell, loan, lease, pledge, offer as security, transfer or assign the Wiley Materials on a stand-alone

basis, or any of the rights granted to you hereunder to any other person.

- The Wiley Materials and all of the intellectual property rights therein shall at all times remain the exclusive property of John Wiley & Sons Inc, the Wiley Companies, or their respective licensors, and your interest therein is only that of having possession of and the right to reproduce the Wiley Materials pursuant to Section 2 herein during the continuance of this Agreement. You agree that you own no right, title or interest in or to the Wiley Materials or any of the intellectual property rights therein. You shall have no rights hereunder other than the license as provided for above in Section 2. No right, license or interest to any trademark, trade name, service mark or other branding ("Marks") of WILEY or its licensors is granted hereunder, and you agree that you shall not assert any such right, license or interest with respect thereto

- NEITHER WILEY NOR ITS LICENSORS MAKES ANY WARRANTY OR REPRESENTATION OF ANY KIND TO YOU OR ANY THIRD PARTY, EXPRESS, IMPLIED OR STATUTORY, WITH RESPECT TO THE MATERIALS OR THE ACCURACY OF ANY INFORMATION CONTAINED IN THE MATERIALS, INCLUDING, WITHOUT LIMITATION, ANY IMPLIED WARRANTY OF MERCHANTABILITY, ACCURACY, SATISFACTORY QUALITY, FITNESS FOR A PARTICULAR PURPOSE, USABILITY, INTEGRATION OR NON-INFRINGEMENT AND ALL SUCH WARRANTIES ARE HEREBY EXCLUDED BY WILEY AND ITS LICENSORS AND WAIVED BY YOU.

- WILEY shall have the right to terminate this Agreement immediately upon breach of this Agreement by you.

- You shall indemnify, defend and hold harmless WILEY, its Licensors and their respective directors, officers, agents and employees, from and against any actual or threatened claims, demands, causes of action or proceedings arising from any breach of this Agreement by you.

- IN NO EVENT SHALL WILEY OR ITS LICENSORS BE LIABLE TO YOU OR ANY OTHER PARTY OR ANY OTHER PERSON OR ENTITY FOR ANY SPECIAL, CONSEQUENTIAL, INCIDENTAL, INDIRECT, EXEMPLARY OR PUNITIVE DAMAGES, HOWEVER CAUSED, ARISING OUT OF OR IN CONNECTION WITH THE DOWNLOADING, PROVISIONING, VIEWING OR USE OF THE MATERIALS REGARDLESS OF THE FORM OF ACTION, WHETHER FOR BREACH OF CONTRACT, BREACH OF WARRANTY, TORT, NEGLIGENCE, INFRINGEMENT OR OTHERWISE (INCLUDING, WITHOUT LIMITATION, DAMAGES BASED ON LOSS OF PROFITS, DATA, FILES, USE, BUSINESS OPPORTUNITY OR CLAIMS OF THIRD PARTIES), AND WHETHER OR NOT THE PARTY HAS BEEN ADVISED OF THE POSSIBILITY OF SUCH DAMAGES. THIS LIMITATION SHALL APPLY NOTWITHSTANDING ANY FAILURE OF ESSENTIAL PURPOSE OF ANY LIMITED REMEDY PROVIDED HEREIN.

- Should any provision of this Agreement be held by a court of competent jurisdiction to be illegal, invalid, or unenforceable, that provision shall be deemed amended to achieve as nearly as possible the same economic effect as the original provision, and

the legality, validity and enforceability of the remaining provisions of this Agreement shall not be affected or impaired thereby.

- The failure of either party to enforce any term or condition of this Agreement shall not constitute a waiver of either party's right to enforce each and every term and condition of this Agreement. No breach under this agreement shall be deemed waived or excused by either party unless such waiver or consent is in writing signed by the party granting such waiver or consent. The waiver by or consent of a party to a breach of any provision of this Agreement shall not operate or be construed as a waiver of or consent to any other or subsequent breach by such other party.

- This Agreement may not be assigned (including by operation of law or otherwise) by you without WILEY's prior written consent.

- Any fee required for this permission shall be non-refundable after thirty (30) days from receipt by the CCC.

- These terms and conditions together with CCC's Billing and Payment terms and conditions (which are incorporated herein) form the entire agreement between you and WILEY concerning this licensing transaction and (in the absence of fraud) supersedes all prior agreements and representations of the parties, oral or written. This Agreement may not be amended except in writing signed by both parties. This Agreement shall be binding upon and inure to the benefit of the parties' successors, legal representatives, and authorized assigns.

- In the event of any conflict between your obligations established by these terms and conditions and those established by CCC's Billing and Payment terms and conditions, these terms and conditions shall prevail.

- WILEY expressly reserves all rights not specifically granted in the combination of (i) the license details provided by you and accepted in the course of this licensing transaction, (ii) these terms and conditions and (iii) CCC's Billing and Payment terms and conditions.

- This Agreement will be void if the Type of Use, Format, Circulation, or Requestor Type was misrepresented during the licensing process.

- This Agreement shall be governed by and construed in accordance with the laws of the State of New York, USA, without regards to such state's conflict of law rules. Any legal action, suit or proceeding arising out of or relating to these Terms and Conditions or the breach thereof shall be instituted in a court of competent jurisdiction in New York County in the State of New York in the United States of America and each party hereby consents and submits to the personal jurisdiction of such court, waives any objection to venue in such court and consents to service of process by registered or certified mail, return receipt requested, at the last known address of such party.

WILEY OPEN ACCESS TERMS AND CONDITIONS

Wiley Publishes Open Access Articles in fully Open Access Journals and in Subscription journals offering Online Open. Although most of the fully Open Access journals publish open access articles under the terms of the Creative Commons Attribution (CC BY) License

only, the subscription journals and a few of the Open Access Journals offer a choice of Creative Commons Licenses. The license type is clearly identified on the article.

The Creative Commons Attribution License

The Creative Commons Attribution License (CC-BY) allows users to copy, distribute and transmit an article, adapt the article and make commercial use of the article. The CC-BY license permits commercial and non-

Creative Commons Attribution Non-Commercial License

The Creative Commons Attribution Non-Commercial (CC-BY-NC)License permits use, distribution and reproduction in any medium, provided the original work is properly cited and is not used for commercial purposes.(see below)

Creative Commons Attribution-Non-Commercial-NoDerivs License

The Creative Commons Attribution Non-Commercial-NoDerivs License (CC-BY-NC-ND) permits use, distribution and reproduction in any medium, provided the original work is properly cited, is not used for commercial purposes and no modifications or adaptations are made. (see below)

Use by commercial "for-profit" organizations

Use of Wiley Open Access articles for commercial, promotional, or marketing purposes requires further explicit permission from Wiley and will be subject to a fee.
Further details can be found on Wiley Online Library
http://olabout.wiley.com/WileyCDA/Section/id-410895.html

Other Terms and Conditions:

v1.10 Last updated September 2015

Questions? customercare@copyright.com or +1-855-239-3415 (toll free in the US) or +1-978-646-2777.

Title: Hollow Cobalt-Based Bimetallic Sulfide Polyhedra for Efficient All-pH-Value Electrochemical and Photocatalytic Hydrogen Evolution

Author: Zhen-Feng Huang, Jiajia Song, Ke Li, et al

Publication: Journal of the American Chemical Society

Publisher: American Chemical Society

Date: Feb 1, 2016

PERMISSION/LICENSE IS GRANTED FOR YOUR ORDER AT NO CHARGE

This type of permission/license, instead of the standard Terms & Conditions, is sent to you because no fee is being charged for your order. Please note the following:

- Permission is granted for your request in both print and electronic formats, and translations.
- If figures and/or tables were requested, they may be adapted or used in part.
- Please print this page for your records and send a copy of it to your publisher/graduate school.
- Appropriate credit for the requested material should be given as follows: "Reprinted (adapted) with permission from (COMPLETE REFERENCE CITATION). Copyright (YEAR) American Chemical Society." Insert appropriate information in place of the capitalized words.
- One-time permission is granted only for the use specified in your request. No additional uses are granted (such as derivative works or other editions). For any other uses, please submit a new request.

If credit is given to another source for the material you requested, permission must be obtained from that source.

BACK CLOSE WINDOW

NATURE PUBLISHING GROUP LICENSE TERMS AND CONDITIONS

May 24, 2017

This Agreement between Ms. Ping Liang ("You") and Nature Publishing Group ("Nature Publishing Group") consists of your license details and the terms and conditions provided by Nature Publishing Group and Copyright Clearance Center.

License Number	4115310345911
License date	May 24, 2017
Licensed Content Publisher	Nature Publishing Group
Licensed Content Publication	Nature Energy
Licensed Content Title	A metal–organic framework-derived bifunctional oxygen electrocatalyst
Licensed Content Author	Bao Yu Xia, Ya Yan, Nan Li, Hao Bin Wu, Xiong Wen (David) Lou et al.
Licensed Content Date	Jan 11, 2016
Licensed Content Volume	1
Licensed Content Issue	1
Type of Use	reuse in a dissertation / thesis
Requestor type	academic/educational
Format	print and electronic
Portion	figures/tables/illustrations
Number of figures/tables/illustrations	3
High-res required	no
Figures	Figure 1, Figure 5, Figure 7
Author of this NPG article	no
Your reference number	
Title of your thesis / dissertation	Synthesis and Evaluation of Nanostructured Membrane Catalytic Systems for Water Treatment
Expected completion date	Jun 2017
Estimated size (number of pages)	200
Requestor Location	Ms. Ping Liang 4-31 nottingham street, east vic park perth, WA 6101 Australia Attn: Ms. Ping Liang
Billing Type	Invoice
Billing Address	Ms. Ping Liang

4-31 nottingham street, east vic park

perth, Australia 6101
Attn: Ms. Ping Liang

Total 0.00 AUD

Terms and Conditions

Terms and Conditions for Permissions

Nature Publishing Group hereby grants you a non-exclusive license to reproduce this material for this purpose, and for no other use,subject to the conditions below:

1. NPG warrants that it has, to the best of its knowledge, the rights to license reuse of this material. However, you should ensure that the material you are requesting is original to Nature Publishing Group and does not carry the copyright of another entity (as credited in the published version). If the credit line on any part of the material you have requested indicates that it was reprinted or adapted by NPG with permission from another source, then you should also seek permission from that source to reuse the material.

2. Permission granted free of charge for material in print is also usually granted for any electronic version of that work, provided that the material is incidental to the work as a whole and that the electronic version is essentially equivalent to, or substitutes for, the print version.Where print permission has been granted for a fee, separate permission must be obtained for any additional, electronic re-use (unless, as in the case of a full paper, this has already been accounted for during your initial request in the calculation of a print run).NB: In all cases, web-based use of full-text articles must be authorized separately through the 'Use on a Web Site' option when requesting permission.

3. Permission granted for a first edition does not apply to second and subsequent editions and for editions in other languages (except for signatories to the STM Permissions Guidelines, or where the first edition permission was granted for free).

4. Nature Publishing Group's permission must be acknowledged next to the figure, table or abstract in print. In electronic form, this acknowledgement must be visible at the same time as the figure/table/abstract, and must be hyperlinked to the journal's homepage.

5. The credit line should read:
   Reprinted by permission from Macmillan Publishers Ltd: [JOURNAL NAME] (reference citation), copyright (year of publication)
   For AOP papers, the credit line should read:
   Reprinted by permission from Macmillan Publishers Ltd: [JOURNAL NAME], advance online publication, day month year (doi: 10.1038/sj.[JOURNAL ACRONYM].XXXXX)

   Note: For republication from the *British Journal of Cancer,* the following credit lines apply.
   Reprinted by permission from Macmillan Publishers Ltd on behalf of Cancer Research UK: [JOURNAL NAME] (reference citation), copyright (year of publication)For AOP papers, the credit line should read:
   Reprinted by permission from Macmillan Publishers Ltd on behalf of Cancer Research UK: [JOURNAL NAME], advance online publication, day month year (doi: 10.1038/sj.[JOURNAL ACRONYM].XXXXX)

6. Adaptations of single figures do not require NPG approval. However, the adaptation should be credited as follows:

   Adapted by permission from Macmillan Publishers Ltd: [JOURNAL NAME] (reference citation), copyright (year of publication)

Note: For adaptation from the *British Journal of Cancer,* the following credit line applies.
Adapted by permission from Macmillan Publishers Ltd on behalf of Cancer Research UK: [JOURNAL NAME] (reference citation), copyright (year of publication)

7. Translations of 401 words up to a whole article require NPG approval. Please visit http://www.macmillanmedicalcommunications.com for more information.Translations of up to a 400 words do not require NPG approval. The translation should be credited as follows:

   Translated by permission from Macmillan Publishers Ltd: [JOURNAL NAME] (reference citation), copyright (year of publication).

   Note: For translation from the *British Journal of Cancer,* the following credit line applies.
   Translated by permission from Macmillan Publishers Ltd on behalf of Cancer Research UK: [JOURNAL NAME] (reference citation), copyright (year of publication)

We are certain that all parties will benefit from this agreement and wish you the best in the use of this material. Thank you.
Special Terms:
v1.1

Questions? customercare@copyright.com or +1-855-239-3415 (toll free in the US) or +1-978-646-2777.

JOHN WILEY AND SONS LICENSE TERMS AND CONDITIONS

May 24, 2017

This Agreement between Ms. Ping Liang ("You") and John Wiley and Sons ("John Wiley and Sons") consists of your license details and the terms and conditions provided by John Wiley and Sons and Copyright Clearance Center.

License Number	4115280972275
License date	May 24, 2017
Licensed Content Publisher	John Wiley and Sons
Licensed Content Publication	Advanced Materials
Licensed Content Title	MOF-Derived Porous ZnO/ZnFe2O4/C Octahedra with Hollow Interiors for High-Rate Lithium-Ion Batteries
Licensed Content Author	Feng Zou,Xianluo Hu,Zhen Li,Long Qie,Chenchen Hu,Rui Zeng,Yan Jiang,Yunhui Huang
Licensed Content Date	Aug 14, 2014
Licensed Content Pages	7
Type of use	Dissertation/Thesis
Requestor type	University/Academic
Format	Print and electronic
Portion	Figure/table
Number of figures/tables	3
Original Wiley figure/table number(s)	Figure 1, Figure 3, Figure 4
Will you be translating?	No
Title of your thesis / dissertation	Synthesis and Evaluation of Nanostructured Membrane Catalytic Systems for Water Treatment
Expected completion date	Jun 2017
Expected size (number of pages)	200
Requestor Location	Ms. Ping Liang 4-31 nottingham street, east vic park perth, WA 6101 Australia Attn: Ms. Ping Liang
Publisher Tax ID	EU826007151
Billing Type	Invoice
Billing Address	Ms. Ping Liang 4-31 nottingham street, east vic park

perth, Australia 6101
Attn: Ms. Ping Liang

Total 0.00 AUD

Terms and Conditions

TERMS AND CONDITIONS

This copyrighted material is owned by or exclusively licensed to John Wiley & Sons, Inc. or one of its group companies (each a"Wiley Company") or handled on behalf of a society with which a Wiley Company has exclusive publishing rights in relation to a particular work (collectively "WILEY"). By clicking "accept" in connection with completing this licensing transaction, you agree that the following terms and conditions apply to this transaction (along with the billing and payment terms and conditions established by the Copyright Clearance Center Inc., ("CCC's Billing and Payment terms and conditions"), at the time that you opened your RightsLink account (these are available at any time at http://myaccount.copyright.com).

Terms and Conditions

- The materials you have requested permission to reproduce or reuse (the "Wiley Materials") are protected by copyright.

- You are hereby granted a personal, non-exclusive, non-sub licensable (on a stand-alone basis), non-transferable, worldwide, limited license to reproduce the Wiley Materials for the purpose specified in the licensing process. This license, **and any CONTENT (PDF or image file) purchased as part of your order,** is for a one-time use only and limited to any maximum distribution number specified in the license. The first instance of republication or reuse granted by this license must be completed within two years of the date of the grant of this license (although copies prepared before the end date may be distributed thereafter). The Wiley Materials shall not be used in any other manner or for any other purpose, beyond what is granted in the license. Permission is granted subject to an appropriate acknowledgement given to the author, title of the material/book/journal and the publisher. You shall also duplicate the copyright notice that appears in the Wiley publication in your use of the Wiley Material. Permission is also granted on the understanding that nowhere in the text is a previously published source acknowledged for all or part of this Wiley Material. Any third party content is expressly excluded from this permission.

- With respect to the Wiley Materials, all rights are reserved. Except as expressly granted by the terms of the license, no part of the Wiley Materials may be copied, modified, adapted (except for minor reformatting required by the new Publication), translated, reproduced, transferred or distributed, in any form or by any means, and no derivative works may be made based on the Wiley Materials without the prior permission of the respective copyright owner.**For STM Signatory Publishers clearing permission under the terms of the STM Permissions Guidelines only, the terms of the license are extended to include subsequent editions and for editions in other languages, provided such editions are for the work as a whole in situ and does not involve the separate exploitation of the permitted figures or extracts,** You may not alter, remove or suppress in any manner any copyright, trademark or other notices displayed by the Wiley Materials. You may not license, rent, sell, loan, lease, pledge, offer as security, transfer or assign the Wiley Materials on a stand-alone basis, or any of the rights granted to you hereunder to any other person.

- The Wiley Materials and all of the intellectual property rights therein shall at all times remain the exclusive property of John Wiley & Sons Inc, the Wiley Companies, or their respective licensors, and your interest therein is only that of having possession of and the right to reproduce the Wiley Materials pursuant to Section 2 herein during the continuance of this Agreement. You agree that you own no right, title or interest in or to the Wiley Materials or any of the intellectual property rights therein. You shall have no rights hereunder other than the license as provided for above in Section 2. No right, license or interest to any trademark, trade name, service mark or other branding ("Marks") of WILEY or its licensors is granted hereunder, and you agree that you shall not assert any such right, license or interest with respect thereto

- NEITHER WILEY NOR ITS LICENSORS MAKES ANY WARRANTY OR REPRESENTATION OF ANY KIND TO YOU OR ANY THIRD PARTY, EXPRESS, IMPLIED OR STATUTORY, WITH RESPECT TO THE MATERIALS OR THE ACCURACY OF ANY INFORMATION CONTAINED IN THE MATERIALS, INCLUDING, WITHOUT LIMITATION, ANY IMPLIED WARRANTY OF MERCHANTABILITY, ACCURACY, SATISFACTORY QUALITY, FITNESS FOR A PARTICULAR PURPOSE, USABILITY, INTEGRATION OR NON-INFRINGEMENT AND ALL SUCH WARRANTIES ARE HEREBY EXCLUDED BY WILEY AND ITS LICENSORS AND WAIVED BY YOU.

- WILEY shall have the right to terminate this Agreement immediately upon breach of this Agreement by you.

- You shall indemnify, defend and hold harmless WILEY, its Licensors and their respective directors, officers, agents and employees, from and against any actual or threatened claims, demands, causes of action or proceedings arising from any breach of this Agreement by you.

- IN NO EVENT SHALL WILEY OR ITS LICENSORS BE LIABLE TO YOU OR ANY OTHER PARTY OR ANY OTHER PERSON OR ENTITY FOR ANY SPECIAL, CONSEQUENTIAL, INCIDENTAL, INDIRECT, EXEMPLARY OR PUNITIVE DAMAGES, HOWEVER CAUSED, ARISING OUT OF OR IN CONNECTION WITH THE DOWNLOADING, PROVISIONING, VIEWING OR USE OF THE MATERIALS REGARDLESS OF THE FORM OF ACTION, WHETHER FOR BREACH OF CONTRACT, BREACH OF WARRANTY, TORT, NEGLIGENCE, INFRINGEMENT OR OTHERWISE (INCLUDING, WITHOUT LIMITATION, DAMAGES BASED ON LOSS OF PROFITS, DATA, FILES, USE, BUSINESS OPPORTUNITY OR CLAIMS OF THIRD PARTIES), AND WHETHER OR NOT THE PARTY HAS BEEN ADVISED OF THE POSSIBILITY OF SUCH DAMAGES. THIS LIMITATION SHALL APPLY NOTWITHSTANDING ANY FAILURE OF ESSENTIAL PURPOSE OF ANY LIMITED REMEDY PROVIDED HEREIN.

- Should any provision of this Agreement be held by a court of competent jurisdiction to be illegal, invalid, or unenforceable, that provision shall be deemed amended to achieve as nearly as possible the same economic effect as the original provision, and the legality, validity and enforceability of the remaining provisions of this Agreement

shall not be affected or impaired thereby.

- The failure of either party to enforce any term or condition of this Agreement shall not constitute a waiver of either party's right to enforce each and every term and condition of this Agreement. No breach under this agreement shall be deemed waived or excused by either party unless such waiver or consent is in writing signed by the party granting such waiver or consent. The waiver by or consent of a party to a breach of any provision of this Agreement shall not operate or be construed as a waiver of or consent to any other or subsequent breach by such other party.

- This Agreement may not be assigned (including by operation of law or otherwise) by you without WILEY's prior written consent.

- Any fee required for this permission shall be non-refundable after thirty (30) days from receipt by the CCC.

- These terms and conditions together with CCC's Billing and Payment terms and conditions (which are incorporated herein) form the entire agreement between you and WILEY concerning this licensing transaction and (in the absence of fraud) supersedes all prior agreements and representations of the parties, oral or written. This Agreement may not be amended except in writing signed by both parties. This Agreement shall be binding upon and inure to the benefit of the parties' successors, legal representatives, and authorized assigns.

- In the event of any conflict between your obligations established by these terms and conditions and those established by CCC's Billing and Payment terms and conditions, these terms and conditions shall prevail.

- WILEY expressly reserves all rights not specifically granted in the combination of (i) the license details provided by you and accepted in the course of this licensing transaction, (ii) these terms and conditions and (iii) CCC's Billing and Payment terms and conditions.

- This Agreement will be void if the Type of Use, Format, Circulation, or Requestor Type was misrepresented during the licensing process.

- This Agreement shall be governed by and construed in accordance with the laws of the State of New York, USA, without regards to such state's conflict of law rules. Any legal action, suit or proceeding arising out of or relating to these Terms and Conditions or the breach thereof shall be instituted in a court of competent jurisdiction in New York County in the State of New York in the United States of America and each party hereby consents and submits to the personal jurisdiction of such court, waives any objection to venue in such court and consents to service of process by registered or certified mail, return receipt requested, at the last known address of such party.

WILEY OPEN ACCESS TERMS AND CONDITIONS

Wiley Publishes Open Access Articles in fully Open Access Journals and in Subscription journals offering Online Open. Although most of the fully Open Access journals publish open access articles under the terms of the Creative Commons Attribution (CC BY) License only, the subscription journals and a few of the Open Access Journals offer a choice of

Creative Commons Licenses. The license type is clearly identified on the article.

The Creative Commons Attribution License

The Creative Commons Attribution License (CC-BY) allows users to copy, distribute and transmit an article, adapt the article and make commercial use of the article. The CC-BY license permits commercial and non-

Creative Commons Attribution Non-Commercial License

The Creative Commons Attribution Non-Commercial (CC-BY-NC)License permits use, distribution and reproduction in any medium, provided the original work is properly cited and is not used for commercial purposes.(see below)

Creative Commons Attribution-Non-Commercial-NoDerivs License

The Creative Commons Attribution Non-Commercial-NoDerivs License (CC-BY-NC-ND) permits use, distribution and reproduction in any medium, provided the original work is properly cited, is not used for commercial purposes and no modifications or adaptations are made. (see below)

Use by commercial "for-profit" organizations

Use of Wiley Open Access articles for commercial, promotional, or marketing purposes requires further explicit permission from Wiley and will be subject to a fee.

Further details can be found on Wiley Online Library

http://olabout.wiley.com/WileyCDA/Section/id-410895.html

Other Terms and Conditions:

v1.10 Last updated September 2015

Questions? customercare@copyright.com or +1-855-239-3415 (toll free in the US) or +1-978-646-2777.

JOHN WILEY AND SONS LICENSE TERMS AND CONDITIONS

May 24, 2017

This Agreement between Ms. Ping Liang ("You") and John Wiley and Sons ("John Wiley and Sons") consists of your license details and the terms and conditions provided by John Wiley and Sons and Copyright Clearance Center.

License Number	4115281460052
License date	May 24, 2017
Licensed Content Publisher	John Wiley and Sons
Licensed Content Publication	Angewandte Chemie International Edition
Licensed Content Title	Formation of CoS2 Nanobubble Hollow Prisms for Highly Reversible Lithium Storage
Licensed Content Author	Le Yu,Jing Fan Yang,Xiong Wen (David) Lou
Licensed Content Date	Aug 16, 2016
Licensed Content Pages	5
Type of use	Dissertation/Thesis
Requestor type	University/Academic
Format	Print and electronic
Portion	Figure/table
Number of figures/tables	2
Original Wiley figure/table number(s)	Figure 3, Figure 4
Will you be translating?	No
Title of your thesis / dissertation	Synthesis and Evaluation of Nanostructured Membrane Catalytic Systems for Water Treatment
Expected completion date	Jun 2017
Expected size (number of pages)	200
Requestor Location	Ms. Ping Liang 4-31 nottingham street, east vic park perth, WA 6101 Australia Attn: Ms. Ping Liang
Publisher Tax ID	EU826007151
Billing Type	Invoice
Billing Address	Ms. Ping Liang 4-31 nottingham street, east vic park perth, Australia 6101

Attn: Ms. Ping Liang

Total 0.00 AUD

Terms and Conditions

TERMS AND CONDITIONS

This copyrighted material is owned by or exclusively licensed to John Wiley & Sons, Inc. or one of its group companies (each a"Wiley Company") or handled on behalf of a society with which a Wiley Company has exclusive publishing rights in relation to a particular work (collectively "WILEY"). By clicking "accept" in connection with completing this licensing transaction, you agree that the following terms and conditions apply to this transaction (along with the billing and payment terms and conditions established by the Copyright Clearance Center Inc., ("CCC's Billing and Payment terms and conditions"), at the time that you opened your RightsLink account (these are available at any time at http://myaccount.copyright.com).

Terms and Conditions

- The materials you have requested permission to reproduce or reuse (the "Wiley Materials") are protected by copyright.

- You are hereby granted a personal, non-exclusive, non-sub licensable (on a stand-alone basis), non-transferable, worldwide, limited license to reproduce the Wiley Materials for the purpose specified in the licensing process. This license, **and any CONTENT (PDF or image file) purchased as part of your order,** is for a one-time use only and limited to any maximum distribution number specified in the license. The first instance of republication or reuse granted by this license must be completed within two years of the date of the grant of this license (although copies prepared before the end date may be distributed thereafter). The Wiley Materials shall not be used in any other manner or for any other purpose, beyond what is granted in the license. Permission is granted subject to an appropriate acknowledgement given to the author, title of the material/book/journal and the publisher. You shall also duplicate the copyright notice that appears in the Wiley publication in your use of the Wiley Material. Permission is also granted on the understanding that nowhere in the text is a previously published source acknowledged for all or part of this Wiley Material. Any third party content is expressly excluded from this permission.

- With respect to the Wiley Materials, all rights are reserved. Except as expressly granted by the terms of the license, no part of the Wiley Materials may be copied, modified, adapted (except for minor reformatting required by the new Publication), translated, reproduced, transferred or distributed, in any form or by any means, and no derivative works may be made based on the Wiley Materials without the prior permission of the respective copyright owner.**For STM Signatory Publishers clearing permission under the terms of the STM Permissions Guidelines only, the terms of the license are extended to include subsequent editions and for editions in other languages, provided such editions are for the work as a whole in situ and does not involve the separate exploitation of the permitted figures or extracts,** You may not alter, remove or suppress in any manner any copyright, trademark or other notices displayed by the Wiley Materials. You may not license, rent, sell, loan, lease, pledge, offer as security, transfer or assign the Wiley Materials on a stand-alone basis, or any of the rights granted to you hereunder to any other person.

- The Wiley Materials and all of the intellectual property rights therein shall at all times remain the exclusive property of John Wiley & Sons Inc, the Wiley Companies, or their respective licensors, and your interest therein is only that of having possession of and the right to reproduce the Wiley Materials pursuant to Section 2 herein during the continuance of this Agreement. You agree that you own no right, title or interest in or to the Wiley Materials or any of the intellectual property rights therein. You shall have no rights hereunder other than the license as provided for above in Section 2. No right, license or interest to any trademark, trade name, service mark or other branding ("Marks") of WILEY or its licensors is granted hereunder, and you agree that you shall not assert any such right, license or interest with respect thereto

- NEITHER WILEY NOR ITS LICENSORS MAKES ANY WARRANTY OR REPRESENTATION OF ANY KIND TO YOU OR ANY THIRD PARTY, EXPRESS, IMPLIED OR STATUTORY, WITH RESPECT TO THE MATERIALS OR THE ACCURACY OF ANY INFORMATION CONTAINED IN THE MATERIALS, INCLUDING, WITHOUT LIMITATION, ANY IMPLIED WARRANTY OF MERCHANTABILITY, ACCURACY, SATISFACTORY QUALITY, FITNESS FOR A PARTICULAR PURPOSE, USABILITY, INTEGRATION OR NON-INFRINGEMENT AND ALL SUCH WARRANTIES ARE HEREBY EXCLUDED BY WILEY AND ITS LICENSORS AND WAIVED BY YOU.

- WILEY shall have the right to terminate this Agreement immediately upon breach of this Agreement by you.

- You shall indemnify, defend and hold harmless WILEY, its Licensors and their respective directors, officers, agents and employees, from and against any actual or threatened claims, demands, causes of action or proceedings arising from any breach of this Agreement by you.

- IN NO EVENT SHALL WILEY OR ITS LICENSORS BE LIABLE TO YOU OR ANY OTHER PARTY OR ANY OTHER PERSON OR ENTITY FOR ANY SPECIAL, CONSEQUENTIAL, INCIDENTAL, INDIRECT, EXEMPLARY OR PUNITIVE DAMAGES, HOWEVER CAUSED, ARISING OUT OF OR IN CONNECTION WITH THE DOWNLOADING, PROVISIONING, VIEWING OR USE OF THE MATERIALS REGARDLESS OF THE FORM OF ACTION, WHETHER FOR BREACH OF CONTRACT, BREACH OF WARRANTY, TORT, NEGLIGENCE, INFRINGEMENT OR OTHERWISE (INCLUDING, WITHOUT LIMITATION, DAMAGES BASED ON LOSS OF PROFITS, DATA, FILES, USE, BUSINESS OPPORTUNITY OR CLAIMS OF THIRD PARTIES), AND WHETHER OR NOT THE PARTY HAS BEEN ADVISED OF THE POSSIBILITY OF SUCH DAMAGES. THIS LIMITATION SHALL APPLY NOTWITHSTANDING ANY FAILURE OF ESSENTIAL PURPOSE OF ANY LIMITED REMEDY PROVIDED HEREIN.

- Should any provision of this Agreement be held by a court of competent jurisdiction to be illegal, invalid, or unenforceable, that provision shall be deemed amended to achieve as nearly as possible the same economic effect as the original provision, and the legality, validity and enforceability of the remaining provisions of this Agreement shall not be affected or impaired thereby.

- The failure of either party to enforce any term or condition of this Agreement shall not constitute a waiver of either party's right to enforce each and every term and condition of this Agreement. No breach under this agreement shall be deemed waived or excused by either party unless such waiver or consent is in writing signed by the party granting such waiver or consent. The waiver by or consent of a party to a breach of any provision of this Agreement shall not operate or be construed as a waiver of or consent to any other or subsequent breach by such other party.

- This Agreement may not be assigned (including by operation of law or otherwise) by you without WILEY's prior written consent.

- Any fee required for this permission shall be non-refundable after thirty (30) days from receipt by the CCC.

- These terms and conditions together with CCC's Billing and Payment terms and conditions (which are incorporated herein) form the entire agreement between you and WILEY concerning this licensing transaction and (in the absence of fraud) supersedes all prior agreements and representations of the parties, oral or written. This Agreement may not be amended except in writing signed by both parties. This Agreement shall be binding upon and inure to the benefit of the parties' successors, legal representatives, and authorized assigns.

- In the event of any conflict between your obligations established by these terms and conditions and those established by CCC's Billing and Payment terms and conditions, these terms and conditions shall prevail.

- WILEY expressly reserves all rights not specifically granted in the combination of (i) the license details provided by you and accepted in the course of this licensing transaction, (ii) these terms and conditions and (iii) CCC's Billing and Payment terms and conditions.

- This Agreement will be void if the Type of Use, Format, Circulation, or Requestor Type was misrepresented during the licensing process.

- This Agreement shall be governed by and construed in accordance with the laws of the State of New York, USA, without regards to such state's conflict of law rules. Any legal action, suit or proceeding arising out of or relating to these Terms and Conditions or the breach thereof shall be instituted in a court of competent jurisdiction in New York County in the State of New York in the United States of America and each party hereby consents and submits to the personal jurisdiction of such court, waives any objection to venue in such court and consents to service of process by registered or certified mail, return receipt requested, at the last known address of such party.

WILEY OPEN ACCESS TERMS AND CONDITIONS

Wiley Publishes Open Access Articles in fully Open Access Journals and in Subscription journals offering Online Open. Although most of the fully Open Access journals publish open access articles under the terms of the Creative Commons Attribution (CC BY) License only, the subscription journals and a few of the Open Access Journals offer a choice of Creative Commons Licenses. The license type is clearly identified on the article.

The Creative Commons Attribution License
The Creative Commons Attribution License (CC-BY) allows users to copy, distribute and transmit an article, adapt the article and make commercial use of the article. The CC-BY license permits commercial and non-
Creative Commons Attribution Non-Commercial License
The Creative Commons Attribution Non-Commercial (CC-BY-NC)License permits use, distribution and reproduction in any medium, provided the original work is properly cited and is not used for commercial purposes.(see below)

Creative Commons Attribution-Non-Commercial-NoDerivs License
The Creative Commons Attribution Non-Commercial-NoDerivs License (CC-BY-NC-ND) permits use, distribution and reproduction in any medium, provided the original work is properly cited, is not used for commercial purposes and no modifications or adaptations are made. (see below)
Use by commercial "for-profit" organizations
Use of Wiley Open Access articles for commercial, promotional, or marketing purposes requires further explicit permission from Wiley and will be subject to a fee.
Further details can be found on Wiley Online Library
http://olabout.wiley.com/WileyCDA/Section/id-410895.html

Other Terms and Conditions:

v1.10 Last updated September 2015

Questions? customercare@copyright.com or +1-855-239-3415 (toll free in the US) or +1-978-646-2777.

JOHN WILEY AND SONS LICENSE TERMS AND CONDITIONS

May 24, 2017

This Agreement between Ms. Ping Liang ("You") and John Wiley and Sons ("John Wiley and Sons") consists of your license details and the terms and conditions provided by John Wiley and Sons and Copyright Clearance Center.

License Number	4115291365639
License date	May 24, 2017
Licensed Content Publisher	John Wiley and Sons
Licensed Content Publication	Advanced Functional Materials
Licensed Content Title	3D Metal Carbide@Mesoporous Carbon Hybrid Architecture as a New Polysulfide Reservoir for Lithium-Sulfur Batteries
Licensed Content Author	Weizhai Bao,Dawei Su,Wenxue Zhang,Xin Guo,Guoxiu Wang
Licensed Content Date	Oct 31, 2016
Licensed Content Pages	11
Type of use	Dissertation/Thesis
Requestor type	University/Academic
Format	Print and electronic
Portion	Figure/table
Number of figures/tables	2
Original Wiley figure/table number(s)	Figure 1, Figure 5
Will you be translating?	No
Title of your thesis / dissertation	Synthesis and Evaluation of Nanostructured Membrane Catalytic Systems for Water Treatment
Expected completion date	Jun 2017
Expected size (number of pages)	200
Requestor Location	Ms. Ping Liang 4-31 nottingham street, east vic park perth, WA 6101 Australia Attn: Ms. Ping Liang
Publisher Tax ID	EU826007151
Billing Type	Invoice
Billing Address	Ms. Ping Liang 4-31 nottingham street, east vic park perth, Australia 6101

Attn: Ms. Ping Liang

Total 0.00 AUD

Terms and Conditions

TERMS AND CONDITIONS

This copyrighted material is owned by or exclusively licensed to John Wiley & Sons, Inc. or one of its group companies (each a"Wiley Company") or handled on behalf of a society with which a Wiley Company has exclusive publishing rights in relation to a particular work (collectively "WILEY"). By clicking "accept" in connection with completing this licensing transaction, you agree that the following terms and conditions apply to this transaction (along with the billing and payment terms and conditions established by the Copyright Clearance Center Inc., ("CCC's Billing and Payment terms and conditions"), at the time that you opened your RightsLink account (these are available at any time at http://myaccount.copyright.com).

Terms and Conditions

- The materials you have requested permission to reproduce or reuse (the "Wiley Materials") are protected by copyright.

- You are hereby granted a personal, non-exclusive, non-sub licensable (on a stand-alone basis), non-transferable, worldwide, limited license to reproduce the Wiley Materials for the purpose specified in the licensing process. This license, **and any CONTENT (PDF or image file) purchased as part of your order,** is for a one-time use only and limited to any maximum distribution number specified in the license. The first instance of republication or reuse granted by this license must be completed within two years of the date of the grant of this license (although copies prepared before the end date may be distributed thereafter). The Wiley Materials shall not be used in any other manner or for any other purpose, beyond what is granted in the license. Permission is granted subject to an appropriate acknowledgement given to the author, title of the material/book/journal and the publisher. You shall also duplicate the copyright notice that appears in the Wiley publication in your use of the Wiley Material. Permission is also granted on the understanding that nowhere in the text is a previously published source acknowledged for all or part of this Wiley Material. Any third party content is expressly excluded from this permission.

- With respect to the Wiley Materials, all rights are reserved. Except as expressly granted by the terms of the license, no part of the Wiley Materials may be copied, modified, adapted (except for minor reformatting required by the new Publication), translated, reproduced, transferred or distributed, in any form or by any means, and no derivative works may be made based on the Wiley Materials without the prior permission of the respective copyright owner.**For STM Signatory Publishers clearing permission under the terms of the STM Permissions Guidelines only, the terms of the license are extended to include subsequent editions and for editions in other languages, provided such editions are for the work as a whole in situ and does not involve the separate exploitation of the permitted figures or extracts,** You may not alter, remove or suppress in any manner any copyright, trademark or other notices displayed by the Wiley Materials. You may not license, rent, sell, loan, lease, pledge, offer as security, transfer or assign the Wiley Materials on a stand-alone basis, or any of the rights granted to you hereunder to any other person.

- The Wiley Materials and all of the intellectual property rights therein shall at all times remain the exclusive property of John Wiley & Sons Inc, the Wiley Companies, or their respective licensors, and your interest therein is only that of having possession of and the right to reproduce the Wiley Materials pursuant to Section 2 herein during the continuance of this Agreement. You agree that you own no right, title or interest in or to the Wiley Materials or any of the intellectual property rights therein. You shall have no rights hereunder other than the license as provided for above in Section 2. No right, license or interest to any trademark, trade name, service mark or other branding ("Marks") of WILEY or its licensors is granted hereunder, and you agree that you shall not assert any such right, license or interest with respect thereto

- NEITHER WILEY NOR ITS LICENSORS MAKES ANY WARRANTY OR REPRESENTATION OF ANY KIND TO YOU OR ANY THIRD PARTY, EXPRESS, IMPLIED OR STATUTORY, WITH RESPECT TO THE MATERIALS OR THE ACCURACY OF ANY INFORMATION CONTAINED IN THE MATERIALS, INCLUDING, WITHOUT LIMITATION, ANY IMPLIED WARRANTY OF MERCHANTABILITY, ACCURACY, SATISFACTORY QUALITY, FITNESS FOR A PARTICULAR PURPOSE, USABILITY, INTEGRATION OR NON-INFRINGEMENT AND ALL SUCH WARRANTIES ARE HEREBY EXCLUDED BY WILEY AND ITS LICENSORS AND WAIVED BY YOU.

- WILEY shall have the right to terminate this Agreement immediately upon breach of this Agreement by you.

- You shall indemnify, defend and hold harmless WILEY, its Licensors and their respective directors, officers, agents and employees, from and against any actual or threatened claims, demands, causes of action or proceedings arising from any breach of this Agreement by you.

- IN NO EVENT SHALL WILEY OR ITS LICENSORS BE LIABLE TO YOU OR ANY OTHER PARTY OR ANY OTHER PERSON OR ENTITY FOR ANY SPECIAL, CONSEQUENTIAL, INCIDENTAL, INDIRECT, EXEMPLARY OR PUNITIVE DAMAGES, HOWEVER CAUSED, ARISING OUT OF OR IN CONNECTION WITH THE DOWNLOADING, PROVISIONING, VIEWING OR USE OF THE MATERIALS REGARDLESS OF THE FORM OF ACTION, WHETHER FOR BREACH OF CONTRACT, BREACH OF WARRANTY, TORT, NEGLIGENCE, INFRINGEMENT OR OTHERWISE (INCLUDING, WITHOUT LIMITATION, DAMAGES BASED ON LOSS OF PROFITS, DATA, FILES, USE, BUSINESS OPPORTUNITY OR CLAIMS OF THIRD PARTIES), AND WHETHER OR NOT THE PARTY HAS BEEN ADVISED OF THE POSSIBILITY OF SUCH DAMAGES. THIS LIMITATION SHALL APPLY NOTWITHSTANDING ANY FAILURE OF ESSENTIAL PURPOSE OF ANY LIMITED REMEDY PROVIDED HEREIN.

- Should any provision of this Agreement be held by a court of competent jurisdiction to be illegal, invalid, or unenforceable, that provision shall be deemed amended to achieve as nearly as possible the same economic effect as the original provision, and the legality, validity and enforceability of the remaining provisions of this Agreement shall not be affected or impaired thereby.

- The failure of either party to enforce any term or condition of this Agreement shall not constitute a waiver of either party's right to enforce each and every term and condition of this Agreement. No breach under this agreement shall be deemed waived or excused by either party unless such waiver or consent is in writing signed by the party granting such waiver or consent. The waiver by or consent of a party to a breach of any provision of this Agreement shall not operate or be construed as a waiver of or consent to any other or subsequent breach by such other party.

- This Agreement may not be assigned (including by operation of law or otherwise) by you without WILEY's prior written consent.

- Any fee required for this permission shall be non-refundable after thirty (30) days from receipt by the CCC.

- These terms and conditions together with CCC's Billing and Payment terms and conditions (which are incorporated herein) form the entire agreement between you and WILEY concerning this licensing transaction and (in the absence of fraud) supersedes all prior agreements and representations of the parties, oral or written. This Agreement may not be amended except in writing signed by both parties. This Agreement shall be binding upon and inure to the benefit of the parties' successors, legal representatives, and authorized assigns.

- In the event of any conflict between your obligations established by these terms and conditions and those established by CCC's Billing and Payment terms and conditions, these terms and conditions shall prevail.

- WILEY expressly reserves all rights not specifically granted in the combination of (i) the license details provided by you and accepted in the course of this licensing transaction, (ii) these terms and conditions and (iii) CCC's Billing and Payment terms and conditions.

- This Agreement will be void if the Type of Use, Format, Circulation, or Requestor Type was misrepresented during the licensing process.

- This Agreement shall be governed by and construed in accordance with the laws of the State of New York, USA, without regards to such state's conflict of law rules. Any legal action, suit or proceeding arising out of or relating to these Terms and Conditions or the breach thereof shall be instituted in a court of competent jurisdiction in New York County in the State of New York in the United States of America and each party hereby consents and submits to the personal jurisdiction of such court, waives any objection to venue in such court and consents to service of process by registered or certified mail, return receipt requested, at the last known address of such party.

WILEY OPEN ACCESS TERMS AND CONDITIONS

Wiley Publishes Open Access Articles in fully Open Access Journals and in Subscription journals offering Online Open. Although most of the fully Open Access journals publish open access articles under the terms of the Creative Commons Attribution (CC BY) License only, the subscription journals and a few of the Open Access Journals offer a choice of Creative Commons Licenses. The license type is clearly identified on the article.

The Creative Commons Attribution License
The Creative Commons Attribution License (CC-BY) allows users to copy, distribute and transmit an article, adapt the article and make commercial use of the article. The CC-BY license permits commercial and non-
Creative Commons Attribution Non-Commercial License
The Creative Commons Attribution Non-Commercial (CC-BY-NC)License permits use, distribution and reproduction in any medium, provided the original work is properly cited and is not used for commercial purposes.(see below)

Creative Commons Attribution-Non-Commercial-NoDerivs License
The Creative Commons Attribution Non-Commercial-NoDerivs License (CC-BY-NC-ND) permits use, distribution and reproduction in any medium, provided the original work is properly cited, is not used for commercial purposes and no modifications or adaptations are made. (see below)
Use by commercial "for-profit" organizations
Use of Wiley Open Access articles for commercial, promotional, or marketing purposes requires further explicit permission from Wiley and will be subject to a fee.
Further details can be found on Wiley Online Library
http://olabout.wiley.com/WileyCDA/Section/id-410895.html

Other Terms and Conditions:

v1.10 Last updated September 2015

Questions? customercare@copyright.com or +1-855-239-3415 (toll free in the US) or +1-978-646-2777.

Title:	"Brick-and-mortar" sandwiched porous carbon building constructed by metal-organic framework and graphene: Ultrafast charge/discharge rate up to 2Vs−1 for supercapacitors
Author:	Lan Wang,Tong Wei,Lizhi Sheng,Lili Jiang,Xiaoliang Wu,Qihang Zhou,Bao Yuan,Jingming Yue,Zheng Liu,Zhuangjun Fan
Publication:	Nano Energy
Publisher:	Elsevier
Date:	December 2016

Order Completed

Thank you for your order.

This Agreement between Ms. Ping Liang ("You") and Elsevier ("Elsevier") consists of your license details and the terms and conditions provided by Elsevier and Copyright Clearance Center.

Your confirmation email will contain your order number for future reference.

Printable details.

License Number	4115300529993
License date	May 24, 2017
Licensed Content Publisher	Elsevier
Licensed Content Publication	Nano Energy
Licensed Content Title	"Brick-and-mortar" sandwiched porous carbon building constructed by metal-organic framework and graphene: Ultrafast charge/discharge rate up to 2Vs−1 for supercapacitors
Licensed Content Author	Lan Wang,Tong Wei,Lizhi Sheng,Lili Jiang,Xiaoliang Wu,Qihang Zhou,Bao Yuan,Jingming Yue,Zheng Liu,Zhuangjun Fan
Licensed Content Date	Dec 1, 2016
Licensed Content Volume	30
Licensed Content Issue	n/a
Licensed Content Pages	9
Type of Use	reuse in a thesis/dissertation
Portion	figures/tables/illustrations
Number of figures/tables/illustrations	1
Format	both print and electronic
Are you the author of this Elsevier article?	No
Will you be translating?	No
Order reference number	
Original figure numbers	Figure 4
Title of your thesis/dissertation	Synthesis and Evaluation of Nanostructured Membrane Catalytic Systems for Water Treatment
Expected completion date	Jun 2017
Estimated size (number	200

of pages)	
Elsevier VAT number	GB 494 6272 12
Requestor Location	Ms. Ping Liang 4-31 nottingham street, east vic park perth, WA 6101 Australia Attn: Ms. Ping Liang
Total	0.00 AUD

ORDER MORE CLOSE WINDOW

ELSEVIER LICENSE
TERMS AND CONDITIONS

May 24, 2017

This Agreement between Ms. Ping Liang ("You") and Elsevier ("Elsevier") consists of your license details and the terms and conditions provided by Elsevier and Copyright Clearance Center.

License Number	4115300529993
License date	May 24, 2017
Licensed Content Publisher	Elsevier
Licensed Content Publication	Nano Energy
Licensed Content Title	"Brick-and-mortar" sandwiched porous carbon building constructed by metal-organic framework and graphene: Ultrafast charge/discharge rate up to 2Vs−1 for supercapacitors
Licensed Content Author	Lan Wang,Tong Wei,Lizhi Sheng,Lili Jiang,Xiaoliang Wu,Qihang Zhou,Bao Yuan,Jingming Yue,Zheng Liu,Zhuangjun Fan
Licensed Content Date	Dec 1, 2016
Licensed Content Volume	30
Licensed Content Issue	n/a
Licensed Content Pages	9
Start Page	84
End Page	92
Type of Use	reuse in a thesis/dissertation
Intended publisher of new work	other
Portion	figures/tables/illustrations
Number of figures/tables/illustrations	1
Format	both print and electronic
Are you the author of this Elsevier article?	No
Will you be translating?	No
Order reference number	
Original figure numbers	Figure 4
Title of your thesis/dissertation	Synthesis and Evaluation of Nanostructured Membrane Catalytic Systems for Water Treatment
Expected completion date	Jun 2017
Estimated size (number of pages)	200
Elsevier VAT number	GB 494 6272 12
Requestor Location	Ms. Ping Liang

4-31 nottingham street, east vic park

perth, WA 6101
Australia
Attn: Ms. Ping Liang

Total 0.00 AUD

Terms and Conditions

INTRODUCTION

1. The publisher for this copyrighted material is Elsevier. By clicking "accept" in connection with completing this licensing transaction, you agree that the following terms and conditions apply to this transaction (along with the Billing and Payment terms and conditions established by Copyright Clearance Center, Inc. ("CCC"), at the time that you opened your Rightslink account and that are available at any time at http://myaccount.copyright.com).

GENERAL TERMS

2. Elsevier hereby grants you permission to reproduce the aforementioned material subject to the terms and conditions indicated.
3. Acknowledgement: If any part of the material to be used (for example, figures) has appeared in our publication with credit or acknowledgement to another source, permission must also be sought from that source. If such permission is not obtained then that material may not be included in your publication/copies. Suitable acknowledgement to the source must be made, either as a footnote or in a reference list at the end of your publication, as follows:
"Reprinted from Publication title, Vol /edition number, Author(s), Title of article / title of chapter, Pages No., Copyright (Year), with permission from Elsevier [OR APPLICABLE SOCIETY COPYRIGHT OWNER]." Also Lancet special credit - "Reprinted from The Lancet, Vol. number, Author(s), Title of article, Pages No., Copyright (Year), with permission from Elsevier."
4. Reproduction of this material is confined to the purpose and/or media for which permission is hereby given.
5. Altering/Modifying Material: Not Permitted. However figures and illustrations may be altered/adapted minimally to serve your work. Any other abbreviations, additions, deletions and/or any other alterations shall be made only with prior written authorization of Elsevier Ltd. (Please contact Elsevier at permissions@elsevier.com). No modifications can be made to any Lancet figures/tables and they must be reproduced in full.
6. If the permission fee for the requested use of our material is waived in this instance, please be advised that your future requests for Elsevier materials may attract a fee.
7. Reservation of Rights: Publisher reserves all rights not specifically granted in the combination of (i) the license details provided by you and accepted in the course of this licensing transaction, (ii) these terms and conditions and (iii) CCC's Billing and Payment terms and conditions.
8. License Contingent Upon Payment: While you may exercise the rights licensed immediately upon issuance of the license at the end of the licensing process for the transaction, provided that you have disclosed complete and accurate details of your proposed use, no license is finally effective unless and until full payment is received from you (either by publisher or by CCC) as provided in CCC's Billing and Payment terms and conditions. If full payment is not received on a timely basis, then any license preliminarily granted shall be deemed automatically revoked and shall be void as if never granted. Further, in the event that you breach any of these terms and conditions or any of CCC's Billing and Payment

terms and conditions, the license is automatically revoked and shall be void as if never granted. Use of materials as described in a revoked license, as well as any use of the materials beyond the scope of an unrevoked license, may constitute copyright infringement and publisher reserves the right to take any and all action to protect its copyright in the materials.
9. Warranties: Publisher makes no representations or warranties with respect to the licensed material.
10. Indemnity: You hereby indemnify and agree to hold harmless publisher and CCC, and their respective officers, directors, employees and agents, from and against any and all claims arising out of your use of the licensed material other than as specifically authorized pursuant to this license.
11. No Transfer of License: This license is personal to you and may not be sublicensed, assigned, or transferred by you to any other person without publisher's written permission.
12. No Amendment Except in Writing: This license may not be amended except in a writing signed by both parties (or, in the case of publisher, by CCC on publisher's behalf).
13. Objection to Contrary Terms: Publisher hereby objects to any terms contained in any purchase order, acknowledgment, check endorsement or other writing prepared by you, which terms are inconsistent with these terms and conditions or CCC's Billing and Payment terms and conditions. These terms and conditions, together with CCC's Billing and Payment terms and conditions (which are incorporated herein), comprise the entire agreement between you and publisher (and CCC) concerning this licensing transaction. In the event of any conflict between your obligations established by these terms and conditions and those established by CCC's Billing and Payment terms and conditions, these terms and conditions shall control.
14. Revocation: Elsevier or Copyright Clearance Center may deny the permissions described in this License at their sole discretion, for any reason or no reason, with a full refund payable to you. Notice of such denial will be made using the contact information provided by you. Failure to receive such notice will not alter or invalidate the denial. In no event will Elsevier or Copyright Clearance Center be responsible or liable for any costs, expenses or damage incurred by you as a result of a denial of your permission request, other than a refund of the amount(s) paid by you to Elsevier and/or Copyright Clearance Center for denied permissions.

LIMITED LICENSE

The following terms and conditions apply only to specific license types:
15. **Translation**: This permission is granted for non-exclusive world **English** rights only unless your license was granted for translation rights. If you licensed translation rights you may only translate this content into the languages you requested. A professional translator must perform all translations and reproduce the content word for word preserving the integrity of the article.
16. **Posting licensed content on any Website**: The following terms and conditions apply as follows: Licensing material from an Elsevier journal: All content posted to the web site must maintain the copyright information line on the bottom of each image; A hyper-text must be included to the Homepage of the journal from which you are licensing at http://www.sciencedirect.com/science/journal/xxxxx or the Elsevier homepage for books at http://www.elsevier.com; Central Storage: This license does not include permission for a scanned version of the material to be stored in a central repository such as that provided by Heron/XanEdu.
Licensing material from an Elsevier book: A hyper-text link must be included to the Elsevier homepage at http://www.elsevier.com . All content posted to the web site must maintain the copyright information line on the bottom of each image.

Posting licensed content on Electronic reserve: In addition to the above the following clauses are applicable: The web site must be password-protected and made available only to bona fide students registered on a relevant course. This permission is granted for 1 year only. You may obtain a new license for future website posting.

17. **For journal authors:** the following clauses are applicable in addition to the above:

Preprints:

A preprint is an author's own write-up of research results and analysis, it has not been peer-reviewed, nor has it had any other value added to it by a publisher (such as formatting, copyright, technical enhancement etc.).

Authors can share their preprints anywhere at any time. Preprints should not be added to or enhanced in any way in order to appear more like, or to substitute for, the final versions of articles however authors can update their preprints on arXiv or RePEc with their Accepted Author Manuscript (see below).

If accepted for publication, we encourage authors to link from the preprint to their formal publication via its DOI. Millions of researchers have access to the formal publications on ScienceDirect, and so links will help users to find, access, cite and use the best available version. Please note that Cell Press, The Lancet and some society-owned have different preprint policies. Information on these policies is available on the journal homepage.

Accepted Author Manuscripts: An accepted author manuscript is the manuscript of an article that has been accepted for publication and which typically includes author-incorporated changes suggested during submission, peer review and editor-author communications.

Authors can share their accepted author manuscript:

- immediately
    - via their non-commercial person homepage or blog
    - by updating a preprint in arXiv or RePEc with the accepted manuscript
    - via their research institute or institutional repository for internal institutional uses or as part of an invitation-only research collaboration work-group
    - directly by providing copies to their students or to research collaborators for their personal use
    - for private scholarly sharing as part of an invitation-only work group on commercial sites with which Elsevier has an agreement
- After the embargo period
    - via non-commercial hosting platforms such as their institutional repository
    - via commercial sites with which Elsevier has an agreement

In all cases accepted manuscripts should:

- link to the formal publication via its DOI
- bear a CC-BY-NC-ND license - this is easy to do
- if aggregated with other manuscripts, for example in a repository or other site, be shared in alignment with our hosting policy not be added to or enhanced in any way to appear more like, or to substitute for, the published journal article.

Published journal article (JPA): A published journal article (PJA) is the definitive final record of published research that appears or will appear in the journal and embodies all value-adding publishing activities including peer review co-ordination, copy-editing, formatting, (if relevant) pagination and online enrichment.

Policies for sharing publishing journal articles differ for subscription and gold open access

articles:
Subscription Articles: If you are an author, please share a link to your article rather than the full-text. Millions of researchers have access to the formal publications on ScienceDirect, and so links will help your users to find, access, cite, and use the best available version.
Theses and dissertations which contain embedded PJAs as part of the formal submission can be posted publicly by the awarding institution with DOI links back to the formal publications on ScienceDirect.
If you are affiliated with a library that subscribes to ScienceDirect you have additional private sharing rights for others' research accessed under that agreement. This includes use for classroom teaching and internal training at the institution (including use in course packs and courseware programs), and inclusion of the article for grant funding purposes.
Gold Open Access Articles: May be shared according to the author-selected end-user license and should contain a CrossMark logo, the end user license, and a DOI link to the formal publication on ScienceDirect.
Please refer to Elsevier's posting policy for further information.
18. **For book authors** the following clauses are applicable in addition to the above:
Authors are permitted to place a brief summary of their work online only. You are not allowed to download and post the published electronic version of your chapter, nor may you scan the printed edition to create an electronic version. **Posting to a repository:** Authors are permitted to post a summary of their chapter only in their institution's repository.
19. **Thesis/Dissertation**: If your license is for use in a thesis/dissertation your thesis may be submitted to your institution in either print or electronic form. Should your thesis be published commercially, please reapply for permission. These requirements include permission for the Library and Archives of Canada to supply single copies, on demand, of the complete thesis and include permission for Proquest/UMI to supply single copies, on demand, of the complete thesis. Should your thesis be published commercially, please reapply for permission. Theses and dissertations which contain embedded PJAs as part of the formal submission can be posted publicly by the awarding institution with DOI links back to the formal publications on ScienceDirect.

Elsevier Open Access Terms and Conditions
You can publish open access with Elsevier in hundreds of open access journals or in nearly 2000 established subscription journals that support open access publishing. Permitted third party re-use of these open access articles is defined by the author's choice of Creative Commons user license. See our open access license policy for more information.
Terms & Conditions applicable to all Open Access articles published with Elsevier:
Any reuse of the article must not represent the author as endorsing the adaptation of the article nor should the article be modified in such a way as to damage the author's honour or reputation. If any changes have been made, such changes must be clearly indicated.
The author(s) must be appropriately credited and we ask that you include the end user license and a DOI link to the formal publication on ScienceDirect.
If any part of the material to be used (for example, figures) has appeared in our publication with credit or acknowledgement to another source it is the responsibility of the user to ensure their reuse complies with the terms and conditions determined by the rights holder.
Additional Terms & Conditions applicable to each Creative Commons user license:
CC BY: The CC-BY license allows users to copy, to create extracts, abstracts and new works from the Article, to alter and revise the Article and to make commercial use of the Article (including reuse and/or resale of the Article by commercial entities), provided the user gives appropriate credit (with a link to the formal publication through the relevant DOI), provides a link to the license, indicates if changes were made and the licensor is not

represented as endorsing the use made of the work. The full details of the license are available at http://creativecommons.org/licenses/by/4.0.
CC BY NC SA: The CC BY-NC-SA license allows users to copy, to create extracts, abstracts and new works from the Article, to alter and revise the Article, provided this is not done for commercial purposes, and that the user gives appropriate credit (with a link to the formal publication through the relevant DOI), provides a link to the license, indicates if changes were made and the licensor is not represented as endorsing the use made of the work. Further, any new works must be made available on the same conditions. The full details of the license are available at http://creativecommons.org/licenses/by-nc-sa/4.0.
CC BY NC ND: The CC BY-NC-ND license allows users to copy and distribute the Article, provided this is not done for commercial purposes and further does not permit distribution of the Article if it is changed or edited in any way, and provided the user gives appropriate credit (with a link to the formal publication through the relevant DOI), provides a link to the license, and that the licensor is not represented as endorsing the use made of the work. The full details of the license are available at http://creativecommons.org/licenses/by-nc-nd/4.0.
Any commercial reuse of Open Access articles published with a CC BY NC SA or CC BY NC ND license requires permission from Elsevier and will be subject to a fee.
Commercial reuse includes:

- Associating advertising with the full text of the Article
- Charging fees for document delivery or access
- Article aggregation
- Systematic distribution via e-mail lists or share buttons

Posting or linking by commercial companies for use by customers of those companies.

20. **Other Conditions**:

v1.9

Questions? customercare@copyright.com or +1-855-239-3415 (toll free in the US) or +1-978-646-2777.

ELSEVIER LICENSE
TERMS AND CONDITIONS

May 24, 2017

This Agreement between Ms. Ping Liang ("You") and Elsevier ("Elsevier") consists of your license details and the terms and conditions provided by Elsevier and Copyright Clearance Center.

License Number	4115301071974
License date	May 24, 2017
Licensed Content Publisher	Elsevier
Licensed Content Publication	Applied Catalysis B: Environmental
Licensed Content Title	Synthesis of ternary Ag/ZnO/ZnFe2O4 porous and hollow nanostructures with enhanced photocatalytic activity
Licensed Content Author	Shikui Wu,Xiaoping Shen,Guoxing Zhu,Hu Zhou,Zhenyuan Ji,Kangmin Chen,Aihua Yuan
Licensed Content Date	Jan 1, 0005
Licensed Content Volume	184
Licensed Content Issue	n/a
Licensed Content Pages	9
Start Page	328
End Page	336
Type of Use	reuse in a thesis/dissertation
Intended publisher of new work	other
Portion	figures/tables/illustrations
Number of figures/tables/illustrations	1
Format	both print and electronic
Are you the author of this Elsevier article?	No
Will you be translating?	No
Order reference number	
Original figure numbers	Figure 8
Title of your thesis/dissertation	Synthesis and Evaluation of Nanostructured Membrane Catalytic Systems for Water Treatment
Expected completion date	Jun 2017
Estimated size (number of pages)	200
Elsevier VAT number	GB 494 6272 12
Requestor Location	Ms. Ping Liang 4-31 nottingham street, east vic park

perth, WA 6101
Australia
Attn: Ms. Ping Liang

Total 0.00 AUD

Terms and Conditions

INTRODUCTION

1. The publisher for this copyrighted material is Elsevier. By clicking "accept" in connection with completing this licensing transaction, you agree that the following terms and conditions apply to this transaction (along with the Billing and Payment terms and conditions established by Copyright Clearance Center, Inc. ("CCC"), at the time that you opened your Rightslink account and that are available at any time at http://myaccount.copyright.com).

GENERAL TERMS

2. Elsevier hereby grants you permission to reproduce the aforementioned material subject to the terms and conditions indicated.
3. Acknowledgement: If any part of the material to be used (for example, figures) has appeared in our publication with credit or acknowledgement to another source, permission must also be sought from that source. If such permission is not obtained then that material may not be included in your publication/copies. Suitable acknowledgement to the source must be made, either as a footnote or in a reference list at the end of your publication, as follows:
"Reprinted from Publication title, Vol /edition number, Author(s), Title of article / title of chapter, Pages No., Copyright (Year), with permission from Elsevier [OR APPLICABLE SOCIETY COPYRIGHT OWNER]." Also Lancet special credit - "Reprinted from The Lancet, Vol. number, Author(s), Title of article, Pages No., Copyright (Year), with permission from Elsevier."
4. Reproduction of this material is confined to the purpose and/or media for which permission is hereby given.
5. Altering/Modifying Material: Not Permitted. However figures and illustrations may be altered/adapted minimally to serve your work. Any other abbreviations, additions, deletions and/or any other alterations shall be made only with prior written authorization of Elsevier Ltd. (Please contact Elsevier at permissions@elsevier.com). No modifications can be made to any Lancet figures/tables and they must be reproduced in full.
6. If the permission fee for the requested use of our material is waived in this instance, please be advised that your future requests for Elsevier materials may attract a fee.
7. Reservation of Rights: Publisher reserves all rights not specifically granted in the combination of (i) the license details provided by you and accepted in the course of this licensing transaction, (ii) these terms and conditions and (iii) CCC's Billing and Payment terms and conditions.
8. License Contingent Upon Payment: While you may exercise the rights licensed immediately upon issuance of the license at the end of the licensing process for the transaction, provided that you have disclosed complete and accurate details of your proposed use, no license is finally effective unless and until full payment is received from you (either by publisher or by CCC) as provided in CCC's Billing and Payment terms and conditions. If full payment is not received on a timely basis, then any license preliminarily granted shall be deemed automatically revoked and shall be void as if never granted. Further, in the event that you breach any of these terms and conditions or any of CCC's Billing and Payment terms and conditions, the license is automatically revoked and shall be void as if never

granted. Use of materials as described in a revoked license, as well as any use of the materials beyond the scope of an unrevoked license, may constitute copyright infringement and publisher reserves the right to take any and all action to protect its copyright in the materials.
9. Warranties: Publisher makes no representations or warranties with respect to the licensed material.
10. Indemnity: You hereby indemnify and agree to hold harmless publisher and CCC, and their respective officers, directors, employees and agents, from and against any and all claims arising out of your use of the licensed material other than as specifically authorized pursuant to this license.
11. No Transfer of License: This license is personal to you and may not be sublicensed, assigned, or transferred by you to any other person without publisher's written permission.
12. No Amendment Except in Writing: This license may not be amended except in a writing signed by both parties (or, in the case of publisher, by CCC on publisher's behalf).
13. Objection to Contrary Terms: Publisher hereby objects to any terms contained in any purchase order, acknowledgment, check endorsement or other writing prepared by you, which terms are inconsistent with these terms and conditions or CCC's Billing and Payment terms and conditions. These terms and conditions, together with CCC's Billing and Payment terms and conditions (which are incorporated herein), comprise the entire agreement between you and publisher (and CCC) concerning this licensing transaction. In the event of any conflict between your obligations established by these terms and conditions and those established by CCC's Billing and Payment terms and conditions, these terms and conditions shall control.
14. Revocation: Elsevier or Copyright Clearance Center may deny the permissions described in this License at their sole discretion, for any reason or no reason, with a full refund payable to you. Notice of such denial will be made using the contact information provided by you. Failure to receive such notice will not alter or invalidate the denial. In no event will Elsevier or Copyright Clearance Center be responsible or liable for any costs, expenses or damage incurred by you as a result of a denial of your permission request, other than a refund of the amount(s) paid by you to Elsevier and/or Copyright Clearance Center for denied permissions.

LIMITED LICENSE

The following terms and conditions apply only to specific license types:
15. **Translation**: This permission is granted for non-exclusive world **English** rights only unless your license was granted for translation rights. If you licensed translation rights you may only translate this content into the languages you requested. A professional translator must perform all translations and reproduce the content word for word preserving the integrity of the article.
16. **Posting licensed content on any Website**: The following terms and conditions apply as follows: Licensing material from an Elsevier journal: All content posted to the web site must maintain the copyright information line on the bottom of each image; A hyper-text must be included to the Homepage of the journal from which you are licensing at http://www.sciencedirect.com/science/journal/xxxxx or the Elsevier homepage for books at http://www.elsevier.com; Central Storage: This license does not include permission for a scanned version of the material to be stored in a central repository such as that provided by Heron/XanEdu.
Licensing material from an Elsevier book: A hyper-text link must be included to the Elsevier homepage at http://www.elsevier.com . All content posted to the web site must maintain the copyright information line on the bottom of each image.

Posting licensed content on Electronic reserve: In addition to the above the following clauses are applicable: The web site must be password-protected and made available only to bona fide students registered on a relevant course. This permission is granted for 1 year only. You may obtain a new license for future website posting.
17. **For journal authors:** the following clauses are applicable in addition to the above:
Preprints:
A preprint is an author's own write-up of research results and analysis, it has not been peer-reviewed, nor has it had any other value added to it by a publisher (such as formatting, copyright, technical enhancement etc.).
Authors can share their preprints anywhere at any time. Preprints should not be added to or enhanced in any way in order to appear more like, or to substitute for, the final versions of articles however authors can update their preprints on arXiv or RePEc with their Accepted Author Manuscript (see below).
If accepted for publication, we encourage authors to link from the preprint to their formal publication via its DOI. Millions of researchers have access to the formal publications on ScienceDirect, and so links will help users to find, access, cite and use the best available version. Please note that Cell Press, The Lancet and some society-owned have different preprint policies. Information on these policies is available on the journal homepage.
Accepted Author Manuscripts: An accepted author manuscript is the manuscript of an article that has been accepted for publication and which typically includes author-incorporated changes suggested during submission, peer review and editor-author communications.
Authors can share their accepted author manuscript:

- immediately
    - via their non-commercial person homepage or blog
    - by updating a preprint in arXiv or RePEc with the accepted manuscript
    - via their research institute or institutional repository for internal institutional uses or as part of an invitation-only research collaboration work-group
    - directly by providing copies to their students or to research collaborators for their personal use
    - for private scholarly sharing as part of an invitation-only work group on commercial sites with which Elsevier has an agreement
- After the embargo period
    - via non-commercial hosting platforms such as their institutional repository
    - via commercial sites with which Elsevier has an agreement

In all cases accepted manuscripts should:

- link to the formal publication via its DOI
- bear a CC-BY-NC-ND license - this is easy to do
- if aggregated with other manuscripts, for example in a repository or other site, be shared in alignment with our hosting policy not be added to or enhanced in any way to appear more like, or to substitute for, the published journal article.

Published journal article (JPA): A published journal article (PJA) is the definitive final record of published research that appears or will appear in the journal and embodies all value-adding publishing activities including peer review co-ordination, copy-editing, formatting, (if relevant) pagination and online enrichment.
Policies for sharing publishing journal articles differ for subscription and gold open access articles:

Subscription Articles: If you are an author, please share a link to your article rather than the full-text. Millions of researchers have access to the formal publications on ScienceDirect, and so links will help your users to find, access, cite, and use the best available version. Theses and dissertations which contain embedded PJAs as part of the formal submission can be posted publicly by the awarding institution with DOI links back to the formal publications on ScienceDirect.
If you are affiliated with a library that subscribes to ScienceDirect you have additional private sharing rights for others' research accessed under that agreement. This includes use for classroom teaching and internal training at the institution (including use in course packs and courseware programs), and inclusion of the article for grant funding purposes.
Gold Open Access Articles: May be shared according to the author-selected end-user license and should contain a CrossMark logo, the end user license, and a DOI link to the formal publication on ScienceDirect.
Please refer to Elsevier's posting policy for further information.
18. **For book authors** the following clauses are applicable in addition to the above: Authors are permitted to place a brief summary of their work online only. You are not allowed to download and post the published electronic version of your chapter, nor may you scan the printed edition to create an electronic version. **Posting to a repository:** Authors are permitted to post a summary of their chapter only in their institution's repository.
19. **Thesis/Dissertation**: If your license is for use in a thesis/dissertation your thesis may be submitted to your institution in either print or electronic form. Should your thesis be published commercially, please reapply for permission. These requirements include permission for the Library and Archives of Canada to supply single copies, on demand, of the complete thesis and include permission for Proquest/UMI to supply single copies, on demand, of the complete thesis. Should your thesis be published commercially, please reapply for permission. Theses and dissertations which contain embedded PJAs as part of the formal submission can be posted publicly by the awarding institution with DOI links back to the formal publications on ScienceDirect.

Elsevier Open Access Terms and Conditions
You can publish open access with Elsevier in hundreds of open access journals or in nearly 2000 established subscription journals that support open access publishing. Permitted third party re-use of these open access articles is defined by the author's choice of Creative Commons user license. See our open access license policy for more information.
Terms & Conditions applicable to all Open Access articles published with Elsevier:
Any reuse of the article must not represent the author as endorsing the adaptation of the article nor should the article be modified in such a way as to damage the author's honour or reputation. If any changes have been made, such changes must be clearly indicated.
The author(s) must be appropriately credited and we ask that you include the end user license and a DOI link to the formal publication on ScienceDirect.
If any part of the material to be used (for example, figures) has appeared in our publication with credit or acknowledgement to another source it is the responsibility of the user to ensure their reuse complies with the terms and conditions determined by the rights holder.
Additional Terms & Conditions applicable to each Creative Commons user license:
CC BY: The CC-BY license allows users to copy, to create extracts, abstracts and new works from the Article, to alter and revise the Article and to make commercial use of the Article (including reuse and/or resale of the Article by commercial entities), provided the user gives appropriate credit (with a link to the formal publication through the relevant DOI), provides a link to the license, indicates if changes were made and the licensor is not represented as endorsing the use made of the work. The full details of the license are

available at http://creativecommons.org/licenses/by/4.0.
CC BY NC SA: The CC BY-NC-SA license allows users to copy, to create extracts, abstracts and new works from the Article, to alter and revise the Article, provided this is not done for commercial purposes, and that the user gives appropriate credit (with a link to the formal publication through the relevant DOI), provides a link to the license, indicates if changes were made and the licensor is not represented as endorsing the use made of the work. Further, any new works must be made available on the same conditions. The full details of the license are available at http://creativecommons.org/licenses/by-nc-sa/4.0.
CC BY NC ND: The CC BY-NC-ND license allows users to copy and distribute the Article, provided this is not done for commercial purposes and further does not permit distribution of the Article if it is changed or edited in any way, and provided the user gives appropriate credit (with a link to the formal publication through the relevant DOI), provides a link to the license, and that the licensor is not represented as endorsing the use made of the work. The full details of the license are available at http://creativecommons.org/licenses/by-nc-nd/4.0.
Any commercial reuse of Open Access articles published with a CC BY NC SA or CC BY NC ND license requires permission from Elsevier and will be subject to a fee.
Commercial reuse includes:

- Associating advertising with the full text of the Article
- Charging fees for document delivery or access
- Article aggregation
- Systematic distribution via e-mail lists or share buttons

Posting or linking by commercial companies for use by customers of those companies.

20. **Other Conditions**:

v1.9

Questions? customercare@copyright.com or +1-855-239-3415 (toll free in the US) or +1-978-646-2777.